frontiers | Research Topics

The brain meets the body: Neural basis of cognitive contribution in movement for healthy and neurological populations

Edited by
Daniela De Bartolo, Valeria Belluscio, Alex Martino Cinnera and Viviana Betti

Published in
Frontiers in Human Neuroscience

ISSN 1664-8714
ISBN 978-2-8325-3839-5
DOI 10.3389/978-2-8325-3839-5

About Frontiers

Frontiers is more than just an open access publisher of scholarly articles: it is a pioneering approach to the world of academia, radically improving the way scholarly research is managed. The grand vision of Frontiers is a world where all people have an equal opportunity to seek, share and generate knowledge. Frontiers provides immediate and permanent online open access to all its publications, but this alone is not enough to realize our grand goals.

Frontiers journal series

The Frontiers journal series is a multi-tier and interdisciplinary set of open-access, online journals, promising a paradigm shift from the current review, selection and dissemination processes in academic publishing. All Frontiers journals are driven by researchers for researchers; therefore, they constitute a service to the scholarly community. At the same time, the *Frontiers journal series* operates on a revolutionary invention, the tiered publishing system, initially addressing specific communities of scholars, and gradually climbing up to broader public understanding, thus serving the interests of the lay society, too.

Dedication to quality

Each Frontiers article is a landmark of the highest quality, thanks to genuinely collaborative interactions between authors and review editors, who include some of the world's best academicians. Research must be certified by peers before entering a stream of knowledge that may eventually reach the public - and shape society; therefore, Frontiers only applies the most rigorous and unbiased reviews. Frontiers revolutionizes research publishing by freely delivering the most outstanding research, evaluated with no bias from both the academic and social point of view. By applying the most advanced information technologies, Frontiers is catapulting scholarly publishing into a new generation.

What are Frontiers Research Topics?

Frontiers Research Topics are very popular trademarks of the *Frontiers journals series*: they are collections of at least ten articles, all centered on a particular subject. With their unique mix of varied contributions from Original Research to Review Articles, Frontiers Research Topics unify the most influential researchers, the latest key findings and historical advances in a hot research area.

Find out more on how to host your own Frontiers Research Topic or contribute to one as an author by contacting the Frontiers editorial office: frontiersin.org/about/contact

The brain meets the body: Neural basis of cognitive contribution in movement for healthy and neurological populations

Topic editors

Daniela De Bartolo — Vrije Universiteit Amsterdam, Netherlands
Valeria Belluscio — Foro Italico University of Rome, Italy
Alex Martino Cinnera — Santa Lucia Foundation (IRCCS), Italy
Viviana Betti — Sapienza University of Rome, Italy

Citation

De Bartolo, D., Belluscio, V., Cinnera, A. M., Betti, V., eds. (2023). *The brain meets the body: Neural basis of cognitive contribution in movement for healthy and neurological populations*. Lausanne: Frontiers Media SA.
doi: 10.3389/978-2-8325-3839-5

Table of contents

frontiers | Frontiers in Human Neuroscience

TYPE Editorial
PUBLISHED 18 October 2023
DOI 10.3389/fnhum.2023.1306252

OPEN ACCESS

EDITED AND REVIEWED BY
Julie Duque,
Université Catholique de Louvain, Belgium

*CORRESPONDENCE
Daniela De Bartolo
✉ d.de.bartolo@vu.nl

RECEIVED 03 October 2023
ACCEPTED 09 October 2023
PUBLISHED 18 October 2023

CITATION
Belluscio V, Betti V, Martino Cinnera A and De Bartolo D (2023) Editorial: The brain meets the body: neural basis of cognitive contribution in movement for healthy and neurological populations.
Front. Hum. Neurosci. 17:1306252.
doi: 10.3389/fnhum.2023.1306252

Editorial: The brain meets the body: neural basis of cognitive contribution in movement for healthy and neurological populations

Valeria Belluscio[1,2], Viviana Betti[2,3], Alex Martino Cinnera[1,2] and Daniela De Bartolo[2,4]*

[1]Department of Movement, Human and Health Sciences, Interuniversity Centre of Bioengineering of the Human Neuromusculoskeletal System, University of Rome "Foro Italico", Rome, Italy, [2]IRCCS Fondazione Santa Lucia, Rome, Italy, [3]Department of Psychology, Sapienza University of Rome, Rome, Italy, [4]Department of Human Movement Sciences, Faculty of Behavioural and Movement Sciences, Amsterdam Movement Sciences and Institute for Brain and Behaviour Amsterdam, Vrije Universiteit Amsterdam, Amsterdam, Netherlands

KEYWORDS

brain dynamics, motor control, measurement, cognitive-motor interplay, neuroscience

Editorial on the Research Topic
The brain meets the body: neural basis of cognitive contribution in movement for healthy and neurological populations

Cortical activation in movement

The human brain comprises billions of neurons forming an intricate network of interactions (Baars and Gage, 2010). Our understanding of brain function has progressed in recent decades (Sakkalis, 2011), delving into the basis of human behavior and function.

Most of everyday human movements are deceptively complex and only appear easy because of extensive practice. Cortical and subcortical networks, known to be involved in the planning and execution of movement (Meirhaeghe et al., 2023), are difficult to assess with imaging techniques in real-time (Sisti et al.). Therefore, modern research is increasingly interested in understanding this mechanism through dual-task conditions, exploiting external stimulations, such as acoustic or visual stimuli, to investigate cortical functioning in motor tasks execution (Bajaj et al., 2015; De Bartolo et al., 2020, 2021; Verna et al., 2020). In this Research Topic, Li et al. investigated whether Tai Chi (TC) practice can improve the brain connectivity of the prefrontal lobe. The authors showed a positive effect of TC on the frontal and temporal networks associated with decision making and abstract thinking. Furthermore, this study investigated the role of cognitive control in the realization of a motor performance, thus linking the improved activation of the prefrontal lobes to the enhancement of the brain functional neuroplasticity. Therefore, authors suggested that TC has a crucial role in improving the physical and mental health of college students, providing scientific guidance for the promotion of TC on campus.

Using fNIRS and virtual reality (VR), Zheng et al. detected the activation of the cerebral cortex under different VR interaction modes, exploring the optimal feedback associated to the improvement and the effectiveness of rehabilitation training with robots. Authors evaluated the effects of multiple VR interaction modalities based on force-haptic feedback combined with visual or auditory stimuli, finding that the multisensory integration is conducive to a stronger cortical activation due to the interaction effect between visual and auditory feedback. These results provided a theoretical basis for the optimal design of rehabilitation robots thus formulating potential VR-based clinical schemes.

Song et al. detected with fNIRS a strong network activity in the bilateral prefrontal, motor, and occipital cortex following a motor exertion based on a race-walking task. These real-time changes reflected different brain network-specific characteristics, suggesting that a more extensive brain activation is needed to process information about speed. Authors suggested that increased motor activity may facilitate the integration of proprioception and motor planning involved in coordinated actions. Finally, in this Research Topic Strong et al. used fMRI to identify brain regions associated with the proprioceptive sense of joint position of the knee in people with injury to the anterior cruciate ligament. Using a knee joint position sense test during simultaneous fMRI, the authors observed significant correlations with increased ipsilateral response in the anterior cingulate, supramarginal gyrus and insula, and sensorimotor processes, body schema and interoception These results provided further insights into brain response to proprioception among different populations.

Postural control and the neuro-muscular investigation

Regulation and control of posture represent a challenge for the body's neuromuscular control system (Hayes, 1982; Munoz-Martel et al., 2019; Martino Cinnera et al., 2022) and its dysfunction affects the daily living activity of neurological patients (Nonnekes et al., 2018). The review proposed by Chaudhary et al., addressed the role of the visual system and its interaction with the vestibular system to maintain postural stability. Authors outlined how visual-vestibular interactions enhance postural stability by interpreting the head's position and generating eye movements accordingly, which helps differentiate self-motion or external motion and achieve gaze stabilization and postural control. Indirect measurement of brain responses to postural changes is also addressed through the assessment of neuromuscular and motor functions, as in the investigation of defense mechanisms adopted to keep the body away from the stimulus (Graziano and Cooke, 2006; Belluscio et al., 2023). In humans the space directly surrounding the body at a grasping distance has been depicted as defensive peripersonal space for tactile (Rizzolatti et al., 1997) or auditory stimulation (Ladavas et al., 2001), closer the stimulation to the head stronger behavioral response was found (Versace et al., 2019). Hamada et al. used EMG to investigate how the prediction of an auditory stimulus site of the head may induce a defense response of the body swaying in the opposite direction, unraveling the specific contribution of the gastrocnemius muscle.

Zipser-Mohammadzada et al. investigated the relationship between intramuscular coherence and corticospinal dynamic balance control during a visually guided walking treadmill task through EMG recordings in a group of incomplete spinal cord injury patients (iSCI). This study provided a reliable measure of adaptive walking ability in individuals with iSCI, thus contributing to new knowledge about supra-spinal locomotor control.

Finally, Schueren et al. explored the role of a somatosensory illusion influencing the postural after-effects of standing on an inclined surface. Using a force plate, the authors showed that lower extremity manipulation is a useful intervention to treat postural stability. This study contributes to the growing body of evidence that manipulation of the lower extremities can drive global postural changes, as well as influence standing behavior.

This Research Topic collected significant contributions to the advancement of the motor-cognitive interplay. The integrative use of novel neuroscientific techniques strives for an in-depth investigation of motor behavior, assuming a multidisciplinary approach to the study of brain–behavior relations also in neurological populations. This will enable neuroscientific knowledge to be effectively translated for clinical practice.

Author contributions

VBel: Methodology, Writing—original draft, Writing—review and editing. VBet: Writing—review and editing. AM: Writing—review and editing. DD: Writing—review and editing, Conceptualization, Investigation, Methodology, Project administration, Supervision, Writing—original draft.

Funding

The author(s) declare that no financial support was received for the research, authorship, and/or publication of this article.

Conflict of interest

The authors declare that the research was conducted in the absence of any commercial or financial relationships that could be construed as a potential conflict of interest.

Publisher's note

References

Baars, B. J., and Gage, N. M. (2010). Cognition, *Brain*, and *Consciousness: Introduction to Cognitive[[Inline Image]] Neuroscience*. Cambridge, MA: Academic Press. doi: 10.1016/B978-0-12-375070-9.00008-5

Bajaj, S., Butler, A. J., Drake, D., and Dhamala, M. (2015). Brain effective connectivity during motor-imagery and execution following stroke and rehabilitation. *Neuroimage: Clin.* 8, 572–582. doi: 10.1016/j.nicl.2015.06.006

Belluscio, V., Cartocci, G., Terbojevich, T., Di Feo, P., Inguscio, B. M. S., Ferrari, M., et al. (2023). Facilitating or disturbing? An investigation about the effects of auditory frequencies on prefrontal cortex activation and postural sway. *Front. Neurosci.* 17, 1197733. doi: 10.3389/fnins.2023.1197733

De Bartolo, D., Belluscio, V., Vannozzi, G., Morone, G., Antonucci, G., Giordani, G., et al. (2020). Sensorized assessment of dynamic locomotor imagery in people with stroke and healthy subjects. *Sensors* 20, 4545. doi: 10.3390/s20164545

De Bartolo, D., De Giorgi, C., Compagnucci, L., Betti, V., Antonucci, G., Morone, G., et al. (2021). Effects of cognitive workload on heart and locomotor rhythms coupling. *Neurosci. Lett.* 762, 136140. doi: 10.1016/j.neulet.2021.136140

Graziano, M. S., and Cooke, D. F. (2006). Parieto-frontal interactions, personal space, and defensive behavior. *Neuropsychologia* 44, 2621–2635. doi: 10.1016/j.neuropsychologia.2005.09.011

Hayes, K. C. (1982). Biomechanics of postural control. *Exerc. Sport Sci. Rev.* 10, 363. doi: 10.1249/00003677-198201000-00011

Ladavas, E., Pavani, F., and Farne, A. (2001). Auditory peripersonal space in humans: a case of auditory-tactile extinction. *Neurocase* 7, 97–103. doi: 10.1093/neucas/7.2.97

Martino Cinnera, A., Princi, A. A., Leone, E., Marrano, S., Pucello, A., Paolucci, S., et al. (2022). The effects of sternocleidomastoid muscle taping on postural control in healthy young adults: a pilot crossover study. *Healthcare* 10, 946. doi: 10.3390/healthcare10050946

Meirhaeghe, N., Riehle, A., and Brochier, T. (2023). Parallel movement planning is achieved via an optimal preparatory state in motor cortex. *Cell Rep.* 42, 112136. doi: 10.1016/j.celrep.2023.112136

Munoz-Martel, V., Santuz, A., Ekizos, A., and Arampatzis, A. (2019). Neuromuscular organisation and robustness of postural control in the presence of perturbations. *Sci. Rep.* 9, 12273. doi: 10.1038/s41598-019-47613-7

Nonnekes, J., Goselink, R. J., RuŽička, E., Fasano, A., Nutt, J. G., and Bloem, B. R. (2018). Neurological disorders of gait, balance and posture: a sign-based approach. *Nat. Rev. Neurol.* 14, 183–189. doi: 10.1038/nrneurol.2017.178

Rizzolatti, G., Fadiga, L., Fogassi, L., and Gallese, V. (1997). The space around us. *Science* 277, 190–191. doi: 10.1126/science.277.5323.190

Sakkalis, V. (2011). Review of advanced techniques for the estimation of brain connectivity measured with EEG/MEG. *Comput. Biol. Med.* 41, 1110–1117. doi: 10.1016/j.compbiomed.2011.06.020

Verna, V., De Bartolo, D., Iosa, M., Fadda, L., Pinto, G., Caltagirone, C., et al. (2020). Te.M.P.O., an app for using temporal musical mismatch in post-stroke neurorehabilitation: a preliminary randomized controlled study. *NeuroRehabilitation* 47, 201–208. doi: 10.3233/NRE-203126

Versace, V., Campostrini, S., Sebastianelli, L., Saltuari, L., and Kofler, M. (2019). Modulation of exteroceptive electromyographic responses in defensive peripersonal space. *J. Neurophysiol.* 121, 1111–1124. doi: 10.1152/jn.00554.2018

frontiers in Human Neuroscience

REVIEW
published: 08 February 2022
doi: 10.3389/fnhum.2022.697739

The Differentiation of Self-Motion From External Motion Is a Prerequisite for Postural Control: A Narrative Review of Visual-Vestibular Interaction

Shikha Chaudhary, Nicola Saywell and Denise Taylor*

Rehabilitation Innovation Centre, Faculty of Health and Environmental Science, Health and Rehabilitation Research Institute, Auckland University of Technology, Auckland, New Zealand

The visual system is a source of sensory information that perceives environmental stimuli and interacts with other sensory systems to generate visual and postural responses to maintain postural stability. Although the three sensory systems; the visual, vestibular, and somatosensory systems work concurrently to maintain postural control, the visual and vestibular system interaction is vital to differentiate self-motion from external motion to maintain postural stability. The visual system influences postural control playing a key role in perceiving information required for this differentiation. The visual system's main afferent information consists of optic flow and retinal slip that lead to the generation of visual and postural responses. Visual fixations generated by the visual system interact with the afferent information and the vestibular system to maintain visual and postural stability. This review synthesizes the roles of the visual system and their interaction with the vestibular system, to maintain postural stability.

Keywords: visual system, postural control, visual-vestibular interaction, visual fixations, retinal slip, optic flow, self-motion perception

OPEN ACCESS

Edited by:
Pilwon Hur,
Gwangju Institute of Science and Technology, South Korea

Reviewed by:
Tsukasa Kimura,
Osaka University, Japan
Binal Motawar,
University of Missouri, United States

****Correspondence:***
Shikha Chaudhary
shikha.chaudhary@aut.ac.nz

Specialty section:
This article was submitted to Motor Neuroscience, a section of the journal Frontiers in Human Neuroscience

Received: *20 April 2021*
Accepted: *18 January 2022*
Published: *08 February 2022*

Citation:
Chaudhary S, Saywell N and Taylor D (2022) The Differentiation of Self-Motion From External Motion Is a Prerequisite for Postural Control: A Narrative Review of Visual-Vestibular Interaction. Front. Hum. Neurosci. 16:697739. doi: 10.3389/fnhum.2022.697739

INTRODUCTION

Postural control requires continuous regulation of information from three systems- the visual, the vestibular, and the somatosensory (Massion, 1994; Samuel et al., 2015; Ivanenko and Gurfinkel, 2018). A key prerequisite for postural control is accurate interpretation and integration of information from the visual and vestibular systems. The interpretation and integration allow differentiation between self-motion and external motion (Redfern et al., 2001; Júnior and Barela, 2004; Guerraz and Bronstein, 2008; Rogers et al., 2017). This review focuses on fundamental concepts of the visual system and its interaction with the vestibular system required for this differentiation and will outline how it underpins efficient postural control. Postural control during conditions when vision is occluded, is not included in this review. For the purpose of this review proprioceptive information from the extraocular muscles is included as a part of the visual system, however, a more comprehensive discussion of the proprioceptive system is beyond the scope of this review. Balance is a complex function and involves multiple

systems including the somatosensory, visual, and vestibular systems along with contributions from a variety of reflex control mechanisms. Whilst these are all important for postural control, this review focuses on the integration of the visual and vestibular systems.

Self-motion and motion of an object in the environment whilst a person is stationary cause a similar visual stimulation (Redfern et al., 2001; Fushiki et al., 2005; Melcher, 2011). For example, a head turn causes movement of a scene relative to the retina similar to that caused by an object's movement within an environment, yet we perceive the environment as stationary when turning the head (Wallach, 1987; Melcher, 2011; Ivanenko and Gurfinkel, 2018). The differentiation of self-motion and external motion is essential as many everyday tasks such as walking, and driving require accurate interpretation of motion to perform each task effectively.

There are a number of reviews discussing the roles of the visual system and the vestibular system in postural control (Guerraz and Bronstein, 2008; Cullen, 2012). However, the authors of this review identified a need to synthesize key concepts of the interaction between the visual and vestibular systems. The current review outlines how this interaction underpins the differentiation of self-motion and external motion to maintain visual and postural stability.

OVERVIEW OF THE VISUAL SYSTEM

The visual system consists of the central visual system (fovea) and the peripheral visual system. The central visual system recognizes objects and object motion, whereas the peripheral vision is sensitive to moving scenes and dominates the awareness of self-motion and postural control (Dichgans and Brandt, 1978; Warren and Kurtz, 1992; Nougier et al., 1997; Berencsi et al., 2005; Guerraz and Bronstein, 2008). To maintain postural control and navigate in an environment, we need a balance between the central and peripheral vision to determine the spatial orientation of self and objects in an environment. As we move, the relationship between self, and objects in the environment changes. Accurate interpretation of these relationships using information from the visual system, helps differentiate self-motion from external motion. The following paragraph introduces three key concepts that help achieve this differentiation, optic flow, retinal slip, and visual fixations.

Optic flow is the pattern of motion of the external world over the retina and forms a part of the afferent information to the visual system (Koenderink, 1986; Warren et al., 2001; William, 2004). For example, when walking past a line of trees, there is a changing pattern of optic flow generated on the retina. Retinal slip is the movement of the visual image on the surface of the retina due to movement of the eyes and head (Strupp et al., 2003; Gielen et al., 2004; Glasauer et al., 2005). Visual fixations allow maintenance of gaze on a point and have a key role in suppressing optic flow and retinal slip, which then improves visual and postural stability (Martinez-Conde et al., 2004; Martinez-Conde, 2006; Martinez-Conde and Macknik, 2008; Otero-Millan et al., 2014). The review will focus on these three central concepts of the visual system and their interaction with the vestibular system.

OVERVIEW OF THE VESTIBULAR SYSTEM

The vestibular system comprises the peripheral and central vestibular systems and serves a wide variety of functions such as postural control, gaze stabilization, conscious perception, autonomic regulation, and navigation. This review will focus on its role in postural control and gaze stabilization (Highstein et al., 2004; Tascioglu, 2005; Kanegaonkar et al., 2012; Khan and Chang, 2013; Dieterich and Brandt, 2015; Casale et al., 2020). It mediates our position in space relative to gravity and perception of self-motion by providing the sensory input to adjust position of the eye, head, and body.

The peripheral vestibular receptors provide information about the motion of the head in three dimensions. The central vestibular pathways use this information to control the reflexes and perception of self-motion (Raphan et al., 2001; Roy and Cullen, 2002; Dieterich and Brandt, 2015). The vestibulo-ocular reflex and the optokinetic reflex interact with the visual system to maintain visual and postural stability (Pettorossi et al., 1996; Kandel et al., 2000; Raphan and Cohen, 2002).

The vestibulo-ocular reflex (VOR) is a gaze stabilizing reflex which stabilizes the retinal image by rotating the eyes in the opposite direction to head movements (Paige et al., 1998; Straube, 2007; Dieterich and Brandt, 2015). It is divided into two parts: the angular VOR and the translational VOR. The angular VOR, mediated by semi-circular canals, compensates for rotational movements of the head. The translational VOR is mediated by otoliths and compensates for translation movements of the head. Gaze stabilization mediated by the VOR helps reduce optic flow and therefore retinal slip generated in response to self-motion or external motion.

Visually perceived orientation of the environment provides cues to verticality but can sometimes confound orientation. To interpret visual cues properly, the contributions of object-in-world and eye-in-world orientations from the retinal images must be reconciled to ensure an accurate perception of verticality (Sunkara et al., 2015). The vestibular system as a gravitational receptor has a fundamental role in verticality perception (Dakin and Rosenberg, 2018). This vestibular contribution to verticality perception helps to transform visual information from an eye-centered reference frame into a gravity-centered reference frame to achieve stable postural control (Dakin and Rosenberg, 2018).

INTEGRATION

The generation of vestibular reflexes in response to visual input signifies an intimate relationship between the visual and the vestibular system such as seen in the optokinetic reflex. This reflex responds to input from the otolith organs and regulates eye position during head rotation and tilting (Mestre and Masson, 1997; Kandel et al., 2000; Tsutsumi et al., 2007). It is a

combination of slow-phase and fast-phase eye movements where the eyes momentarily follow a moving object, then rapidly reset to the initial position. The optokinetic reflex is generated in response to large field movements and movement of objects in the peripheral visual field. The following sections outline visual-vestibular interactions at a functional and neuronal level.

There are three sections: (1) optic flow and postural control: this section describes how optic flow is generated, what it is used for and its role in postural control, (2) retinal slip, vestibulo-ocular reflex, and postural control: this section emphasizes how the retinal slip is interpreted and its interaction with the vestibular system to maintain postural control, (3) visual fixations and postural control: this section incorporates the role visual fixations play in postural control by interaction with the optic flow and the retinal slip. Finally, visual-vestibular interaction is discussed at the neuronal level.

Optic Flow and Postural Control

When a person moves in an environment, it is necessary to differentiate self-motion from external motion to maintain postural stability (Wertheim, 1994; Redfern et al., 2001; Fajen and Matthis, 2013; Ramkhalawansingh et al., 2018). This distinction is dependent on perceiving whether the motion of an image on the retina is the result of a person moving relative to an object or an object moving relative to the person.

Movement of an observer in a stationary environment is interpreted as self-motion as it generates patterns of optic flow specific to self-motion (Gibson, 1950; Lappe et al., 1999; Barela et al., 2009; Fajen and Matthis, 2013). In the presence of object motion along with self-motion, the resultant optic flow is the vector sum of the object motion and self-motion components (Warren et al., 2001; Royden and Connors, 2010; Fajen and Matthis, 2013). Therefore, to achieve differentiation between self-motion and object motion, the visual system must separate the object motion component from the self-motion component. This is achieved by comparing visual information of self-motion and non-visual information of self-motion (Rushton and Warren, 2005; Guerraz and Bronstein, 2008; Royden and Connors, 2010; Fajen and Matthis, 2013). Visual information is known as retinal signal and non-visual information as the reference signal. The reference signal includes proprioceptive feedback from the extraocular muscles, the somatosensory system, vestibular afferents, and cognition. When the retinal and reference signals match, the object is perceived as stationary (the person is moving relative to the object; self-motion), when they differ, object motion is perceived (the object is moving relative to the person; object motion) (Wertheim, 1994; Wolsley et al., 1996b; Freeman, 2007; Guerraz and Bronstein, 2008; Bogadhi et al., 2013).

The optic flow pattern created during self-motion is not consistent throughout the visual field (William, 2004; DeAngelis and Angelaki, 2012). During self-motion, optic flow expands radially outwards and is projected on to the center of the retina with a focus of expansion aligned with the direction of movement, known as radial flow. In the peripheral field, optic flow remains parallel to the line of motion and sweeps past the observer, known as lamellar flow (Warren et al., 2001; Turano et al., 2005; Guerraz and Bronstein, 2008; Royden and Connors, 2010). If the object is not moving parallel to the observer, the direction of optic flow deviates from the radially expanding background flow and allows detection of the object motion during self-motion. These optic flow patterns from the environment also provide spatial-temporal information required for spatial orientation and visual navigation (Redlick et al., 2001; Warren et al., 2001; Angelaki and Hess, 2005).

In addition to optic flow, vestibular signals are important for inferring self-motion (Telford et al., 1995; Ohmi, 1996; Warren et al., 2001; Fetsch et al., 2007, 2009; Gu et al., 2008; Dokka et al., 2015). The visual and the vestibular systems have their optimal frequency ranges for providing precise cues for self-motion. The vestibular system provides information about the angular and linear acceleration of head in space, providing inputs for detecting self-motion. Information from the vestibular system is important in instances when optic flow elicits an illusion of self-motion known as vection (Brandt et al., 1972; Berthoz et al., 1975; Telford et al., 1995; Harris et al., 2000; Bertin and Berthoz, 2004). The most common real-life example of vection is, when sitting in a stationary train, movement of a neighboring train causes illusory movement of the stationary train. In such instances, a combination of information from the visual and vestibular systems is necessary to determine self-motion accurately.

Retinal Slip, Vestibulo-Ocular Reflex, and Postural Control

Retinal slip is the afferent signal used to generate visually evoked postural reactions (Wertheim, 1994; Wolsley et al., 1996a; Guerraz and Bronstein, 2008; Lacour et al., 2018). These postural reactions' objective is to lessen the amplitude of optic flow changes (Masson et al., 1995; Barela et al., 2009). Retinal slip is used as feedback for compensatory sway by the central nervous system (Wolsley et al., 1996a; Strupp et al., 2003; Guerraz and Bronstein, 2008).

During self-motion, objects within the visual scene move on the retina generating retinal slip, this can lead to a blurry perception of the scene and the object. To avoid this, visual and vestibular systems co-function to compensate for retinal slip by generating compensatory eye movements (Miles and Busettini, 1992; Miles, 1998; Angelaki and Hess, 2005). The eye movements comprise a vestibular driven foveal stabilization reflex known as the translational vestibular-ocular reflex (TVOR) and the visual system induced ocular following reflex (OFRs) (Miles and Wallman, 1993; Miles, 1998; Yang et al., 1999). The compensatory eye movements help maintain the target stationary on the retina while objects at different distances in the scene move relative to one another thus minimizing retinal slip (Miles and Busettini, 1992; Angelaki et al., 2003; Angelaki and Hess, 2005). The TVOR generates eye movements with an amplitude corresponding with the viewing distance (Schwarz and Miles, 1991; Angelaki and McHenry, 1999; Hess and Angelaki, 2003). The amplitude of TVOR eye movements increases as the target gets closer to the observer, enabling quick compensation for the retinal slip induced by self-motion (Angelaki and McHenry, 1999; Angelaki and Hess, 2005). The remaining retinal slip is stabilized by the

ocular following reflexes (OFRs). OFRs generated in response to lamellar flow comprise conjugate vertical and horizontal eye movements. To compensate for radial flow, vergence OFRs are generated. Like TVOR, generation of OFR also depends on the viewing distance. However, TVOR dominates the compensation for first 10 milliseconds of self-motion (Schwarz and Miles, 1991; Busettini et al., 1997; Ramat and Zee, 2003).

The complexity of retinal slip increases when the observer moves closer to an object, or the object lies at an angle to the direction of motion. To maintain the body in a stable position, retinal slip must be minimized (Gielen et al., 2004). To minimize retinal slip, the amplitude of postural sway should be equal to movement of the optic flow in a direction that decreases the overall amplitude of the optic flow, which can be destabilizing for the observer (Strupp et al., 2003). To prevent destabilization, the nervous system receives information about the retinal slip by the compensatory eye movements, the TVOR, and OFR. The eye movements break down the optic flow into three components: translation, divergence, and rotational components. The disintegration minimizes the retinal slip providing cues to the central nervous system regarding the resultant retinal slip against which the compensatory postural sway is generated (Gielen et al., 2004; Angelaki and Hess, 2005). Thus, both TVOR and the OFR eliminate retinal slip maintaining visual acuity on the fovea and enabling the nervous system to provide a compensatory sway allowing the observer to maintain upright stance (Strupp et al., 2003; Angelaki and Hess, 2005).

The functioning of the VOR depends on three significant context variables; the head movement characteristics (known as stimulus context), fixation during head movements (known as fixational context), and the motion of visual target (known as visual context) (Paige, 1996; Paige et al., 1998). The head movement characteristics mainly involve the frequency and amplitude of motion. Both AVOR and LVOR operate at high frequencies (Paige et al., 1998; King and Shanidze, 2011).

For maintained fixation during head movement, VOR compensates for both translational and rotational components. Compensation is dependent on fixation distance. Fixation on a distant target requires little eye movement, as the object gets closer a larger amplitude of ocular responses is generated (Schwarz and Miles, 1991; Paige et al., 1998; Telford et al., 1998).

The mode of visual-vestibular interaction is dependent on whether the visual target is stationary or moving. If a visual target is stationary, the VOR efficiently compensates for any sudden perturbations of the head in space. Activities such as locomotion achieve gaze stability by activating semi-circular canal afferents through head movements, triggering the VOR. The eye movements generated are so accurate that there is no retinal slip, maintaining high visual acuity and gaze stability (Paige et al., 1998; Straube, 2007; Fetsch et al., 2009; Dokka et al., 2015).

Visual Fixations and Postural Control

Visual fixations keep our eyes fixed on a target while viewing a scene. Visual fixations occur between saccades, contribute to 80% of the visual experience and are essential for visual processing (Martinez-Conde, 2006; Martinez-Conde and Macknik, 2008; Otero-Millan et al., 2014; Snodderly, 2016). Within periods of visual fixations, there are small eye movements. These small eye movements are required to overcome the neural mechanisms that lead to normalizing responses in cases of constant or uniform visual stimulation (Murakami and Cavanagh, 2001; Martinez-Conde et al., 2004; Martinez-Conde, 2006; Martinez-Conde and Macknik, 2008; Otero-Millan et al., 2012, 2014; Rucci and Poletti, 2015; Snodderly, 2016).

Visual fixations have an important role in reducing optic flow, minimizing retinal slip, and suppressing the optokinetic response (Pola et al., 1995; Glennerster et al., 2001; Murakami and Cavanagh, 2001; Uchiyama and Demura, 2009; Hoppes et al., 2018). Minimizing optic flow and retinal slip is essential as sometimes information from optic flow is destabilizing leading to generation of vection or an optokinetic response (Brandt et al., 1972; Dichgans and Brandt, 1978; Júnior and Barela, 2004; Barela et al., 2009; Dokka et al., 2015). Both instances can erroneously evoke destabilizing postural responses making a person feel unsteady and in the worst case can contribute to a fall. Interpreting information from optic flow becomes more complicated in naturalistic conditions and is significantly altered during eye and head movements and by motion of objects in the visual field (Barela et al., 2009; Fajen and Matthis, 2013; Hoppes et al., 2018). By maintaining the gaze at a single point within a scene, visual fixations increase visual stability and enhance postural control by suppressing the perception of motion within the visual field. This helps maximize the peripheral vision and provide a steady image to amplify the visual signals of self-motion (Bense et al., 2005; Martinez-Conde and Macknik, 2008; Fetsch et al., 2009; Dokka et al., 2015; Thomas et al., 2016). Sensory information from extraocular muscles then helps implementation of postural reactions (Wolsley et al., 1996b; Ivanenko and Gurfinkel, 2018).

Large field visual motion typically generates the optokinetic response (Mestre and Masson, 1997; Valmaggia and Gottlob, 2002; Tsutsumi et al., 2010). Such stimuli can lead to two interpretations; a normal one in which the observer perceives himself stationary in a moving environment or an abnormal one leading to a perception of self-motion, where moving surroundings appear stationary. Naturally, the optokinetic response is suppressed by maintaining visual fixation (Chambers and Gresty, 1982; Pola et al., 1995; Bense et al., 2005; Tsutsumi et al., 2007). Suppression of optokinetic response is required to maintain a steady image and perceive a stable world; visual-vestibular interaction is essential for visual and postural control (Bense et al., 2005; Roberts et al., 2013; Garzorz and MacNeilage, 2017). An example of this is while driving; the driver moves rapidly past stationary and moving objects, seen in the peripheral vision which would generate a rapid ocular response, if visual fixation was not able to be maintained on the road.

Visual fixations have a key role in maintaining postural stability as visually fixating on a target decreases postural sway (Wyatt et al., 1988, 1995; Miles and Wallman, 1993; Wallman, 1993; Uchiyama and Demura, 2009; Thomas et al., 2016; Murphy et al., 2019). Two theories have been used to explain visual fixations' role in postural stability (Murakami and Cavanagh, 2001; Guerraz and Bronstein, 2008). The inflow theory

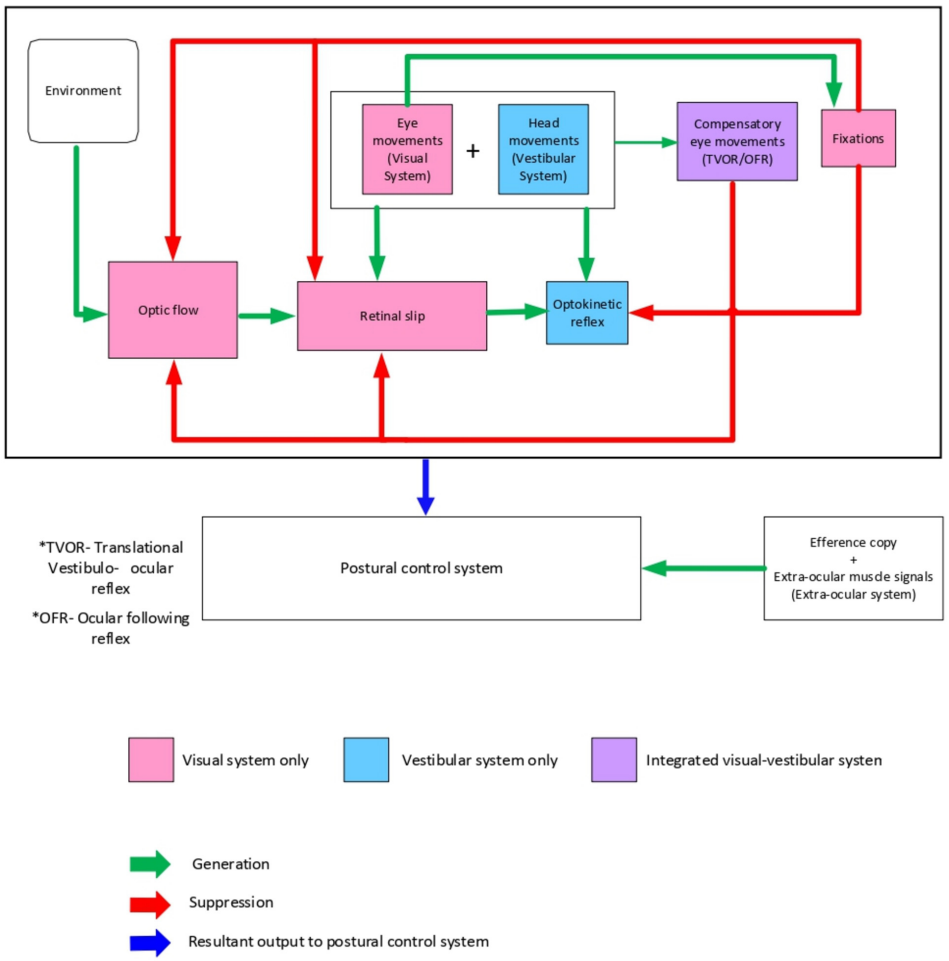

FIGURE 1 | Conceptual model of visual-vestibular interaction to differentiate self-motion from external motion to maintain postural stability.

suggests that proprioceptors in the extraocular muscles provide information about the degree of eye movements, leading to an interpretation of body shifts during postural sway. However, the outflow theory has now superseded the inflow theory. It suggests a feedforward mechanism based on the efferent copy of a motor command utilized by the central nervous system to maintain visual consistency. In this theory the magnitude of eye movements is anticipated in a feed-forward manner which provides a better explanation of what we see **Figure 1**.

NEURONAL CONTROL OF VISUAL-VESTIBULAR INTERACTION

There is a large literature around neuronal control of visual-vestibular interaction. For this review, we are restricting discussion to brain areas involved in visual-vestibular interaction, neuronal mechanism for visual fixation control and interaction between these areas to maintain gaze and postural stability.

Visual-vestibular interaction is necessary to estimate and continuously update the body position in space and to distinguish self-motion from external motion. Explanation of this interaction has been widely studied in Macaque monkeys. The exact neural mechanisms for visual-vestibular integration in humans is less well understood (Roberts et al., 2017; Smith et al., 2017). Early studies have reported activation of the occipito-temporal cortex, posterior parietal cortex, and subcortical structures with reduced activation within posterior insular cortex during visual motion (Brandt et al., 1998; Dieterich et al., 1998; Kleinschmidt et al., 2002; Bense et al., 2006). Studies using caloric vestibular stimulation identified activation of similar regions with increased activity in posterior insular cortex (Bense et al., 2005, 2006).

These findings led to the current hypothesis of reciprocal visual-vestibular interaction based on reciprocal inhibition (Brandt et al., 1998). Visual-vestibular interaction depends on the pattern of visual motion as well as the active postural and locomotor tasks. This requires the nervous system to weigh out the more reliable sensory information and is known as sensory reweighting (see following for a more detailed discussion, Peterka, 2002; Assländer and Peterka, 2014). Functionally, during a constant visual input, there should be a decrease in the vestibular system's sensitivity to head acceleration. This is

essential to avoid mismatch between visual and vestibular inputs during involuntary head accelerations such as sitting facing in the opposite direction to that of the train in which you are traveling. Continuous vestibular inputs in such situations can be misleading with the perception of self-motion (Bense et al., 2005; Dokka et al., 2015). To avoid such mismatches there is a reciprocal inhibitory interaction between the visual and vestibular system (Brandt et al., 1998) where both systems suppress the other to produce a coherent sense of self-motion. Deactivation of the vestibular cortex prevents conflict between vestibular information of head motion from visually induced perception of motion and vice versa. Recent studies have identified areas of cortical activation during optic flow stimulation which are consistent with detection of self-motion (Wall and Smith, 2008; Cardin and Smith, 2010). These are regions within the intraparietal sulcus and cingulate sulcus visual area. Parieto-insular vestibular cortex and posterior insular cortex are also found to be activated during object motion (Frank et al., 2014).

A large number of areas have been associated with resolving perceptual conflicts (Nachev et al., 2008; Sharp et al., 2010; Roberts and Husain, 2015; Kolling et al., 2016). These include the insular cortex, inferior frontal gyrus, and medial frontal structures pre supplementary motor area. During conflicting visual-vestibular information there is activation of parieto-insular vestibular cortex.

Additionally, the existence of visual targets in the environment requires a combination of eye and head orientation to achieve gaze stability. The visual-vestibular interaction to shift gaze toward a target and then maintain fixation is regulated by omni-directional pause neurons (OP neurons), located in nucleus raphe interpositus of the paramedian pontine reticular formation (Prsa and Galiana, 2007; Krauzlis et al., 2017). These neurons fire during fixations and stop firing during saccades. Activity of the neurons have an inhibitory influence on saccades. They prevent firing of saccade-related premotor burst neurons which are in the mesencephalic and pontomedullary reticular formations. However, a pause in their activity allows resumption of the saccade-related burst driving the motor neurons that innervate the extraocular muscles (Krauzlis et al., 2017).

The input to the OP neurons is a weighted sum of the vestibular and visual inputs (Krauzlis et al., 2017). This comprises three signals- 1. the gaze motor error- uses a range of sensory inputs (auditory, somatosensory, and cognitive) and is the difference between the present gaze position and the final required gaze position, 2. the head velocity signal detected by the semi-circular canals by vestibular neuron and 3. the eye velocity signal. When the sum total of afferent signals surpasses a threshold the OPN's are turned off leading to a halt in activity allowing the saccadic activity, whereas when the sum is below a threshold, OPN's turn on and induce fixation on the target (Prsa and Galiana, 2007).

Therefore, there is a continued interaction between visual and vestibular systems for postural control to maintain body and eye stability during various transitions involving head movements and constant visual motion.

CONCLUSION

The visual information regarding movements of self and objects in the environment is fundamental to postural control. Information from the optic flow patterns helps differentiate self-motion from external motion. Concurrent information of self-motion is also provided by the vestibular system using angular and linear acceleration of head in space. This information is necessary in instances when information from optic flow generates a false perception of self-motion known as vection or stimulates an optokinetic response. Optic flow patterns generate retinal slip on the retina constituting the main afferent signal to generate visually evoked postural reactions. To maintain visual and postural stability, the visual system, and the vestibular system co- function by generating TVOR and OFR's respectively to stabilize the image on retina. Stabilization of retinal image eliminates retinal slip, providing information to the nervous system to maintain an upright stance by generating compensatory postural sway.

A key determinant of visual and postural stability is visual fixations which keep eyes fixed on a target while viewing a scene. Visual fixations suppress the optic flow and minimize retinal slip by maximizing the peripheral vision and suppressing the generation of vection. They also have a major role in suppressing the optokinetic response which can destabilize an observer. Further, they maintain visual stability during tracking a moving target by suppressing the VOR.

The current review outlines how visual-vestibular interactions enhance postural stability by interpreting the head's position and generating eye movements accordingly, which helps differentiate self-motion or external motion and achieve gaze stabilization and postural control.

AUTHOR CONTRIBUTIONS

SC drafted the manuscript. DT and NS provided Ph.D. supervision for SC. All authors critically revised the manuscript read and approved the final manuscript.

REFERENCES

Angelaki, D. E., and Hess, B. J. (2005). Self-motion-induced eye movements: Effects on visual acuity and navigation. *Nat. Rev. Neurosci.* 6, 966–976. doi: 10.1038/nrn1804

Angelaki, D. E., and McHenry, M. Q. (1999). Short-latency primate vestibuloocular responses during translation. *J. Neurophysiol.* 82, 1651–1654. doi: 10.1152/jn.1999.82.3.1651

Angelaki, D. E., Zhou, H.-H., and Wei, M. (2003). Foveal versus full-field visual stabilization strategies for translational and rotational head movements. *J. Neurosci.* 23, 1104–1108. doi: 10.1523/jneurosci.23-04-01104.2003

Assländer, L., and Peterka, R. J. (2014). Sensory reweighting dynamics in human postural control. *J. Neurophysiol.* 111, 1852–1864.

Barela, A. M., Barela, J. A., Rinaldi, N. M., and de Toledo, D. R. (2009). Influence of imposed optic flow characteristics and intention on postural responses. *Motor Cont.* 13, 119–129.

Bense, S., Janusch, B., Schlindwein, P., Bauermann, T., Vucurevic, G., Brandt, T., et al. (2006). Direction-dependent visual cortex activation during horizontal optokinetic stimulation (fMRI study). *Human Brain Mapp.* 27, 296–305. doi: 10.1002/hbm.20185

Bense, S., Stephan, T., Bartenstein, P., Schwaiger, M., Brandt, T., and Dieterich, M. (2005). Fixation suppression of optokinetic nystagmus modulates cortical visual–vestibular interaction. *Neuroreport* 16, 887–890. doi: 10.1097/00001756-200506210-00003

Berencsi, A., Ishihara, M., and Imanaka, K. (2005). The functional role of central and peripheral vision in the control of posture. *Human Movem. Sci.* 24, 689–709. doi: 10.1016/j.humov.2005.10.014

Berthoz, A., Pavard, B., and Young, L. (1975). Perception of linear horizontal self-motion induced by peripheral vision (linearvection) basic characteristics and visual-vestibular interactions. *Exp. Brain Res.* 23, 471–489. doi: 10.1007/bf00234916

Bertin, R., and Berthoz, A. (2004). Visuo-vestibular interaction in the reconstruction of travelled trajectories. *Exp. Brain Res.* 154, 11–21. doi: 10.1007/s00221-003-1524-3

Bogadhi, A. R., Montagnini, A., and Masson, G. S. (2013). Dynamic interaction between retinal and extraretinal signals in motion integration for smooth pursuit. *J. Vision* 13, 5–5. doi: 10.1167/13.13.5

Brandt, T., Bartenstein, P., Janek, A., and Dieterich, M. (1998). Reciprocal inhibitory visual-vestibular interaction. Visual motion stimulation deactivates the parieto-insular vestibular cortex. *Brain* 121, 1749–1758. doi: 10.1093/brain/121.9.1749

Brandt, T., Dichgans, J., and Koenig, E. (1972). Perception of self-rotation (circular vection) induced by optokinetic stimuli. *Pflugers Archiv. Eur. J. Physiol.* 332:R398.

Busettini, C., Masson, G., and Miles, F. (1997). Radial optic flow induces vergence eye movements with ultra-short latencies. *Nature* 390, 512–515. doi: 10.1038/37359

Cardin, V., and Smith, A. T. (2010). Sensitivity of human visual and vestibular cortical regions to egomotion-compatible visual stimulation. *Cereb. Cortex* 20, 1964–1973. doi: 10.1093/cercor/bhp268

Casale, J., Browne, T., Murray, I., and Gupta, G. (2020). *Physiology, vestibular system*. Treasure Island: StatPearls

Chambers, B., and Gresty, M. (1982). Effects of fixation and optokinetic stimulation on vestibulo-ocular reflex suppression. *J. Neurol. Neurosurg. Psychiatry* 45, 998–1004. doi: 10.1136/jnnp.45.11.998

Cullen, K. E. (2012). The vestibular system: multimodal integration and encoding of self-motion for motor control. *Trends Neurosci.* 35, 185–196.

Dakin, C. J., and Rosenberg, A. (2018). Gravity estimation and verticality perception. *Handbook Clin. Neurol.* 159, 43–59.

DeAngelis, G. C., and Angelaki, D. E. (2012). *Visual–vestibular integration for self-motion perception. In The neural bases of multisensory processes*. Boca Raton: CRC Press. doi: 10.1201/b11092-39

Dichgans, J., and Brandt, T. (1978). "Visual-Vestibular Interaction: Effects on Self-Motion Perception and Postural Control," in *Perception*, eds R. Held, H. W. Leibowitz, and H.-L. Teuber (Berlin: Springer), 755–804. doi: 10.1007/978-3-642-46354-9_25

Dieterich, M., and Brandt, T. (2015). The bilateral central vestibular system: its pathways, functions, and disorders. *Ann. NY Acad. Sci.* 1343, 10–26. doi: 10.1111/nyas.12585

Dieterich, M., Bucher, S. F., Seelos, K. C., and Brandt, T. (1998). Horizontal or vertical optokinetic stimulation activates visual motion-sensitive, ocular motor and vestibular cortex areas with right hemispheric dominance. An fMRI study. *Brain* 121, 1479–1495. doi: 10.1093/brain/121.8.1479

Dokka, K., DeAngelis, G. C., and Angelaki, D. E. (2015). Multisensory integration of visual and vestibular signals improves heading discrimination in the presence of a moving object. *J. Neurosci.* 35, 13599–13607. doi: 10.1523/jneurosci.2267-15.2015

Fajen, B. R., and Matthis, J. S. (2013). Visual and non-visual contributions to the perception of object motion during self-motion. *PLoS One* 8:e55446. doi: 10.1167/11.11.920

Fetsch, C. R., Turner, A. H., DeAngelis, G. C., and Angelaki, D. E. (2009). Dynamic reweighting of visual and vestibular cues during self-motion perception. *J. Neurosci.* 29, 15601–15612. doi: 10.1523/jneurosci.2574-09.2009

Fetsch, C. R., Wang, S., Gu, Y., DeAngelis, G. C., and Angelaki, D. E. (2007). Spatial reference frames of visual, vestibular, and multimodal heading signals in the dorsal subdivision of the medial superior temporal area. *J. Neurosci.* 27, 700–712. doi: 10.1523/jneurosci.3553-06.2007

Frank, S. M., Baumann, O., Mattingley, J. B., and Greenlee, M. W. (2014). Vestibular and visual responses in human posterior insular cortex. *J. Neurophysiol.* 112, 2481–2491. doi: 10.1152/jn.00078.2014

Freeman, T. C. (2007). Simultaneous adaptation of retinal and extra-retinal motion signals. *Vision Res.* 47, 3373–3384. doi: 10.1016/j.visres.2007.10.002

Fushiki, H., Kobayashi, K., Asai, M., and Watanabe, Y. (2005). Influence of visually induced self-motion on postural stability. *Acta Oto-Laryngologica* 125, 60–64. doi: 10.1080/00016480410015794

Garzorz, I. T., and MacNeilage, P. R. (2017). Visual-vestibular conflict detection depends on fixation. *Curr. Biol.* 27, 2856–2861. doi: 10.1016/j.cub.2017.08.011

Gibson, J. J. (1950). *The perception of the visual world*. Boston: Houghton Mifflin.

Gielen, C., Gabel, S., and Duysens, J. (2004). Retinal slip during active head motion and stimulus motion. *Exp. Brain Res.* 155, 211–219. doi: 10.1007/s00221-003-1722-z

Glasauer, S., Schneider, E., Jahn, K., Strupp, M., and Brandt, T. (2005). How the eyes move the body. *Neurology* 65, 1291–1293. doi: 10.1212/01.wnl.0000175132.01370.fc

Glennerster, A., Hansard, M. E., and Fitzgibbon, A. W. (2001). Fixation could simplify, not complicate, the interpretation of retinal flow. *Vision Res.* 41, 815–834. doi: 10.1016/s0042-6989(00)00300-x

Gu, Y., Angelaki, D. E., and DeAngelis, G. C. (2008). Neural correlates of multisensory cue integration in macaque MSTd. *Nat. Neurosci.* 11, 1201–1210. doi: 10.1038/nn.2191

Guerraz, M., and Bronstein, A. (2008). Ocular versus extraocular control of posture and equilibrium. *Clin. Neurophysiol.* 38, 391–398. doi: 10.1016/j.neucli.2008.09.007

Harris, L. R., Jenkin, M., and Zikovitz, D. C. (2000). Visual and non-visual cues in the perception of linear self motion. *Exp. Brain Res.* 135, 12–21. doi: 10.1007/s002210000504

Hess, B. J., and Angelaki, D. E. (2003). Vestibular contributions to gaze stability during transient forward and backward motion. *J. Neurophysiol.* 90, 1996–2004. doi: 10.1152/jn.00302.2003

Highstein, S. M., Fay, R. R., and Popper, A. N. (2004). *The vestibular system*. Berlin: Springer, doi: 10.1007/b97280

Hoppes, C. W., Sparto, P. J., Whitney, S. L., Furman, J. M., and Huppert, T. J. (2018). Functional near-infrared spectroscopy during optic flow with and without fixation. *PLoS One* 13:e0193710. doi: 10.1371/journal.pone.0193710

Ivanenko, Y., and Gurfinkel, V. S. (2018). Human postural control. *Front. Neurosci.* 12:171. doi: 10.3389/fnins.2018.00171

Júnior, P. B. F., and Barela, J. A. (2004). Postural control as a function of self- and object-motion perception. *Neurosci. Lett.* 369, 64–68. doi: 10.1016/j.neulet.2004.07.075

Kandel, E. R., Schwartz, J. H., Jessell, T. M., Biochemistry, D. O., Jessell, M. B. T., Siegelbaum, S., et al. (2000). *Principles of neural science*. New York: McGraw-hill.

Kanegaonkar, R., Amin, K., and Clarke, M. (2012). The contribution of hearing to normal balance. *J. Laryngol. Otol.* 126, 984–988. doi: 10.1017/s002221511200179x

Khan, S., and Chang, R. (2013). Anatomy of the vestibular system: A review. *NeuroRehabilitation* 32, 437–443. doi: 10.3233/nre-130866

King, W., and Shanidze, N. (2011). Anticipatory eye movements stabilize gaze during self-generated head movements. *Ann. NY Acad. Sci.* 1233:219.

Kleinschmidt, A., Thilo, K. V., Büchel, C., Gresty, M. A., Bronstein, A. M., and Frackowiak, R. S. (2002). Neural correlates of visual-motion perception as object-or self-motion. *Neuroimage* 16, 873–882. doi: 10.1006/nimg.2002.1181

Koenderink, J. J. (1986). Optic flow. *Vision Res.* 26, 161–179. doi: 10.1016/0042-6989(86)90078-7

Kolling, N., Wittmann, M. K., Behrens, T. E., Boorman, E. D., Mars, R. B., and Rushworth, M. F. (2016). Value, search, persistence and model updating in anterior cingulate cortex. *Nat. Neurosci.* 19, 1280–1285. doi: 10.1038/nn.4382

Krauzlis, R. J., Goffart, L., and Hafed, Z. M. (2017). Neuronal control of fixation and fixational eye movements. *Philos. Trans. R Soc. B: Biol. Sci.* 372:20160205. doi: 10.1098/rstb.2016.0205

Lacour, M., Dosso, N. Y., Heuschen, S., Thiry, A., Van Nechel, C., and Toupet, M. (2018). How eye movements stabilize posture in patients with bilateral vestibular hypofunction. *Front. Neurol.* 9:744.

Lappe, M., Bremmer, F., and Van den Berg, A. (1999). Perception of self-motion from visual flow. *Trends Cogn. Sci.* 3, 329–336. doi: 10.1016/s1364-6613(99)01364-9

Martinez-Conde, S. (2006). Fixational eye movements in normal and pathological vision. *Prog. Brain Res.* 154, 151–176.

Martinez-Conde, S., and Macknik, S. L. (2008). Fixational eye movements across vertebrates: Comparative dynamics, physiology, and perception. *J. Vision* 8, 28–28. doi: 10.1167/8.14.28

Martinez-Conde, S., Macknik, S. L., and Hubel, D. H. (2004). The role of fixational eye movements in visual perception. *Nat. Rev. Neurosci.* 5, 229–240.

Massion, J. (1994). Postural control system. *Curr. Opin. Neurobiol.* 4, 877–887. doi: 10.1016/0959-4388(94)90137-6

Masson, G., Mestre, D., and Pailhous, J. (1995). Effects of the spatio-temporal structure of optical flow on postural readjustments in man. *Exp. Brain Res.* 103, 137–150. doi: 10.1007/bf00241971

Melcher, D. (2011). Visual stability. *Philos. Trans. R Soc. B: Biol. Sci.* 366, 468–475. doi: 10.1098/rstb.2010.0277

Mestre, D., and Masson, G. (1997). Ocular responses to motion parallax stimuli: The role of perceptual and attentional factors. *Vision Res.* 37, 1627–1641. doi: 10.1016/s0042-6989(96)00314-8

Miles, F. (1998). The neural processing of 3-D visual information: evidence from eye movements. *Eur. J. Neurosci.* 10, 811–822. doi: 10.1046/j.1460-9568.1998.00112.x

Miles, F. A., and Wallman, J. (1993). *Visual Motion and its role in the stabilization of gaze*. Amsterdam: Elsevier Science Limited.

Miles, F., and Busettini, C. (1992). Ocular compensation for self-motion. Visual mechanisms. *Ann. NY Acad. Sci.* 656, 220–232. doi: 10.1111/j.1749-6632.1992.tb25211.x

Murakami, I., and Cavanagh, P. (2001). Visual jitter: Evidence for visual-motion-based compensation of retinal slip due to small eye movements. *Vision Res.* 41, 173–186. doi: 10.1016/s0042-6989(00)00237-6

Murphy, C., Kapusta, M., and Overbury, O. (2019). The influence of fixation stability on balance in central vision loss. *Int. J. Orient. Mobil.* 10, 1–9. doi: 10.21307/ijom-2019-003

Nachev, P., Kennard, C., and Husain, M. (2008). Functional role of the supplementary and pre-supplementary motor areas. *Nat. Rev. Neurosci.* 9, 856–869. doi: 10.1038/nrn2478

Nougier, V., Bard, C., Fleury, M., and Teasdale, N. (1997). Contribution of central and peripheral vision to the regulation of stance. *Gait Posture* 5, 34–41. doi: 10.1016/s0966-6362(96)01071-5

Ohmi, M. (1996). Egocentric perception through interaction among many sensory systems. *Cogn. Brain Res.* 5, 87–96. doi: 10.1016/s0926-6410(96)00044-4

Otero-Millan, J., Macknik, S. L., and Martinez-Conde, S. (2012). Microsaccades and blinks trigger illusory rotation in the "rotating snakes" illusion. *J. Neurosci.* 32, 6043–6051. doi: 10.1523/jneurosci.5823-11.2012

Otero-Millan, J., Macknik, S. L., and Martinez-Conde, S. (2014). Fixational eye movements and binocular vision. *Front. Integ. Neurosci.* 8:52. doi: 10.3389/fnint.2014.00052

Paige, G. (1996). *How does the linear vestibulo-ocular reflex compare with the angular vestibulo-ocular reflex*. Oxford: Oxford University Press.

Paige, G. D., Telford, L., Seidman, S. H., and Barnes, G. R. (1998). Human vestibuloocular reflex and its interactions with vision and fixation distance during linear and angular head movement. *J. Neurophysiol.* 80, 2391–2404. doi: 10.1152/jn.1998.80.5.2391

Peterka, R. J. (2002). Sensorimotor integration in human postural control. *J. Neurophysiol.* 88, 1097–1118.

Pettorossi, V. E., Errico, P., Ferraresi, A., and Manni, E. (1996). Influence of the extraocular muscle proprioceptors on the orientation of the vestibulo-ocular reflex. *Acta Oto-Laryngol.* 116, 198–200. doi: 10.3109/00016489609137822

Pola, J., Wyatt, H. J., and Lustgarten, M. (1995). Visual fixation of a target and suppression of optokinetic nystagmus: effects of varying target feedback. *Vision Res.* 35, 1079–1087. doi: 10.1016/0042-6989(94)00215-8

Prsa, M., and Galiana, H. L. (2007). Visual-vestibular interaction hypothesis for the control of orienting gaze shifts by brain stem omnipause neurons. *J. Neurophysiol.* 97, 1149–1162. doi: 10.1152/jn.00856.2006

Ramat, S., and Zee, D. S. (2003). Ocular motor responses to abrupt interaural head translation in normal humans. *J. Neurophysiol.* 90, 887–902. doi: 10.1152/jn.01121.2002

Ramkhalawansingh, R., Butler, J. S., and Campos, J. L. (2018). Visual–vestibular integration during self-motion perception in younger and older adults. *Psychol. Aging* 33, 798–813. doi: 10.1037/pag0000271

Raphan, T., and Cohen, B. (2002). The vestibulo-ocular reflex in three dimensions. *Exp. Brain Res.* 145, 1–27. doi: 10.1007/s00221-002-1067-z

Raphan, T., Imai, T., Moore, S. T., and Cohen, B. (2001). Vestibular compensation and orientation during locomotion. *Ann. NY Acad. Sci.* 942, 128–138. doi: 10.1111/j.1749-6632.2001.tb03740.x

Redfern, M. S., Yardley, L., and Bronstein, A. M. (2001). Visual influences on balance. *J. Anx. Disord.* 15, 81–94. doi: 10.1016/s0887-6185(00)00043-8

Redlick, F. P., Jenkin, M., and Harris, L. R. (2001). Humans can use optic flow to estimate distance of travel. *Vision Res.* 41, 213–219. doi: 10.1016/s0042-6989(00)00243-1

Roberts, E., Bronstein, A., and Seemungal, B. (2013). Visual-vestibular interaction: Basic science to clinical relevance. *Adv. Clin. Neurosci. Rehab.* 13, 8–12.

Roberts, R. E., Ahmad, H., Arshad, Q., Patel, M., Dima, D., Leech, R., et al. (2017). Functional neuroimaging of visuo-vestibular interaction. *Brain Struct. Funct.* 222, 2329–2343. doi: 10.1007/s00429-016-1344-4

Roberts, R. E., and Husain, M. (2015). A dissociation between stopping and switching actions following a lesion of the pre-supplementary motor area. *Cortex* 63, 184–195. doi: 10.1016/j.cortex.2014.08.004

Rogers, C., Rushton, S. K., and Warren, P. A. (2017). Peripheral visual cues contribute to the perception of object movement during self-movement. *I-Perception* 8, 2041669517736072. doi: 10.1177/2041669517736072

Roy, J. E., and Cullen, K. E. (2002). Vestibuloocular reflex signal modulation during voluntary and passive head movements. *J. Neurophysiol.* 87, 2337–2357. doi: 10.1152/jn.2002.87.5.2337

Royden, C. S., and Connors, E. M. (2010). The detection of moving objects by moving observers. *Vision Res.* 50, 1014–1024. doi: 10.1016/j.visres.2010.03.008

Rucci, M., and Poletti, M. (2015). Control and functions of fixational eye movements. *Ann. Rev. Vision Sci.* 1, 499–518. doi: 10.1146/annurev-vision-082114-035742

Rushton, S. K., and Warren, P. A. (2005). Moving observers, relative retinal motion and the detection of object movement. *Curr. Biol.* 15, R542–R543. doi: 10.1016/j.cub.2005.07.020

Samuel, A. J., Solomon, J., and Mohan, D. (2015). A critical review on the normal postural control. *Physiother. Occup. Ther. J.* 8, 71–75. doi: 10.21088/potj.0974.5777.8215.4

Schwarz, U., and Miles, F. (1991). Ocular responses to translation and their dependence on viewing distance. I. Motion of the observer. *J. Neurophysiol.* 66, 851–864. doi: 10.1152/jn.1991.66.3.851

Sharp, D., Bonnelle, V., De Boissezon, X., Beckmann, C., James, S., Patel, M., et al. (2010). Distinct frontal systems for response inhibition, attentional capture, and error processing. *Proc. Nat. Acad. Sci.* 107, 6106–6111. doi: 10.1073/pnas.1000175107

Smith, A. T., Greenlee, M. W., DeAngelis, G. C., and Angelaki, D. E. (2017). Distributed visual–vestibular processing in the cerebral cortex of man and macaque. *Multisen. Res.* 30, 91–120. doi: 10.1163/22134808-00002568

Snodderly, D. M. (2016). A physiological perspective on fixational eye movements. *Vision Res.* 118, 31–47. doi: 10.1016/j.visres.2014.12.006

Straube, A. (2007). Anatomy of the Oculomotor System. *Dev. Ophthalmol.* 40, 1–14. doi: 10.1159/000100345

Strupp, M., Glasauer, S., Jahn, K., Schneider, E., Krafczyk, S., and Brandt, T. (2003). Eye movements and balance. *Ann. NY Acad. Sci.* 1004, 352–358. doi: 10.1196/annals.1303.033

Sunkara, A., DeAngelis, G. C., and Angelaki, D. E. (2015). Role of visual and non-visual cues in constructing a rotation-invariant representation of heading in parietal cortex. *Elife* 4:e04693.

Tascioglu, A. B. (2005). Brief review of vestibular system anatomy and its higher order projections. *Neuroanatomy* 4, 24–27.

Telford, L., Howard, I. P., and Ohmi, M. (1995). Heading judgments during active and passive self-motion. *Exp. Brain Res.* 104, 502–510. doi: 10.1007/bf00231984

Telford, L., Seidman, S. H., and Paige, G. D. (1998). Canal-otolith interactions in the squirrel monkey vestibulo-ocular reflex and the influence of fixation distance. *Exp. Brain Res.* 118, 115–125. doi: 10.1007/s002210050261

Thomas, N. M., Bampouras, T. M., Donovan, T., and Dewhurst, S. (2016). Eye movements affect postural control in young and older females. *Front. Aging Neurosci.* 8:216. doi: 10.3389/fnagi.2016.00216

Tsutsumi, T., Inaoka, H., Fukuoka, Y., Masuda, T., and Kitamura, K. (2007). Cross-coupling in a body-translating reaction: Interaural optokinetic stimulation reflects a gravitational cue. *Acta Oto-Laryngol.* 127, 273–279. doi: 10.1080/00016480600868422

Tsutsumi, T., Murakami, M., Kawaishi, J., Chida, W., Fukuoka, Y., and Watanabe, K. (2010). Postural stability during visual stimulation and the contribution from the vestibular apparatus. *Acta Oto-Laryngol.* 130, 464–471. doi: 10.3109/00016480903292718

Turano, K. A., Yu, D., Hao, L., and Hicks, J. C. (2005). Optic-flow and egocentric-direction strategies in walking: Central vs peripheral visual field. *Vision Res.* 45, 3117–3132. doi: 10.1016/j.visres.2005.06.017

Uchiyama, M., and Demura, S. (2009). The role of eye movement in upright postural control. *Sport Sci. Health* 5, 21–27. doi: 10.1007/s11332-009-0072-z

Valmaggia, C., and Gottlob, I. (2002). Optokinetic nystagmus elicited by filling-in in adults with central scotoma. *Invest. Ophthalmol. Visual Sci.* 43, 1804–1808.

Wall, M. B., and Smith, A. T. (2008). The representation of egomotion in the human brain. *Curr. Biol.* 18, 191–194. doi: 10.1016/j.cub.2007.12.053

Wallach, H. (1987). Perceiving a stable environment when one moves. *Ann. Rev. Psychol.* 38, 1–29. doi: 10.1146/annurev.ps.38.020187.000245

Wallman, J. (1993). Subcortical optokinetic mechanisms. *Rev. Oculomotor Res.* 5:321.

Warren, W. H., and Kurtz, K. J. (1992). The role of central and peripheral vision in perceiving the direction of self-motion. *Percep. Psychophys.* 51, 443–454. doi: 10.3758/bf03211640

Warren, W. H., Kay, B. A., Zosh, W. D., Duchon, A. P., and Sahuc, S. (2001). Optic flow is used to control human walking. *Nat. Neurosci.* 4, 213–216. doi: 10.1038/84054

Wertheim, A. H. (1994). Motion perception during selfmotion: The direct versus inferential controversy revisited. *Behav. Brain Sci.* 17, 293–311. doi: 10.1017/s0140525x00034646

William, H. W. (2004). "Optic Flow," in *The Visual Neurosciences*, ed. L. C. J. Werner Cambridge: MIT Press, 1247–1259.

Wolsley, C., Sakellari, V., and Bronstein, A. (1996b). Reorientation of visually evoked postural responses by different eye-in-orbit and head-on-trunk angular positions. *Exp. Brain Res.* 111, 283–288. doi: 10.1007/bf00227305

Wolsley, C., Buckwell, D., Sakellari, V., and Bronstein, A. (1996a). The effect of eye/head deviation and visual conflict on visually evoked postural responses. *Brain Res. Bullet.* 40, 437–441. doi: 10.1016/0361-9230(96)00139-6

Wyatt, H. J., Pola, J., and Lustgarten, M. (1988). "Passive suppression" of optokinesis by stabilized targets. *Vision Res.* 28, 1023–1029. doi: 10.1016/0042-6989(88)90079-x

Wyatt, H. J., Pola, J., Lustgarten, M., and Aksionoff, E. (1995). Optokinetic nystagmus (OKN) suppression by fixation of a stabilized target: the effect of OKN-stimulus predictability. *Vision Res.* 35, 2903–2910. doi: 10.1016/0042-6989(95)00062-5

Yang, D.-S., Fitzgibbon, E., and Miles, F. (1999). Short-latency vergence eye movements induced by radial optic flow in humans: Dependence on ambient vergence level. *J. Neurophysiol.* 81, 945–949. doi: 10.1152/jn.1999.81.2.945

Conflict of Interest: The authors declare that the research was conducted in the absence of any commercial or financial relationships that could be construed as a potential conflict of interest.

Publisher's Note: All claims expressed in this article are solely those of the authors and do not necessarily represent those of their affiliated organizations, or those of the publisher, the editors and the reviewers. Any product that may be evaluated in this article, or claim that may be made by its manufacturer, is not guaranteed or endorsed by the publisher.

frontiers in Human Neuroscience

ORIGINAL RESEARCH
published: 22 March 2022
doi: 10.3389/fnhum.2022.841874

Brain Response to a Knee Proprioception Task Among Persons With Anterior Cruciate Ligament Reconstruction and Controls

Andrew Strong[1], Helena Grip[2], Carl-Johan Boraxbekk[2,3,4,5], Jonas Selling[1] and Charlotte K. Häger[1]*

[1] Department of Community Medicine and Rehabilitation, Physiotherapy, Umeå University, Umeå, Sweden, [2] Department of Radiation Sciences, Umeå University, Umeå, Sweden, [3] Danish Research Centre for Magnetic Resonance (DRCMR), Centre for Functional and Diagnostic Imaging and Research, Copenhagen University Hospital Hvidovre, Copenhagen, Denmark, [4] Umeå Center for Functional Brain Imaging (UFBI), Umeå University, Umeå, Sweden, [5] Institute of Sports Medicine Copenhagen (ISMC), Copenhagen University Hospital Bispebjerg, Copenhagen, Denmark

Knee proprioception deficits and neuroplasticity have been indicated following injury to the anterior cruciate ligament (ACL). Evidence is, however, scarce regarding brain response to knee proprioception tasks and the impact of ACL injury. This study aimed to identify brain regions associated with the proprioceptive sense of joint position at the knee and whether the related brain response of individuals with ACL reconstruction differed from that of asymptomatic controls. Twenty-one persons with unilateral ACL reconstruction (mean 23 months post-surgery) of either the right (n = 10) or left (n = 11) knee, as well as 19 controls (CTRL) matched for sex, age, height, weight and current activity level, performed a knee joint position sense (JPS) test during simultaneous functional magnetic resonance imaging (fMRI). Integrated motion capture provided real-time knee kinematics to activate test instructions, as well as accurate knee angles for JPS outcomes. Recruited brain regions during knee angle reproduction included somatosensory cortices, prefrontal cortex and insula. Neither brain response nor JPS errors differed between groups, but across groups significant correlations revealed that greater errors were associated with greater ipsilateral response in the anterior cingulate (r = 0.476, P = 0.009), supramarginal gyrus (r = 0.395, P = 0.034) and insula (r = 0.474, P = 0.008). This is the first study to capture brain response using fMRI in relation to quantifiable knee JPS. Activated brain regions have previously been associated with sensorimotor processes, body schema and interoception. Our innovative paradigm can help to guide future research investigating brain response to lower limb proprioception.

Keywords: anterior cruciate ligament, anterior cruciate ligament reconstruction, knee, rehabilitation, position sense, magnetic resonance imaging, neuronal plasticity

OPEN ACCESS

Edited by:
Jason Friedman,
Tel Aviv University, Israel

Reviewed by:
Tim Lehmann,
University of Paderborn, Germany
Zengyong Li,
National Research Center for Rehabilitation Technical Aids, China

****Correspondence:***
Andrew Strong
andrew.strong@umu.se

Specialty section:
This article was submitted to Motor Neuroscience, a section of the journal Frontiers in Human Neuroscience

Received: *22 December 2021*
Accepted: *25 February 2022*
Published: *22 March 2022*

Citation:
Strong A, Grip H, Boraxbekk C-J, Selling J and Häger CK (2022) Brain Response to a Knee Proprioception Task Among Persons With Anterior Cruciate Ligament Reconstruction and Controls. Front. Hum. Neurosci. 16:841874. doi: 10.3389/fnhum.2022.841874

INTRODUCTION

Rupture of the anterior cruciate ligament (ACL) is a common knee injury among athletic populations (Majewski et al., 2006), with a reported 30% rate of secondary ACL injury up to 15 years post-reconstruction (Leys et al., 2012) and a four times higher risk for knee osteoarthritis (Poulsen et al., 2019). Evidence further indicates that individuals with ACL reconstruction (ACLR)

have lesser bilateral corticospinal excitability than those without injury, which may have a detrimental effect on muscle recovery (Rush et al., 2021). The initial trauma and potential surgical reconstruction causes loss of neural elements such as Golgi tendon organ-like receptors (Cabuk et al., 2022). These receptors contribute with afferent information to the central nervous system (CNS) regarding proprioceptive sensations such as movement and position (Dhillon et al., 2012). Of the proprioceptive senses, joint position sense (JPS) is one of the most commonly tested, typically involving the passive or active reproduction of joint angles with the confounding sense of vision occluded (Hillier et al., 2015). Outcomes are based on the difference in degrees between the target and reproduced angles, thus reflecting the kinematic errors. Identifying deficient knee JPS is believed important as it may contribute to errors in coordination which can subsequently expose the joint to positions deemed to increase the risk for injury (Needle et al., 2017). Meta-analyses have found significantly greater knee JPS errors for ACL-injured knees compared to both the contralateral non-injured knees of the same individuals (Relph et al., 2014; Kim et al., 2017; Strong et al., 2021a) and to those of asymptomatic persons (Relph et al., 2014; Strong et al., 2021a). The clinical significance of these findings is, however, unclear given the small absolute differences of $< 1°$ knee flexion angle. Existing JPS tests have also been criticized for lacking reliability and validity (Hillier et al., 2015). Therefore, despite the belief that neurosensory information and knee proprioception may be impaired following ACL injury (Nyland et al., 2017), simply comparing knee JPS errors may be insufficient in detecting intricate alterations to the CNS (Baumeister et al., 2008). Thus, although knee JPS tests appear not to reveal clinically significant levels of deficient proprioception following ACL injury, reorganization of the CNS has nonetheless been hypothesized (Kapreli and Athanasopoulos, 2006). It is specifically believed that effects on the somatosensory and motor cortices may lead to proprioception-related deficits in preparatory and reactive motor abilities, consequently contributing to the increased risk for secondary injury (Needle et al., 2017).

Brain response associated with lower limb proprioceptive acuity is unclear. Callaghan et al. (2012) implemented a single-joint knee JPS task during functional magnetic resonance imaging (fMRI) among asymptomatic controls and found greater blood-oxygen-level-dependent (BOLD) response in the supplementary motor area, ventral tegmental area, primary sensory cortex, cerebellum and precentral gyrus compared to a similar movement without angle reproduction. However, no outcomes of the JPS test were recorded, the sample size was small ($n = 8$) and the authors recommended a multi-joint movement to better represent normal functional tasks. In the same study, patellar taping, hypothesized to increase proprioceptive input, decreased response in the anterior cingulate and cerebellum. Based on a similar hypothesis, Thijs et al. (2010) investigated the influence of a knee brace and knee sleeve on brain response during lower limb multi-joint movements among asymptomatic individuals. Compared with no garment, greater response was found in the frontal lobe and paracentral lobule for the knee brace, as well as for the parietal lobe and superior parietal lobule for the knee sleeve. The combined findings of these studies indicate that changes to afferent information at the knee alters brain response during lower limb movements.

Injury to the ACL is believed to cause adaptations to the CNS (Needle et al., 2017). A recent scoping review of the topic by Neto et al. (2019) indeed found evidence for greater brain response compared to controls in mainly cortical areas associated with sensory and motor processes. One electroencephalography (EEG) study by Baumeister et al. (2008) incorporated a test of knee JPS and found greater frontal Theta-power for individuals with ACLR compared to controls. This response was believed to generate from the anterior cingulate cortex due to attentional demands and task complexity. Correlations for both groups additionally showed a reduction of JPS errors over time together with decreased processing in the parietal somatosensory cortex. However, EEG is limited in providing exact locations of the electrical sources from scalp recordings, while fMRI provides a higher spatial resolution (Ritter and Villringer, 2006). The only studies which used fMRI were those by Kapreli et al. (2009) and Grooms et al. (2017) who used similar task designs of single-joint knee flexion and extension. Both studies found less cerebellum activation and greater activation of secondary somatosensory areas for their ACL groups compared to their respective control groups, but also some inconsistent results for other regions. Differences between the ACL populations, such as treatment strategy, i.e., with or without reconstruction, and contrasting activity levels may have contributed to the divergent results. Grooms et al. (2017) suggested that multi-joint movements would improve the clinical applicability of future investigations. A more recent study thus included repetitive multi-joint heel slide movements and found that individuals with ACLR had greater response in areas associated with visual-spatial cognition and orientation compared with asymptomatic matched controls (Criss et al., 2020). It has, however, been recommended to improve the clinical applicability of such findings by increasing the motor control demands of such tasks by including, e.g., a proprioceptive goal-oriented element such as position matching (Grooms et al., 2017; Criss et al., 2020).

To summarize, brain response to proprioceptive tasks of the lower extremities remains unclear. Injury to the ACL may cause deficits to knee proprioception and related adaptations of the CNS. We have previously developed a supine knee JPS test which can be adapted for use in an fMRI setting (Strong et al., 2021b). Importantly, our standardized knee JPS test is unique for an fMRI setting in retaining otherwise common methods, whereby repetitions of knee angle memorization and subsequent reproduction are performed. Additionally, an integrated motion capture system not only provides test instructions to the participant based on their real-time kinematics, but is also used to identify knee movement phases for extraction of fMRI data during only relevant time periods. The kinematics further make possible the accurate reporting of angular errors to assess proprioceptive acuity and its potential association with response in specific brain regions. We therefore aimed to investigate the possibility of characterizing brain response using fMRI during simultaneous performance of a novel quantifiable knee JPS test among asymptomatic controls and individuals with unilateral

ACLR. The specific research questions were: (1) Does our knee JPS test evoke a different brain response compared to a similar knee flexion movement without an angle reproduction task? (2) Is brain response different in persons with ACLR compared to asymptomatic persons during our knee JPS test? (3) Does brain response correlate to knee JPS test errors captured by kinematics? We hypothesized that our knee JPS test would recruit somatosensory and motor cortices more than during simple knee flexion and that individuals with ACLR would show greater response in such regions compared to asymptomatic persons. We further hypothesized that knee JPS errors would correlate with BOLD response in associated brain regions.

MATERIALS AND METHODS

Participant Selection

For this cross-sectional study, participants were recruited from April 2017 to May 2019 using convenience sampling *via* orthopedic clinics, sports clubs, advertisements at the local University, social media and *via* word of mouth. Screening ensured the following eligibility criteria were met: aged 17–35 years, magnetic resonance imaging compliance, current Tegner activity score (Tegner and Lysholm, 1985) of at least 4, ability to understand either Swedish or English language, no known previous or ongoing injuries or diseases (other than ACLR and possible concomitant meniscus injury in the previous 5 years) that could affect the CNS or leg movements. Specific criteria for participants of the ACLR group required unilateral hamstring autograft reconstructive surgery performed 6 months to 5 years prior to testing, limited to only one ACL injury and subsequent surgery. All ACLR participants had to be cleared for full return to activity by their physical therapist. Asymptomatic controls were to be right-side dominant (leg preferred to kick a ball) and matched to ACLR participants with regard to sex, age, height, mass and current Tegner activity score. Our study is the first to incorporate this JPS paradigm during fMRI and thus data was not available to perform power calculations to estimate the required sample sizes. Considering previous similar research, one fMRI study comparing a different knee JPS task to a similar movement without a JPS task included eight healthy males (Callaghan et al., 2012). Previous fMRI studies comparing individuals with ACL injury to controls have included groups of either 15 (Grooms et al., 2017; Criss et al., 2020) or 17/18 (Kapreli et al., 2009), whereas a previous EEG study incorporating a knee JPS test included groups of 10/12 (Baumeister et al., 2008), respectively. Considering that our task design was calculated to result in fewer brain volumes than the aforementioned studies, we estimated that a pooled group of 40 participants would be required to investigate the brain regions recruited by our JPS test and 20 per group to examine potential differences in brain response between the ACLR and asymptomatic groups. The project was approved by the Regional Ethical Review Board in Umeå, Sweden (Dnr. 2015/67-31) and was performed in accordance with the relevant guidelines and regulations stated in the Declaration of Helsinki. All participants provided their written informed consent prior to participation.

Procedures

Data collection occurred between June 2017 and May 2019. All participants completed the Marx Activity Scale (Marx et al., 2001) and the Tegner Activity Scale (Tegner and Lysholm, 1985). The following questionnaires were also completed by the ACLR participants: 2000 International Knee Documentation Committee Subjective Knee Form (IKDC; Irrgang et al., 2001); Lysholm Scale (Lysholm and Gillquist, 1982); and the Swedish version of the Tampa Scale of Kinesiophobia (TSK; Lundberg et al., 2004). Participants then performed a supine knee JPS test in the U-motion laboratory at Umeå University, Sweden to familiarize themselves with the task. Approximately 1 h later they performed the knee JPS test in an MRI scanner at the Umeå center for Functional Brain Imaging, University Hospital of Umeå, Sweden.

Knee Joint Position Sense Test Protocol

A knee JPS test was specifically designed for fMRI compatibility by using a supine position, slow active movements and additional rest blocks. It was considered important that the test reflect those typically applied in the literature whereby target angle memorization is performed immediately prior to each attempt to reproduce the angle (Han et al., 2016). It was further important to assess brain response only during blocks for which proprioceptive signal processing was considered to be most pertinent for perception and movement control. This is in contrast to a previous study in which brain imaging analyses were performed without memorization prior to each reproduction attempt and during movement to a start position for which proprioception was less relevant and represented half of the brain images assessed (Callaghan et al., 2012). Standardized written test instructions were provided to each participant and any questions were answered. A three-camera motion capture system (Oqus MRI Qualisys AB, Gothenburg, Sweden, 120 Hz) provided real-time kinematic data for the lower limbs. Passive retro-reflective spherical markers were affixed with participants in standing on the skin overlying the greater trochanter and lateral epicondyle of each femur using skin-friendly double-sided adhesive tape. The greater trochanter markers were placed on sticks 56 mm in length (wand markers) to improve their visibility. Participants then lay supine with their feet in foot holders of a custom-made low-friction knee flexion/extension board (see **Figure 1**). Elastic bands with hook-and-loop fasteners secured each foot and lower shank to the foot holders to ensure a 90° ankle joint angle. A strap over the torso and cushions in the head coil limited head movement. Wand markers with 46 mm sticks were affixed on the lateral part of each foot holder in line with the lateral malleolus in the sagittal plane. Kinematic data of the knee were based on the three respective markers for each leg in the sagittal plane. To provide an asymmetrical marker set and thus more stable real-time marker tracking, two markers were additionally affixed on the middle distal edge of the right footplate and one on the left footplate of the sliding board. Participants were positioned to allow a maximum knee flexion angle of approximately 100° when reaching an in-built physical stop at the proximal end of the board. For all movements, a constant knee angular velocity of

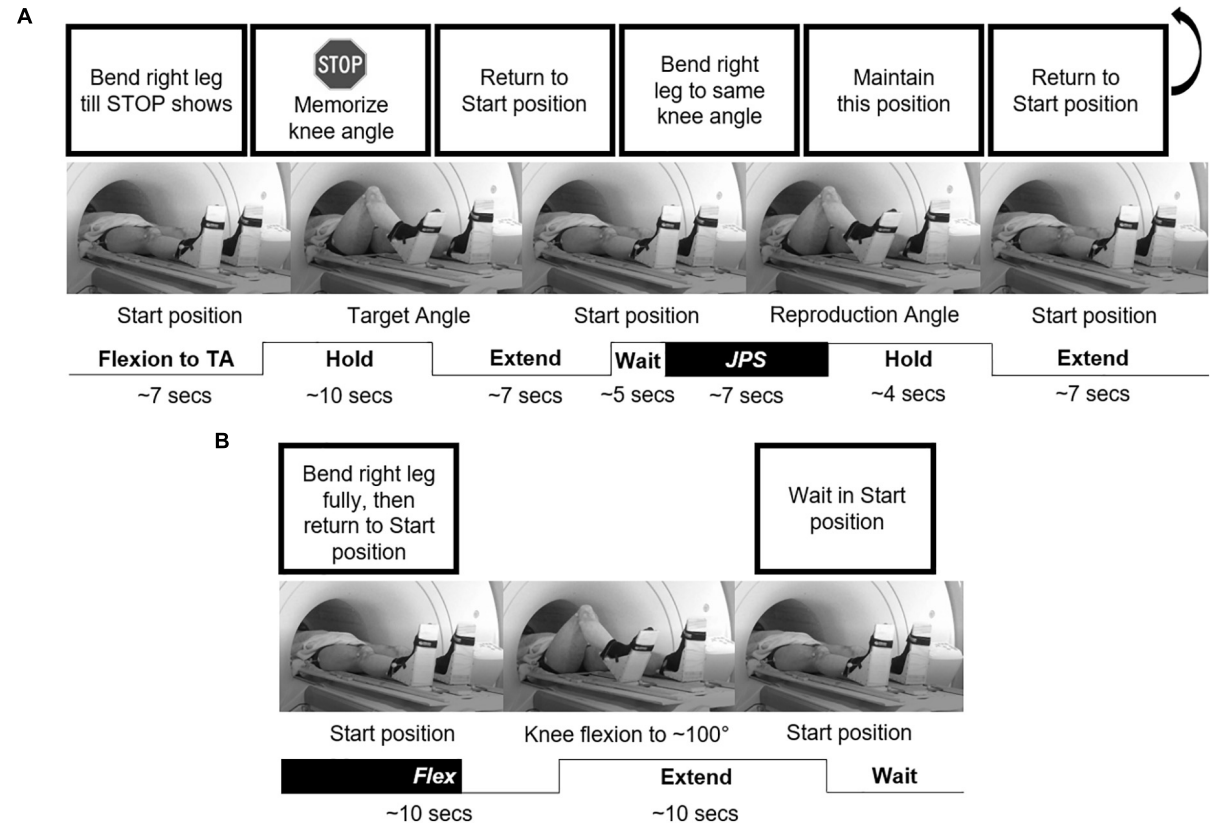

FIGURE 1 | An illustration of the experimental setup. The individual is performing with their right leg **(A)** one repetition of the JPS test with a target angle of 65°, and **(B)** one repetition of the *Flex* condition. Example instructions shown at the top were displayed on a screen at the rear of the scanner visible to the participant *via* a tilted mirror attached to the head coil. BOLD response was measured during the highlighted "*JPS*" (from Start position to reproduction angle) and "*Flex*" (from Start position to 65° knee flexion) blocks, respectively, as well as for a "*Rest*" block (Start position for 15 s). TA, target angle.

10°/s was attempted. This was practiced during familiarization using real-time graphical feedback for three trials per leg. If knee angular velocity fluctuated by more than 5°/s for consecutive trials of the MRI protocol, participants were verbally reminded to move slower or faster accordingly. Automated instructions were provided throughout the tests based on knee angle and angular velocity calculated from the real-time kinematic data as further described henceforth.

While supine in the Start position (legs fully extended), participants were instructed to flex a specified leg (randomized order) until a stop sign appeared (randomly activated at 35° or 60° knee flexion, but participants told angles were random). Two seconds after stopping, participants were instructed to maintain the position and memorize the knee (target) angle. Eight seconds later, they were instructed to return to the Start position and then 5 s after returning were instructed to reproduce the same angle. Four seconds after stopping, participants were instructed to return to the Start position. This was performed eight times per angle on each leg, resulting in a total of 16 repetitions for the JPS test on each leg. Additionally, knee flexion to the physical stop at ∼100° was performed on eight separate occasions per leg, with the timeframe from 0–65° extracted for brain imaging analysis for a *Flex* condition. The *JPS* and *Flex* conditions were pseudorandomized with a maximum two consecutive repetitions of the same condition and a minimum 7 s between trials. A *Rest* condition (Start position for 15 s) was also included five times at evenly-spaced intervals throughout testing. Thus, the task had a block design, individualized based on kinematic data. We utilized three different experimental conditions: (1) *JPS* condition – active knee flexion during angle reproduction (start/end at onset/cessation of flexion, respectively), (2) *Flex* condition – active knee flexion without angle reproduction (start at onset of flexion and end when reaching 65° knee angle), and (3) *Rest* condition – Start position (start/end at cessation of extension and onset of flexion, respectively). The protocol lasted approximately 40 min, resulting in 1240 whole-brain sets.

The current fMRI-adapted knee JPS test was also assessed for test-retest reliability in our movement laboratory among a separate group of 15 (9 males) asymptomatic persons (mean ± SD: age 25.0 ± 3.1 years, height 1.78 ± 0.09 m, mass 74.4 ± 11.2 kg) who performed the test on two occasions 7 days apart. Reliability was estimated with Intraclass Correlation Coefficients (ICC) and 95% confidence intervals (CI) based on a mean rating (k = 10), two-way mixed effects model with absolute agreement and Standard Error of Measurement (SEM), calculated as the mean square error term from the ANOVA,

separately for the non-dominant [ICC 3,10 = 0.64 (CI 0.02–0.87), SEM = 0.67°] and dominant leg [ICC 3,10 = 0.78 (CI 0.34–0.93), SEM = 0.86°].

Image Acquisition

A 3T General Electric MR scanner with a 32-channel head coil was used to acquire the MR images. A T1 structural image was first acquired to create a study-specific template using the following parameters: 180 slices; 1 mm thickness; repetition time 8.2 ms; echo time 3.2 ms; flip angle 12°; field of view 25 × 25 cm. The functional gradient-echo-planar imaging sequence was collected with the following scanning parameters: repetition time = 2000 ms, echo time = 30 ms, flip angle = 80°, field of view = 25 × 25 cm. Thirty-seven transaxial slices with a thickness of 3.4 mm (0.5 mm gap) were acquired in an interleaved order. Ten initial dummy scans were collected and discarded prior to analysis. Test instructions were presented on a computer screen, which were seen *via* a tilted mirror attached to the head coil. The computer parallel port was used to detect the trigger output signal from the MR scanner to synchronize kinematic data with fMRI data in later analyses.

Data Processing and Analysis

Motion capture data were exported to Visual3D software (v.5.02.19, C-Motion Inc., Germantown, MD, United States) and filtered with a 6 Hz fourth-order low-pass zero-lag Butterworth filter. Automated scripts set events based on knee angles and knee angular velocities in the sagittal plane. Target and reproduction angles were extracted 2 s after cessation of flexion during the respective phases. All events were checked visually by the lead researcher and adjusted if deemed incorrect. No data were removed from analyses. Data were exported to IBM SPSS Statistics for Windows, version 25 (IBM Corp., Armonk, N.Y., United States) in which all statistical analyses for knee JPS outcome measures, participant characteristics and patient-reported outcomes were performed.

SPM12 software (Wellcome Department of Cognitive Neurology, London, United Kingdom) run under MATLAB R 2016 b (MathWorks, Inc., Natick, MA, United States) was used for automated batching, pre-processing and data analysis. SPM was used for visualization of statistical maps and MarsBaR 0.44 (Brett et al., 2002) was used to calculate the percentage of BOLD signal change. Data were pre-processed in the following way: slice timing correction (interleaved order, first image set to reference slice), movement correction by unwarping and realigning all subsequent scans to the first image, co-registration of the mean functional image set and the structural T1 image set, segmentation of the co-registered structural image, normalization to a sample-specific template based on white and gray matter segments from the segmented, co-registered, structural image [using DARTEL (Ashburner, 2007)] and affine alignment to Montreal Neurological Institute (MNI) standard space and smoothing with an 8-mm FWHM Gaussian kernel. The final voxel size was 2 × 2 × 2 mm.

Statistical Analyses

The ACLR group was subdivided into those with right-side (R-ACLR) and left-side (L-ACLR) reconstruction. Sex distribution between groups was analyzed with a Chi-square test. Age and current activity level (Tegner current and Marx activity) between all groups, as well as pre-injury activity level of the ACLR groups to current activity level of CTRL, were analyzed with Kruskal-Wallis tests and Dunn-Bonferroni *post hoc* tests for significant results. The questionnaires TSK, IKDC and Lysholm Scale were compared between ACLR groups with Mann-Whitney *U* tests. A One-way analysis of variance (ANOVA) compared body height and mass between all groups, as well as months since reconstruction between ACLR groups.

Between-group comparisons for kinematic data and brain response were made between the injured leg of ACLR and the matched leg of CTRL. Thus, the R-ACLR group was compared to controls only when the right leg was active for each group and the L-ACLR group were compared to controls only when the left leg was active for each group. Knee JPS error was defined in degrees as the absolute difference [absolute error (AE)] between the target and reproduction angles of the knee for each repetition

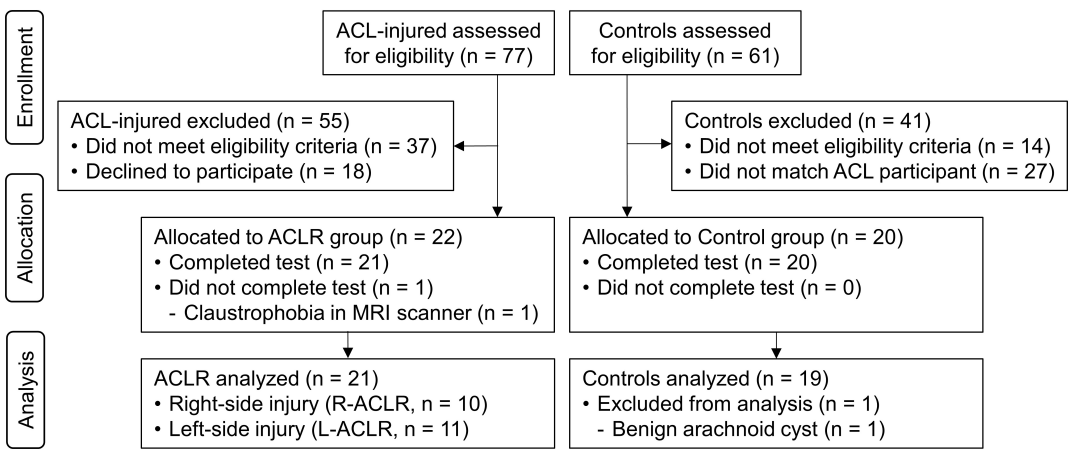

FIGURE 2 | Flow diagram illustrating the recruitment process.

of the JPS test. Mean AE was calculated for each leg by pooling the 40° and 65° angle conditions for each participant. Outliers in the data set were assessed for eligibility at group level, but none were removed due to a lack of evidence to the contrary. Shapiro-Wilk tests of normality and analysis of distribution graphs confirmed non-normally distributed group-level data. Knee JPS data were thus log transformed and were subsequently considered normally distributed according to further Shapiro-Wilk tests. Independent samples t-tests were used to compare the log transformed knee JPS AE between groups. Significance levels were set *a priori* ($\alpha = 0.05$).

Brain imaging data for each angle condition were pooled so that each participant contributed with data from 16 *JPS* trials per leg. The first-order (single-subject) analyses were set up by including the experimental conditions as regressors of interest in the general linear model, convolved with the hemodynamic response function. Six realignment parameters (head rotations and translations) were included as covariates of no interest to account for movement artifacts. The following contrasts were set up for each participant: (1) (*JPS* > *Rest*) and (2) (*Flex* > *Rest*). Second-order (group) analyses were based on flexible factorial models (Gläscher and Gitelman, 2008) of the (*JPS* > *Rest*) and (*Flex* > *Rest*) contrasts from each participant, including participant, group (two levels, R-ACLR or L-ACLR and CTRL), condition (two levels, *JPS* and *Flex*) and the interaction (group × condition) as factors. Separate analyses of the conditions used in the flexible factorial design (*JPS* > *Rest*) and (*Flex* > *Rest*) were also performed to investigate activation patterns in comparison to *Rest*. These analyses are included as supplementary material. The main effect from condition [(*JPS* > *Rest*) > (*Flex* > *Rest*)] and the interaction (group × condition) was analyzed [family-wise error (FWE) rate corrected, 0.05; voxel limit 15]. Brain regions were defined and labeled according to the MNI coordinates, which relate to the peak activity within the cluster, using automated anatomic labeling in SPM (Tzourio-Mazoyer et al., 2002). Brain regions that showed significant activation for any of these analyses were further analyzed by calculating the percentage of BOLD signal change during the *JPS* condition (i.e., the original beta values) in the significant region, compared to the overall mean brain activity of the session. The percentage of BOLD change values were exported to SPSS where Spearman's rho was used to analyze correlations of participant mean values between percentage of BOLD change and JPS errors.

TABLE 1 | Participant characteristics of the study groups.

	R-ACLR	L-ACLR	CTRL
Participants, n	10	11	19
Age, y, mean (SD)	24.8 (4.2)	28.2 (4.7)	27.1 (4.6)
Male:female, n	4:6	4:7	7:12
Months since reconstruction, mean (SD)	20.0 (9.7)	28.5 (18.6)	–
Body height, m, mean (SD)	1.72 (0.09)	1.73 (0.09)	1.75 (0.08)
Body mass, kg, mean (SD)	72.6 (7.8)	72.1 (11.0)	73.1 (9.9)
Patient-reported outcome scales, median (IQR)			
IKDC 2000,% of maximum	77.6 (14.1)	77.0 (15.0)	–
Lysholm score	86.0 (12.5)	86.0 (5.0)	–
Marx activity score	12.0 (6.5)	10.0 (7.0)	11.0 (7.0)
Tegner pre-injury score	8.5 (1.2)†,‡	8.0 (2.0)	–
Tegner current score	5.5 (2.2)	7.0 (4.0)	6.0 (4.0)
TSK score	36.5 (11.5)	33.0 (5.0)	–
Injury mechanism, non-contact:contact, n	8:2	11:0	–
Leg dominance, right:left, n	10:0	8:3	19:0
Injury activity, n			
Soccer	4	2	
Downhill skiing	2	4	
Martial arts	0	2	
Basketball	0	1	
Dancing	1	0	
Floorball	1	0	
Gymnastics	0	1	
Rugby	1	0	
Snowboard	1	0	
Volleyball	0	1	

†*Significantly greater than R-ACLR Tegner current score (P = 0.011).*
‡*Significantly greater than CTRL Tegner current score (P = 0.010).*
CTRL, asymptomatic control group; IKDC 2000, International Knee Documentation Committee Subjective Knee Form; IQR, interquartile range; L-ACLR, left-side anterior cruciate ligament-reconstructed group; R-ACLR, right-side anterior cruciate ligament-reconstructed group; TSK, Tampa Scale of Kinesiophobia.

RESULTS

Of 77 persons with ACL injury and 61 potential controls who expressed an interest in participating, 55 and 14, respectively, were considered ineligible due to either another existing injury, too low physical activity level, left leg dominance for controls, older age, or a combination of those factors. Thus, 22 individuals with ACLR and 47 asymptomatic controls were considered eligible for the study. To ensure matching of characteristics between groups, controls were invited to participate only after a matching ACLR participant had completed testing. One ACLR participant did not complete the fMRI procedure due to claustrophobic feelings in the MRI scanner. Despite completing testing, one asymptomatic control was not included in the analyses due to the presence of a benign arachnoid cyst, unknown prior to participation, which would have confounded brain imaging analyses. Thus, 10 R-ACLR, 11 L-ACLR and 19 CTRL completed testing and were included in the analyses (see **Figure 2** for a flow diagram of the recruitment process and **Table 1** for group characteristics). Due to a technical issue, one L-ACLR participant completed a shortened protocol of 12, instead of 16, repetitions per leg. Also, due to slow performance of the test, one participant from each group performed one less repetition on both legs. Current activity level of CTRL was significantly lower than pre-injury level of R-ACLR ($P = 0.010$). No groups differed significantly with regard to sex, age, height, weight or the remaining patient-report outcome measures. Months since reconstruction did not differ significantly between the ACLR groups. For the

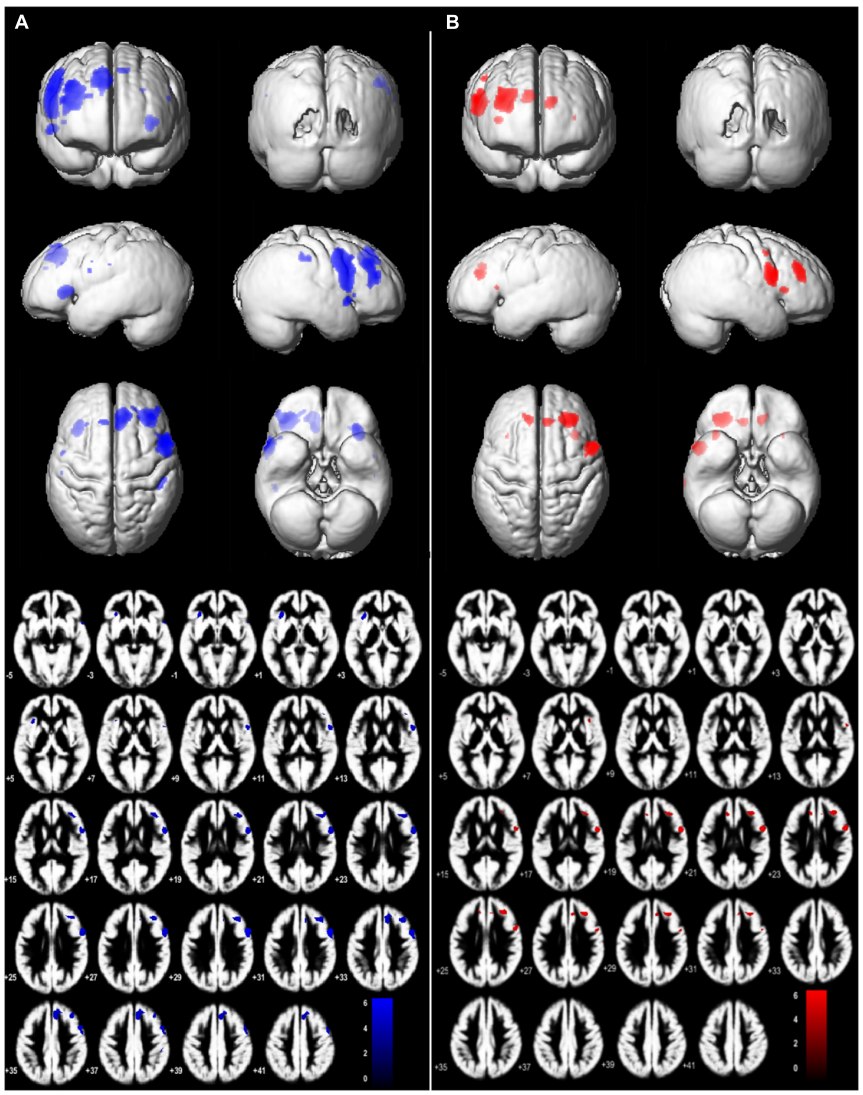

FIGURE 3 | Brain regions with significant main effect condition in (*JPS* > *Rest*) > (*Flex* > *Rest*), *P* = 0.05, family-wise corrected, voxel limit 15. Slices –5:2:38 mm (MNI) in inferior-superior direction are shown. Group mean brains (Dartel) are used for the illustration for **(A)** left-side analyses – L-ACLR moving their injured left leg and CTRL moving their left non-dominant leg, and **(B)** right-side analyses – R-ACLR moving their right injured leg and CTRL moving their right non-dominant leg.

knee JPS test, no statistically significant differences in errors were seen between either the left reconstructed/non-dominant leg of L-ACLR [median (Mdn) 5.10° (Q1 4.04°, Q3 6.82°)] and CTRL [Mdn 4.17° (Q1 2.89°, Q3 4.95°)], respectively, or between the right reconstructed/dominant leg of R-ACLR [Mdn 4.89° (Q1 3.54°, Q3 6.85°)] and CTRL [4.55° (Q1 3.64°, Q3 6.56°)], respectively.

Brain Response During the Knee Joint Position Sense Test

The JPS condition evoked significantly greater BOLD response (*P* = 0.05, FWE corrected; voxel limit 15) in seven brain regions for each leg compared to the Flex condition without a JPS task. These included prefrontal regions, the precentral gyrus, cingulate gyri and insula (see **Figures 3**, **4** and **Table 2** for all significant regions with voxel extent, exact statistics, and MNI coordinates).

Between-Group Comparisons of Brain Response During the Knee Joint Position Sense Test

No significant between-group differences were found on the corrected level (FWE 0.05).

Correlations Between Brain Response and Knee Joint Position Sense Errors

Correlation analyses were performed for the seven regions per test side that were found to have significantly greater BOLD response during the JPS condition compared to the Flex

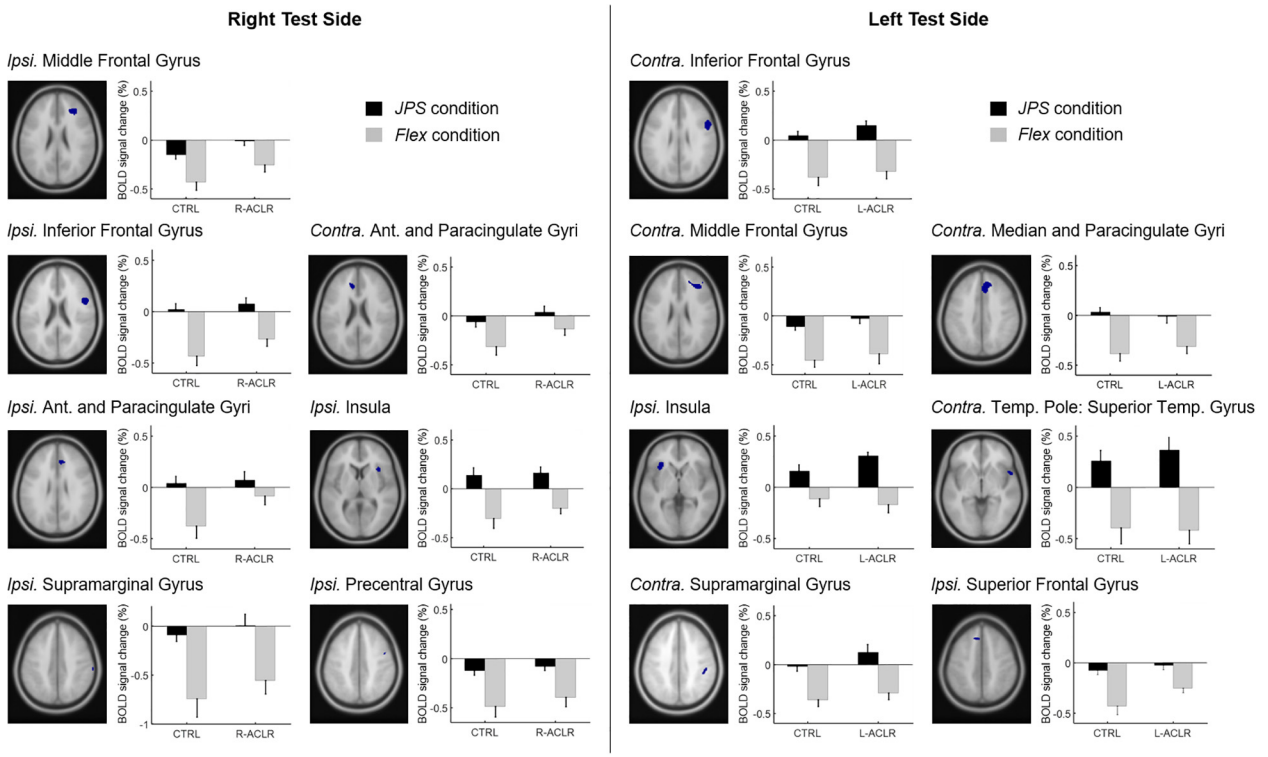

FIGURE 4 | BOLD signal change (%) during angle reproduction of the JPS test for the brain regions with a significant main effect from condition [(*JPS* > *Rest*) > (*Flex* > *Rest*)]. Ant., Anterior; *Contra.*, contralateral; CTRL, asymptomatic control group; *Flex*, flex condition; *Ipsi.*, ipsilateral; JPS, joint position sense condition; L-ACLR, left side anterior cruciate ligament-reconstructed group; R-ACL, right-side anterior cruciate ligament-reconstructed group; Temp., Temporal.

condition (see **Table 2** for a list of the regions). When performing the test with the right leg (R-ACL and CTRL, $n = 29$), significant positive correlations were found between JPS errors and BOLD signal percentage change (i.e., greater JPS AE correlated with greater BOLD response) in the ipsilateral anterior cingulate ($r = 0.476$, $P = 0.009$; **Figure 5A**) as well as the ipsilateral supramarginal gyrus ($r = 0.395$, $P = 0.034$; **Figure 5B**). Close to significance was also the ipsilateral middle frontal gyrus ($r = 0.364$, $P = 0.052$). For the left leg (L-ACLR and CTRL, $n = 30$), a significant positive correlation was found for the ipsilateral insula ($r = 0.474$, $P = 0.008$; **Figure 5C**).

DISCUSSION

We aimed to characterize brain response during a knee JPS test among asymptomatic controls and individuals with ACL reconstruction. We further investigated whether brain response would differ between groups and whether brain response would correlate with knee JPS errors. Our hypothesis that our knee JPS test would evoke greater response in somatosensory and motor cortices compared to simple knee flexion was confirmed by observations of greater response during angle reproduction in, for example, the precentral gyrus, middle frontal gyrus, insula and cingulate gyri. The lack of significant differences between individuals with ACL reconstruction compared to asymptomatic controls was, however, contradictory to our hypothesis. Greater knee JPS errors correlated with BOLD response in the insula, anterior cingulate and supramarginal gyrus, thus confirming our hypothesis of correlations between brain response and knee JPS errors.

Brain Response During a Knee Proprioception Test

Our knee JPS test evoked response in the *ipsilateral* precentral gyrus for the right test side and cingulate gyri for both test sides. Response in these regions has also been observed among asymptomatic individuals during active knee flexion tasks of JPS (Callaghan et al., 2012) and force matching (Grooms et al., 2021). Response in the right middle frontal gyrus was seen for both test sides and has been previously associated with switching between external and internal focus of attention (Japee et al., 2015), relevant for our JPS task where the focus of attention changes from external instructions on a screen to internal sensations related to proprioception. Also common for both test sides was recruitment of the *ipsilateral* insula, previously associated with sensorimotor processes such as active and passive stepping motions (Jaeger et al., 2014). This finding also aligns with the body image and body schema concepts of body representations (Head and Holmes, 1911), in which current understandings attribute the insula with conscious perceptual representation of the body and memory (Dijkerman and De Haan, 2007). The

insula and anterior cingulate are further thought to play a key role in interoception, a term originally introduced by Sherrington (1906) to describe visceral sensations, but now often used as a broader term encompassing the subjective experience of the body state (Ceunen et al., 2016) and even proprioception (Hillier et al., 2015). In fact damage to the insula due to stroke has been associated with poor position sense of the upper limbs (Findlater et al., 2016). The same study also found similar associations for the inferior frontal and superior temporal gyri, two areas that were activated during our JPS test in the current study. Thus, our findings add to previous evidence of distributed neural networks involved when processing proprioceptive tasks and expand these to those associated with the lower limbs. Interestingly, 11 of the 14 regions with significantly greater BOLD response during the *JPS* condition compared with the *Flex* condition were of the right hemisphere (**Table 2**). A general dominance of the right hemisphere for proprioception in the lower limbs is supported by previous findings for a foot position matching task among healthy individuals who were right hand and foot dominant, suggesting a role for position sense of the right parietal and frontal cortex (Iandolo et al., 2018). In fact, research into body representations further seems to implicate the right hemisphere with kinesthetic sensations (Naito et al., 2016). If future research confirms these results, the traditional network of brain regions believed to be associated with proprioception of the lower limbs should thus be extended and include an emphasis on the right hemisphere. To improve our understanding further, extended mapping of associated neural networks is required.

TABLE 2 | Brain regions with significantly greater bold response during *JPS* than *Flex* [(*JPS* > *Rest*)] > (*Flex* > *Rest*)][†].

Test side	Brain regions	Voxel #	*P*	Z max	MNI coordinates		
					X	*Y*	*Z*
Left	*Contra.* Inferior frontal gyrus	1608	0.000	6.15	51	9	30
	Contra. Middle frontal gyrus	1049	0.000	5.33	36	30	33
	Contra. Median and Paracingulate gyri	864	0.000	5.29	8	29	36
	Ipsi. Insula[‡]	330	0.001	5.63	−32	24	2
	Contra. Temp. Pole: Superior temp. Gyrus	97	0.008	5.17	54	11	−5
	Contra. Supramarginal gyrus	84	0.010	4.60	48	−29	38
	Ipsi. Superior frontal gyrus	43	0.018	4.57	−9	29	47
Right	*Ipsi.* Middle frontal gyrus	666	0.000	5.51	29	33	26
	Ipsi. Inferior frontal gyrus	596	0.000	5.76	51	5	20
	Contra. Ant. and Paracingulate gyri	152	0.005	4.98	−9	33	21
	Ipsi. Ant. and Paracingulate gyri[‡]	135	0.006	4.67	8	33	26
	Ipsi. Insula	61	0.015	4.70	35	20	6
	Contra. Supramarginal gyrus[‡]	15	0.031	4.70	65	−26	42
	Ipsi. Precentral gyrus	15	0.031	4.42	47	0	42

[†]*Seven brain regions for each test side showed significantly greater BOLD response during the JPS condition compared with the Flex condition across groups.*

[‡]*Significant correlation between knee JPS AE and BOLD percentage change. For left test side n = 30 (L-ACLR 11 and CTRL 19), right test side n = 29 (R-ACLR 10 and CTRL 19).*

Test side: the leg that was active during the JPS test; Voxel #: indicates number of activated voxels in this cluster; P: 0.05 family wise error rate corrected (cluster level); Z max: Z-score of the voxel with the highest activity for main effect from condition; MNI: voxel with the highest activity in MNI-space. Ant., anterior; Contra., contralateral; CTRL, asymptomatic control group; Flex, flex condition; Ipsi., ipsilateral; JPS, joint position sense condition; L-ACLR, left-side anterior cruciate ligament-reconstructed group; MNI, Montreal Neurological Institute; Rest, rest condition; R-ACLR, right-side anterior cruciate ligament-reconstructed group; Temp., temporal.

Brain Response of Individuals With Anterior Cruciate Ligament Reconstruction Compared to Matched Controls

There were no significant between-group differences for brain response nor for knee JPS errors. Previous research investigating knee JPS and somatosensory evoked potentials of individuals 18 months after surgical reconstruction of the ACL also found a lack of difference compared with controls as evidence of sensory neurone regeneration (Ochi et al., 1999). The original version of the current supine knee JPS test also did not detect any significant differences in errors for a separate ACLR group approximately 2 years after surgical reconstruction compared with matched athletes (Strong et al., 2021b). In that study, less-active controls instead showed significantly greater JPS errors compared to the ACLR group, suggesting that activity level is a more important factor in this context. It is therefore possible that deficits in proprioception were not present among the individuals of our ACLR group, who were active and participated on average 23 months after surgical reconstruction. Additionally, a recent meta-analysis found that only knee JPS tests with passive rather than active movements differentiate between ACL-injured knees and those of asymptomatic controls (Strong et al., 2021a). The active movements of the current test, which also incorporated the hip, may further have contributed to the lack of between-group difference seen here. The target angles of 40° and 65° knee flexion used in our JPS test both lie close to the mid-range of motion for the joint. These angles may not have been optimal for elucidating differences between groups where joint receptors are the focus of investigation, given that they are believed to play a more predominant role toward the limits of joint rotation (Proske and Chen, 2021). It is also possible that small group sizes (due to separating ACLR into right and left leg analyses), as well as the contrast to such a similar movement, may have reduced the sensitivity of our analysis.

Correlations Between Brain Response and Knee Joint Position Sense Errors

Our results showed that greater knee JPS errors, i.e., poorer knee proprioceptive acuity, was associated with greater brain response in the ipsilateral insula for the left test side, as well as the

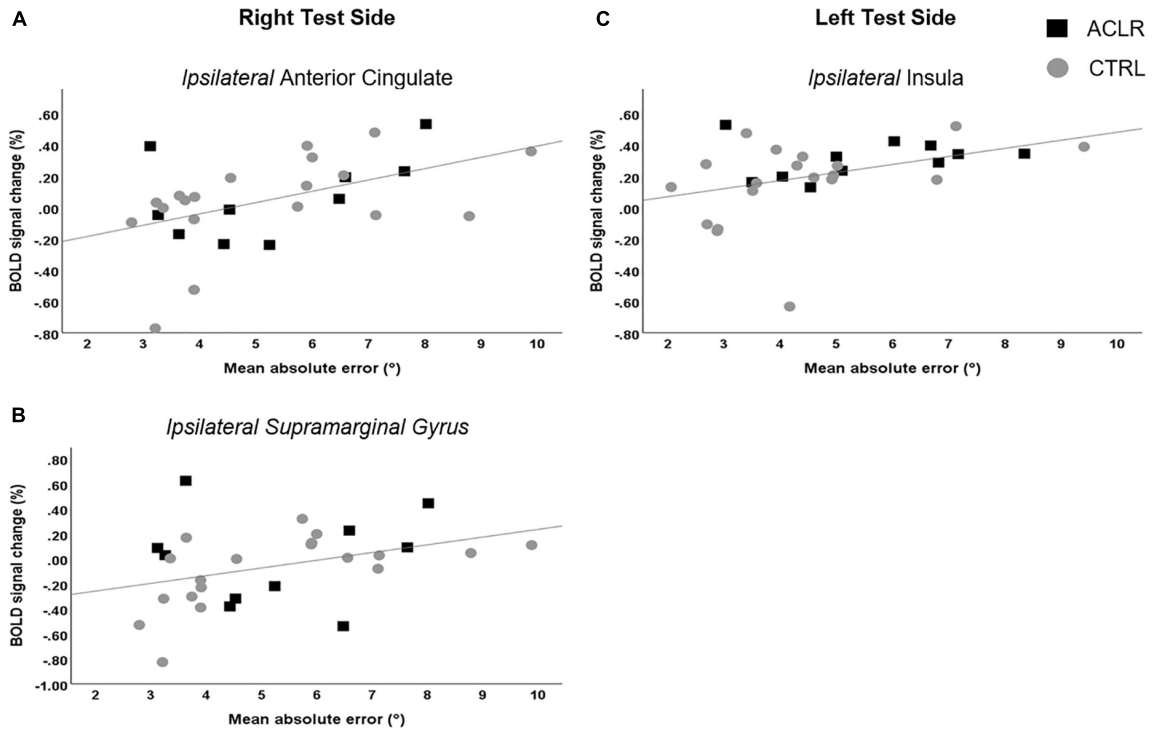

FIGURE 5 | Scatter plots illustrating the significant correlations between mean knee joint position sense absolute errors and simultaneous percentage change in BOLD response for the right test side **(A,B)** and the left test side **(C)**.

ipsilateral anterior, paracingulate and supramarginal gyri for the right test side. These results are line with the Embodied Predictive Interoception Coding (EPIC) model proposed by Barrett and Simons (Barrett and Simmons, 2015), which describes the process of active inference in interoception. Part of this model describes the role of the mid- and posterior insula in computing and transmitting prediction errors as well as the integration of other agranular visceromotor cortices such as the cingulate cortex in this process. This model may thus be relevant for proprioceptive tasks. The importance of the insula to position sense is further supported by findings previously mentioned here for the upper limbs following stroke, whereby lesions in this region were associated with greater errors when attempting to actively move the unaffected arm to the mirror-matched position of the passively moved contralateral arm (Findlater et al., 2016). Associated response for the right supramarginal gyrus is supported by previous findings of greater response during a proprioceptive task of force matching at the knee among asymptomatic females (Grooms et al., 2021).

Limitations of the Study

A limitation of our study was the additional task of attempting a constant knee angular velocity, although this was similar for the contrast *Flex* condition. Further, the active movement of the whole lower limb meant that proprioceptive feedback was not isolated to the knee, but also incorporated the hip. Although this is more similar to everyday activities and thus may enhance the ecological validity of the task compared with a single-joint movement, compensations at the hip joint for potential deficits at the knee are possible. Despite the active task, head movement (range 0.14 – 0.88 mm) did not confound brain imaging analyses. Due to challenges in recruiting participants, we included ACLR individuals who had injured either knee, but a control group with only right-side dominance. Comparisons were thus made to the non-dominant and dominant legs of CTRL for the L-ACLR and R-ACLR groups, respectively. Evidence regarding whether leg dominance influences knee proprioception among healthy controls has, however, shown both positive (Azevedo et al., 2020) and negative (Cug et al., 2016; Galamb et al., 2018) findings. Defining leg dominance for an unfamiliar task is also complicated given evidence of task specificity (Van Melick et al., 2017). It is thus unclear whether leg dominance influenced our results. Further, having to split the ACL participants into two groups meant that the sample sizes for between-groups comparisons were not in line with our aims. We acknowledge this as an important limitation of the current study. Future studies with a greater number of and more homogenous participants are likely required to further elucidate potential group differences. Additionally, both sexes were represented in each of our groups. Two similar fMRI studies have, however, indicated potentially different functional brain connectivity between males (Diekfuss et al., 2020) and females (Diekfuss et al., 2019) who later suffered an ACL injury. Our eligibility criteria required a minimum physical activity level score of four according to the Tegner activity scale. Although we matched current activity level between groups, a sub-analysis using Wilcoxon Signed Ranks

tests compared pre-injury and current activity levels within the ACLR groups and found that R-ACLR had significantly reduced their activity level ($P = 0.011$), but the level was not significantly changed among L-ACLR. A difference in activity level change from pre- to post-injury was thus a potentially confounding factor in our analyses. To explore this further, a Mann-Whitney U test to compare change in activity level between the groups found no significant between-group difference. A significant reduction in activity level following ACL injury is, however, considered a useful outcome for defining non-copers (Button et al., 2006). Future studies may thus benefit from analyses that consider coping classification of individuals with ACL injury. To improve the sensitivity of the analyses, future test designs should also consider how to increase the number of brain images during movements which require proprioceptive processing. This could, for example, be done by increasing the duration of the proprioceptive element of such tasks.

CONCLUSION

Our paradigm found greater BOLD response for a number of brain regions which have previously been associated with processes that can be linked to proprioception. These results thus indicate that the experimental design was successful in recruiting brain regions involved in proprioception and adds valuable information regarding central processing of such tasks. The lack of differences between groups adds to the mixed evidence of proprioceptive deficits among individuals nearly 2 years post-ACLR. The small sample sizes as a result of splitting the ACLR group into left and right-side injuries may, however, have been a contributing factor to the lack of significance. The significant correlations between knee JPS error and activation in some brain regions further indicates that demands were placed on the proprioceptive acuity of the participants. The novel integration of kinematics with fMRI thus provided added value to the paradigm by providing behavioral data as well as specific time frames for extraction of brain images to isolate such processes. Our unique paradigm demonstrates a method to expand these findings and provide further insights into brain response to proprioception at the knee and other joints as well as among different populations.

DATA AVAILABILITY STATEMENT

The raw data supporting the conclusions of this article will be made available by the authors, without undue reservation.

ETHICS STATEMENT

The studies involving human participants were reviewed and approved by Regionala etikprövningsnämnden i Umeå. The patients/participants provided their written informed consent to participate in this study.

AUTHOR CONTRIBUTIONS

JS created the integrated software used for data collection. AS and CH recruited participants. AS and JS performed data collection. AS and HG processed and analyzed the kinematic and brain imaging data. AS, HG, and C-JB performed statistical analyses. AS wrote the first draft of the manuscript. HG and JS wrote sections of the manuscript. All authors contributed to the conception and design of the study and contributed to manuscript revision, read, and approved the submitted version.

FUNDING

This study was funded by the Swedish Research Council (Grant No. 2017-00892), Region Västerbotten (Grant No. ALF VLL548501, VLL838421 and Strategic funding VLL-358901; Project No. 7002795), the Swedish Research Council for Sports Science (Grant No. Dnr CIF P2018-0104; P2019-0068), and Umeå University School of Sport Science (Grant No. Dnr IH 5.3-13-2017). King Gustaf V and Queen Victoria's Foundation of Freemasons. C-JB was supported by The Novo Nordisk Foundation grant to Team Danmark. The funders did not have any role in the study design or outcomes.

ACKNOWLEDGMENTS

We acknowledge the Umeå Center for Functional Brain Imaging (UFBI) for collaboration and assistance, Ashokan Arumugam and Ph.D. student Adam Grinberg for assistance during data collection, and all of the study participants.

SUPPLEMENTARY MATERIAL

The Supplementary Material for this article can be found online at: https://www.frontiersin.org/articles/10.3389/fnhum.2022.841874/full#supplementary-material

REFERENCES

Ashburner, J. (2007). A fast diffeomorphic image registration algorithm. *Neuroimage* 38, 95–113. doi: 10.1016/j.neuroimage.2007.07.007

Azevedo, J., Rodrigues, S., and Seixas, A. (2020). The influence of sports practice, dominance and gender on the knee joint position sense. *Knee* 28, 117–123. doi: 10.1016/j.knee.2020.11.013

Barrett, L. F., and Simmons, W. K. (2015). Interoceptive predictions in the brain. *Nat. Rev. Neurosci.* 16, 419–429. doi: 10.1038/nrn3950

Baumeister, J., Reinecke, K., and Weiss, M. (2008). Changed cortical activity after anterior cruciate ligament reconstruction in a joint position paradigm: an EEG study. *Scand. J. Med. Sci. Sports* 18, 473–484. doi: 10.1111/j.1600-0838.2007.00702.x

Brett, M., Anton, J.-L., Valabregue, R., and Poline, J.-B. (2002). Modeling & analysis. *NeuroImage* 16, 769–1198.

Button, K., Van Deursen, R., and Price, P. (2006). Classification of functional recovery of anterior cruciate ligament copers, non-copers, and adapters. *Br. J. Sports Med.* 40, 853–859. doi: 10.1136/bjsm.2006.028258

Cabuk, H., Kusku Cabuk, F., and Turan, K. (2022).). The time from injury to surgery is an important factor affecting the mechanoreceptors at stump of torn anterior cruciate ligament. *Arch. Orthop. Trauma. Surg.* [Epub online ahead of print]. doi: 10.1007/s00402-021-04310-3

Callaghan, M. J., Mckie, S., Richardson, P., and Oldham, J. A. (2012). Effects of patellar taping on brain activity during knee joint proprioception tests using functional magnetic resonance imaging. *Phys. Ther.* 92, 821–830. doi: 10.2522/ptj.20110209

Ceunen, E., Vlaeyen, J. W. S., and Van Diest, I. (2016). On the Origin of Interoception. *Front. Psychol.* 7:743–743. doi: 10.3389/fpsyg.2016.00743

Criss, C. R., Onate, J. A., and Grooms, D. R. (2020). Neural activity for hip-knee control in those with anterior cruciate ligament reconstruction: a task-based functional connectivity analysis. *Neurosci. Lett.* 730:134985. doi: 10.1016/j.neulet.2020.134985

Cug, M., Wikstrom, E. A., Golshaei, B., and Kirazci, S. (2016). The Effects of Sex, Limb Dominance, and Soccer Participation on Knee Proprioception and Dynamic Postural Control. *J. Sport Rehab.* 25, 31–39. doi: 10.1123/jsr.2014-0250

Dhillon, M. S., Bali, K., and Prabhakar, S. (2012). Differences among mechanoreceptors in healthy and injured anterior cruciate ligaments and their clinical importance. *Muscles Ligaments Tendons J.* 2, 38–43.

Diekfuss, J. A., Grooms, D. R., Nissen, K. S., Schneider, D. K., Foss, K. D. B., Thomas, S., et al. (2020). Alterations in knee sensorimotor brain functional connectivity contributes to ACL injury in male high-school football players: a prospective neuroimaging analysis. *Braz. J. Phys. Ther.* 24, 415–423. doi: 10.1016/j.bjpt.2019.07.004

Diekfuss, J. A., Grooms, D. R., Yuan, W., Dudley, J., Barber Foss, K. D., Thomas, S., et al. (2019). Does brain functional connectivity contribute to musculoskeletal injury? *A preliminary prospective analysis of a neural biomarker of ACL injury risk*. *J. Sci. Med. Sport* 22, 169–174. doi: 10.1016/j.jsams.2018.07.004

Dijkerman, H. C., and De Haan, E. H. (2007). Somatosensory processes subserving perception and action. *Behav. Brain Sci.* 30, 189–201. doi: 10.1017/S0140525X07001392

Findlater, S. E., Desai, J. A., Semrau, J. A., Kenzie, J. M., Rorden, C., Herter, T. M., et al. (2016). Central perception of position sense involves a distributed neural network - Evidence from lesion-behavior analyses. *Cortex* 79, 42–56. doi: 10.1016/j.cortex.2016.03.008

Galamb, K., Szilagyi, B., Magyar, O. M., Hortobagyi, T., Nagatomi, R., Vaczi, M., et al. (2018). Effects of side-dominance on knee joint proprioceptive target-matching asymmetries. *Physiol. Int.* 105, 257–265. doi: 10.1556/2060.105.2018.3.22

Gläscher, J. P., and Gitelman, D. (2008). *Contrast Weights in Flexible Factorial Design With Multiple Groups of Subjects.* Unpublished tutorial. Available: http://www.jiscmail.ac.uk/cgi-bin/webadmin?A2=ind0803&L=SPM&P=R16629 (accessed July, 2020).

Grooms, D. R., Criss, C. R., Simon, J. E., Haggerty, A. L., and Wohl, T. R. (2021). Neural Correlates of Knee Extension and Flexion Force Control: a Kinetically-Instrumented Neuroimaging Study. *Front. Hum. Neurosci.* 14:622637. doi: 10.3389/fnhum.2020.622637

Grooms, D. R., Page, S. J., Nichols-Larsen, D. S., Chaudhari, A. M., White, S. E., and Onate, J. A. (2017). Neuroplasticity associated with anterior cruciate ligament reconstruction. *J. Orthop. Sports Phys. Ther.* 47, 180–189. doi: 10.2519/jospt.2017.7003

Han, J., Waddington, G., Adams, R., Anson, J., and Liu, Y. (2016). Assessing proprioception: a critical review of methods. *J. Sport Health Sci.* 5, 80–90.

Head, H., and Holmes, G. (1911). Sensory Disturbances from Cerebral Lesions. *Brain* 34, 102–254. doi: 10.1016/S0304-3959(99)00123-2

Hillier, S., Immink, M., and Thewlis, D. (2015). Assessing Proprioception: a Systematic Review of Possibilities. *Neurorehabil. Neural Repair* 29, 933–949. doi: 10.1177/1545968315573055

Iandolo, R., Bellini, A., Saiote, C., Marre, I., Bommarito, G., Oesingmann, N., et al. (2018). Neural correlates of lower limbs proprioception: an fMRI study of foot position matching. *Hum. Brain Mapp.* 39, 1929–1944. doi: 10.1002/hbm.23972

Irrgang, J. J., Anderson, A. F., Boland, A. L., Harner, C. D., Kurosaka, M., Neyret, P., et al. (2001). Development and validation of the international knee documentation committee subjective knee form. *Am. J. Sports Med.* 29, 600–613.

Jaeger, L., Marchal-Crespo, L., Wolf, P., Riener, R., Michels, L., and Kollias, S. (2014). Brain activation associated with active and passive lower limb stepping. *Front. Hum. Neurosci.* 8:828. doi: 10.3389/fnhum.2014.00828

Japee, S., Holiday, K., Satyshur, M. D., Mukai, I., and Ungerleider, L. G. (2015). A role of right middle frontal gyrus in reorienting of attention: a case study. *Front. Syst. Neurosci.* 9:23. doi: 10.3389/fnsys.2015.00023

Kapreli, E., and Athanasopoulos, S. (2006). The anterior cruciate ligament deficiency as a model of brain plasticity. *Med. Hypothes.* 67, 645–650. doi: 10.1016/j.mehy.2006.01.063

Kapreli, E., Athanasopoulos, S., Gliatis, J., Papathanasiou, M., Peeters, R., Strimpakos, N., et al. (2009). Anterior cruciate ligament deficiency causes brain plasticity: a functional MRI study. *Am. J. Sports Med.* 37, 2419–2426. doi: 10.1177/0363546509343201

Kim, H. J., Lee, J. H., and Lee, D. H. (2017). Proprioception in Patients With Anterior Cruciate Ligament Tears: a Meta-analysis Comparing Injured and Uninjured Limbs. *Am. J. Sports Med.* 45, 2916–2922. doi: 10.1177/0363546516682231

Leys, T., Salmon, L., Waller, A., Linklater, J., and Pinczewski, L. (2012). Clinical results and risk factors for reinjury 15 years after anterior cruciate ligament reconstruction: a prospective study of hamstring and patellar tendon grafts. *Am. J. Sports Med.* 40, 595–605. doi: 10.1177/0363546511430375

Lundberg, M. K. E., Styf, J., and Carlsson, S. G. (2004). A psychometric evaluation of the Tampa Scale for Kinesiophobia — from a physiotherapeutic perspective. *Physiother. Theor. Prac.* 20, 121–133. doi: 10.1080/09593980490453002

Lysholm, J., and Gillquist, J. (1982). Evaluation of knee ligament surgery results with special emphasis on use of a scoring scale. *Am. J. Sports Med.* 10, 150–154. doi: 10.1177/036354658201000306

Majewski, M., Susanne, H., and Klaus, S. (2006). Epidemiology of athletic knee injuries: a 10-year study. *Knee* 13, 184–188. doi: 10.1016/j.knee.2006.01.005

Marx, R. G., Stump, T. J., Jones, E. C., Wickiewicz, T. L., and Warren, R. F. (2001). Development and Evaluation of an Activity Rating Scale for Disorders of the Knee. *Am. J. Sports Med.* 29, 213–218. doi: 10.1177/03635465010290021601

Naito, E., Morita, T., and Amemiya, K. (2016). Body representations in the human brain revealed by kinesthetic illusions and their essential contributions to motor control and corporeal awareness. *Neurosci. Res.* 104, 16–30. doi: 10.1016/j.neures.2015.10.013

Needle, A., Lepley, A., and Grooms, D. (2017). Central Nervous System Adaptation After Ligamentous Injury: a Summary of Theories. *Evid. Clin. Interpret. Sports Med.* 47, 1271–1288. doi: 10.1007/s40279-016-0666-y

Neto, T., Sayer, T., Theisen, D., and Mierau, A. (2019). Functional Brain Plasticity Associated with ACL Injury: a Scoping Review of Current Evidence. *Neural Plast.* 2019:3480512. doi: 10.1155/2019/3480512

Nyland, J., Gamble, C., Franklin, T., and Caborn, D. N. M. (2017). Permanent knee sensorimotor system changes following ACL injury and surgery. *Knee Surg. Sports Traumatol. Arthrosc.* 25, 1461–1474. doi: 10.1007/s00167-017-4432-y

Ochi, M., Iwasa, J., Uchio, Y., Adachi, N., and Sumen, Y. (1999). The regeneration of sensory neurones in the reconstruction of the anterior cruciate ligament. *J. Bone. Joint Surg. Br.* 81, 902–906. doi: 10.1302/0301-620x.81b5.9202

Poulsen, E., Goncalves, G. H., Bricca, A., Roos, E. M., Thorlund, J. B., and Juhl, C. B. (2019). Knee osteoarthritis risk is increased 4-6 fold after knee injury - a systematic review and meta-analysis. *Br. J. Sports Med.* 53, 1454–1463. doi: 10.1136/bjsports-2018-100022

Proske, U., and Chen, B. (2021). Two senses of human limb position: methods of measurement and roles in proprioception. *Exp. Brain Res.* 239, 3157–3174. doi: 10.1007/s00221-021-06207-4

Relph, N., Herrington, L., and Tyson, S. (2014). The effects of ACL injury on knee proprioception: a meta-analysis. *Physiotherapy* 100, 187–195. doi: 10.1016/j.physio.2013.11.002

Ritter, P., and Villringer, A. (2006). Simultaneous EEG–fMRI. *Neurosci. Biobehav. Rev.* 30, 823–838.

Rush, J. L., Glaviano, N. R., and Norte, G. E. (2021). Assessment of Quadriceps Corticomotor and Spinal-Reflexive Excitability in Individuals with a History of Anterior Cruciate Ligament Reconstruction: A Systematic Review and Meta-analysis. *Sports Med.* 51, 961–990. doi: 10.1007/s40279-020-01403-8

Sherrington, C. S. (1906). *The Integrative Action of the Nervous System*. New Haven, CT, US: Yale University Press.

Strong, A., Arumugam, A., Tengman, E., Röijezon, U., and Häger, C. K. (2021a). Properties of Knee Joint Position Sense Tests for Anterior

Cruciate Ligament Injury: a Systematic Review and Meta-analysis. *Orthop. J. Sports Med.* 9, 23259671211007878. doi: 10.1177/2325967121 1007878

Strong, A., Srinivasan, D., and Häger, C. K. (2021b). Development of supine and standing knee joint position sense tests. *Phys. Ther. Sport* 49, 112–121. doi: 10.1016/j.ptsp.2021.02.010

Tegner, Y., and Lysholm, J. (1985). Rating systems in the evaluation of knee ligament injuries. *Clin Orthop. Relat. Res.* 198, 43–49.

Thijs, Y., Vingerhoets, G., Pattyn, E., Rombaut, L., and Witvrouw, E. (2010). Does bracing influence brain activity during knee movement: an fMRI study. *Knee Surg. Sports Traumatol. Arthrosc.* 18, 1145–1149. doi: 10.1007/s00167-009-1012-9

Tzourio-Mazoyer, N., Landeau, B., Papathanassiou, D., Crivello, F., Etard, O., Delcroix, N., et al. (2002). Automated Anatomical Labeling of Activations in SPM Using a Macroscopic Anatomical Parcellation of the MNI MRI Single-Subject Brain. *NeuroImage* 15, 273–289.

Van Melick, N., Meddeler, B. M., Hoogeboom, T. J., Nijhuis-Van Der, Sanden, M. W. G., and Van Cingel, R. E. H. (2017). How to determine leg dominance: the agreement between self-reported and observed performance in healthy adults. *PLoS One* 12:e0189876. doi: 10.1371/journal.pone.018 9876

Conflict of Interest: The authors declare that the research was conducted in the absence of any commercial or financial relationships that could be construed as a potential conflict of interest.

Publisher's Note: All claims expressed in this article are solely those of the authors and do not necessarily represent those of their affiliated organizations, or those of the publisher, the editors and the reviewers. Any product that may be evaluated in this article, or claim that may be made by its manufacturer, is not guaranteed or endorsed by the publisher.

frontiers | Frontiers in Human Neuroscience

ORIGINAL RESEARCH
published: 24 June 2022
doi: 10.3389/fnhum.2022.912276

Relationship Between the Practice of Tai Chi for More Than 6 Months With Mental Health and Brain in University Students: An Exploratory Study

Xiaoyuan Li[1,2], Jintao Geng[1], Xiaoyu Du[1], Hongyu Si[2] and Zhenlong Wang[3]**

[1] School of Electrical Engineering, Zhengzhou University, Zhengzhou, China, [2] School of Physical Education, Zhengzhou University, Zhengzhou, China, [3] School of Life Sciences, Zhengzhou University, Zhengzhou, China

To study whether Tai Chi (TC) practice can improve the brain connectivity of the prefrontal lobe of college students, the positive psychological capital questionnaires and resting EEG signals were acquired from 50 college students including 25 TC practitioners and 25 demographically matched TC healthy controls. The results showed that the score of the positive psychological capital questionnaire of the TC group was significantly higher than that of the control group, and the node degree of the frontal lobe and temporal lobe of both groups was positively correlated with the score of the positive psychological capital questionnaire. In addition, the response time of the TC group under auditory stimulation was significantly shorter than that of the control group, and there was a significant positive correlation between response time and its characteristic path length, and a significant negative correlation with global efficiency. Meanwhile, during the selected range of sparsity, the difference in global network parameters between two groups is significant in the alpha band. Under all single sparsity, the clustering coefficient, global efficiency, and local efficiency of the TC group have a higher trend, while the characteristic path length tended to be shorter. In the analysis of the local characteristics of the resting brain functional network, it was found that the node degree of the frontal lobe and temporal lobe of the TC group was higher, and the difference was significant in some nodes. These results all point to the fact that TC practice has a certain impact on specific brain areas of the brain.

Keywords: brain connectivity, Tai Chi, EEG signal, functional brain network, network metrics

OPEN ACCESS

Edited by:
Redha Taiar, Université de Reims Champagne-Ardenne, France

Reviewed by:
Víctor Manuel Mendoza-Núñez, Universidad Nacional Autónoma de México, Mexico
Antonio Ivano Triggiani, National Institute of Neurological Disorders and Stroke (NIH), United States

****Correspondence:***
Hongyu Si
sihongyu005@163.com
Zhenlong Wang
wzl@zzu.edu.cn

Specialty section:
This article was submitted to Motor Neuroscience, a section of the journal Frontiers in Human Neuroscience

Received: *05 April 2022*
Accepted: *25 May 2022*
Published: *24 June 2022*

Citation:
Li X, Geng J, Du X, Si H and Wang Z (2022) Relationship Between the Practice of Tai Chi for More Than 6 Months With Mental Health and Brain in University Students: An Exploratory Study. Front. Hum. Neurosci. 16:912276. doi: 10.3389/fnhum.2022.912276

INTRODUCTION

With the increasing complexity of knowledge, the accelerating pace of life, and the intensifying pressure of social competition, college students invest more and more time in knowledge learning, which leads to the psychological pressure faced by college students and its adverse consequences are becoming more evident (Yanxiao et al., 2021). On the other hand, due to the spread of network media, the increasing fragmented reading among college students has become a common phenomenon, thus ignoring systematic and in-depth reading learning (Xiaoyan and Yunbo, 2020). Many college students lack the abilities of self-management and restraint and make learning less efficient. Based on the above phenomena, it is urgent to find a way to improve brain function to cope with the great learning pressure, so as to improve learning efficiency.

Physical exercise is a very important way. Martial art is a kind of inherited technique of ancient military war created for fighting on the battlefield, which is equivalent to modern aerobic physical training (Tan, 2010). It is a full-body exercise that focuses more on flexible limb movements, so as to strengthen the body and have the ability of defend and attack (He, 2012). Meditation is a meditation technique used in yoga, with its emphasis on mindfulness and mental management, and the ultimate goal of which is to lead one to a state of liberation (Ryu and Jung, 2014). Neuroscientists have found that if you meditate regularly, you not only become good at it but also improve your self-control, self-knowledge, attention, stress management, and the ability to resist impulses (Friese et al., 2012). However, beginners often have difficulty concentrating when practicing meditation, resulting in poor training results. TC is a comprehensive mind-body exercise with both martial arts and meditation components and has the unique advantage of being easy to learn, safe and effective. Compared to other martial arts, there are no hard and fast requirements for learning TC (Bu et al., 2010), and it is suitable for both young and old. Since the practice of TC requires moderate aerobic exercise and mental exertion, it will exhibit similar or better executive neurological function than meditation and other exercises (Hawkes et al., 2014). At present, TC courses are offered in most universities in China, and it has been popularized all over the world in recent years. Existing studies have shown that TC has a very significant effect in terms of exercise intervention, which can not only improve physical fitness, including fall prevention (Lin et al., 2006), hypertension reduction (Guan et al., 2020), and cardiac rehabilitation (Cheng et al., 2020), but also has certain benefits to mental health, including improvement of quality of life and self-efficacy, emotional processing and other problems (Caldwell et al., 2009), and even has some beneficial effects on the improvement of patients with depression (Laird et al., 2018). Meanwhile, TC can also significantly improve people's sleep quality and mental state (Li et al., 2020).

Up to now, there are many studies on the human physiological and psychological effects of TC. Previous researchers preferred the ways of observation and questionnaire investigation. In recent years, many novel research methods have emerged to explore the effects of TC practicing on brain function, including electroencephalogram (EEG) processing and functional magnetic resonance imaging (fMRI). In 2010, Field observed that performances on math computations (including speed and accuracy) of participants were significantly improved by a 20-min TC training course and associated with an increase in frontal EEG theta activity (Field et al., 2010). Moreover, the practice of TC can also enhance the cognitive function of the elderly (Wayne et al., 2014). Wei used resting-state functional magnetic resonance images (rs-fMRI) to find that TC can influence the intrinsic functional architecture of the human brain (Wei et al., 2014). Compared with the control group, the TC Group has significant performance gains on attention network behavior tests.

Long-term TC practice could modulate mental control function and functional connections of cognitive control networks in older adults, demonstrating the potential of TC exercises in preventing cognitive decline (Tao et al., 2017). A systematic review study by Pan et al. (2018) found that TC intervention gives rise to beneficial neurological changes in the human brain through three neuroimaging techniques including fMRI (N = 6), EEG (N = 4), and MRI (N = 1). Eight weeks of TC exercise had a stronger effect on brain plasticity in college students compared to general aerobic exercise (Cui et al., 2019). In, Wang et al. (2004) compared the SF-36v2 health survey questionnaire scores before and after practicing TC and found that TC exercise had positive effects on the self-assessed physical and mental health of college students (Wang et al., 2004). Therefore, this study aims to integrate EEG technology and psychological questionnaire to evaluate the positive impact of TC practice on improving the physical and mental health of college students, so as to provide scientific guidance for the promotion of TC on campus.

MATERIALS AND METHODS

Participants

Participants were recruited from college students at Zhengzhou University. The sample size was determined by G*Power to ensure that an effect of 0.8 was obtained with $\alpha = 0.05$ and test efficacy of 0.8, requiring a minimum of 21 samples per group (Faul et al., 2009). 25 volunteers (17 M/8 F, age 20–24 years, mean ± SD = 21.20 ± 1.190 years) who have practiced TC for more than 6 months (Practice TC at least twice a week for 100 min each time in addition to regular physical courses) in the Wushu Association of Zhengzhou University were recruited to participate this study. Another total of 25 subjects (19 M/6 F, age 21–22 years, mean ± SD = 21.60 ± 0.577 years) without TC practice (Do little exercise except for physical education class once a week) was screened as the control group. All subjects were recruited at random, covering the natural sciences, social sciences, and humanities (**Table 1**), all of them were right-handed, without any neurological or mental illness, and their naked or the corrected visual acuity of both eyes was normal. This study was approved by the Institutional Review Board of Zhengzhou University. All study participants provided written informed consent before they were enrolled in the study. There was no significant difference in age (two-sample t-test, $t = -1.512$ and $p = 0.140$) and gender [χ^2-test, $\chi^2_{(1)} = 0.397$, and $p = 0.529$] between the TC group and the control group.

Electroencephalogram Data Acquisition

Data were analyzed in a quiet, dark, room at room temperature, where each participant was asked to sit in a comfortable chair, keeping their eyes closed and relaxed, especially keeping their body and head still. At the same time, they were asked to stay awake and try to avoid thinking about anything. The data were derived with Ag-AgCl disc electrodes placed on frontal, vertex, temporal, parietal, and occipital recording sites of the international 10–20 system against the right earlobe as reference. Electrode impedances were maintained at less than 5 KΩ. The sampling frequency was set to 250 Hz, we used additional EEG filters (0.36–70 Hz bandpass) just for

TABLE 1 | Demographic characteristics.

	Tai Chi (*N* = 25)				Control (*N* = 25)		
No.	**Age**	**Sex**	**Subject**	**Number of months of TC practice(m)**	**Age**	**Sex**	**Subject**
1	24	Female	Economics	18	21	Male	Engineering
2	23	Female	Economics	6	21	Male	Engineering
3	22	Male	Engineering	6	21	Male	Engineering
4	20	Male	Engineering	6	21	Male	Engineering
5	20	Male	Engineering	6	22	Female	Engineering
6	20	Male	Philosophy	6	23	Male	Education
7	21	Male	Science	6	22	Male	Arts
8	21	Male	Science	6	22	Female	Arts
9	21	Male	Science	6	22	Male	Arts
10	23	Male	Literature	6	22	Male	Law
11	21	Male	Literature	6	22	Male	Law
12	21	Female	Management	6	22	Male	Law
13	23	Male	Management	6	21	Female	Law
14	22	Male	Management	6	21	Male	Management
15	21	Male	Engineering	18	22	Male	Management
16	22	Male	Engineering	18	21	Male	Management
17	20	Male	Engineering	18	22	Male	Management
18	22	Male	Law	6	21	Male	Science
19	22	Male	Law	6	21	Male	Agriculture
20	21	Female	Philosophy	6	22	Male	Agriculture
21	20	Female	Philosophy	6	21	Male	Philosophy
22	20	Female	Philosophy	6	22	Male	Literature
23	20	Female	Education	6	22	Female	Literature
24	20	Female	Education	6	22	Female	Literature
25	20	Male	Education	6	21	Female	Literature
	21.20 ± 1.190	17M/8F			21.6 ± 0.577	19M/6F	

observing the filtered data and not applying these filters to the final saved data. The whole resting state EEG signals were collected with eyes closed continuously for 4 min. In addition to collecting EEG signals from the subjects, we also administered the "Oddball" auditory stimulation paradigm, in which we used two different tones as stimulus sources, with the low frequency of 1,000 Hz as the interference tone and the high frequency of 1,500 Hz as the target stimulus tone, both of which occurred randomly, with the interference tone accounting for 85 and 15% of the target tone. Each subject performed 200 trials per auditory "Oddball" paradigm, with 30 target tones, and each subject performed two auditory "Oddball" experiments, and the final results of the two "Oddball" experiments were compared. The average response time of the subject was obtained by averaging the 60 keystroke response times obtained from the 60 target tones in the two "Oddball" experiments.

The EEG electrode lead is used as the network node, and the connection network is established between the nodes, and the nodes represent the brain region. The whole brain was divided into five zones, frontal lobe (FP1, FP2, F7, F8, F3, F4, FZ, FC3, FCz, FC4), parietal lobe (CP3, CPz, CP4, P3, Pz, P4), temporal lobe (FT7, FT8, T3, T4, TP7, TP8, T5, T6), and occipital lobe (O1, OZ, O2).

Data Pre-processing

The pre-processing of EEG data was adopted by using the EEGLAB (Delorme and Makeig, 2004) toolbox based on MATLAB[1] in order to obtain high validity of the data, including filtering (0.5–30 Hz band-passed filtering, 50 Hz notch filtering). Standardization of reference values using RE-reference (Reference Electrode Standardization Technique, REST)(Yao, 2001; Dong et al., 2017), segmentation (The raw EEGs of each subject were randomly divided into 8 non-overlapping epochs, each lasting for 15 s), and invalid data removal (Bad channels were removed manually *via* visual inspection off-line, and artifacts of eye movement, muscular movement or other disturbances were removed by blind source separation algorithm based on independent component analysis)(Mognon et al., 2011).

Functional Network Construction

The EEG electrodes of 30 effective channels were used as nodes in principle, and the synchrony measures among all nodes were quantified as the value of network edges to construct a functional brain network. In this study, the Phase-Locking value (PLV)(Lachaux et al., 1999), one of the estimation methods for

[1]https://sccn.ucsd.edu/eeglab/index.php

functional connection of phase synchronization, was calculated among all nodes to generate a correlation matrix for each subject. Then, the functional brain networks of the two groups were constructed based on four EEG sub-bands of interest: *delta* (0.5–4 Hz), *theta* (4–7 Hz), *alpha* (8–12 Hz), *beta* (13–30 Hz), respectively. Phase synchronization in practical applications usually means that the phase difference between two signals is bounded (the bound has to be smaller than 2π). Therefore, for two real-valued EEG signals *x(t)* and *y(t)*, the phase lock condition is:

$$\Delta\Phi(t) = \left|\Phi_x(t) - \Phi_y(t)\right| < c \tag{1}$$

Where Φ_x(t) and Φ_y(t) represent the phase of signal *x(t)* and signal *y(t)*, respectively, and $\Delta\Phi$(t) represents the phase difference between them, and *c* is constant.

Use cyclic phase under conditions of phase lock, that is, the relative phase difference $\Delta\Phi_{rel}$, which can be defined as:

$$PLV = \left|\left\langle e^{i\Delta\Phi_{rel}(t)}\right\rangle\right| = \left|\frac{1}{N}\sum_{n=1}^{N} e^{i\Delta\Phi_{rel}(t_n)}\right|$$
$$= \sqrt{\langle\cos\Delta\Phi_{rel}(t)\rangle^2 + \langle\sin\Delta\Phi_{rel}(t)\rangle^2} \tag{2}$$

Where $\langle . \rangle$ means averaging in the time domain. The range of PLV was [0,1]. The PLV describes the phase synchronization between any two EEG sequences in a certain frequency band, using the phase information of the signal. The higher PLV means the higher the degree of phase synchronization between the two signals and the more consistent the phase difference. When PLV = 0, it indicates that there is no phase synchronization between two signals. Conversely, when PLV = 1, it declares that there is complete phase synchronization between them. The larger the PLV of two EEG signals is, the greater the degree of phase synchronization between the two cerebral cortex regions is, indicating that they have higher information interaction efficiency and stronger cooperative working ability.

Network Analysis

Threshold Selection

We converted the PLV correlation matrix into an adjacency matrix (binary matrix) with the same sparsity by selecting the appropriate threshold, which is an undirected and non-weighted functional brain network. In some current studies, a functional brain network with the same number of nodes and edges always is constructed by sparsity (fixed connection density method) (Wang et al., 2016). Sparsity is defined as the ratio between the total number of existing edges *K* and the possible maximum number of edges *N(N-1)/2*, where *N* is the number of nodes (*N* = 30 in our study)(Zhang et al., 2018). This approach ensures that any graphical differences between groups are caused purely by the reconfiguration of specific functional connections, not by overall connectivity in the network topology.

It is vital for us to select an appropriate sparsity threshold since the characteristic parameters of the functional brain network will change with different levels of sparsity. However, there is no standard for selecting the optimal sparsity threshold at present. Some studies have shown that the level of sparsity is too small to obtain a stable topology of networks. On the contrary, the network with too large sparsity loses the small-world topology property that is characteristic of human brains and becomes more and more inclined to the random network (Achard and Bullmore, 2007). In this study, we constructed a series of functional brain networks at a large range of sparsity (from 12 to 40%, 1% step) to compare the differences between the two groups of participants (Meng et al., 2014).

Global Parameters

The characteristic path length (*L*) of a network is defined as the minimum number of edges connecting a pair of nodes, averaged over all pairs of nodes (Shang, 2011). It can describe the ability of information transmission within the network and reflect the strength of functional integration among brain regions. The shorter the path length, the greater the intensity of functional integration. The definition of characteristic path length can be expressed as:

$$L = \frac{2\sum_{i\geq j} L_{ij}}{N(N-1)} \tag{3}$$

Where L_{ij} represents the geodesic length between node *i* and node *j*, and *N* is the number of nodes.

Another commonly used measure is global efficiency (Bryan et al., 2015), which is used to measure how efficiently the functional brain network transmits and processes information. The global efficiency is equal to the average of the reciprocal of the shortest path on the numerical, defined as follows:

$$E_{global} = \frac{1}{N(N-1)}\sum_{i\neq j}\frac{1}{L_{ij}} \tag{4}$$

The definition of clustering coefficient is the average fraction of pairs of neighbors of a node that are also neighbors of each other (Wang, 2002). The clustering coefficient c_i of node *i* is defined as the ratio between the number E_i of edges that actually exist between these k_i nodes and the total number k_i (k_i - 1)/2, namely,

$$C_i = \frac{2E_i}{k_i(k_i-1)} \tag{5}$$

Similarly, the clustering coefficient *C* of a network is given by the average of the C_i over all nodes in the network:

$$C = \frac{1}{N}\sum_{i=1}^{N} C_i \tag{6}$$

In addition, a global parameter, local efficiency is used to quantify the fault-tolerant ability for a complex network, which means the information transmission ability of the subgraph formed by the nodes directly connected with the node after removing a node (Boccaletti et al., 2006). For the local efficiency of the whole network, its definition is described as the average of the shortest path of the neighbor subgraph of all nodes, with the formula as follows:

$$E_{local} = \frac{1}{N}\sum_{i\in V} E_{global}(G_i) \tag{7}$$

Where G_i represents a subgraph formed by nodes directly connected to node i (no node i included). It is always used to assess the information transmission capacity of the network at the local level, which is essentially the extension of the clustering coefficient.

Nodal Parameters

Among all the centrality metrics, degree centrality is the most basic and important metric in the network. The degree k_i of the node i in an undirected network is the total number of edges directly connected to it. The average of k_i over all nodes i is called the average degree of the network and is denoted as $\overline{k}$. Given the adjacency matrix $A = (a_{ij})_{N \times N}$ of network G, we have:

$$k_i = \sum_{j=1}^{N} a_{ij} = \sum_{j=1}^{N} a_{ji}$$
$$\overline{k} = \frac{1}{N} \sum_{j=1}^{N} k_i = \frac{1}{N} \sum_{i,j=1}^{N} a_{ij} \quad (8)$$

Statistical Analysis

Two-sample t-test and ^{2}-test in SPSS were conducted to analyze age and sex statistics involving 25 practitioners in TC group and 25 healthy controls. The correlation coefficient and p-value between reaction time and global network topological properties were analyzed using the corrcoef procedure (MATLAB corrcoef). The non-parametric permutation test was used to assess statistical group differences in brain functional network parameters for the TC group and the control group. Differences were considered statistically significant when the $p < 0.05$. The images were drawn with GraphPad Prism 9 and Visio 2019.

RESULTS

Differences of the Component Positive Psychological Capital Questionnaire

In order to analyze the difference in a psychological state between the TC group and the control group, we completed the positive psychological capital questionnaire before the EEG signal acquisition. Psychological capital is divided into four core components: Self-efficacy, Resiliency, Hope, and Optimism.

As shown in **Figure 1**, the total score of the positive psychological capital questionnaire in the TC group was significantly higher than that in the control group by non-parametric substitution test analysis. In terms of the four core components, the TC group was significantly higher than the control group in self-efficacy, resilience, and optimism. In terms of hope, although the TC group still showed a higher trend compared to the control group, the difference was not significant.

Relationship Between Brain Connectivity Analysis and Reaction Time

We made a statistical analysis of the reaction time of the subjects under the auditory "Oddball" experiment. The results, as shown in **Figure 2**, showed that the reaction time of the TC group was faster than that of the control group, and the difference was significant by the non-parametric replacement test. Compared with the control group, the subjects in the TC group seemed to have a faster reaction speed.

Based on the previous study, we analyzed the correlation between the global topological characteristics of the brain functional network in the resting state and the response time in the auditory "Oddball" experiment. **Figure 3** was the scatter plot of the correlation between global network topology characteristics and the reaction time. The correlations between response time and characteristic path length of subjects in the TC group ($r = 0.4314$, $p = 0.0313$) and in the control group ($r = 0.2939$, $p = 0.1539$) were shown in **Figure 3A**, indicating that there was a significant positive correlation between them in TC group, while there was no significant correlation in the control group. **Figure 3B** showed the correlation between reaction time and global efficiency in the TC group ($r = -0.4501$, $p = 0.0240$) and in the control group ($r = -0.3885$, $p = 0.0550$). The results revealed a significant negative correlation between reaction time and global efficiency in the TC group, while no significant correlation was found in the control group. Unfortunately, no significant correlations between reaction time and clustering coefficient, response time, and local efficiency in either the TC group or the control group were found.

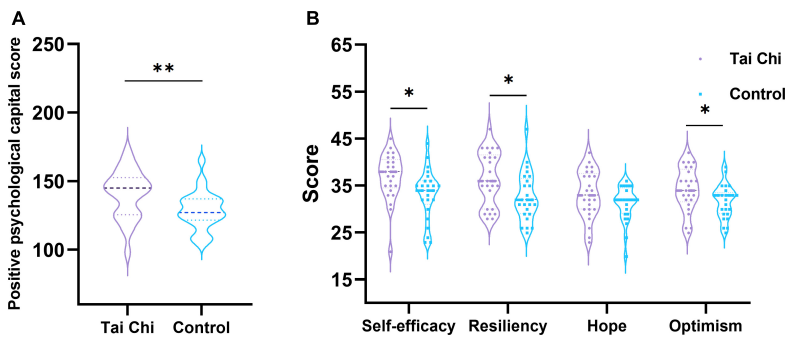

FIGURE 1 | Analysis of psychological questionnaire scores in TC group and control group. **(A)** The score difference of positive psychological capital questionnaire between groups. **(B)** Inter group score difference of four core components. *Indicated significant difference between groups, $p < 0.05$, **indicated significant difference between groups, $p < 0.01$.

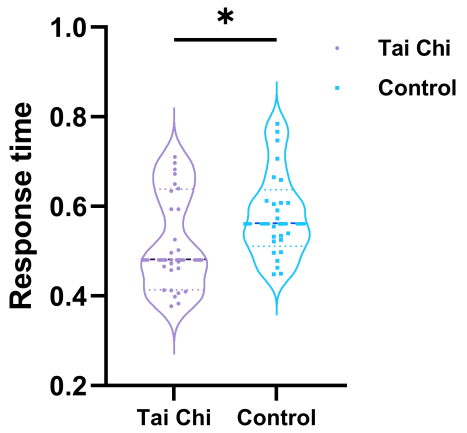

FIGURE 2 | Reaction time of TC group and control group under auditory "Oddball" experiment. *Indicated significant difference between groups, $p < 0.05$.

Function Network Construction Based on Phase-Locking Value

For the four frequency bands of *delta, theta, alpha*, and *beta,* the PLV values between 30 electrode channels of each participant were calculated respectively, which were taken as the connecting edge of the network, and thus the 30 × 30 PLV correlation matrix for each subject at each frequency band was obtained. Finally, according to the previously set sparsity threshold, these PLV correlation matrices were binarized into adjacency matrices to generate the PLV functional network for all of the subjects (as shown in **Figure 4**).

Brain Connectivity Analysis

For the constructed PLV brain function network, we compared the differences in global parameters between the two groups in different frequency bands (*delta, theta, alpha,* and *beta*), and analyzed whether there are differences in brain function network between TC and control groups. According to the statistical analysis of the non-parameter replacement test, As shown in **Figures 5A,C,E**, the inter-group differences in clustering coefficient, characteristic path length, and global efficiency between TC and control groups were only significant in *alpha* band, there were no significant differences in *delta*, *theta,* and *beta* bands. Then we targeted the *alpha* band that showed significance for inter-group differences at each single sparsity threshold to compare L, C, and E_{local} in the TC and control groups. **Figures 5B,D,F,H** showed that under all the sparsity thresholds, the TC group was higher than the control group, and the difference was significant under some sparsity thresholds. At the same time, the characteristic path length of the TC group was shorter than that of the control group, and the difference was more significant when the sparsity level was lower.

Although the boxplot of **Figure 5G** showed that the maximum value of local efficiency in the TC group was lower than that in the control group in the *beta* frequency band, the median value of the TC group was significantly higher. From the perspective of distribution, the local efficiency distribution of the TC group was more compact. Under most of the selected sparsity, the local efficiency of the TC group was significantly higher than that of the control group.

Nodal Characteristics of Brain Regions

Because the *alpha* band in global parameters analysis displayed the most significant difference, we analyzed the average value difference between the node degrees of each sparsity level in the two groups in the brain function network, and the statistical analysis method used non-parametric replacement inspection.

As shown in **Figure 6**, the degree of each node in the frontal lobe of the brain was compared between the TC group and the control group, it can be found that the values of all nodes in the frontal lobe in the TC group are almost higher than those in the control group. Meanwhile, through the statistical analysis of the non-parametric replacement test, the values of FP1 and

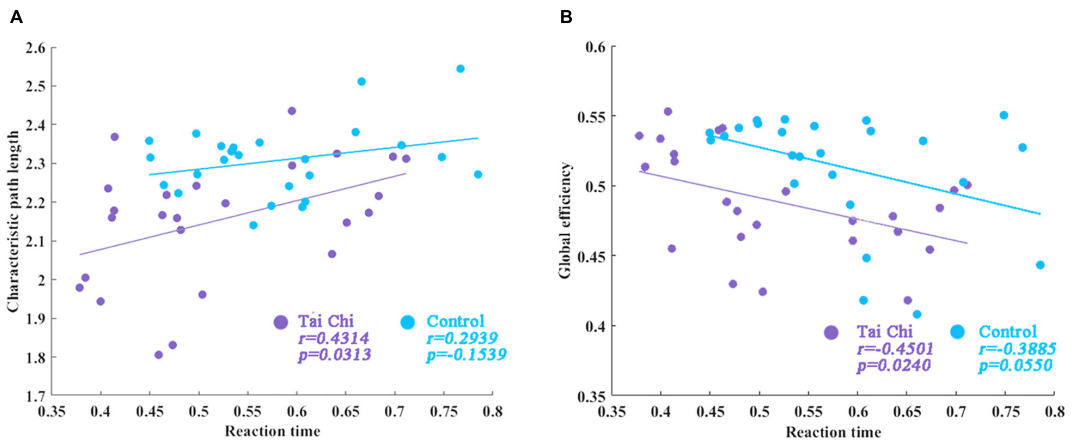

FIGURE 3 | The correlation between reaction time and global network topological properties. **(A)** The correlations between response time and characteristic path length of subjects in TC group. **(B)** Correlation between reaction time and global efficiency in the TC group.

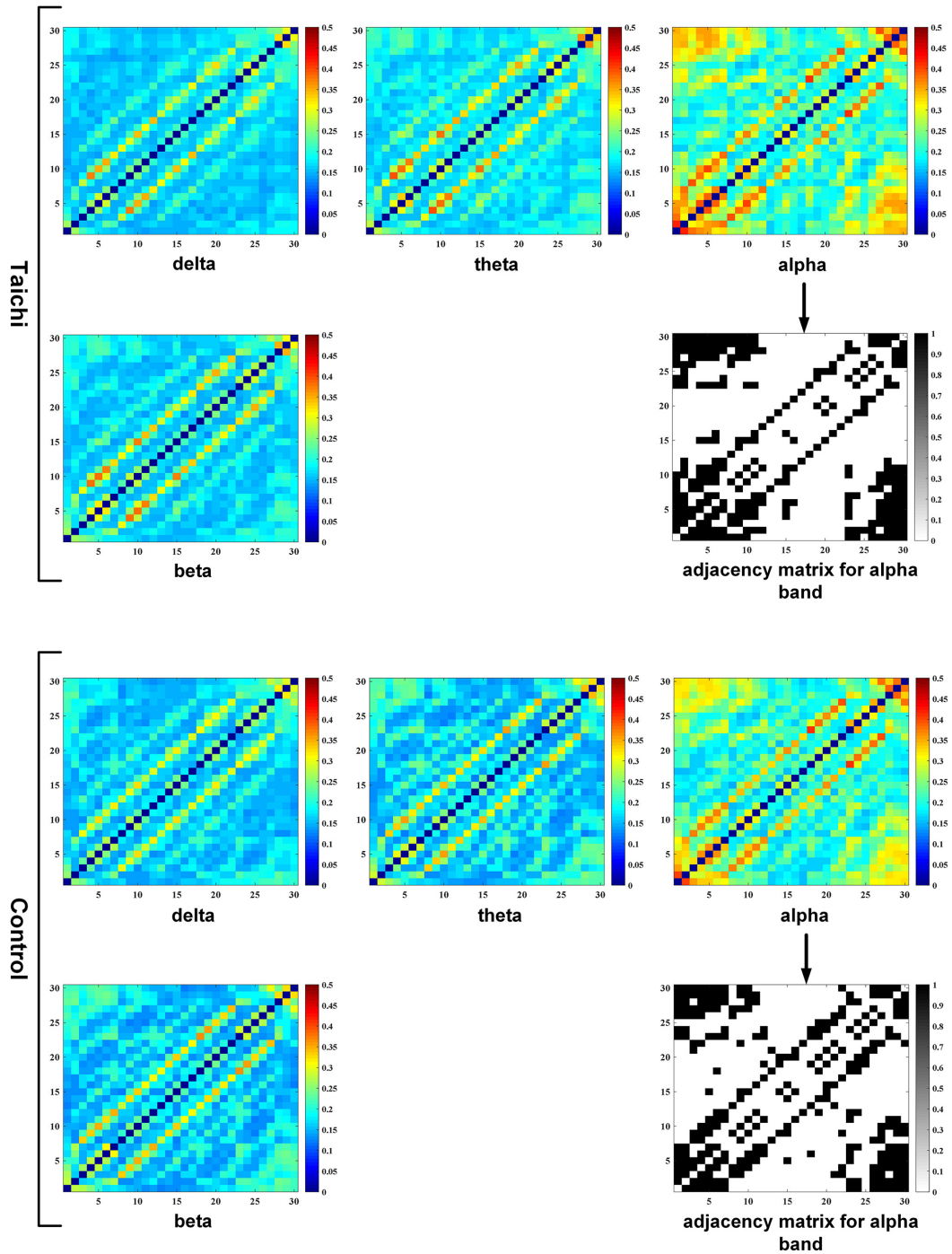

FIGURE 4 | PLV correlation matrix and adjacency matrix of TC and control.

FP2 nodes in the TC group (FP1:12.81 ± 1.51, FP2:12.42 ± 1.80) were higher than those in the control group (FP1:11.52 ± 1.50, FP2:11.37 ± 1.77), and the difference was significant. Degree values of nodes T3 and T4 in the TC group (T3:3.59 ± 1.26, T4:3.46 ± 1.80) were significantly higher than those in the control group (T3:2.78 ± 1.46, T4:2.54 ± 1.26), and the difference was significant in some nodes. As shown in **Figure 7**, it was found that the node degree of the frontal lobe and temporal lobe of the TC group was higher. These results all point to the fact that TC practice has a certain impact on specific brain areas of the brain. There was no significant difference between the TC group and the control group for the nodes of the parietal and occipital lobes. There was no significant difference between the TC group and the control group for the nodes of the parietal and occipital lobes.

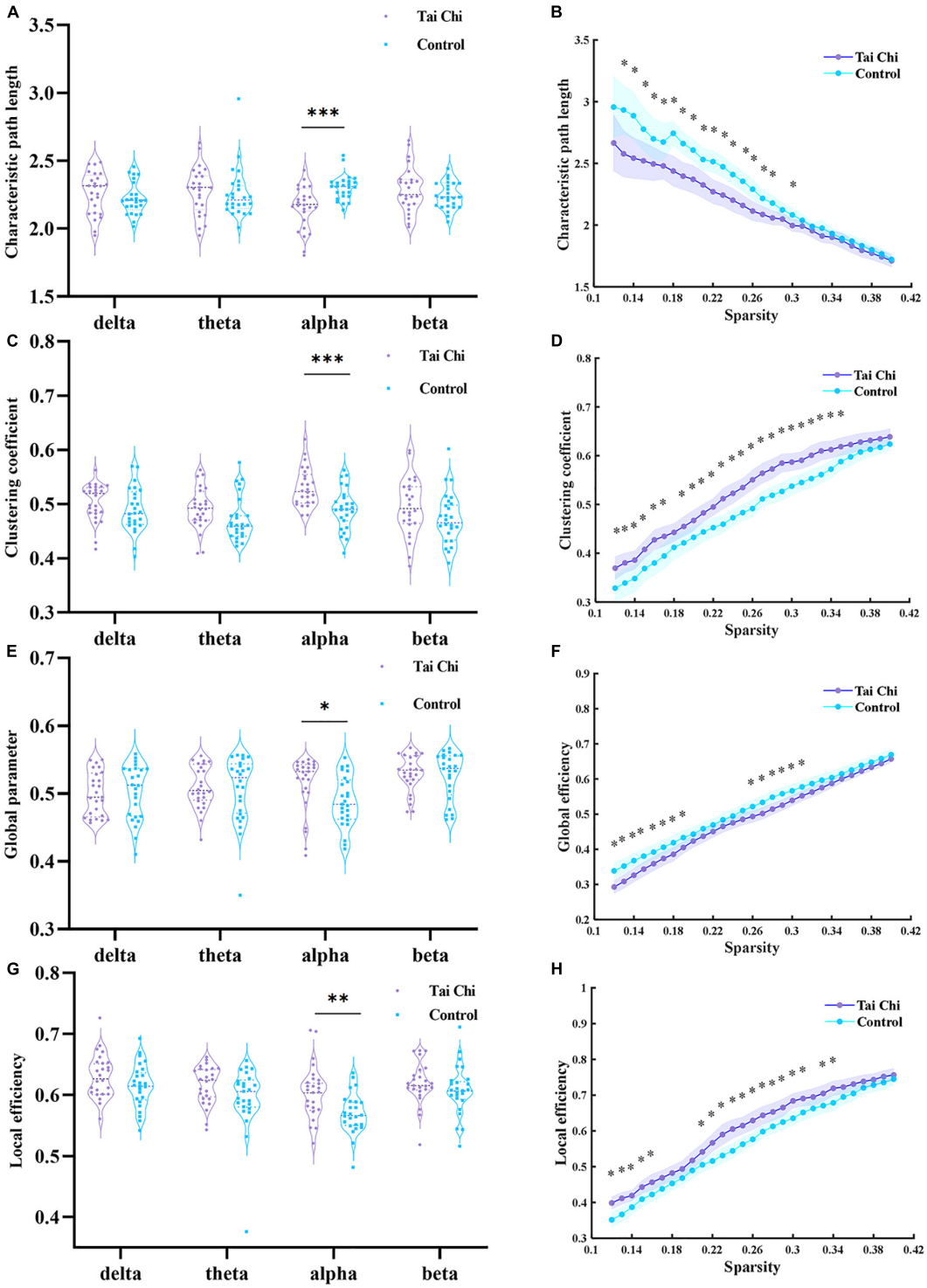

FIGURE 5 | Panels **(A,C,E,G)** showed the inter-group differences of clustering coefficient, characteristic path length, global efficiency and local efficiency within the selected sparsity threshold range at each frequency band, respectively. Panels **(B,D,F,H)** represented the inter-group differences of clustering coefficient, characteristic path length, global efficiency, and local efficiency of two groups of subjects under each single sparsity threshold at alpha frequency band, respectively. The purple and blue shading represented 95% confidence intervals of the TC group and the control group, *indicated significant difference between groups, $p < 0.05$, **indicated significant difference between groups, $p < 0.01$; and ***indicated a very significant difference between groups, $p < 0.001$.

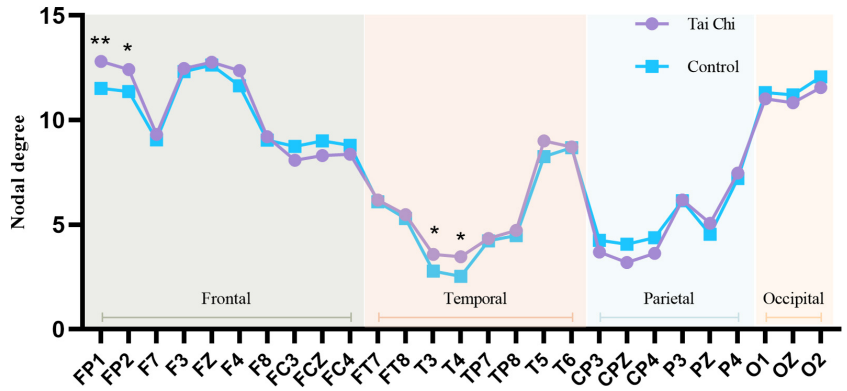

FIGURE 6 | Line chart of nodal degree of each brain region in alpha frequency band of TC group and control group. *Indicated significant difference between groups, $p < 0.05$, **indicated significant difference between groups, $p < 0.01$.

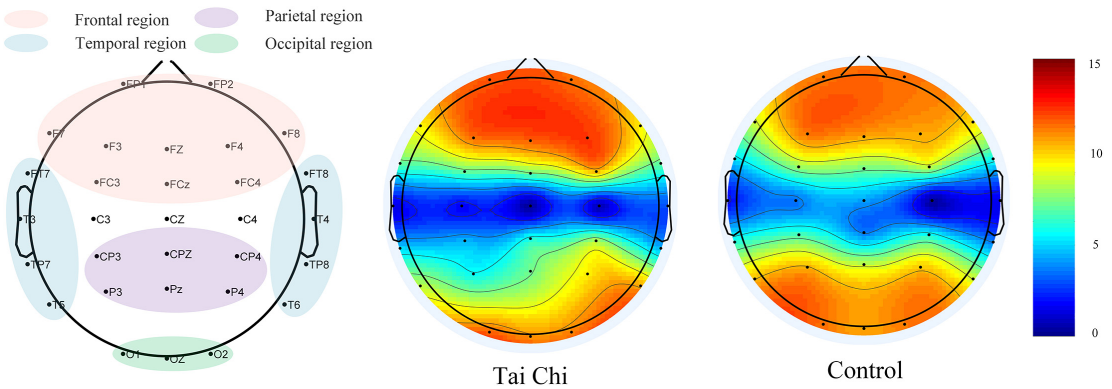

FIGURE 7 | Node location and node degree topographic map.

DISCUSSION

The alpha band analysis of EEG showed that TC practice significantly improved the activation of the prefrontal lobes of the practitioners, enhanced functional neuroplasticity of the brain (Cui et al., 2021), and also increased the reaction speed of the practitioners.

Increased Brain Functional Connectivity

The nodal degree of the two groups was significantly different in the FP1 and FP2 nodes of the frontal lobe and the T3 and T4 nodes of the temporal lobe. with advanced cognitive functions, such as learning, language, decision making, abstract thinking, emotion, and so on, while the temporal lobe is related to memory and emotion, and the amygdala in the anterior temporal lobe is the core area that regulates emotion (Sergerie et al., 2006). The node degree of the frontal lobe and temporal lobe in the TC group was higher than that in the control group, which indirectly reflected that the practice of TC had a positive effect on the advanced cognitive functions. From the perspective of physical exercise, TC belongs to aerobic exercise (Wayne et al., 2014), which has been proved to improve memory function (Erickson et al., 2011; Li et al., 2014).

After the practice of TC, the shortest path length between the nodes in the brain functional network of the TC group became shorter, that is, the number of edges from one node to another decreased. Furthermore, under a single sparse degree, the TC group showed higher global efficiency, which further indicated that compared with the control group, the transmission efficiency of the information carried by each node in the TC group is higher at the global level of the brain. This indirectly proved that after the practice of TC, the degree of functional integration within the brain is enhanced (Gu et al., 2022). On the other hand, a higher clustering coefficient in the TC group revealed that the nodes in the brain functional network of the TC group had a higher degree of aggregation at the local level of the brain, that is, for the whole brain region, the connection density between nodes decreased, while the higher local efficiency of the TC group showed that the information transmission efficiency of the nodes in the brain functional network of the TC group was higher than that of the control group at the local level (Taya et al., 2014).

There is a strong anatomical link between the prefrontal cortex and the hippocampus, which is consistent with the idea that the prefrontal cortex and hippocampus interact to support memory (Bu et al., 2010). Activation of the prefrontal lobe also has a dramatic improvement in input and output to the

hippocampus, thereby improving the cognitive ability of the practitioner to learn.

TC practitioners were significantly higher than the controls in the total score of positive psychological capital (You, 2016) and the three core components of self-efficacy, resilience, and optimism, indicating participants who have practiced TC for more than 6 months have a more positive mental state than the control group. TC and paced breathing have variously been linked to improvements in vagal tone (Larkey et al., 2009), and TC exercise had positive effects on the self-assessed physical and mental health of college students (Wang et al., 2004).

Previous studies have found that anxious people have abnormal connections in the frontal lobe, temporal lobe, and parietal lobe, and the node degree in the frontal lobe and temporal lobe is lower than that of normal people. At the same time, the clustering coefficient of the brain network of anxious people was found to be lower than that of the normal group, and the degree of clustering within the brain network and the information transmission capacity of the network of anxious people were reduced (Ji et al., 2020). Whalen's research also proved that anxiety was related to the weakening of the functional connection between the amygdala and medial prefrontal cortex (Kim et al., 2011). TC practice may lead the practitioner to a positive mental state and keep them away from negative mental states such as anxiety and depression. Regarding the characteristics of TC movement, TC practice incorporates elements of meditation, the movement of the limbs is coordinated with the breathing (Jingfang et al., 2018). The whole process not only tones up the body but also regulates the psychology. After long-term practice, the frontal lobe and temporal lobe of the brain will also be changed imperceptibly. Therefore, practicing TC can liberate practitioners from stress. Studies have also shown that TC is effective in improving depression, anxiety and quality of life in drug users (Cui et al., 2022), suggesting that TC can also be used as a new type of intervention for the prevention and cessation of internet addiction among college students.

Tai Chi Practice Can Make College Students React Faster

The key response time of the "oddball" experiment in the TC group was shorter than that in the controls, which indirectly reflected that the TC group had a faster response to the sudden stimulus. Meanwhile, the reaction time in the TC group showed a significant positive correlation with the characteristic path length extracted from the functional network and a significant negative correlation with its global efficiency. That is to say, the shorter the characteristic path length and the higher the global efficiency of the TC group is, the faster the reaction speed. This phenomenon was also reflected in the research results of Field. In their research, the mathematical calculation speed and accuracy of subjects were significantly improved after 20 min of TC (Field et al., 2010). Indeed, related studies confirmed that TC intervention could cause significant changes in the functional connectivity and homogeneity of the brain and the neural function of the executive network (Pan et al., 2018). It is supposed that executive control is susceptible to TC training in multiple ways.

Due to the popularity of electronic devices, university students are increasingly reading in fragments, making it difficult to concentrate during study and work. TC practice not only regulates physical activities, but also requires the brain to maintain continuous focus, and need to perform multiple action tasks at the same time, which also plays a certain role in maintaining concentration. Therefore, such physical and mental exercise may also have a positive impact on cognitive function. Previous studies have shown that the functional connections of the prefrontal cortex of the TC group have an enhanced trend in multiple frequency bands, and these functional enhancements are related to the improvement of memory scores (Tao et al., 2017). TC and other similar mindfulness training can regulate attention, working memory, and its central executive function through norepinephrine, and it also has a certain alleviating effect on mental illness (Russell and Arcuri, 2015).

Limitations

There were several limitations to the current research. First, the subjects in this study were concentrated in the same university and lacked research on various age and career groups for a small sample size, which potentially limits the generalization of the analysis results. Second, our research analysis only targeted college students with and without TC practice and investigated the effects of TC practice on college students' brain functional networks and psychological states. The further stratified analysis by the number of months of TC practice was not carried out, which could not provide a theoretical basis for clinical application. Furthermore, only the resting-state brain functional network was constructed in this study, and the differences in the brain functional network between both groups of subjects in the task state would be investigated in the future. Finally, the study design is cross-sectional and therefore its findings are not explanatory. Therefore, further clinical trials on the improved efficacy of TC practice with long term follow-up for promoting an effective exercise need to be performed.

CONCLUSION

Compared to matched controls, TC practitioners exhibited higher mental scores and faster response times, in the alpha band, increased connectivity, transitivity, and clustering associated with higher modularity were observed. Since PLV values reflected the degree of phase synchronization between the two signals, it indicated that the TC group had stronger synchronization between the cerebral cortex, that is to say, higher efficiency of information interaction and stronger collaborative ability. The results have demonstrated that TC exercises have a positive impact on the brain connectivity of the prefrontal lobe for college students. It can be concluded that after TC practice, the frontal and temporal lobes of the subjects have significant effects, with the improvement of the prefrontal cortex being the most obvious. Previous studies have shown that the prefrontal cortex is closely related to

executive cognitive function and emotion of the brain, and plays positive guidance in mental health (Fuster, 2001). This conclusion is consistent with the phenomenon we observed. Since PLV values reflected the degree of phase synchronization between the two signals, it indicated that the TC group had stronger synchronization between the cerebral cortex, that is to say, higher efficiency of information interaction and stronger collaborative ability. In the follow-up study, the direction information of the network or the connection weight information can be appropriately added, so as to better realize EEG traceability and functional connection analysis on the brain source.

DATA AVAILABILITY STATEMENT

The raw data supporting the conclusions of this article will be made available by the authors, without undue reservation.

ETHICS STATEMENT

The studies involving human participants were reviewed and approved by the Institutional Review Committee of Zhengzhou University. The patients/participants provided their written informed consent to participate in this study.

AUTHOR CONTRIBUTIONS

XL designed the conception. ZW conceived and designed the paradigm. HS instructed the Tai Chi group to practice Tai Chi. JG performed the data collection work and analyzed the data. XL, JG, XD, and ZW wrote the main manuscript text. All authors contributed to the development of this manuscript and reviewed the manuscript.

FUNDING

This research was supported by the Department of Science and Technology of Henan Province focuses on R&D and promotion grant (192102310026), Education and Teaching Reform research and Practice project of Zhengzhou University (2021ZZUJGLX038), and Philosophy and Social Science planning project of Henan Province (2019BTY007).

ACKNOWLEDGMENTS

We would like to thank all the participants in this study. We would also like to thank Jiaozuo Qigong Association for providing technical guidance.

REFERENCES

Achard, S., and Bullmore, E. T. (2007). Efficiency and cost of economical brain functional networks. *PLoS Comput. Biol.* 3:174–183. doi: 10.1371/journal.pcbi.0030017

Boccaletti, S., Latora, V., Moreno, Y., Chavez, M., and Hwang, D. U. (2006). Complex networks: structure and dynamics. *Phys. Rep. Rev. Sec. Phys. Lett.* 424, 175–308. doi: 10.1016/j.physrep.2005.10.009

Bryan, E. K., VerSchneider, C., and Narayan, D. A. (2015). Global efficiency of graphs. *Akce Int. J. Graphs Combinat.* 12, 1–13. doi: 10.1016/j.akcej.2015.06.001

Bu, B., Haijun, H., Yong, L., Chaohui, Z., Xiaoyuan, Y., and Singh, M. F. (2010). Effects of martial arts on health status: a systematic review. *J. Evid. Based Med.* 3, 205–219. doi: 10.1111/j.1756-5391.2010.01107.x

Caldwell, K., Harrison, M., Adams, M., and Triplett, N. T. (2009). Effect of Pilates and taiji quan training on self-efficacy, sleep quality, mood, and physical performance of college students. *J. Bodywork Mov. Ther.* 13, 155–163. doi: 10.1016/j.jbmt.2007.12.001

Cheng, D., Wang, B., Li, Q., Guo, Y., and Wang, L. (2020). Research on function and mechanism of Tai Chi on cardiac rehabilitation. *Chin. J. Integrat. Med.* 26, 393–400. doi: 10.1007/s11655-020-3262-9

Cui, J., Liu, F., Liu, X., Li, R., Chen, X., and Zeng, H. (2022). The impact of Qigong and Tai Chi exercise on drug addiction: a systematic review and meta-analysis. *Front. Psychiatry* 13:826187. doi: 10.3389/fpsyt.2022.826187

Cui, L., Tao, S., Yin, H. C., Shen, Q. Q., Wang, Y., Zhu, L. N., et al. (2021). Tai Chi Chuan alters brain functional network plasticity and promotes cognitive flexibility. *Front. Psychol.* 12:665419. doi: 10.3389/fpsyg.2021.665419

Cui, L., Yin, H. C., Lyu, S. J., Shen, Q. Q., Wang, Y., Li, X. J., et al. (2019). Tai Chi Chuan vs general aerobic exercise in brain plasticity: a multimodal MRI study. *Sci. Rep.* 9:17264. doi: 10.1038/s41598-019-53731-z

Delorme, A., and Makeig, S. (2004). EEGLAB: an open source toolbox for analysis of single-trial EEG dynamics including independent component analysis. *J. Neurosci. Methods* 134, 9–21. doi: 10.1016/j.jneumeth.2003.10.009

Dong, L., Li, F., Liu, Q., Wen, X., Lai, Y., Xu, P., et al. (2017). MATLAB toolboxes for reference electrode standardization technique (REST) of scalp EEG. *Front. Neurosci.* 11:601. doi: 10.3389/fnins.2017.00601

Erickson, K. I., Voss, M. W., Prakash, R. S., Basak, C., Szabo, A., Chaddock, L., et al. (2011). Exercise training increases size of hippocampus and improves memory. *Proc. Natl. Acad. Sci. U.S.A.* 108, 3017–3022.

Faul, F., Erdfelder, E., Buchner, A., and Lang, A. G. (2009). Statistical power analyses using G*Power 3.1: tests for correlation and regression analyses. *Behav. Res. Methods* 41, 1149–1160. doi: 10.3758/brm.41.4.1149

Field, T., Diego, M., and Hernandez-Reif, M. (2010). Tai chi/yoga effects on anxiety, heartrate, EEG and math computations. *Complement. Ther. Clin. Pract.* 16, 235–238. doi: 10.1016/j.ctcp.2010.05.014

Friese, M., Messner, C., and Schaffner, Y. (2012). Mindfulness meditation counteracts self-control depletion. *Conscious. Cogn.* 21, 1016–1022. doi: 10.1016/j.concog.2012.01.008

Fuster, J. M. (2001). The prefrontal cortex–an update: time is of the essence. *Neuron* 30, 319–333. doi: 10.1016/s0896-6273(01)00285-9

Gu, F., Gong, A. M., Qu, Y., Bao, A. Y., Wu, J., Jiang, C. H., et al. (2022). From expert to elite? - research on top Archer's EEG network topology. *Front. Hum. Neurosci.* 16:759330. doi: 10.3389/fnhum.2022.759330

Guan, Y., Hao, Y., Guan, Y., and Wang, H. (2020). Effects of Tai Chi on essential hypertension and related risk factors: a meta-analysis of randomized controlled trials. *J. Rehab. Med.* 52:jrm00057. doi: 10.2340/16501977-2683

Hawkes, T. D., Manselle, W., and Woollacott, M. H. (2014). Tai Chi and meditation-plus-exercise benefit neural substrates of executive function: a cross-sectional, controlled study. *J. Complement. Integr. Med.* 11, 279–288. doi: 10.1515/jcim-2013-0031

He, H. L. (2012). "Study of offensive and defensive skills in martial arts education," in *Proceedings of the International Symposium on Sports Innovation and Development of Universities and Colleges*, Wuhan, 109–112.

Ji, S., Su, X., Xun, X., Bu, X., and Xu, Q. (2020). Study on brain function network of emotional conflict response in college students with anxiety. *Chin. J. Biomed. Eng.* 39, 145–151.

Jingfang, C., Yingying, L., and Hongyu, S. (2018). On the lmprovement of Sub-health status of contemporary college students by Taijiquan exercise prescription. *Wushu Stud.* 3, 61–63.

Kim, M. J., Gee, D. G., Loucks, R. A., Davis, F. C., and Whalen, P. J. (2011). Anxiety dissociates dorsal and ventral medial prefrontal cortex functional connectivity

with the amygdala at rest. *Cereb. Cortex* 21, 1667–1673. doi: 10.1093/cercor/bhq237

Lachaux, J. P., Rodriguez, E., Martinerie, J., and Varela, F. J. (1999). Measuring phase synchrony in brain signals. *Hum. Brain Mapp.* 8, 194–208. doi: 10.1002/(sici)1097-019319998:4<194::Aid-hbm4<3.0.Co;2-c

Laird, K. T., Paholpak, P., Roman, M., Rahi, B., and Lavretsky, H. (2018). Mind-body therapies for late-life mental and cognitive health. *Curr. Psychiatry Rep.* 20:2. doi: 10.1007/s11920-018-0864-4

Larkey, L., Jahnke, R., Etnier, J., and Gonzalez, J. (2009). Meditative movement as a category of exercise: implications for research. *J. Phys. Act. Health* 6, 230–238. doi: 10.1123/jpah.6.2.230

Li, H., Chen, J., Xu, G., Duan, Y., Huang, D., Tang, C., et al. (2020). The effect of Tai Chi for improving sleep quality: a systematic review and meta-analysis. *J. Affect. Disord.* 274, 1102–1112. doi: 10.1016/j.jad.2020.05.076

Li, L., Men, W.-W., Chang, Y.-K., Fan, M.-X., Ji, L., and Wei, G.-X. (2014). Acute aerobic exercise increases cortical activity during working memory: a functional MRI study in female college students. *PLoS One* 9:e99222. doi: 10.1371/journal.pone.0099222

Lin, M.-R., Hwang, H.-F., Wang, Y.-W., Chang, S.-H., and Wolf, S. L. (2006). Community-based tai chi and its effect on injurious falls, balance, gait, and fear of falling in older people. *Phys. Ther.* 86, 1189–1201. doi: 10.2522/ptj.20040408

Meng, C., Brandl, F., Tahmasian, M., Shao, J., Manoliu, A., Scherr, M., et al. (2014). Aberrant topology of striatum's connectivity is associated with the number of episodes in depression. *Brain* 137, 598–609. doi: 10.1093/brain/awt290

Mognon, A., Jovicich, J., Bruzzone, L., and Buiatti, M. (2011). ADJUST: an automatic EEG artifact detector based on the joint use of spatial and temporal features. *Psychophysiology* 48, 229–240. doi: 10.1111/j.1469-8986.2010.01061.x

Pan, Z. J., Su, X. W., Fang, Q., Hou, L. J., Lee, Y. H., Chen, C. C., et al. (2018). The effects of Tai Chi intervention on healthy elderly by means of neuroimaging and EEG: a systematic review. *Front. Aging Neurosci.* 10:110. doi: 10.3389/fnagi.2018.00110

Russell, T. A., and Arcuri, S. M. (2015). A neurophysiological and neuropsychological consideration of mindful movement: clinical and research implications. *Front. Hum. Neurosci.* 9:282. doi: 10.3389/fnhum.2015.00282

Ryu, H. M., and Jung, K.-C. (2014). A meta-analysis on the intervention effects of various meditation types, such as yoga, buddhism, mindfulness, and combined-related meditation. *J. Arts Psychothr.* 10, 1–17.

Sergerie, K., Lepage, M., and Armony, J. L. (2006). A process-specific functional dissociation of the amygdala in emotional memory. *J. Cogn. Neurosci.* 18, 1359–1367. doi: 10.1162/jocn.2006.18.8.1359

Shang, Y. (2011). Estimation of the shortest average distance in bipartite networks with given density. *J. Phys. Soc. Japan* 80, 055001–055002.

Tan, Z. J. (2010). "On development of Chinese martial arts from the perspective of their functionsŠ evolution," in *Proceedings of the 21st Pan-Asian Congress of Sports and Physical Education*, Nanchang, 271–274.

Tao, J., Chen, X. L., Liu, J., Egorova, N., Xue, X. H., Liu, W. L., et al. (2017). Tai Chi Chuan and Baduanjin mind-body training changes resting-state low-frequency fluctuations in the frontal lobe of older adults: a resting-state fMRI study. *Front. Hum. Neurosci.* 11:514. doi: 10.3389/fnhum.2017.00514

Taya, F., Sun, Y., Thakor, N., and Bezerianos, A. (2014). "Information transfer efficiency during rest and task a functional connectome approach," in *Proceedings of the IEEE Biomedical Circuits and Systems Conference (BioCAS*, Lausanne, 101–104.

Wang, J., Lu, M., Fan, Y., Wen, X., Zhang, R., Wang, B., et al. (2016). Exploring brain functional plasticity in world class gymnasts: a network analysis. *Brain Struct. Funct.* 221, 3503–3519. doi: 10.1007/s00429-015-1116-6

Wang, X. F. (2002). Complex networks: topology, dynamics and synchronization. *Int. J. Bifurcat. Chaos* 12, 885–916. doi: 10.1142/s0218127402004802

Wang, Y., Taylor, L., Pearl, M., and Chang, L. S. (2004). Effects of Tai Chi exercise on physical and mental health of college students. *Am. J. Chin. Med.* 32, 453–459. doi: 10.1142/s0192415x04002107

Wayne, P. M., Walsh, J. N., Taylor-Piliae, R. E., Wells, R. E., Papp, K. V., Donovan, N. J., et al. (2014). Effect of Tai Chi on cognitive performance in older adults: systematic review and meta-analysis. *J. Am. Geriatr. Soc.* 62, 25–39. doi: 10.1111/jgs.12611

Wei, G.-X., Dong, H.-M., Yang, Z., Luo, J., and Zuo, X.-N. (2014). Tai Chi Chuan optimizes the functional organization of the intrinsic human brain architecture in older adults. *Front. Aging Neurosci.* 6:74. doi: 10.3389/fnagi.2014.00074

Xiaoyan, Z., and Yunbo, X. (2020). The dialectical thinking and development trend of fragmented reading among college students. *J. Anshan Norm. Univ.* 22, 95–98+103.

Yanxiao, R., Jiawen, Z., Yixin, H., Ruihan, L., and Yiran, S. (2021). Integration and construction: structural psychological stress of college students and its influencing factors. *PR World*29, 6–7.

Yao, D. (2001). A method to standardize a reference of scalp EEG recordings to a point at infinity. *Physiol. Meas.* 22, 693–711. doi: 10.1088/0967-3334/22/4/305

You, J. W. (2016). The relationship among college students' psychological capital, learning empowerment, and engagement. *Learn. Individ. Dif.* 49, 17–24. doi: 10.1016/j.lindif.2016.05.001

Zhang, M., Zhou, H., Liu, L., Feng, L., Yang, J., Wang, G., et al. (2018). Randomized EEG functional brain networks in major depressive disorders with greater resilience and lower rich-club coefficient. *Clin. Neurophysiol.* 129, 743–758. doi: 10.1016/j.clinph.2018.01.017

Conflict of Interest: The authors declare that the research was conducted in the absence of any commercial or financial relationships that could be construed as a potential conflict of interest.

Publisher's Note: All claims expressed in this article are solely those of the authors and do not necessarily represent those of their affiliated organizations, or those of the publisher, the editors and the reviewers. Any product that may be evaluated in this article, or claim that may be made by its manufacturer, is not guaranteed or endorsed by the publisher.

frontiers | Frontiers in Human Neuroscience

TYPE Original Research
PUBLISHED 03 August 2022
DOI 10.3389/fnhum.2022.927704

OPEN ACCESS

EDITED BY
John Martin,
City College of New York (CUNY),
United States

REVIEWED BY
Jens Bo Nielsen,
University of Copenhagen, Denmark
Supriyo Choudhury,
Institute of Neurosciences Kolkata
(I-NK), India

*CORRESPONDENCE
Freschta Zipser-Mohammadzada
Freschta.Zipser-
Mohammadzada@balgrist.ch

SPECIALTY SECTION
This article was submitted to
Motor Neuroscience,
a section of the journal
Frontiers in Human Neuroscience

RECEIVED 24 April 2022
ACCEPTED 15 July 2022
PUBLISHED 03 August 2022

CITATION
Zipser-Mohammadzada F, Conway BA,
Halliday DM, Zipser CM, Easthope CA,
Curt A and Schubert M (2022)
Intramuscular coherence during
challenging walking in incomplete
spinal cord injury: Reduced
high-frequency coherence reflects
impaired supra-spinal control.
Front. Hum. Neurosci. 16:927704.
doi: 10.3389/fnhum.2022.927704

Intramuscular coherence during challenging walking in incomplete spinal cord injury: Reduced high-frequency coherence reflects impaired supra-spinal control

Freschta Zipser-Mohammadzada[1]*, Bernard A. Conway[2], David M. Halliday[3,4], Carl Moritz Zipser[1], Chris A. Easthope[1,5], Armin Curt[1] and Martin Schubert[1]

[1]Spinal Cord Injury Center, Department of Neurophysiology, Balgrist University Hospital, Zurich, Switzerland, [2]Department of Biomedical Engineering, University of Strathclyde, Glasgow, United Kingdom, [3]Department of Electronic Engineering, University of York, York, United Kingdom, [4]York Biomedical Research Institute, University of York, York, United Kingdom, [5]Cereneo Foundation, Center for Interdisciplinary Research, Vitznau, Switzerland

Individuals regaining reliable day-to-day walking function after incomplete spinal cord injury (iSCI) report persisting unsteadiness when confronted with walking challenges. However, quantifiable measures of walking capacity lack the sensitivity to reveal underlying impairments of supra-spinal locomotor control. This study investigates the relationship between intramuscular coherence and corticospinal dynamic balance control during a visually guided Target walking treadmill task. In thirteen individuals with iSCI and 24 controls, intramuscular coherence and cumulant densities were estimated from pairs of Tibialis anterior surface EMG recordings during normal treadmill walking and a Target walking task. The approximate center of mass was calculated from pelvis markers. Spearman rank correlations were performed to evaluate the relationship between intramuscular coherence, clinical parameters, and center of mass parameters. In controls, we found that the Target walking task results in increased high-frequency (21–44 Hz) intramuscular coherence, which negatively related to changes in the center of mass movement, whereas this modulation was largely reduced in individuals with iSCI. The impaired modulation of high-frequency intramuscular coherence during the Target walking task correlated with neurophysiological and functional readouts, such as motor-evoked potential amplitude and outdoor mobility score, as well as center of mass trajectory length. The Target walking effect, the difference between Target and Normal walking intramuscular coherence, was significantly higher in controls than in individuals with iSCI [$F(1.0,35.0) = 13.042$, $p < 0.001$]. Intramuscular coherence obtained during challenging walking in individuals with iSCI may provide information on

corticospinal gait control. The relationships between biomechanics, clinical scores, and neurophysiology suggest that intramuscular coherence assessed during challenging tasks may be meaningful for understanding impaired supra-spinal control in individuals with iSCI.

KEYWORDS

spinal cord injury, EMG-EMG coherence, intramuscular coherence, gait, visually guided walking, motor control, balance control, center of mass

Introduction

Human walking involves complex stereotyped motion sequences that are continuously adjusted to environmental demands that challenge progression. The integration of multimodal sensory inputs and supra-spinal commands, including visuomotor control, are required to achieve effective adaptive and controlled stepping (Rossignol et al., 2006; Matthis et al., 2017; Pearcey and Zehr, 2019). The supra-spinal and multimodal sensory command processes fail to be properly conducted to and between spinal cord levels following spinal cord injury or degeneration affecting spinal cord tracts. Yet while many individuals with incomplete spinal cord injury (iSCI) can regain walking ability, limb- and balance coordination are impaired (Barbeau et al., 2006; Awai and Curt, 2014; Easthope et al., 2018; Malik et al., 2019), resulting in reduced capacity to adapt to challenging walking when precision in foot placement is a requirement (e.g., walking over irregular surfaces) (Leroux et al., 1999; Desrosiers et al., 2014; Mohammadzada et al., 2022). Whilst such functional deficits are a consequence of spinal tract damage, the integrity of supra-spinal control of human gait is difficult to assess, and the neural mechanisms of visuomotor coordination during gait in individuals with iSCI remain poorly understood.

During outdoor walking on uneven terrain, continuous visuomotor and proprioceptive integration is needed for reactive and anticipatory gait adjustments (Marigold et al., 2011). Individuals with iSCI may utilize different adaptation strategies compared to controls, as shown in studies investigating individuals with iSCI during obstructed walking (Leroux et al., 1999; Ladouceur et al., 2003) and this is likely to be attributed to impaired transmission of descending neural drive to the muscles, which can be assessed non-invasively with coherence analysis (Halliday et al., 1995). Coherence measures provide an estimate of a coupled relationship between two simultaneously recorded signals in terms of common coherent components (Plankar et al., 2013). Corticomuscular coherence represents a coupling feature between muscle activity and cortical activity (Conway et al., 1995), while intermuscular coherence quantifies the coupling or common drive between two separate muscles. Intramuscular coherence quantifies the shared common drive occurring within the active motor units of the same muscle. Coherence analysis can serve as a reliable method to explore sensorimotor integration non-invasively by observing changes in specific physiologically relevant frequency bands. While intra- and intermuscular coherence in the alpha-band (8–12 Hz) is debated to have its origin in spinal- and subcortical systems, as shown in studies analyzing intermuscular coherence in lower (Norton et al., 2003) and upper limbs (Boonstra et al., 2009); the high-frequency bands, such as beta- (15–32) and gamma-band (35–60 Hz), are associated with activation from supra-spinal systems and provide insight on descending influences to muscles during movements as shown in corticomuscular coherence studies investigating sensorimotor cortex contributions to the control of upper limb and in lower limb muscles during walking in neurological intact adults (Conway et al., 1995; Salenius et al., 1997; Halliday et al., 1998; Baker, 2007; Petersen et al., 2012).

In individuals with iSCI and stroke, intra- and intermuscular coherence between muscle pairs in the high-frequency bands are strongly reduced during regular treadmill walking compared to controls (Hansen et al., 2005; Nielsen et al., 2008; Barthélemy et al., 2010); similarly, in upper motor neuron disease, intermuscular coherence in the high-frequency band is either absent or reduced (Fisher et al., 2012). These findings suggest that an intact supra-spinal drive is needed for normal function. Accordingly, high-frequency coherence between and within co-active muscles may be an indicator for supra-spinal drive, notwithstanding that synchronizing contributions from other neural circuits not characterized by common frequency components in EMG records will not be observable (e.g., extrapyramidal motor system, reticulospinal, and ascending sensory tracts).

Precision motor tasks that demand and engage attention may increase coherence in the high-frequency band as shown in corticomuscular coherence studies of the sensorimotor cortex and the contralateral hand (Kristeva-Feige et al., 2002; Kristeva et al., 2007), possibly due to enhanced motor cortex task related contributions to the shaping of motor output (Drew et al., 1996, 2008), and planning of movements (Spedden et al., 2022). In the lower limb, an example of this is observed during visually guided walking where increased Tibialis anterior intramuscular

and corticomuscular beta- and gamma-band coherence is observed during the swing phase when compared to normal walking in a control cohort (Jensen et al., 2018; Spedden et al., 2019a). Thus, using a visually guided walking paradigm provides an opportunity to investigate the relationship between high-frequency coherence and adaptive locomotor capacity. By investigating a cohort of individuals with iSCI, we strive to understand to what extent spinal cord damage impacts high-frequency coherence and how this relates to the capacity for continuous locomotor adaptation in iSCI.

Therefore, our primary aim was to test the hypothesis that, compared to controls, modulation of high-frequency intramuscular coherence is reduced or lacking in individuals with iSCI when challenged with a visually guided Target walking task (TW). We further explored how high-frequency intramuscular coherence relates to kinematics and impairment of gait adaptation in individuals with iSCI to assess whether coherence measures can serve as a potential marker for the pathophysiological underpinnings of impaired gait adaptation.

Materials and methods

Participants

For this study, twenty-four controls without a history of neurological disease and thirteen individuals with iSCI from Balgrist University Hospital were recruited and provided written informed consent. Individuals were older than 18 years old, could stand without physical assistance for over 2 min, and were either in the subacute (3–6 months post-injury) or chronic (≥12 months post-injury) stage. All individuals with iSCI were required to have partially preserved or reacquired walking ability. Individuals were also included if they were dependent on walking aids for recreational activities (see **Table 1**). Individuals were not included when they had a neurological impairment other than iSCI or cognitive impairments liable to interfere with task performance. Both subacute and chronic individuals with iSCI were included in order to cover a broad range of walking abilities. The study was approved by the Zurich cantonal ethics Committee (BASEC-Nr. 2017-01780). All experiments were conducted in accordance with the current 2013 revision of the Declaration of Helsinki.

Recordings

Surface EMGs were recorded wirelessly from proximal (TAp) and distal (TAd) sites of the right Tibialis anterior muscle. Recording sites were prepared by carefully shaving, abrading, and disinfecting the skin areas of interest before attaching bipolar EMG adhesive hydrogel electrodes (Kendall, Covidien) and wireless EMG sensors (myon AG, Switzerland, 2 kHz sampling rate, 10 – 500 Hz bandpass filter).

Full-body kinematics were recorded using a passive infrared motion capture system (Vero, Vicon Motion Systems Ltd, Oxford, United Kingdom) operating at 100 Hz and processed in Nexus 2.2.3 (Vicon, Oxford, United Kingdom) and with custom-written MATLAB scripts (MATLAB R2017b) using 42 reflective markers placed on bony landmarks (diameter = 14 mm). For the step cycle identification, markers were placed on the heel and the second toe (metatarsal 2). The times of heel strike (HS) and toe off were calculated from the zero-crossing of heel and toe marker velocity (Zeni et al., 2008). Approximated center of mass (CoM) was defined as the midpoint between left posterior spina iliac to right anterior spina iliac and left anterior spina iliac to right posterior spina iliac (Havens et al., 2018; Bannwart et al., 2020).

Coherence analysis

EMG signals were processed with custom-written MATLAB scripts. Recordings were zero-phase bandpass filtered (10–500 Hz), full-wave rectified, and normalized to unit variance before analysis in the frequency and time domain. Full-wave rectification suppresses any information related to the motor unit action potential shape (Farmer and Halliday, 2014).

Intramuscular coherences were investigated between TAp and TAd during the entire gait cycle and analyzed with the Neurospec routines using Type 1 analysis (Halliday et al., 1995) (Neurospec 2.0[1]). A complete gait cycle was defined as one stride going from one HS to the next HS with the same leg. The discrete Fourier transform (DFT) was constructed from each non-overlapping stride with a DFT segment length of 4096 samples (4096 samples/2000 Hz = 2048 ms), with zero padding used for strides with fewer samples, resulting in a frequency resolution of 0.49 Hz. Coherence measures assess the linear association between two rectified EMG signals on a scale from 0 to 1 in the frequency domain. The coherence function is defined at frequency λ as

$$|R_{xy}(\lambda)|^2 = \frac{|f_{xy}(\lambda)|^2}{f_{xx}(\lambda) f_{yy}(\lambda)} \quad (1)$$

$f_{xy}(\lambda)$ denotes the cross-spectrum between EMG signals x and y. It is normalized by dividing it by the power spectrum of one EMG signal $f_{xx}(\lambda)$ multiplied by that of the other EMG signal $f_{yy}(\lambda)$. Estimates of the cumulant density function characterize the covariance of the signals in the time domain and give information related to the timing of shared inputs to the motor units contributing to the EMG recordings. It is defined

1 https://www.neurospec.org/

TABLE 1 Incomplete spinal cord injury demographics.

ID	Age (y)	Height (cm)	Sex (m/f)	Walking speed (m/s)		Mean step length (m)		Mean step width (m)		ML accuracy (cm)	AP accuracy (cm)	AIS	Level of injury	Time since injury (y)	Type of Injury	Total sensory score (right)	LEMS score		Max MEP (right TA)	Mean SCIM (max 8)	Walking aids
				NW	TW	NW	TW	NW	TW								R	L			
01	79	170	m	0.35	0.3	0.24	0.35	0.17	0.16	−1.5	4	D	L3	24	Traumatic	50	20	22	0.23	na	Yes
02	42	173	m	0.4	0.4	0.33	0.34	0.13	0.16	na	na	D	C3	1	Degenerative	90	25	25	0.9	5	No
03	65	175	m	1.2	1	0.58	0.45	0.09	0.18	−0.2	7.7	D	C4	1	Traumatic	112	25	25	0.43	6	No
04	57	176	m	0.8	0.8	0.52	0.39	0.09	0.16	−1.7	6.7	D	T4	0.3	Traumatic	71	25	25	0.39	7	No
06	36	180	m	0.8	0.8	0.53	0.43	0.17	0.19	−0.27	6	D	T7	5	Traumatic	112	25	25	0.05	5	No
07	69	167	f	0.6	0.6	0.36	0.40	0.19	0.2	−0.5	6.1	D	C5	6	Traumatic	102	23	23	0.09	3	No
09	48	182	m	0.9	0.8	0.58	0.40	0.15	0.17	−3	11.5	D	L3	18	Traumatic	100	24	24	0.94	7	No
10	58	163	f	0.8	0.6	0.54	0.41	0.14	0.18	−0.7	7.9	D	T4	2	Toxic	80	25	25	0.13	1	Yes
11	58	170	f	1	1	0.61	0.4	0.11	0.16	−1.3	9	D	T7	11	Degenerative	112	25	25	0.63	8	No
13	70	170	m	0.8	0.7	0.52	0.41	0.15	0.2	−2.4	7.6	D	T4	7	Tumor	112	25	25	0.38	4	No
14	66	170	m	0.8	0.7	0.44	0.39	0.15	0.16	−0.9	5.5	D	T3	14	Tumor	76	25	25	0.12	8	No
15	67	177	m	0.55	0.6	0.55	0.43	0.09	0.17	−1.7	1	D	L1	8	Tumor	94	19	16	0.31	6	Yes
16	54	184	m	0.7	0.6	0.55	0.4	0.14	0.16	−0.8	5.4	D	T12	6	Traumatic	90	25	25	0.2	5	No
Median	58	173		0.8	0.7	0.53	0.4	0.14	0.17	−1.1	6.4			6		94	25	25	0.31	5.5	
IQR	13	7.8		0.2	0.2	0.14	0.03	0.05	0.02	1.1	2.4			10		33	1.25	1.25	0.35	2.5	
Stats				$p = 0.02$		$p = 0.006$		$p < 0.001$													

y, years; m, male; f, female; NW, Normal walking; TW, Target walking; ML, medio-lateral; AP, anterio-posterior; AIS, American Spinal Injury Association (ASIA) impairment scale; LEMS, Lower extremities motor score; R, right; L, left; MEP, motor evoked potential; SCIM, spinal cord independence measure; na, not available; IQR, interquartile range; Stats, Statistics; paired wilcoxon test.

10.3389/fnhum.2022.927704

as the inverse Fourier transform of the cross-spectrum and is a function of time lag u

$$q_{xy}(u) = \int_{-\pi}^{\pi} f_{xy}(\lambda)\, e^{i\lambda u} d\lambda \quad (2)$$

A central peak around zero lag reflects the synchronous activity of populations of motor units and suggests the presence of common synaptic input to the motoneurons within the activated motor pool (Halliday et al., 1995, 2003).

Pooled coherence and cumulant density estimates

Pooled coherence and pooled cumulant density measures (Amjad et al., 1997) are helpful to assess systematic task-dependent modulations in the correlation pattern in the gait cycle across subjects (Halliday et al., 2003). Pooled estimates, thus, allow for inferences at the population level in each group, combining all data from each group in a single representative estimate. This study uses the modulation pattern of pooled coherence to determine the frequency bands of interest for further in-depth single-case analysis.

Clinical assessment

A neurological examination following International standards for neurological classification of spinal cord injury (Kirshblum et al., 2011) was performed at enrollment in individuals with iSCI. Motor-evoked potentials (MEPs) of the Tibialis anterior muscle were acquired from individuals in a supine position using single-pulse transcranial magnetic stimulation (TMS; Magstim-200, Magstim Company, Carmarthenshire, Wales, United Kingdom). A double cone coil was used to achieve focal stimulation of the vertex, and MEPs were recorded from the Tibialis anterior muscle with disposable surface EMG electrodes. The individuals were asked to relax and not voluntarily contract the Tibialis anterior muscle. Maximum stimulus output was set to evoke reproducible MEPs at maximum amplitude. In compliance with ethical guidelines, MEPs were not assessed in control participants to avoid unwarranted experimental measurements on volunteers.

Experimental set-up

Participants walked at a self-selected walking speed with their typical, comfortable footwear on a split-belt treadmill with two integrated, synchronized force plates (GRAIL, Gait Realtime Analysis Interactive Lab, Motek Medical B.V., Netherlands). The participants were secured with a harness and were allowed to hold the handrails if needed. The participants completed the TW and Normal walking (NW) tasks in random order.

Target walking

Target walking is a 3 min visually guided walking task requiring the participants to precisely step on to moving circular targets projected onto the treadmill belts. This task is in detailed explained and investigated previously (Mohammadzada et al., 2022) and summarized below.

The circular targets (10 cm diameter, white dots) were projected onto and in front of the right and left treadmill belt (**Figure 1**) and moved toward the participant at the speed of the treadmill belt. Thus, the targets evoked the impression of being stationary compared to the moving treadmill surface (Motek Forcelink, Amsterdam, Netherlands, version 3.34.1). The participants were able to anticipate upcoming targets over three to four step cycles, since the targets were presented with a lead-in of greater than two stride lengths (Matthis et al., 2017). Adjustments of step cycle length (randomly distributed between 40 and 80% of 0.8 m step length) and width (randomly distributed between 40% and 80% of 0.25 m step width) were required to successfully step on to the targets.

In addition to standard markers for gait analysis, foot placement was tracked by a 14 mm reflective marker placed on the base joint of the second toe – metatarsal 2 (MT2). Placement precision was calculated by the distance (error) from MT2 to the center of the target in anterior-posterior (AP) and medio-lateral (ML) directions. Stepping medially and posteriorly from the center of the target resulted in negative error values, whereas stepping laterally and anteriorly resulted in positive error values. Errors were calculated once per step at midstance and recorded for offline analysis; participants did not receive feedback on errors. Due to technical reasons, accuracy measures in the ML- and AP-direction were introduced from participant 15 onward (see **Table 2**). Before data collection commenced, participants were provided with a 1 min task familiarization period.

Normal walking

For the Normal walking condition, participants were asked to look straight ahead and sustain a comfortable self-selected walking speed over a 3 min period in the absence of any projected visual targets.

Statistical analysis

Pooled coherence analyses were performed in order to observe correlation patterns across subjects within each group. Upper and lower 95% confidence limits (CI) are constructed under the assumption of independence and considering the

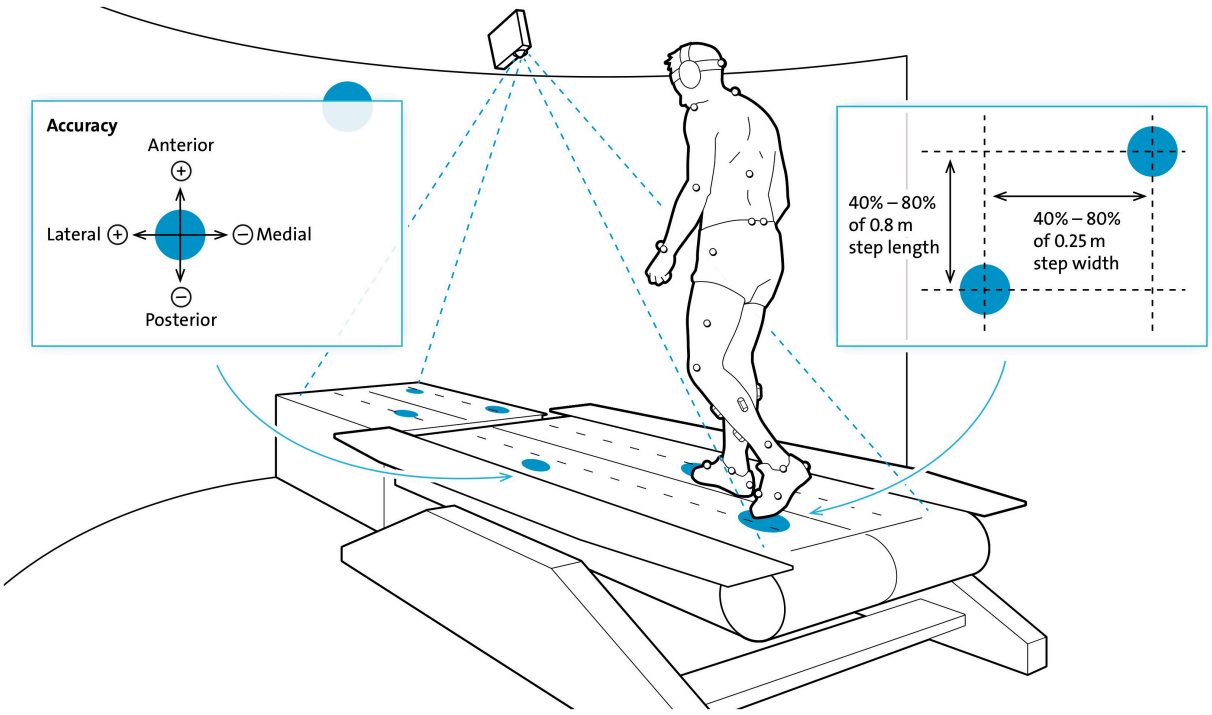

FIGURE 1
Experimental set-up for the Target walking task. Participants walked on moving white circular targets (diameter = 10 cm, here blue) projected on the black treadmill (here white) with their preferred walking speed. Circular targets moved at the same speed and thus, gave the impression of being stationary. Step length and width were changed based on a variability of 40–80% of 0.8 m and 40–80% of 0.25 m, respectively. Participants had to precisely step on to the center of the targets which was tracked by a reflective marker placed on the second toe. Accuracy of foot placement was recorded in the anterior-posterior (AP) and medio-lateral (ML) directions. The harness that was worn for safety and the handrails are not shown in this schematic figure of the Motek GRAIL treadmill system. Modified from Mohammadzada et al. (2022).

number of segments (L) (Halliday et al., 1995; Amjad et al., 1997):

$$CI = 1 - (0.05)^{1/(L-1)} \quad (3)$$

For pooled data, L denotes the combined number of segments across subjects. Additionally, the χ^2 extended difference of coherence test (Amjad et al., 1997) was used to explore differences at each frequency between tasks in each cohort. In the control cohort, we found that TW coherence was higher than NW coherence over the frequency range of 8–12 Hz (alpha band) and 21–44 Hz (high-frequency band). Single-subject coherence estimates were averaged from 8–12 to 21–44 Hz for each participant and used to examine intramuscular coherence at the single-subject level in both walking tasks. The high-frequency band from 21 to 44 Hz is of specific interest since it reflects supraspinal information which is transmitted to the motor neuron pools. The mean high-frequency and alpha band coherence estimates were used to investigate the relationships to clinical and biomechanical parameters.

Details on the biomechanical parameters, such as the 3-D CoM trajectory length $C_{AP-ML-V}$ and the mean Euclidean distance $D_{AP-ML-V}$, are reported in the **Supplementary methods**.

The primary outcome was defined as the modulation effect on intramuscular coherence estimates between TW and NW (TW effect) within iSCI individuals in contrast to controls.

The secondary outcome was the correlation between mean intramuscular coherence, clinical parameters, and CoM trajectory length in individuals with iSCI and controls. Finally, the TW effect, the subtraction of NW high-frequency and alpha coherence from TW high-frequency and alpha coherence, was used to correlate with the mean Euclidean distance between TW and NW and TW speed.

Statistical analyses were performed using Matlab (MATLAB R2017b) and SPSS (IBM SPSS Statistics for Macintosh, Version 27.0). Statistical significance was set at $\alpha = 0.05$. The Kolmogorov–Smirnov test was performed to assess data normality. Two repeated measures ANOVA's were performed separately for high-frequency and alpha band coherence with the within-subjects variable walking task and the between-subject variable group. For that, we used a variance stabilizing transform of the coherence by applying Fisher's transform $\tanh^{-1}$ to the magnitude coherency (Amjad et al., 1997).

TABLE 2 Participant demographics.

ID	Age (years)	Height (cm)	Sex (m/f)	Walking speed (m/s)		Mean step length (m)		Mean step width (m)		ML accuracy (cm)	AP accuracy (cm)
				NW	TW	NW	TW	NW	TW		
05	30	188	m	0.95	0.95	0.6	0.51	0.1	0.3	na	na
06	26	173	m	0.9	0.9	0.6	0.41	0.1	0.2	na	na
08	36	172	m	1.32	1.2	0.7	0.56	0.12	0.2	na	na
09	31	169	f	1.01	1	0.57	0.41	0.15	0.2	na	na
10	27	173	f	1.45	1	0.7	0.4	0.1	0.2	na	na
11	48	175	f	1	0.8	0.59	0.36	0.08	0.16	na	na
12	25	185	m	1.2	1.1	0.6	0.45	0.1	0.2	na	na
13	28	159	f	0.9	0.9	0.5	0.4	0.08	0.18	na	na
15	25	160	f	1.2	1.1	0.64	0.4	0.1	0.2	0.01	8.4
16	31	167	f	0.9	0.8	0.5	0.41	0.15	0.2	na	na
17	29	166	f	1.1	1.1	0.6	0.4	0.12	0.16	na	na
18	26	171	f	1.2	1	0.65	0.4	0.14	0.2	na	na
19	32	161	f	1	0.9	0.6	0.4	0.02	0.13	na	na
20	21	166	f	0.95	0.7	0.6	0.4	0.13	0.25	−0.5	6.7
21	32	168	m	0.95	0.9	0.58	0.41	0.13	0.23	−0.4	6.5
22	26	176	m	1.1	1	0.67	0.4	0.1	0.17	−0.6	7
23	31	150	f	0.8	0.7	0.51	0.42	0.13	0.2	0.2	5.1
24	29	174	m	1	0.9	0.54	0.4	0.13	0.19	0.2	8.4
25	27	173	m	1	0.9	0.58	0.4	0.1	0.19	−0.8	5.7
26	34	178	m	1.3	1.1	0.71	0.4	0.14	0.2	0.1	5.6
27	26	160	m	0.85	0.8	0.5	0.41	0.23	0.26	0.08	5.7
28	27	170	f	1.25	1	0.65	0.4	0.14	0.19	0.07	9.2
29	32	162	f	1	0.9	0.55	0.4	0.16	0.24	0.6	6
30	23	170	f	1	0.9	0.62	0.4	0.14	0.25	0.3	5.6
Median	28.5	170		1.0	0.9	0.6	0.4	0.12	0.2	0.08	6.3
IQR	5.5	9.5		0.25	0.1	0.1	0.01	0.04	0.04	0.7	2.1
Stats				$p < 0.001$		$p < 0.001$		$p < 0.001$			

m, male; f, female; NW, Normal walking; TW, Target walking; ML, medio-lateral; AP, anterio-posterior; na, not available; IQR, interquartile range; Stats, Statistics; paired wilcoxon test.

10.3389/fnhum.2022.927704

Non-paired Wilcoxon rank-sum tests between individuals with iSCI and controls were performed to investigate differences in CoM trajectory length in each task, and the mean Euclidean distance. Paired Wilcoxon tests were used to investigate differences in CoM trajectory length between NW and TW in individuals with iSCI and controls. The Chi-square test of Independence was used to test for sex differences. Descriptive statistics were also used to compare walking speed, step length and -width, and body height within and between controls and individuals. All reported *p*-values for the demographic and biomechanical data were Bonferroni-corrected per comparison group and reported in the results when significance was not met. Results are shown as the median and interquartile range (IQR). Spearman rank correlations were used to assess the relationship between (1) Mean TW coherence in the (21–44 Hz) high-frequency and alpha (8–12 Hz) band and Max MEP amplitude, (2) Mean TW coherence in the high-frequency and alpha band and mean spinal cord independence measure (SCIM) outdoor score, (3) TW effect (TW – NW high-frequency/alpha coherence) and TW speed, (4) TW effect, mean 3-D Euclidean distance, and (5) mean high-frequency/alpha coherence and 3-D CoM trajectory length. SCIM outdoor score was averaged from the acute to the chronic stage to account for the amount of recovery during rehabilitation.

Results

Recruitment

Thirteen participants with subacute or chronic iSCI (ten males; median age 58 years, IQR = 13; one subacute, twelve chronic; see **Table 1**) and twenty-four controls (14 females; median age 28.5 years, IQR = 5.5; see **Table 2**) were enrolled in this study. Individuals with iSCI were older than controls ($T = 400$, $n = 37$, $z = 4.88$, $p < 0.0001$, $r = 0.8$) and sex differences were found between the groups [$\chi^2(1) = 4.22$, $p = 0.04$]. Three iSCI participants who made use of walking aids in everyday walking activity held handrails during both treadmill walking tasks (P01, P10, P15; **Table 1**). Control participants did not require the use of handrails.

Two individuals with iSCI (not listed in **Table 1**) were excluded from the analysis due to missing TW data in one case and inconsistent usage of aids during tasks in the other individual. Details on gait parameters are reported in the **Supplementary Results**.

Modulation of intramuscular coherence

Pooled coherence estimates in **Figure 2A** provide a general summary of the correlation structure in each cohort and task. In the control cohort, we obtained larger coherence magnitudes during TW than NW over the 8–12 Hz and 21–44 Hz range (**Figure 2A**, left upper panel) ($p < 0.05$), whereas in the iSCI cohort no differences were obtained between TW and NW (**Figure 2A**, right upper panel) ($p > 0.05$). Furthermore, lower intramuscular coherence magnitudes were obtained in the iSCI cohort compared to the control cohort. The cumulant density structure (**Figure 2A**, lower panel, second from left) in controls displayed secondary rhythmic peaks at –58/+62 ms for NW and TW and ±30 ms for TW, consistent with the corresponding periodicities of 17.2/16.1 and 33.3 Hz, respectively, found in the coherence plot (**Figure 2A**, left upper panel) and were accompanied by the enhanced central peak at time lag 0 ms (Halliday et al., 1995). In the iSCI cohort, the cumulant density structure for NW showed secondary peaks at ± 190 ms and –310 ms, corresponding to 5.3 and 3.2 Hz, respectively, accompanied by a central peak at time lag 0 ms (**Figure 2A**, lower panel, third from left). The TW effect (calculated by subtracting mean NW coherence from mean TW coherence in the high-frequency band in single participants) was significantly higher in healthy controls compared to individuals with iSCI ($T = 44$, $n = 37$, $z = -3.56$, $p < 0.001$, $r = -0.59$). To illustrate this, examples of the analysis obtained from a control and two individuals with iSCI are given below (**Figure 2B**) and how variation in coherence measures across the iSCI group relates to clinical assessment is explored in the next sections (**Figures 3**, **4**). In a single control (Control 24, **Figure 2Ba**), who showed a median TW effect, we found an enhanced modulation of intramuscular coherence in the 21–44 Hz range. This modulation was also reflected in the respective EMG power spectra and the cumulant had a clear sharp peak at time lag 0 ms. Such enhanced modulation of intramuscular coherence in the frequency band 21–44 Hz was lacking or reduced to various degrees in individual individuals with iSCI (**Figures 2Bb,c**): While iSCI 09 (**Figure 2Bb**) showed increased intramuscular coherence during TW compared to NW with a pointed peak in the cumulant density plot at time lag 0 ms, iSCI 10 (**Figure 2Bc**) showed little intramuscular coherence for TW and NW and the cumulant density plot was broader compared to that of iSCI 09 and Control 24. The repeated measures ANOVA with a Greenhouse–Geisser correction determined that TW high-frequency coherence was significantly higher than NW high-frequency coherence [$F(1.0,35.0) = 25.705$, $p < 0.001$]. Furthermore, there was a statistically significant interaction between TW and NW high-frequency coherence and group [$F(1.0,35.0) = 13.042$, $p < 0.001$]. The repeated measures ANOVA with a Greenhouse–Geisser correction determined that TW alpha band coherence was significantly higher than NW alpha band coherence [$F(1.0,35.0) = 17.147$, $p < 0.001$]. However, there was no statistically significant interaction between TW and NW alpha band coherence and group [$F(1.0,35.0) = 3.266$, $p = 0.079$]. Thus, the change observed between TW and NW alpha band

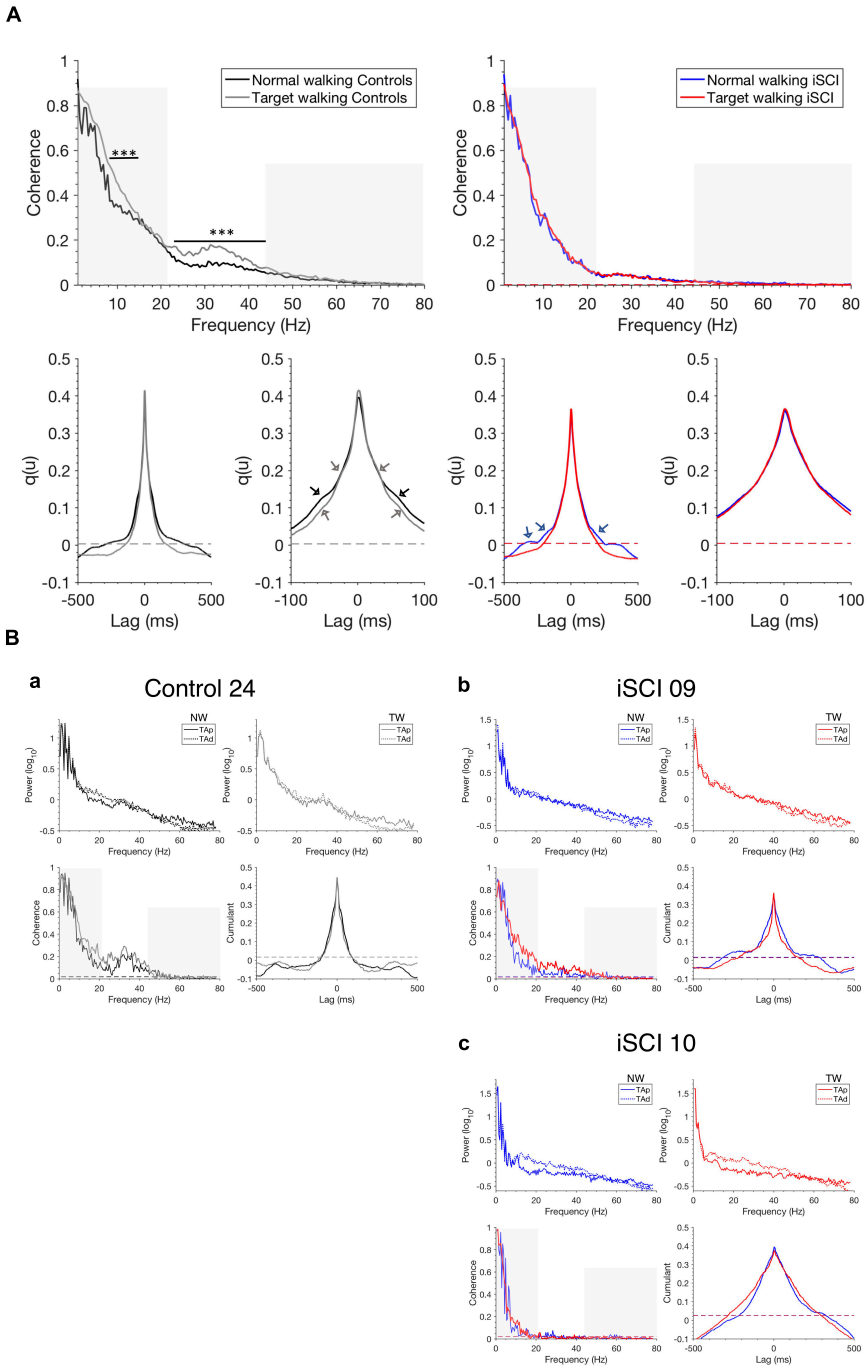

FIGURE 2
Pooled coherence estimates, single-participant coherence, and cumulant densities during walking. **(A)** Pooled TAp-TAd coherence estimates for controls during NW (black) and TW (gray) (top left) and individuals with iSCI during NW (blue) and TW (red) (top right) and the corresponding cumulants are shown (bottom with expanded lag scales in second and fourth position). The non-shaded area indicates the high-frequency range (21–44 Hz) of interest. The pooled cumulant densities are zoomed to allow for better visualization of secondary features (see arrows). Dashed horizontal lines indicate the upper 95% confidence interval limits. **(B)** Single TAp-TAd coherence estimates, power spectra and cumulant densities for **(a)** a control (Control 24) who shows a median effect of increased mean high-frequency intramuscular coherence (non-shaded area) during TW compared to NW. iSCI 09 **(b)** shows high mean high-frequency coherence (non-shaded area) during TW while iSCI 10 **(c)** shows the lowest mean high-frequency coherence (non-shaded area) during TW. Dashed horizontal lines indicate the upper 95% confidence interval limits. The non-shaded area in the single coherence estimates presents the frequency range of interest 21–44 Hz. Note that the *y*-scale is different for the power spectra in **(Ba–c)**. iSCI, incomplete spinal cord injury; TAp, Tibialis anterior proximal; TAd, Tibialis anterior distal; NW, Normal walking; TW, Target walking. ***$P < 0.001$.

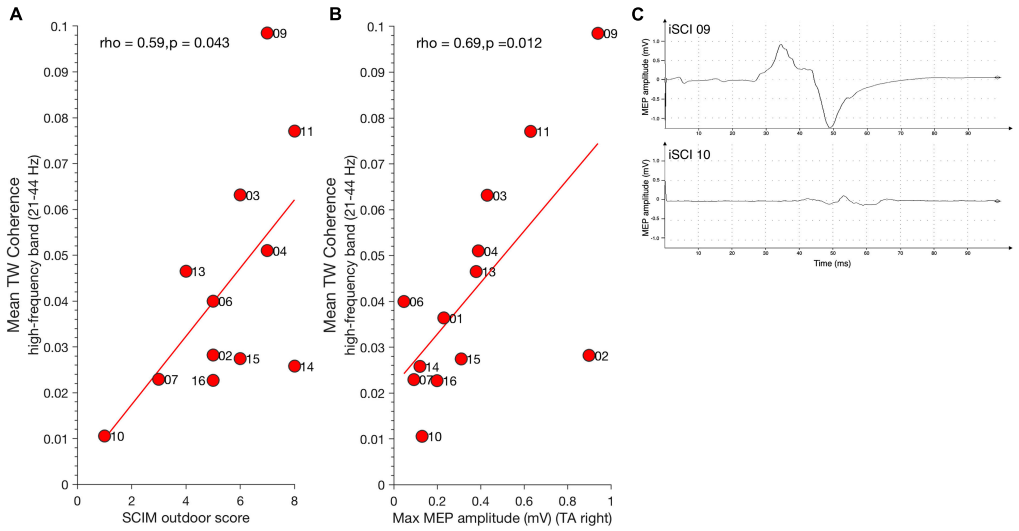

FIGURE 3
Relationship between high-frequency coherence and clinical parameters. **(A)** Mean SCIM outdoor mobility score positively correlates with high-frequency coherence during TW. **(B)** Maximum MEP amplitude of Tibialis anterior muscle (TA) positively correlates with high-frequency coherence during TW. Dots represent individuals with iSCI and their ID. **(C)** Examples for MEP traces of iSCI 09 (top) who has a high MEP amplitude and high mean high-frequency coherence value and iSCI 10 (bottom) who has low a MEP amplitude and low mean high-frequency coherence value. iSCI, incomplete spinal cord injury; MEP, magnetic evoked potential; SCIM, spinal cord Independence measure; TAp, Tibialis anterior proximal; TAd, Tibialis anterior distal; TA, Tibialis anterior muscle; TW, Target walking.

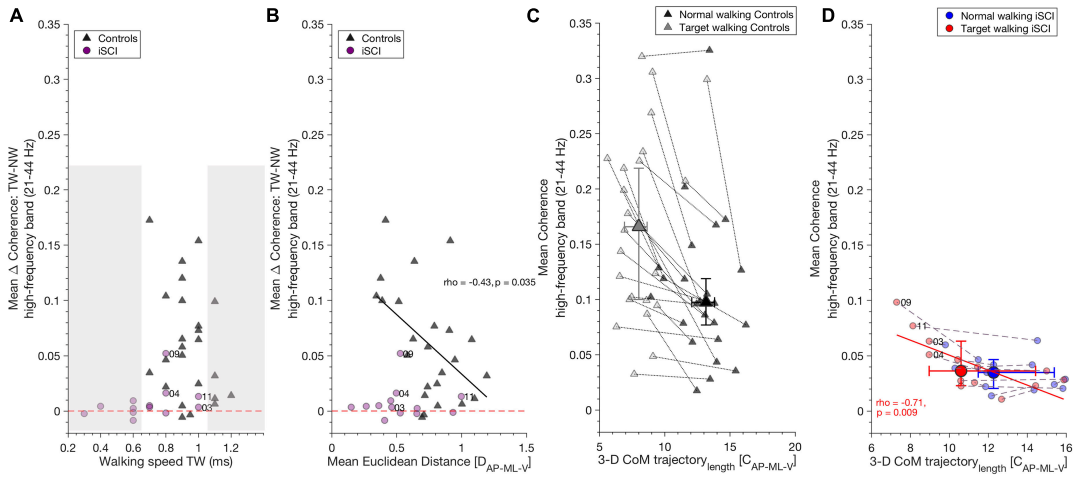

FIGURE 4
High-frequency coherence is related to gait parameters. **(A)** TW speed did not influence increased high-frequency coherence during TW compared to NW, as shown by the TW effect (Target walking – Normal walking): iSCI (purple dots) and controls (dark gray triangles) increased high-frequency band coherence independent of their walking speed in TW. The non-shaded area depicts iSCI and controls with the same walking speeds. Dashed red line indicates the zero value and distinguishes positive and negative TW effects. **(B)** In controls, increase of high-frequency coherence during TW as shown by TW effect (Target walking – Normal walking) correlated negatively with mean Euclidean distance, whereas in iSCI no correlation was found. Thus, controls who were able to adapt their gait pattern during TW showed decreased TW effect compared to those controls who adapted their gait pattern to a lesser extent. Dashed red line, dots and triangles as in **(A)**. **(C)** A reduction of 3-D CoM trajectory length along with an increase in high-frequency coherence is a typical mechanism found during TW in controls but there is no significant relationship between these parameters. **(D)** However, in individuals with iSCI, 3-D CoM trajectory length during TW negatively correlates with mean TW high-frequency coherence in (red dots). No such relationship was found during NW in individuals with iSCI (blue dots). Gray dotted lines and purple dashed lines connect NW and TW for each control and iSCI, respectively. Dots (individuals with iSCI) and triangles (controls) represent single participants and their ID. Large dots and triangles depict the median and their 95% confidence intervals. iSCI's ID's are shown for the skilled or less affected individuals. CoM, center of mass; iSCI, incomplete spinal cord injury; NW, Normal walking; TAp, Tibialis anterior proximal; TAd, Tibialis anterior distal; TW, Target walking. Spearman's rho and *p*-values are presented where significant; regression lines and 95% confidence limits are omitted for clarity.

coherence does not depend on the type of group and further analyses on the alpha band coherence should be interpreted cautiously.

Relationship between coherence and clinical/neurophysiological parameters in individuals with incomplete spinal cord injury

Spinal cord independence measure outdoor mobility score positively correlated with mean TW high-frequency coherence (21–44 Hz) [spearman's $\rho(11) = 0.59$, $p = 0.043$] (**Figure 3A**) but not with mean NW high-frequency coherence [spearman's $\rho(11) = 0.56$, $p = 0.059$]. Thus, individuals with high mean SCIM outdoor scores exhibited greater high-frequency coherence in the TW condition. Significant mean high-frequency coherence estimates obtained during TW correlated positively with maximum MEP amplitude of the right Tibialis anterior muscle [spearman's $\rho(11) = 0.69$, $p = 0.012$] (**Figure 3B**). This is in line with observations previously demonstrating a relationship between MEP amplitude, Tibialis anterior coherence, and ankle dorsiflexion during the swing phase of walking in individuals with iSCI (Barthélemy et al., 2010). There was no relationship between TW high-frequency coherence modulation and MEP latency [spearman's $\rho(11) = -0.36$, $p = 0.224$]. **Figure 3C** shows examples of one iSCI individual with a relatively high MEP amplitude and high-frequency coherence (iSCI 09, top) and another iSCI individual with low MEP amplitude and high-frequency coherence (iSCI 10, bottom). High-frequency coherence obtained in NW did not correlate with MEP amplitude [spearman's $\rho(11) = 0.55$, $p = 0.053$] and latency [spearman's $\rho(11) = -0.26$, $p = 0.373$].

Motor-evoked potentials amplitude correlated positively with mean TW alpha band coherence (8–12 Hz) [$\rho(11) = 0.74$, $p = 0.006$] but not with NW alpha band coherence [$\rho(11) = 0.07$, $p = 0.835$]. No significant correlation was found between mean alpha band coherence and MEP latency for TW [$\rho(11) = -0.33$, $p = 0.271$] and NW [$\rho(11) = 0.03$, $p = 0.935$]. Furthermore, no significant correlation was found between mean alpha band coherence and SCIM for TW [$\rho(11) = 0.24$, $p = 0.451$] and NW [$\rho(11) = 0.18$, $p = 0.582$].

To check whether TW effects are solely obtained for the high-frequency coherence (beta and gamma band, 21–44 Hz), we calculated the mean coherence in the low beta frequency range (13–21 Hz) for TW and NW. MEP amplitude was not correlated with mean low beta frequency coherence during TW [$\rho(11) = 0.44$, $p = 0.135$], nor during NW [$\rho(11) = 0.46$, $p = 0.119$].

High-frequency band coherence is related to gait parameters during Target walking

Target walking effect was calculated by subtracting mean NW coherence from mean TW coherence in the high-frequency band and alpha band (the resulting value describes the increase of coherence during TW).

Target walking speed in the control group or in iSCI did not influence the increase of high-frequency coherence seen during TW in controls [spearman's $\rho(22) = -0.24$, $p = 0.260$] or iSCI [spearman's $\rho(11) = 0.46$, $p = 0.11$] (**Figure 4A**) nor the increase of alpha band coherence during NW in controls [spearman's $\rho(22) = -0.06$, $p = 0.789$] or iSCI [spearman's $\rho(11) = 0.13$, $p = 0.66$]. As the non-shaded area indicates in **Figure 4A**, iSCI and controls with the same TW speed exhibited different TW effects. The mean Euclidean distance was negatively correlated with the TW effect of high-frequency coherence in controls [spearman's $\rho(22) = -0.43$, $p = 0.035$] (**Figure 4B**). Thus, controls who reduced their CoM movement in the TW task and obtained higher mean Euclidean distances between TW and NW exhibited lower TW effects (smaller coherence difference between TW and NW in the high-frequency band). Mean Euclidean distance did not affect TW effect in individuals with iSCI [spearman's $\rho(11) = -0.03$, $p = 0.92$]. The TW effect of alpha band coherence was not significantly correlated with the mean Euclidean distance in either controls [spearman's $\rho(22) = -0.11$, $p = 0.96$] or iSCI [spearman's $\rho(11) = 0.13$, $p = 0.682$].

A significant reduction of TW 3-D CoM trajectory length was observed during TW compared to NW in controls. However, no relationship was found with high-frequency coherence for either task [NW: spearman's $\rho(22) = -0.09$, $p = 0.673$; TW: spearman's rho$(22) = 0.12$, $p = 0.586$] (**Figure 4C**) or alpha band coherence [NW: spearman's $\rho(22) = -0.19$, $p = 0.371$; TW: spearman's rho$(22) = -0.13$, $p = 0.536$]. In individuals with iSCI, 3-D CoM trajectory length on average did not differ between the tasks. However, TW 3-D CoM trajectory length negatively correlated with mean high-frequency coherence during TW [spearman's $\rho(11) = -0.71$, $p = 0.009$] (**Figure 4D**). Thus, the individuals with iSCI who reduced their CoM trajectory length during TW generated greater high-frequency coherence. No significant relationship was found between NW high-frequency coherence and NW 3-D CoM trajectory length in individuals with iSCI [spearman's $\rho(11) = -0.43$, $p = 0.15$] (**Figure 4D**). The alpha band coherence during TW correlated negatively with TW 3-D CoM trajectory length [spearman's $\rho(11) = -0.62$, $p = 0.029$] but not during NW with NW 3-D CoM trajectory length [spearman's $\rho(11) = -0.25$, $p = 0.404$] in individuals with iSCI.

Accuracy in ML-direction differed ($T = 209.5$, $n = 24$, $z = 3.41$, $p = 0.0006$, $r = 0.7$) between individuals with iSCI

and controls, whereas no difference was found in AP-direction ($T = 151$, $n = 24$, $z = 0$, $p > 0.05$, $r = 0$).

Mean high-frequency band coherence did not correlate with task performance (accuracy) in controls [AP: spearman's $\rho(22) = -0.22$, $p = 0.499$, ML: spearman's $\rho(22) = 0.45$, $p = 0.14$] or individuals with iSCI [AP: spearman's $\rho(11) = 0.54$, $p = 0.075$, ML: spearman's $\rho(11) = -0.39$, $p = 0.210$] nor did the alpha band in controls [AP: spearman's $\rho(22) = -0.06$, $p = 0.85$, ML: spearman's $\rho(22) = -0.24$, $p = 0.46$] or individuals with iSCI [AP: spearman's $\rho(11) = 0.27$, $p = 0.40$, ML: spearman's $\rho(11) = -0.36$, $p = 0.256$].

Discussion

This study demonstrates that the magnitude of high-frequency (21–44 Hz) intramuscular coherence over the gait cycle is enhanced during TW and systematically related to adjustments affecting balance control in space (i.e., Euclidean distance between TW and NW) in a control group. However, in the iSCI cohort, high-frequency modulation was severely diminished, indicating impaired task adaptability. Interestingly, in iSCI individuals who regained reasonable skilled walking abilities, high-frequency coherence was preserved reflecting neural adaptability of gait potentiated during TW. This is the first experimental account of a correlation of high-frequency intramuscular coherence with biomechanical proxies for volitional gait adaptation and its systematic correlation with neurophysiological (MEP) and functional scores (self-reported walking performance in SCIM) in iSCI.

Intramuscular coherence during Target walking reflects visuomotor integration

In this study, TW is a proxy for complex outdoor walking where participants need to voluntarily modify their step length and width to accommodate obstacles and adjust the step cycle to the terrain (Dietz, 1992; Drew and Marigold, 2015).

Corticomuscular coherence in high-frequency bands, namely the beta and gamma spectra, is associated with supra-spinal input (Conway et al., 1995; Salenius et al., 1997; Brown et al., 1998; Petersen et al., 2012) as it is modulated by demanding tasks (Brown et al., 1998) requiring attention (Johnson et al., 2011) and precision (Kristeva-Feige et al., 2002). In support of this notion, increased corticomuscular coherence at 15–35 Hz has been observed after visuomotor skill training of the ankle dorsiflexor (Perez et al., 2006). In individuals with iSCI performing regular treadmill walking, previous studies have shown reduced or absent intramuscular TAp-TAd coherence in the high-frequency band, which was attributed to compromised descending motor input (Hansen et al., 2005; Barthélemy et al., 2010). In addition, in this study, the high-frequency coherence modulation as observed in the control subjects was not uniformly expressed in individuals with iSCI. In a majority of iSCI individuals, modulation was lacking during TW (for instance, iSCI 10), while it could be observed in some individuals (for instance, iSCI 09). Interestingly, the individual differences appear to relate to the capability of individuals to adjust their gait to challenging Targeted walking tasks. This finding is novel and expands on previous studies demonstrating the reduction of high-frequency coherence during NW in individuals with iSCI.

The results of the coherence analysis in the iSCI cohort are supported by cumulant estimates, which reveal variations in the size and width of the central peak. Both the central peak amplitude and width in the cumulant are indicative of time domain features that reveal variations in the degree and frequency content of descending inputs contributing to synchronization within the recorded Tibialis anterior EMG (Hansen et al., 2005).

In contrast to the high-frequency observations, the alpha band coherence change from NW to TW was not different between the groups. One reason for this may be that spinal interneurons that drive the spinal motoneurons remain functional in individuals with iSCI (Hansen et al., 2005).

Intramuscular coherence and its relationship to gait adaptability mechanisms in controls and individuals with incomplete spinal cord injury

Effective capacity to adapt gait to external demands can be assessed with the SCIM outdoor mobility score (van Hedel and Dietz, 2009). We found a positive correlation between mean SCIM outdoor score and high-frequency band coherence during TW in individuals with iSCI, indicating that coherence corresponds to self-experienced walking abilities. This is supported by previous results, showing that the ability to reduce the TW 3-D CoM trajectory length correlated with the mean SCIM outdoor mobility score (Mohammadzada et al., 2022). Walking speed is commonly used to quantify walking capacity in individuals with iSCI (van Hedel et al., 2007; van Silfhout et al., 2017) and was lower in individuals with iSCI than in controls. However, in this study, TW speed was unrelated to the increase of intramuscular high-frequency coherence during TW. This is an expected result as walking speed is generally represented by intramuscular coherence in low-frequency bands that capture features related to gait rhythm and the overall EMG burst envelope, while high-frequency features are generally considered to provide insight into common EMG activity features that occur within EMG bursts. Accordingly, the difference in TW speed between both groups cannot explain the difference in high-frequency

coherence found for individuals with iSCI and controls as demonstrated by iSCI and controls walking at similar TW speeds (see **Figure 4A**).

Adjustments of 3-D CoM movement to TW demand were assessed by estimating the mean Euclidean distance between TW and NW. We found that those controls showing high mean Euclidean distance by reducing 3-D CoM movement during TW exhibited smaller increases in high-frequency coherence, thus, smaller relative TW effects on coherence (see **Figure 4B**). As such, a reduction of CoM movement was also found for individuals with iSCI despite their lack of coherence increase; this may point to a strategy to adapt to the TW demands, which may not necessarily rely on an increment of common rhythmic central drive. It may nevertheless involve preserved capacity for supra-spinal control given iSCI's capability to reduce their CoM trajectory length during TW correlated negatively with TW high-frequency coherence (see TW in individuals with iSCI, **Figure 4D**). This suggests that TW provokes a higher demand on the common central drive through intact fibers of descending tracts to the muscles coupled to 3-D CoM trajectory length in some (less affected) individuals with iSCI (i.e., 03, 04, 09, 11). However, this may also indicate that the requirements necessary for the performance of a challenging walking task are coupled to anatomical and/or biomechanical constraints in individuals with iSCI. Thus, individuals with iSCI may be functionally restricted in their ability to adapt their walking pattern during TW due to impaired intralimb coordination, muscle weakness, proprioception (Awai and Curt, 2014), and level of injury (Mohammadzada et al., 2022).

Performance accuracy did not correlate with intramuscular TAp-TAd coherence. We assume that the mere demand of the task was enough to increase high-frequency and alpha band coherence, irrespective of how well the participants hit the target. Furthermore, intramuscular coherence when measured in Tibialis anterior alone may not be sensitive enough to detect minimal errors in ML direction and errors exaggerated in AP direction due to the nature of the task. Studies on the behavior of other muscle groups contributing to successful target hits, particularly in the ML direction are warranted.

The interplay of intramuscular coherence and motor-evoked potentials

In individuals with iSCI, high-frequency and alpha band coherence during TW positively correlated with MEP amplitude, which suggests that individuals with preserved corticospinal integrity adapt better to the challenging walking task.

It has been previously demonstrated that following locomotor training, individuals with iSCI with moderate muscle strength showed increases in maximum MEP size that correlated positively with 24-40 Hz coherence (Norton and Gorassini, 2006). The authors proposed that the increase in high-frequency (24–40 Hz) coherence may be mediated via spared corticospinal tract function in these individuals. Furthermore, as MEPs and intramuscular coherence in Tibialis anterior during early swing have been shown to be correlated with the degree of foot drop in single individuals with iSCI (Barthélemy et al., 2010), it is likely that in TW tasks, where precision in foot placement is a requirement, coherence modulation throughout swing is enhanced. The correlation to MEP amplitude was also present for the alpha band coherence during TW indicating that TW leads to an overall excitability change in neural systems that contribute to the generation of gait in iSCIs. However, in contrast to the high-frequency coherence, the difference between NW and TW alpha band coherence was not significant between the groups, suggesting that the former is a manifestation of mechanisms related to the TW task.

In our cohort, individuals 03, 04, 09, and 11 showed increased high-frequency band coherence during TW. We interpret this as an indication not only that a corticospinal innervation remains active in these individuals but that the innervation is capable of transmitting synchronizing inputs over the range of frequencies represented in the coherence results. In these individuals, TW may have recruited residual corticospinal drive, whilst in those individuals who failed to show enhanced high-frequency coherence together with small or delayed MEPs any residual corticospinal drive may be incapable of sustaining high-frequency synchronization within spinal motor pools. However, given the complex interplay of the corticospinal tract, the extrapyramidal motor system, reticulospinal, and ascending sensory tracts, their contribution to coherence needs to be further investigated. Seven out of 13 individuals with iSCI (01, 02, 04, 10, 14, 15, 16) had sensory scores lower than 100 points (max is 112), whereas the others had higher scores. Of those individuals with low sensory scores, the majority (5 out of 7; 02, 10, 14, 15, 16) had mean high-frequency TW coherence magnitudes lower than 0.03. This points toward an interrelation between sensory impairment and low levels of high-frequency coherence. Previous studies support this notion. For instance, modulation of afferent input via arm cooling has been shown to reduce beta-band corticomuscular coherence in hand- and arm muscles in some controls (Riddle and Baker, 2005). Similarly, digital nerve anesthesia of the hand muscle led to a decrease of beta-band intermuscular coherence in controls (Fisher et al., 2002). The lack of the afferent input also leads to a reduction of intermuscular coherence in the beta range (15–30 Hz) shown in studies investigating a deafferented patient (Kilner et al., 2004; Schmied et al., 2014).

Limitations

Incomplete spinal cord injury characteristics were different in terms of etiology, level of injury, and central and peripheral neurological pathologies. In addition, controls were neither sex-, age-, nor walking speed-matched.

Age may have affected the results, although its effects on intramuscular beta band coherence are ambiguous (Semmler et al., 2003; Jaiser et al., 2016; Spedden et al., 2018; Watanabe et al., 2018) and we found significant sex differences between the cohorts. Moreover, our results suggest that the decrease in intramuscular coherence during TW and NW is due to the individual's neurological impairment since similar results have been obtained in previous studies during NW (Hansen et al., 2005; Barthélemy et al., 2010).

The TW task was not adapted to individual step width and length, which may be comparable to challenges faced when walking outdoors in a natural environment and may similarly affect individuals with iSCI and controls. We are confident that the measurements and analysis conducted were not affected by cross-talk between the muscle pairs, which, if present, would be characterized by significant high-amplitude broad-band coherence and a narrow central peak in the cumulant density (Hansen et al., 2001; Halliday et al., 2003). CoM calculation was not based on a full-body marker set because reliable placement of the torso markers was prevented by the safety harness necessary for this iSCI population. Nevertheless, the approximated CoM model is well understood in its limitations (Gard et al., 2004; Süptitz et al., 2013; Havens et al., 2018).

Although the Tibialis anterior muscle is mainly active during the swing phase of gait, we analyzed intramuscular TAp-TAd coherence for the entire gait cycle. We were interested in the correlation pattern across the entire gait cycle since gait abnormalities in iSCI are not restricted to specific gait phases. However, extending the study to investigate intermuscular coherence between additional lower limb muscles during TW is warranted in order to determine which specific phases of the gait cycle increased high-frequency coherence contributes most. Furthermore, we aimed at investigating the dynamic relationship with the CoM parameters which considers the entire gait cycle as well. We further focused on the intramuscular coherence of the Tibialis anterior since this ankle dorsiflexor muscle is proposed to receive neural drive from supra-spinal systems as shown in controls (Schubert et al., 1997; Halliday et al., 2003; Spedden et al., 2019b) as well as pathological walking (Hansen et al., 2005; Nielsen et al., 2008). Spasticity, which may alter the walking pattern and -capacity in individuals with iSCI (Krawetz and Nance, 1996), was not assessed. The comparison to EEG-EMG coherence literature is limited, as frequency bands were determined in a data-driven approach and not through predefined ranges commonly used in EEG. Future studies are required to investigate the test-retest reliability of intramuscular coherence during TW, as one previous study pointed out limits of agreement and reliability under specific conditions during NW (van Asseldonk et al., 2014).

Conclusion

To our knowledge, this is the first study to demonstrate an interplay between intramuscular coherence and biomechanical features of gait, here quantified by CoM control. Individuals with iSCI generated less coherence in high-frequency bands during TW than controls whereas no difference was found for the alpha band. Furthermore, the extent of reduced modulated high-frequency coherence was related to MEP pathologies, biomechanical proxies for the gait disturbance, and self-reported walking performance (SCIM).

Thus, intramuscular coherence during TW could be used to quantify preserved supra-spinal control in individuals with iSCI since it quantifies subtle gait disturbances. Intramuscular coherence may provide a complementary insight into the recovery of gait function beyond gross motor scores (such as muscle strength and walking distances) where a targeted advancement of fine motor control may benefit gait rehabilitation strategies.

Data availability statement

The original contributions presented in this study are included in the article/**Supplementary material**, further inquiries can be directed to the corresponding author.

Ethics statement

The studies involving human participants were reviewed and approved by Zurich Cantonal Ethics Committee. The patients/participants provided their written informed consent to participate in this study.

Author contributions

FZ-M, CE, and MS designed the study. FZ-M, MS, CZ, CE, BC, DH, and AC assisted in data interpretation, manuscript preparation, and manuscript revision. FZ-M recruited participants and conducted measurements with assistance of CE. CZ and MS did the clinical assessment of

individuals with iSCI. FZ-M performed the data analysis and wrote the manuscript. All authors read and approved the final version of the manuscript.

Funding

This study was supported by Wings for Life grant WFL-CH-21/17 (CE).

Acknowledgments

We thank all individuals with iSCI and controls for their participation in this study. We also thank Charlotte Werner for her assistance during the measurements. This work was also supported by the Swiss Center for clinical Movement Analysis (SCMA), Balgrist Campus AG, Zürich, Switzerland, and the P&K Pühringer Foundation. **Figure 1** was modified from Mohammadzada et al. (2022) published in the Journal of NeuroEngineering and Rehabilitation, and BioMed Central is the original publisher. The article is licensed under Creative Commons Attribution License 4.0 (https://creativecommons.org/licenses/by/4.0/legalcode).

Conflict of interest

The authors declare that the research was conducted in the absence of any commercial or financial relationships that could be construed as a potential conflict of interest.

Publisher's note

Supplementary material

The Supplementary Material for this article can be found online at: https://www.frontiersin.org/articles/10.3389/fnhum.2022.927704/full#supplementary-material

References

Amjad, A. M., Halliday, D. M., Rosenberg, J. R., and Conway, B. A. (1997). An extended difference of coherence test for comparing and combining several independent coherence estimates: theory and application to the study of motor units and physiological tremor. *J Neurosci Methods* 73, 69–79. doi: 10.1016/s0165-0270(96)02214-5

Awai, L., and Curt, A. (2014). Intralimb coordination as a sensitive indicator of motor-control impairment after spinal cord injury. *Front Hum Neurosci* 8:148. doi: 10.3389/fnhum.2014.00148

Baker, S. N. (2007). Oscillatory interactions between sensorimotor cortex and the periphery. *Curr Opin Neurobiol* 17, 649–655.

Bannwart, M., Bayer, S. L., König Ignasiak, N., Bolliger, M., Rauter, G., and Easthope, C. A. (2020). Mediolateral damping of an overhead body weight support system assists stability during treadmill walking. *J Neuroeng Rehabil* 17, 108.

Barbeau, H., Nadeau, S., and Garneau, C. (2006). Physical determinants, emerging concepts, and training approaches in gait of individuals with spinal cord injury. *J Neurotrauma* 23, 571–585. doi: 10.1089/neu.2006.23.571

Barthélemy, D., Willerslev-Olsen, M., Lundell, H., Conway, B. A., Knudsen, H., Biering-Sørensen, F., et al. (2010). Impaired Transmission in the Corticospinal Tract and Gait Disability in Spinal Cord Injured Persons. *Journal of Neurophysiology* 104, 1167–1176.

Boonstra, T. W., Van Wijk, B. C., Praamstra, P., and Daffertshofer, A. (2009). Corticomuscular and bilateral EMG coherence reflect distinct aspects of neural synchronization. *Neurosci Lett* 463, 17–21. doi: 10.1016/j.neulet.2009.07.043

Brown, P., Salenius, S., Rothwell, J. C., and Hari, R. (1998). Cortical correlate of the Piper rhythm in humans. *J Neurophysiol* 80, 2911–2917.

Conway, B. A., Halliday, D. M., Farmer, S. F., Shahani, U., Maas, P., Weir, A. I., et al. (1995). Synchronization between motor cortex and spinal motoneuronal pool during the performance of a maintained motor task in man. *J Physiol* 489(Pt 3), 917–924. doi: 10.1113/jphysiol.1995.sp021104

Desrosiers, E., Duclos, C., and Nadeau, S. (2014). Gait adaptation during walking on an inclined pathway following spinal cord injury. *Clin Biomech (Bristol, Avon)* 29, 500–505. doi: 10.1016/j.clinbiomech.2014.04.004

Dietz, V. (1992). Human neuronal control of automatic functional movements: interaction between central programs and afferent input. *Physiol Rev* 72, 33–69. doi: 10.1152/physrev.1992.72.1.33

Drew, T., and Marigold, D. S. (2015). Taking the next step: cortical contributions to the control of locomotion. *Curr Opin Neurobiol* 33, 25–33. doi: 10.1016/j.conb.2015.01.011

Drew, T., Andujar, J. E., Lajoie, K., and Yakovenko, S. (2008). Cortical mechanisms involved in visuomotor coordination during precision walking. *Brain Res Rev* 57, 199–211. doi: 10.1016/j.brainresrev.2007.07.017

Drew, T., Jiang, W., Kably, B., and Lavoie, S. (1996). Role of the motor cortex in the control of visually triggered gait modifications. *Can J Physiol Pharmacol* 74, 426–442.

Easthope, C. S., Traini, L. R., Awai, L., Franz, M., Rauter, G., Curt, A., et al. (2018). Overground walking patterns after chronic incomplete spinal cord injury show distinct response patterns to unloading. *J Neuroeng Rehabil* 15, 102. doi: 10.1186/s12984-018-0436-1

Farmer, S. F., and Halliday, D. M. (2014). Reply to McClelland et al.: EMG rectification and coherence analysis. *J Neurophysiol* 111, 1151–1152.

Fisher, K. M., Zaaimi, B., Williams, T. L., Baker, S. N., and Baker, M. R. (2012). Beta-band intermuscular coherence: a novel biomarker of upper motor neuron dysfunction in motor neuron disease. *Brain* 135, 2849–2864. doi: 10.1093/brain/aws150

Fisher, R. J., Galea, M. P., Brown, P., and Lemon, R. N. (2002). Digital nerve anaesthesia decreases EMG-EMG coherence in a human precision grip task. *Exp Brain Res* 145, 207–214. doi: 10.1007/s00221-002-1113-x

Gard, S. A., Miff, S. C., and Kuo, A. D. (2004). Comparison of kinematic and kinetic methods for computing the vertical motion of the body center of mass during walking. *Hum Mov Sci* 22, 597–610. doi: 10.1016/j.humov.2003.11.002

Halliday, D. M., Conway, B. A., Christensen, L. O., Hansen, N. L., Petersen, N. P., and Nielsen, J. B. (2003). Functional coupling of motor units is modulated during walking in human subjects. *J Neurophysiol* 89, 960–968. doi: 10.1152/jn.00844.2002

Halliday, D. M., Conway, B. A., Farmer, S. F., and Rosenberg, J. R. (1998). Using electroencephalography to study functional coupling between cortical activity and electromyograms during voluntary contractions in humans. *Neurosci Lett* 241, 5–8.

Halliday, D. M., Rosenberg, J. R., Amjad, A. M., Breeze, P., Conway, B. A., and Farmer, S. F. (1995). A framework for the analysis of mixed time series/point process data–theory and application to the study of physiological tremor, single motor unit discharges and electromyograms. *Prog Biophys Mol Biol* 64, 237–278. doi: 10.1016/s0079-6107(96)00009-0

Hansen, N. L., Conway, B. A., Halliday, D. M., Hansen, S., Pyndt, H. S., Biering-Sorensen, F., et al. (2005). Reduction of common synaptic drive to ankle dorsiflexor motoneurons during walking in patients with spinal cord lesion. *J Neurophysiol* 94, 934–942. doi: 10.1152/jn.00082.2005

Hansen, N. L., Hansen, S., Christensen, L. O., Petersen, N. T., and Nielsen, J. B. (2001). Synchronization of lower limb motor unit activity during walking in human subjects. *J Neurophysiol* 86, 1266–1276.

Havens, K. L., Mukherjee, T., and Finley, J. M. (2018). Analysis of biases in dynamic margins of stability introduced by the use of simplified center of mass estimates during walking and turning. *Gait Posture* 59, 162–167. doi: 10.1016/j.gaitpost.2017.10.002

Jaiser, S. R., Baker, M. R., and Baker, S. N. (2016). Intermuscular Coherence in Normal Adults: Variability and Changes with Age. *PLoS One* 11:e0149029. doi: 10.1371/journal.pone.0149029

Jensen, P., Jensen, N. J., Terkildsen, C. U., Choi, J. T., Nielsen, J. B., and Geertsen, S. S. (2018). Increased central common drive to ankle plantar flexor and dorsiflexor muscles during visually guided gait. *Physiological Reports* 6, e13598. doi: 10.14814/phy2.13598

Johnson, A. N., Wheaton, L. A., and Shinohara, M. (2011). Attenuation of corticomuscular coherence with additional motor or non-motor task. *Clin Neurophysiol* 122, 356–363.

Kilner, J. M., Fisher, R. J., and Lemon, R. N. (2004). Coupling of oscillatory activity between muscles is strikingly reduced in a deafferented subject compared with normal controls. *J Neurophysiol* 92, 790–796. doi: 10.1152/jn.01247.2003

Kirshblum, S. C., Burns, S. P., Biering-Sorensen, F., Donovan, W., Graves, D. E., Jha, A., et al. (2011). International standards for neurological classification of spinal cord injury (revised 2011). *J Spinal Cord Med* 34, 535–546.

Krawetz, P., and Nance, P. (1996). Gait analysis of spinal cord injured subjects: effects of injury level and spasticity. *Arch Phys Med Rehabil* 77, 635–638. doi: 10.1016/s0003-9993(96)90000-3

Kristeva, R., Patino, L., and Omlor, W. (2007). Beta-range cortical motor spectral power and corticomuscular coherence as a mechanism for effective corticospinal interaction during steady-state motor output. *Neuroimage* 36, 785–792. doi: 10.1016/j.neuroimage.2007.03.025

Kristeva-Feige, R., Fritsch, C., Timmer, J., and Lucking, C. H. (2002). Effects of attention and precision of exerted force on beta range EEG-EMG synchronization during a maintained motor contraction task. *Clin Neurophysiol* 113, 124–131. doi: 10.1016/s1388-2457(01)00722-2

Ladouceur, M., Barbeau, H., and Mcfadyen, B. J. (2003). Kinematic adaptations of spinal cord-injured subjects during obstructed walking. *Neurorehabil Neural Repair* 17, 25–31. doi: 10.1177/0888439003251750

Leroux, A., Fung, J., and Barbeau, H. (1999). Adaptation of the walking pattern to uphill walking in normal and spinal-cord injured subjects. *Exp Brain Res* 126, 359–368. doi: 10.1007/s002210050743

Malik, R. N., Eginyan, G., Lynn, A. K., and Lam, T. (2019). Improvements in skilled walking associated with kinematic adaptations in people with spinal cord injury. *J Neuroeng Rehabil* 16, 107. doi: 10.1186/s12984-019-0575-z

Marigold, D. S., Andujar, J. E., Lajoie, K., and Drew, T. (2011). Chapter 6–motor planning of locomotor adaptations on the basis of vision: the role of the posterior parietal cortex. *Prog Brain Res* 188, 83–100. doi: 10.1016/B978-0-444-53825-3.00011-5

Matthis, J. S., Barton, S. L., and Fajen, B. R. (2017). The critical phase for visual control of human walking over complex terrain. *Proc Natl Acad Sci U S A* 114, E6720–E6729.

Mohammadzada, F., Zipser, C. M., Easthope, C. A., Halliday, D. M., Conway, B. A., Curt, A., et al. (2022). Mind your step: Target walking task reveals gait disturbance in individuals with incomplete spinal cord injury. *J Neuroeng Rehabil* 19, 36. doi: 10.1186/s12984-022-01013-7

Nielsen, J. B., Brittain, J. S., Halliday, D. M., Marchand-Pauvert, V., Mazevet, D., and Conway, B. A. (2008). Reduction of common motoneuronal drive on the affected side during walking in hemiplegic stroke patients. *Clin Neurophysiol* 119, 2813–2818. doi: 10.1016/j.clinph.2008.07.283

Norton, J. A., and Gorassini, M. A. (2006). Changes in cortically related intermuscular coherence accompanying improvements in locomotor skills in incomplete spinal cord injury. *J Neurophysiol* 95, 2580–2589. doi: 10.1152/jn.01289.2005

Norton, J. A., Wood, D. E., Marsden, J. F., and Day, B. L. (2003). Spinally generated electromyographic oscillations and spasms in a low-thoracic complete paraplegic. *Mov Disord* 18, 101–106. doi: 10.1002/mds.10298

Pearcey, G. E. P., and Zehr, E. P. (2019). We Are Upright-Walking Cats: Human Limbs as Sensory Antennae During Locomotion. *Physiology* 34, 354–364. doi: 10.1152/physiol.00008.2019

Perez, M. A., Lundbye-Jensen, J., and Nielsen, J. B. (2006). Changes in corticospinal drive to spinal motoneurones following visuo-motor skill learning in humans. *J Physiol* 573, 843–855. doi: 10.1113/jphysiol.2006.105361

Petersen, T. H., Willerslev-Olsen, M., Conway, B. A., and Nielsen, J. B. (2012). The motor cortex drives the muscles during walking in human subjects. *J Physiol* 590, 2443–2452.

Plankar, M., Brezan, S., and Jerman, I. (2013). The principle of coherence in multi-level brain information processing. *Prog Biophys Mol Biol* 111, 8–29. doi: 10.1016/j.pbiomolbio.2012.08.006

Riddle, C. N., and Baker, S. N. (2005). Manipulation of peripheral neural feedback loops alters human corticomuscular coherence. *J Physiol* 566, 625–639. doi: 10.1113/jphysiol.2005.089607

Rossignol, S., Dubuc, R., and Gossard, J.-P. (2006). Dynamic Sensorimotor Interactions in Locomotion. *Physiological Reviews* 86, 89–154.

Salenius, S., Portin, K., Kajola, M., Salmelin, R., and Hari, R. (1997). Cortical control of human motoneuron firing during isometric contraction. *J Neurophysiol* 77, 3401–3405.

Schmied, A., Forget, R., and Vedel, J. P. (2014). Motor unit firing pattern, synchrony and coherence in a deafferented patient. *Front Hum Neurosci* 8:746. doi: 10.3389/fnhum.2014.00746

Schubert, M., Curt, A., Jensen, L., and Dietz, V. (1997). Corticospinal input in human gait: modulation of magnetically evoked motor responses. *Exp Brain Res* 115, 234–246.

Semmler, J. G., Kornatz, K. W., and Enoka, R. M. (2003). Motor-unit coherence during isometric contractions is greater in a hand muscle of older adults. *J Neurophysiol* 90, 1346–1349. doi: 10.1152/jn.00941.2002

Spedden, M. E., Beck, M. M., West, T. O., Farmer, S. F., Nielsen, J. B., and Lundbye-Jensen, J. (2022). Dynamics of cortical and corticomuscular connectivity during planning and execution of visually guided steps in humans. *Cereb Cortex* doi: 10.1093/cercor/bhac066

Spedden, M. E., Choi, J. T., Nielsen, J. B., and Geertsen, S. S. (2019a). Corticospinal control of normal and visually guided gait in healthy older and younger adults. *Neurobiol Aging* 78, 29–41. doi: 10.1016/j.neurobiolaging.2019.02.005

Spedden, M. E., Jensen, P., Terkildsen, C. U., Jensen, N. J., Halliday, D. M., Lundbye-Jensen, J., et al. (2019b). The development of functional and directed corticomuscular connectivity during tonic ankle muscle contraction across childhood and adolescence. *Neuroimage* 191, 350–360. doi: 10.1016/j.neuroimage.2019.02.054

Spedden, M. E., Nielsen, J. B., and Geertsen, S. S. (2018). Oscillatory Corticospinal Activity during Static Contraction of Ankle Muscles Is Reduced in Healthy Old versus Young Adults. *Neural Plast* 2018, 3432649. doi: 10.1155/2018/3432649

Süptitz, F., Moreno Catalá, M., Brüggemann, G. P., and Karamanidis, K. (2013). Dynamic stability control during perturbed walking can be assessed by a reduced kinematic model across the adult female lifespan. *Hum Mov Sci* 32, 1404–1414. doi: 10.1016/j.humov.2013.07.008

van Asseldonk, E. H., Campfens, S. F., Verwer, S. J., Van Putten, M. J., and Stegeman, D. F. (2014). Reliability and agreement of intramuscular coherence in tibialis anterior muscle. *PLoS One* 9:e88428. doi: 10.1371/journal.pone.0088428

van Hedel, H. J., and Dietz, V. (2009). Walking during daily life can be validly and responsively assessed in subjects with a spinal cord injury. *Neurorehabil Neural Repair* 23, 117–124. doi: 10.1177/1545968308320640

van Hedel, H. J., Dietz, V., and Curt, A. (2007). Assessment of walking speed and distance in subjects with an incomplete spinal cord injury. *Neurorehabil Neural Repair* 21, 295–301.

van Silfhout, L., Hosman, A. J. F., Bartels, R., Edwards, M. J. R., Abel, R., Curt, A., et al. (2017). Ten Meters Walking Speed in Spinal

Cord-Injured Patients: Does Speed Predict Who Walks and Who Rolls? *Neurorehabil Neural Repair* 31, 842–850. doi: 10.1177/1545968317723751

Watanabe, T., Saito, K., Ishida, K., Tanabe, S., and Nojima, I. (2018). Coordination of plantar flexor muscles during bipedal and unipedal stances in young and elderly adults. *Exp Brain Res* 236, 1229–1239. doi: 10.1007/s00221-018-5217-3

Zeni, J. A. JR., Richards, J. G., and Higginson, J. S. (2008). Two simple methods for determining gait events during treadmill and overground walking using kinematic data. *Gait Posture* 27, 710–714. doi: 10.1016/j.gaitpost.2007.07.007

frontiers | Frontiers in Human Neuroscience

TYPE Original Research
PUBLISHED 14 October 2022
DOI 10.3389/fnhum.2022.1002793

OPEN ACCESS

EDITED BY
Stephane Perrey,
Université de Montpellier, France

REVIEWED BY
Oliver Seidel-Marzi,
Friedrich Schiller University Jena, Germany
Kanwal Preet Kochhar,
All India Institute of Medical Sciences, India

*CORRESPONDENCE
Hao Wu
wuhao@cupes.edu.cn
Jie Yang
LDDXTY@126.com

SPECIALTY SECTION
This article was submitted to Motor Neuroscience, a section of the journal Frontiers in Human Neuroscience

RECEIVED 29 July 2022
ACCEPTED 28 September 2022
PUBLISHED 14 October 2022

CITATION
Song Q, Cheng X, Zheng R, Yang J and Wu H (2022) Effects of different exercise intensities of race-walking on brain functional connectivity as assessed by functional near-infrared spectroscopy.
Front. Hum. Neurosci. 16:1002793.
doi: 10.3389/fnhum.2022.1002793

Effects of different exercise intensities of race-walking on brain functional connectivity as assessed by functional near-infrared spectroscopy

Qianqian Song[1,2], Xiaodong Cheng[1], Rongna Zheng[3], Jie Yang[3]* and Hao Wu[1]*

[1]Capital University of Physical Education and Sports, Beijing, China, [2]School of Physical Education, Yanshan University, Qinhuangdao, China, [3]School of Physical Education, Ludong University, Yantai, China

Introduction: Race-walking is a sport that mimics normal walking and running. Previous studies on sports science mainly focused on the cardiovascular and musculoskeletal systems. However, there is still a lack of research on the central nervous system, especially the real-time changes in brain network characteristics during race-walking exercise. This study aimed to use a network perspective to investigate the effects of different exercise intensities on brain functional connectivity.

Materials and methods: A total of 16 right-handed healthy young athletes were recruited as participants in this study. The cerebral cortex concentration of oxyhemoglobin was measured by functional near-infrared spectroscopy in the bilateral prefrontal cortex (PFC), the motor cortex (MC) and occipital cortex (OC) during resting and race-walking states. Three specific periods as time windows corresponding to different exercise intensities were divided from the race-walking time of participants, including initial, intermediate and sprint stages. The brain activation and functional connectivity (FC) were calculated to describe the 0.01-0.1 Hz frequency-specific cortical activities.

Results: Compared to the resting state, FC changes mainly exist between MC and OC in the initial stage, while PFC was involved in FC changes in the intermediate stage, and FC changes in the sprint stage were widely present in PFC, MC and OC. In addition, from the initial-development to the sprint stage, the significant changes in FC were displayed in PFC and MC.

Conclusion: This brain functional connectivity-based study confirmed that hemodynamic changes at different exercise intensities reflected different brain network-specific characteristics. During race-walking exercise, more extensive brain activation might increase information processing speed. Increased exercise intensity could facilitate the integration of neural signals

such as proprioception, motor control and motor planning, which may be an important factor for athletes to maintain sustained motor coordination and activity control at high intensity. This study was beneficial to understanding the neural mechanisms of brain networks under different exercise intensities.

KEYWORDS

functional near-infrared spectroscopy, race-walking, exercise intensity, brain activation, functional connectivity

Introduction

Race-walking is a sport that mimics normal walking and running. The rules for this event, set by the International Association of Athletics Federations, require that the supporting leg remains straight at first contact with the ground until the body passes over the sole. In addition, the toes of the back foot should not leave the ground until the heel of the front foot touches the ground to ensure that both feet are not off the ground at the same time. In addition, the rules require the athlete to present a straightened knee from initial contact to the "vertical upright position" and no visible loss of contact. These rules distinguish race-walking from walking and running, making race-walking possesses a unique locomotor strategy different from other sports (Zhang et al., 2019). Physiological studies had shown that race-walking has higher restricted joint biomechanics and muscle energy costs than running (Cronin et al., 2016; Gomez-Ezeiza et al., 2019). Therefore, investigating the motor mechanisms of race-walking might be crucial for practitioners of this discipline.

The race-walking process is controlled by both peripheral and central systems. Traditionally, sports science focused on the effects of the exercise on cardiovascular and musculoskeletal systems. For example, the speed and distance of exercise is determined by the number of motor units that are recruited in our exercising limbs (Katz, 2010), the quality of the muscle fibers that produce force (Rae et al., 2010), and the size of the maximal cardiac output (Levine, 2008; Shephard, 2009). However, the theory that motor performance is primarily limited by the changes in cardiovascular and skeletal muscle metabolism has been generally questioned. With the fatigue development in the peripheral muscle fibers, the brain must regulate additional fresh fibers as compensation to assist those fatiguing fibers to sustain the work rate. This process continues progressively until all available motor units in the active muscle has been recruited. In fact, it has been established that less than 50% of active muscle fibers were recruited during prolonged exercise (Tucker et al., 2004; Amann et al., 2006); Even at maximum exercise intensity, that recruitment is only increased to about 60% (Albertus, 2008). Thus, the regulation of the central nervous system seemed to be the essence that determines the changes in motor performance.

There is growing evidence that the most important factors affecting motor performance begin and end in the brain (Noakes, 2011). Existing studies have described the relationship between the central system and the peripheral system through imaging methods. During incremental exercise, the concentration of oxygenated hemoglobin (HbO_2) in the prefrontal cortex (PFC) continues to increase, and decreases before the end of exercise due to exhaustion (Rupp and Perrey, 2008; Kojima et al., 2022). Since reduced HbO_2 in the PFC is associated with reduced muscle force generation capacity (Rasmussen et al., 2007), this may provide evidence that PFC plays a role in motor termination (Robertson and Marino, 2015). In addition, because of motor related areas could increase muscle power output with increasing exercise intensity, the neural activity of the motor cortex (MC) continues to increase in incremental exercise and it is also reported to decrease before the end of the exercise. However, some studies believe that no changes in neural activity seem to occur in PFC regions during submaximal and maximal exercise (Brümmer et al., 2011; Schneider et al., 2013), while changes in MC seem to be more able to reflect neural changes during movement (Jung et al., 2015). Over all, from the perspective of functional systems theory, the central nervous system determine the effectiveness of exercise (Kolomiets et al., 2017).

Recent research in neuroscience highlights the brain as a widespread and interconnected network that plays a fundamental role in controlling behavioral performance. Thus, analysis of regional activity levels may not adequately reflect the modulation of exercise-induced cortical mechanisms. The functional network throughout the cerebral cortex may be dramatically affected from normal resting to exercise states (Raichlen et al., 2016), and cortical network changes during exercise can be effectively evaluated in connectivity–based approach. Functional connectivity (FC) is defined as the statistical dependencies among remote neurophysiological events, which is a statistically quantifiable and observable phenomenon. Both activation and functional connectivity are parameters for evaluating the brain's function (Stephan et al., 2009). A study of comparison on the effects of aerobic and anaerobic exercise on FC of brain network shows that aerobic exercise could increase the resting state FC in attention network

(Schmitt et al., 2019). Furthermore, low and moderate-intensity exercise could enhance the resting state FC in the attention network as well as sensorimotor network (Rajab et al., 2014; Schmitt et al., 2019; Büchel et al., 2021). Thus, increased functional connectivity may contribute to the maintenance of exercise. In addition, the central executive network can be down-regulated if prolonged exercise is expected, in order to save mental resources (Radel et al., 2017). This might be another mode to the maintenance of exercise. However, how the functional interaction or connectivity changes between brain regions during a sustained high-intensity exercise remains a question that needed to be explored.

With the development of neuroimaging technology, it is possible to use functional near-infrared spectroscopy (fNIRS) to evaluate brain function changes during exercise in real time. The multichannel fNIRS instrument can measure the temporal correlation of cortical region changes and subsequently enable fNIRS-based activation or functional connectivity assessments (Chang-Hwan, 2010; Medvedev, 2014). The fNIRS is an optical imaging method based on the hemodynamic response, which can detect the changes in HbO_2 and deoxygenated hemoglobin (HHb) concentration levels in the microcirculation of brain tissue very effectively, with good spatial and temporal resolution. (Jobsis, 1977; Naseer and Hong, 2015). Simultaneous functional magnetic resonance imaging (fMRI) research revealed that fNIRS measurement of HbO_2 is highly correlated with fMRI measurement of blood oxygen level-dependent, suggesting that fNIRS could be an appropriate substitute for fMRI (Kim et al., 2017; Yücel et al., 2017). Compared with other non-invasive conventional functional imaging tools, such as fMRI and positron emission tomography, in general, fNIRS are characterized as safe, convenient, and inexpensive, and have fewer physical or environmental limitations and taboos (Naseer et al., 2014; Herold et al., 2017). Thus, it is readily applicable in the process of exercise to detect hemodynamic fluctuation in different movement states of athletes. In addition, filtering out cardiac and respiratory noise (Tachtsidis and Scholkmann, 2016; Fantini et al., 2018) can be addressed with the relatively high sampling rate of the fNIRS device (Fantini et al., 2018).

Performing high-intensity motor tasks might require a higher level of attention and sensorimotor processing to integrate visual and proprioceptive. Neuroimaging studies have shown that the PFC contributes to many higher-order behaviors, including motion planning, organization, regulation, speed, and direction of motion, and synthesis of multiple information required for complex behaviors (Hussar and Pasternak, 2013; Nee and D'Esposito, 2016). In addition, the PFC plays a broad role in controlling the process of goal-directed actions (D'Esposito et al., 2000; Miller and Cohen, 2001; Herd et al., 2006). The MC is mainly involved in the coordination and execution of complex motor sensations and motor functions, and controls human movement through spatial sensation and motor planning (Franceschini et al., 2003). The occipital cortex (OC), as visual cortex, is not only related to visual function, but also essential for conscious perception of various parts of the body, and can be modulated by visual stimuli, visually guided attention, and motor actions (Miller et al., 1993; Astafiev et al., 2004). These regions may be involved in responses to race-walking exercise in different coordinated ways. Thus, we measure the changes in cerebral oxyhemoglobin concentrations in the PFC, MC and OC. This study aimed to use a network perspective to investigate the effects of different exercise intensities on brain functional connectivity by the fNIRS imaging. We hypothesized that MC related brain functional connectivity would gradually increase to maintain the ability of the central system to regulate motor behavior in high exercise intensities. The results of this study might broaden our knowledge of the changes of brain functional networks during race-walking exercise. Real-time assessment of the functional status of central nervous system based on network connectivity characteristics helps to determine the strategy of the definite athlete adaptation, and estimates the effectiveness of the exercise process.

Materials and methods

Participants

Sixteen healthy young right-handed athletes aged 18–27 years from Ludong University were recruited to participate in this study. All of them met the competition criteria for the 2016 Rio de Janeiro Olympic Games (male 84-min and female 96-min for 20 km). Among the selected participants, 2 were excluded because of loose detectors during race-walking exercise. Therefore, the number of valid samples for the final analysis was 14 (8 males, accounting for 57%). All participants were screened for any history of significant medical, neurological or psychiatric injuries and disorders, which might affect brain structure or function. The researchers introduced the basic information (including experimental purposes, procedures, schedules, announcements, and contributions) of the experiment to the study participants and obtained their consent. All participants were required to have adequate sleep and were not allowed to participate in exercise within 24 h before the experiment. The Animal Ethics Committee of the Capital University of Physical Education and Sports (Beijing, China) approved all procedures and protocols. All participants signed informed consent before participating in all.

Procedures

The experiment was conducted as a training lesson. Participants were asked to sit quietly for 5–10-min before the

start of the experiment to eliminate the existing hemodynamic response caused by their activity. Subsequently, the research assistant wears the fNIRS equipment for the participants. The experiment was divided into two states, namely the resting state and race-walking state, and fNIRS was implemented continuously throughout the experiment. During the resting state, participants were instructed to stay awake with their eyes closed and remain quiet for 10-min. Then, all participants performed a 20-min warm-up. In race-walking state, participants were required to complete a 20-km race-walking on a treadmill (0% incline) within the required time of routine training. Three specific periods as time-windows corresponding to different exercise intensities were divided from the total time of participants. In order to better distinguish different exercise intensities, the three time-windows should be as far apart as possible. The fNIRS signal of 0.01–0.1 Hz was selected in this study, which was considered to be physiologically important and might reflect spontaneous neural activity (Scholkmann et al., 2014). In addition, more than five low-frequency periods are required to ensure the accuracy of the phase information (Bandrivskyy et al., 2004). Thus, the detection time for each time-window was set to 10-min. The first 10-min of race-walking state was extracted as the initial stage (male, 3.7 m/s; female 3.2 m/s), the middle 10-min as the intermediate stage (male, 3.8 m/s; female 3.3 m/s), and the last 10-min as the sprint stage (male, 4.0 m/s; female, 3.4 m/s). The detailed time schedule of race-walking was shown in **Table 1**.

Basic information including gender, age, height, weight, blood pressure and medical history were recorded by the staff on the day before the experiment. Since heart rate measurement was a useful tool for detecting exercise intensity (Reis et al., 2011), the sports watch was used to monitor real-time heart rate changes during race-walking in the participants. The basic information and behavioral parameters of participants were shown in **Table 2**. In the present study, there were significant differences in the mean heart rates of the participants under the three time-windows, as shown in **Table 3**. The heart rate in each stage was averaged over the corresponding time-window. Therefore, the exercise intensity of the initial, intermediate and sprint stages could be distinguishable, respectively. During the race-walking, the experiment was terminated immediately if any symptoms developed or were suspicious (e.g., pain and tenderness, swelling, fever, redness or discoloration, and distension of the lower extremity surface veins, hypoxia, respiratory events, or chest pain).

Functional near-infrared spectroscopy data acquisition

This experiment adopts the multi-channel fNIRS system (NirSmart, Dan Yang hui gen medical instrument co., LTD.). In addition, the study adopted the 760 nm and 850 nm of two different wavelengths of near-infrared light to detect HbO_2 and HHb concentration level changes. The inter–optode distance was 3 cm and the sampling rate was 10 Hz. Forty measurement channels, consisting of 24 light source probes and 13 detector probes, were established for measurement. The channel filling corresponding to 10/10 electrode positions was determined according to the different head sizes. With the help of the calibration function of the instrument and the corresponding template, the center of the middle probe setting row was placed near the FPz. As shown in **Figure 1**, the template and probe were symmetrically placed in the PFC (lPFC/rPFC), MCs (lMC/rMC), and OCs (lOC /rOC) regions on the left and right sides.

Data pre-processing

The fNIRS signal preprocessing was carried out with the help of the NirSpark software package. During fNIRS, participants would have unavoidable head movements, especially during exercise. The commonly used correction methods for motion artifacts include spline interpolation, wavelet analysis, principal component analysis (PCA), etc., which had attracted extensive attention because of their great role in functional connectivity analysis (Zhang S. et al., 2021). In this study, the following steps were used to preprocess the fNIRS signals. In short, determining the components that may be associated with noise and artifacts requires us to perform PCA and independent component analysis (ICA) of the HbO_2 and HHb signals for each channel. Firstly, PCA was used to reduce the dimension of each channel time series of each fNIRS, and ICA was used to separate the independent components of the same dimension. Through the inverse process of ICA and PCA, the remaining components of interest were reconstructed into signals of the same dimension as the original time series to separate unwanted sources from the hemodynamic response, including blood pressure, skin blood interference and non-evoked hemodynamic components (van de Ven et al., 2004; Zhang et al., 2010). Subsequently, the artifact portion was determined by identifying the impulse or cliff-type jumps caused by the relative sliding of the scalp and probes and was removed by cubic spline interpolation. Thirdly, the six–order Butterworth band–pass filter was used to retain the 0.01–0.1 Hz portion of the filtering signal and improve signal–to–noise ratio. Finally, the modified Beer-Lambert law was used to transform light intensity data into the relative change of the HbO_2 and HHb based on different absorption spectra, the formula is as follows:

$$OD^{\lambda i} = In\frac{I_{Oi}}{I_i} = \left(\varepsilon_{HBO}^{\lambda_i} C_{HBO} + \varepsilon_{HHB}^{\lambda_i} C_{HHB}\right) L_{\lambda_i}\ i = 1, 2 \quad (1)$$

OD is the optical density, I_{Oi} is the intensity of incident light with a wavelength of λi, I_i is the corresponding scattered light

TABLE 1 The detailed time schedule of race-walking.

Distance	Male			Female		
	Segmented time	Speed	Total time	Segmented time	Speed	Total time
0–2 km	9-min	3.7m/s	* 9-min	10-min 10-s	3.2m/s	*10-min 10-s
2–4 km	9-min	3.7m/s	* 18-min	10-min 10-s	3.2m/s	20-min 20-s
4–6 km	8-min 45-s	3.8m/s	26-min 45-s	10-min	3.3m/s	30-min 20-s
6–8 km	8-min 45-s	3.8m/s	35-min 30-s	10-min	3.3m/s	40-min 20-s
8–10 km	8-min 45-s	3.8m/s	& 44-min 15-s	10-min	3.3m/s	&50-min 20-s
10–12 km	8-min 30-s	3.9m/s	& 52-min 45-s	9-min 55-s	3.3m/s	&60-min 15-s
12–14 km	8-min 30-s	3.9m/s	61-min 15-s	9-min 55-s	3.3m/s	70-min 10-s
14–16 km	8-min 30-s	3.9m/s	69-min 45-s	9-min 55-s	3.3m/s	80-min 5-s
16–18 km	8-min 15-s	4.0m/s	# 78-min	9-min 50-s	3.4m/s	#89-min 55-s
18–20 km	8-min 15-s	4.0m/s	# 86-min 15-s	9-min 50-s	3.4m/s	#99-min 45-s

*Represent the start and end points of the initial stage's time-window (male 0-min to 10-min, female 0-min to 10-min), &represent the start and end points of the intermediate stage's time-window (male 38-min 7.5-s to 48-min 7.5-s, female 44-min 52.5-s to 54-min 52.5-s), and #represent the start and end points of the sprint stage's time-window (male 76-min 15-s to 86-min 15-s, female 89-min 45-s to 99-min 45-s).

intensity, and L_{λ_i} is the optical path. $\varepsilon_{HBO}^{\lambda_i} C_{HBO}$ and $\varepsilon_{HHB}^{\lambda_i} C_{HHB}$ represent the light absorption coefficient and concentration of HbO_2 and HHb with a wavelength of λi, respectively. ΔC_{HbOHHb} represents the relative concentration changes in HbO_2 and HHb concentrations. The following equation was used to calculate (Hu et al., 2019; Li et al., 2021):

$$\Delta C_{HbOHHb} = \begin{pmatrix} \varepsilon_{HbO}^{\lambda_1} + HHb \\ \varepsilon_{HbO}^{\lambda_2} + HHb \end{pmatrix}^{-1} \begin{pmatrix} OD^{\lambda_1} / (r \times DPF^{\lambda_1}) \\ OD^{\lambda_2} / (r \times DPF^{\lambda_2}) \end{pmatrix} \quad (2)$$

Studies had shown that HbO_2 was the most sensitive marker of activity-dependent changes in regional cerebral blood flow (Dashtestani et al., 2018; Fang et al., 2018; Sulpizio et al., 2018), specially locomotion-related changes in cerebral oxygenation (Holtzer et al., 2015, 2016, 2017; Hernandez et al., 2016; Lin and Lin, 2016; Verghese et al., 2017). In addition, HbO_2 had a superior contrast-to-noise ratio to HHb. Therefore, HbO_2 signals were analyzed to describe the hemodynamic changes in this study.

Brain activation

The cerebral oxygen signal measured by near infrared spectroscopy has very obvious time-frequency characteristics, and the frequency content can be continuously derived in time. By adjusting the length of the time domain and averaging the content in the time domain, the brain function parameters in a specific time range can be obtained. After preprocessing the original experimental data, a generalized linear model (GLM) was used to analyze the HbO_2 signal time series data. GLM establishes the ideal hemodynamic response function (HRF) for each experimental paradigm and then calculates the degree of match between the experimental HRF value and the ideal HRF value, denoted by β. It represents the peak of the HRF function, and reflects the intensity or activation of the cerebral cortex (Chung et al., 2018; Ge et al., 2021). In this study, a pair of the adjacent light sources and detector forms a channel, and we calculate the intra-group average of β-value at the channel level. Then the image is generated by the interpolation method of inverse distance.

Brain functional network connectivity

Through Pearson correlation analysis, the correlation coefficient between regions could be obtained and the FC intensity also could be studied (Ge et al., 2021; Zhang N. et al., 2021). Therefore, a 6x6 functional connectivity matrix could be calculated for each participant. The formula is as follows:

$$r_{a,b} = \frac{cov(a,b)}{\sigma_a \sigma_b} = \frac{E(ab) - E(a)E(b)}{\sqrt{E(a^2) - E^2(a)}\sqrt{E(b^2) - E^2(b)}} \quad (3)$$

$Cov(a,b)$ represents the covariance of a and b; $E(a)$ and $E(b)$ represent the mean values of a and b, respectively; σ_a and σ_b represent the variance of a and b, respectively. $r_{a,b}$ was used to evaluate the strength of FC. This indicates that there is a strong correlation between the two cortical regions, which is proportional to the r-value.

Statistical analysis

In order to meet the assumptions required for parametric analysis, the normality test (Kolmogorov-Smirnov test) and variance uniformity test (Levene test) were performed on participant data, when $p > 0.05$, the variance was considered homogeneous. In this study, one–way ANOVA was performed

TABLE 2 Basic information of participants and behavioral parameters.

Number	Age (year)	Gender	Education (year)	Height (cm)	Weight (kg)	Heart rate (b.p.m)			Blood diastolic/systolic pressure (mmHg)		Body temperature (°C)	
						Initial	Intermediate	Sprint	Pre	Post	Pre	Post
N1	20	Female	13	172	54	145	171	190	125/75	147/96	36.2	36.7
N2	21	Male	15	173	67	143	168	188	141/79	150/88	36.4	36.8
N3	25	Female	19	168	50	140	176	191	97/66	143/101	36.2	36.8
N4	27	Male	20	178	70	144	169	189	122/92	140/112	36.2	37.5
N5	18	Male	13	180	60	145	170	190	120/90	141/113	36.3	37
N6	21	Male	13	192	75	143	173	191	113/90	137/109	36.4	37.7
N7	25	Male	19	175	53	140	171	189	117/84	148/101	36.5	37.0
N8	25	Female	19	156	45	143	172	186	108/90	126/98	36.2	36.9
N9	24	Male	16	180	73	139	170	185	108/70	138/95	36.5	37
N10	21	Female	15	168	54	146	174	185	112/79	132/92	36.2	36.5
N11	19	Male	13	180	76	141	174	190	114/80	140/92	36.5	37
N12	19	Female	13	161	48	142	170	189	119/86	136/105	36.6	36.8
N13	20	Male	13	178	68	141	169	187	120/90	148/110	36.3	37.2
N14	20	Female	14	160	73	142	171	188	119/86	150/106	36.5	37.0

10.3389/fnhum.2022.1002793

TABLE 3 Statistical analysis of participants in three time-windows.

Time-windows	Heart rate		
	Mean	Standard deviation	*P*-value
Initial stage	142.43	2.10	<0.01
Intermediate stage	171.29	2.27	<0.01
Sprint stage	188.43	2.03	

on the region–wise activation and FC. Bonferroni correction was used for the multiple comparisons. There were six inter-group pair-wise comparisons, including resting vs. initial, resting vs. intermediate, resting vs. sprint, initial vs. intermediate, initial vs. sprint, and intermediate vs. sprint. The corrected p–value threshold was set at $p < 0.0083$ (0.05/6).

Results

Brain activation change

In this study, Figure 2 shows the results of cortical intensity or activation patterns in resting state (a), initial stage (b), intermediate stage (c) and sprint stage (d). The color bar number range on the right represents the β-value in the six brain regions and the purple color represents the higher activation than the blue color. We found that brain activation increased progressively with increasing walking intensity. In addition, the activation regions in the bilateral cerebral hemispheres were different during the initial, intermediate and sprint stages. However, although race-walking could induce a wide range of activation increases, there was no evidence that the β-value ($P > 0.05$) showed significant differences in the race-walking state compared with the resting state, as well as between different stages of race-walking.

Functional connectivity change

We examined changes of FC values in different four states. Figure 3 provided a visual indication of the connectivity significantly change among the cerebral regions between any two states. The line color indicates connectivity intensity, blue dots indicate nodes. We found that the FC changes between resting vs. initial stage mainly exist between MC and OC, as shown in Figure 3A, while PFC was involved in FC changes between resting vs. intermediate as shown in Figure 3B, and resting vs. sprint were widely present in PFC, MC and OC as shown in Figure 3C. In addition, when the initial development

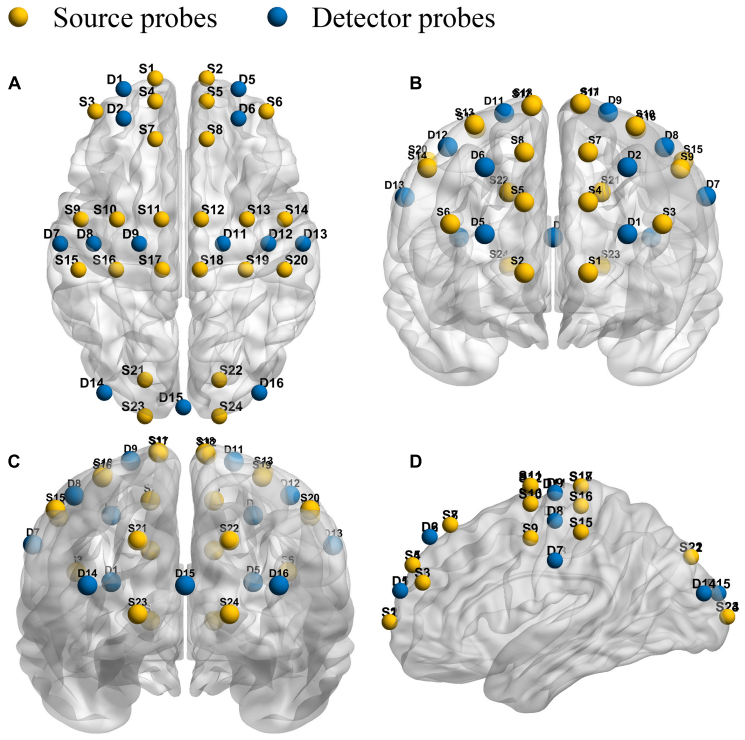

FIGURE 1
Schematic diagram of the fNIRS. Configuration of 24 source probes, 13 detector probes and 40 measurement channels. The top view **(A)**, the front view **(B)**, the rear view **(C)**, and the side view **(D)**.

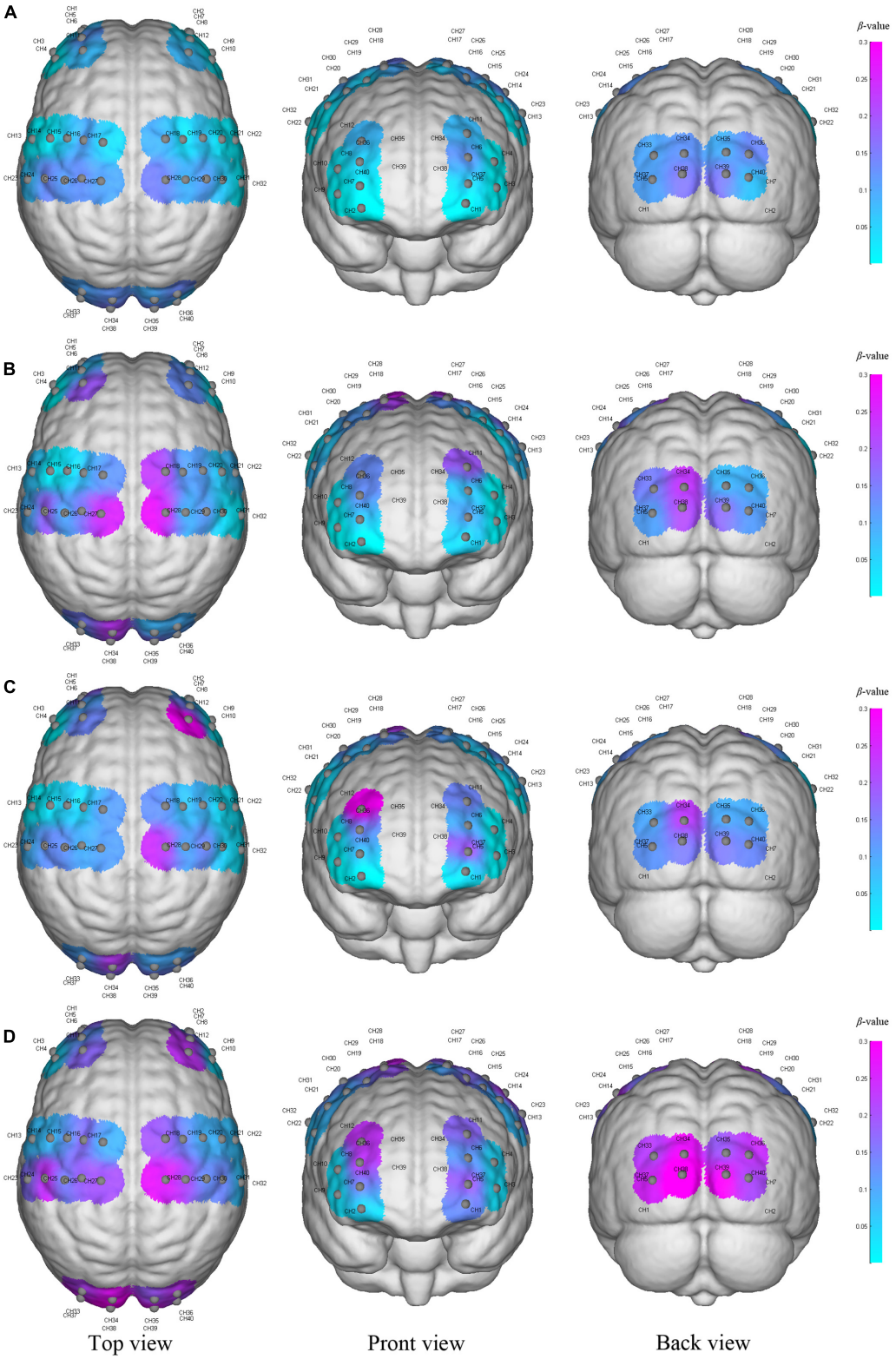

FIGURE 2
The activation of the cerebral cortex during resting state **(A)**, initial stage **(B)**, intermediate stage **(C)** and sprint stage **(D)** under three viewing angles (top view, front view, and back view). The color reflects the mean β-value of each region on the time scale, and the purple color represents higher activation than the blue–colored regions. Gray node represents the channel formed by each light source probe and detector probe, and the CH number is the label of the channel.

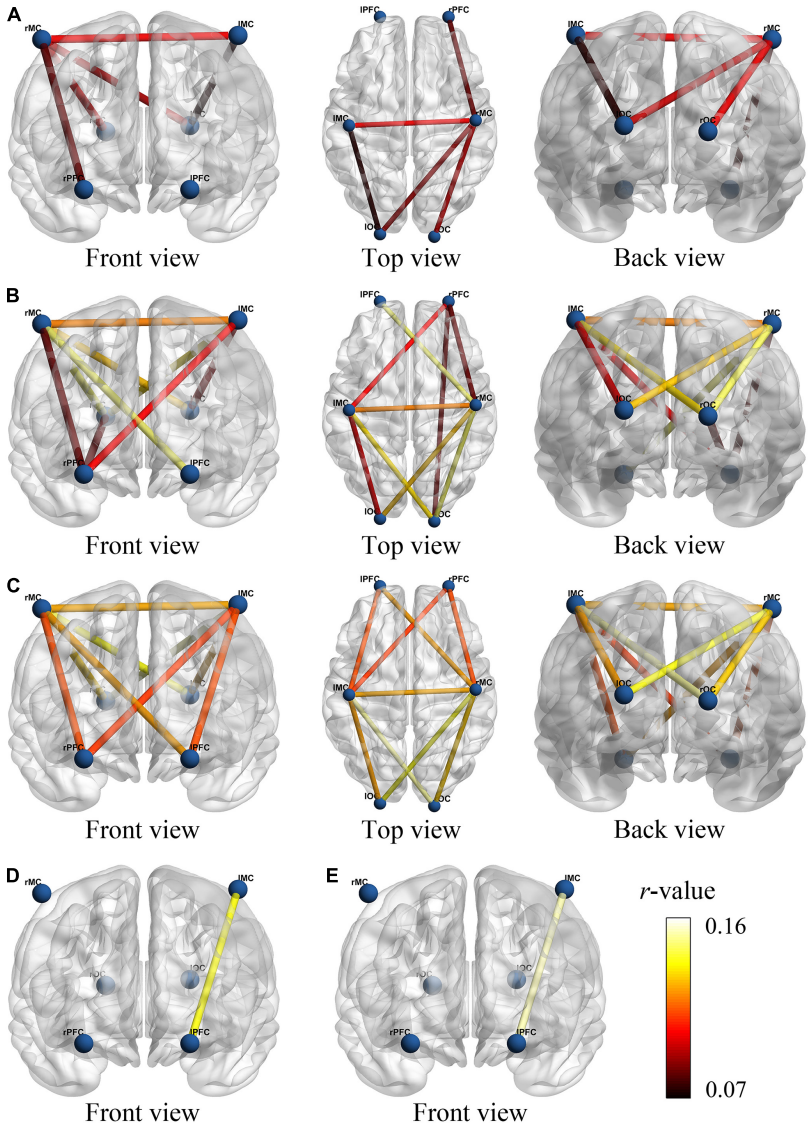

FIGURE 3
The functional connectivity visual map under different viewing angles. The connectivity line indicates the significant changes of *r*-value between resting and initial stage **(A)**, resting and intermediate stage **(B)**, resting and sprint stage **(C)**, initial and intermediate stage **(D)**, initial and sprint stage **(E)**. The blue nodes represent six brain regions. Line color indicates the connectivity intensity, and the brighter color represents higher strength.

to the sprint stage, the significant changes of FC were displayed in PFC and MC, as shown in Figures 3D,E.

In detail, results of FC analysis showed that significant *r*-value increased in connectivity of lMC-lOC ($p = 0.014$), lMC-rMC ($p = 0.001$), lOC-rMC ($p = 0.002$), rPFC-rMC ($p = 0.05$), and rMC-rOC ($p = 0.047$), which was higher in initial stage than that in resting state, as shown in Figure 4A. Compared with resting state, significant increased FC value of lPFC-rMC ($p < 0.001$), lMC-lOC ($p = 0.001$), lMC-rPFC ($p = 0.023$), lMC-rMC ($p < 0.001$), lMC-rOC ($p = 0.008$), lOC-rMC ($p < 0.001$), rPFC-rMC ($p = 0.001$), rPFC-rOC ($p = 0.016$), and rMC-rOC ($p = 0.001$) were observed in intermediate stage, as shown in Figure 4B. The *r*-value exhibited significantly increased in lPFC-lMC ($p = 0.022$), lPFC-rMC ($p = 0.001$), lMC-lOC ($p < 0.001$), lMC-rPFC ($p = 0.01$), lMC-rMC ($p < 0.001$), lMC-rOC ($p = 0.002$), lOC-rMC ($p < 0.001$), rPFC-rMC ($p = 0.003$), and rMC-rOC ($p = 0.004$) in sprint stage compared with resting state, as shown in Figure 4C. In addition, the FC value of lPFC-rMC in intermediate stage ($p = 0.004$) and sprint stage ($p = 0.001$) were significantly increased than initial stage, as shown as Figures 4D,E.

Overall, FC results showed a continuous increase from the resting to the intermediate stage. However, an interesting result was that the FC between several regions, such as lPFC and

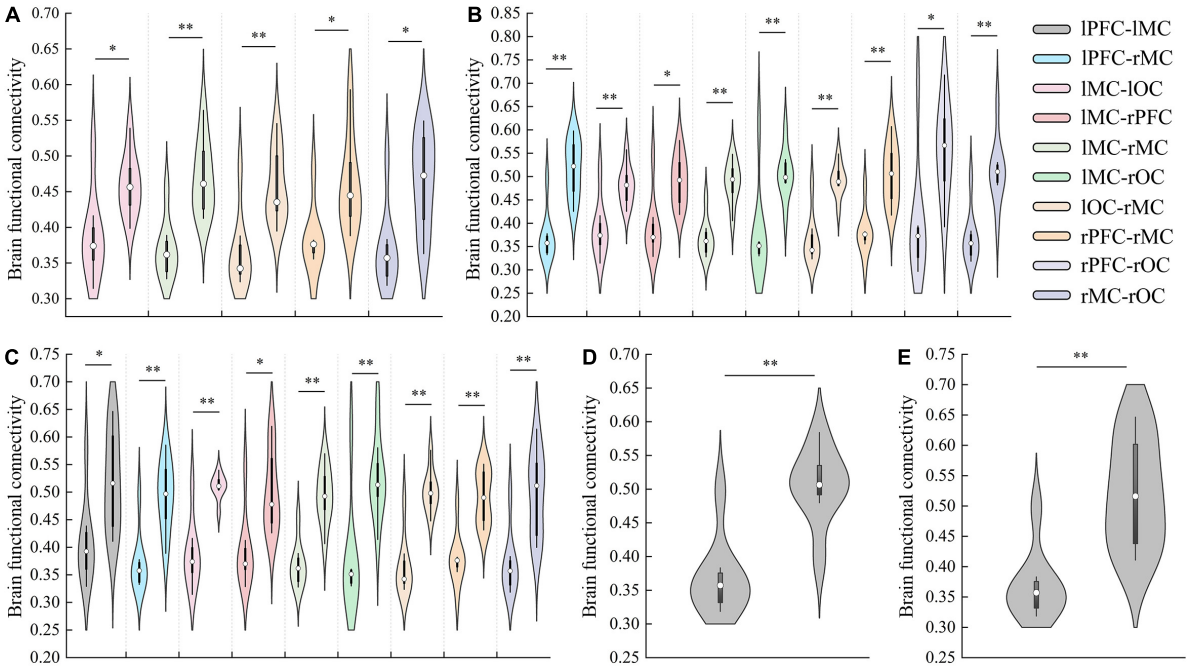

FIGURE 4
The results of significant changes of FC value between resting and initial stage **(A)**, resting and intermediate stage **(B)**, resting and sprint stage **(C)**, initial and intermediate stage **(D)**, initial and sprint stage **(E)**. $^{*}p < 0.05$, $^{**}p < 0.01$.

rMC, decreased in the sprint stage. Moreover, there was no significant difference in FC was found between the sprint and intermediate stages.

Discussion

In this study, portable fNIRS was used to detect the central nervous system activity during different time windows of race-walking, and cortical activation and FC indexes were used to explore the change patterns of brain network mechanisms under different intensity levels. The fNIRS signals were detected mainly in the 0.01–0.1Hz frequency interval, reflecting important neurovascular coupling activity (Scholkmann et al., 2014). This study mainly found that with the continuous development of race-walking, the mode of brain activation had undergone specific changes. In addition, the results of the brain network showed that with the exercise intensity rising, the intensity and number of brain connectivity began to increase significantly.

In this study, a seminal observation was that bilateral MCs activation occurred within 10 min of the beginning of race-walking compared to pre-exercise. Subsequently, hemodynamic responses of the prefrontal region were successfully induced, which might be the neural mechanism by which acute exercise could induce enhanced cognitive and control functions (Basso and Suzuki, 2017; Zaman et al., 2021). In the last 10 min of exercise, almost regional resources, including bilateral PFCs, MCs and OCs, participated in the sprint task. These discrepancies might reflect the following potential acute exercise effect. Our results suggested that spontaneous neural activity in PFC, MC and OC responds differently to exercise intensity. Spontaneous neural activity had been shown to have different physiological sources such as metabolic activity, neurogenic activity and myogenic activity in healthy people study (Xie et al., 2019, 2021), so hemodynamic parameters were closely controlled and regulated by these factors. Some neuroimaging reports believed that cerebrovascular reactivity was associated with chronic and acute exercise, respectively (Svensson et al., 2015; Vilela et al., 2017; Mueller et al., 2020; Vints et al., 2022), which also supports our conclusions. At higher exercise intensity, extensive cortical activation might improve information processing speed (Chang et al., 2012). In addition, the regional allocation of cerebral blood flow during the exercise stage might reflect changes in functional connectivity since others report acute exercise impacts attention-related brain networks (Kamijo et al., 2004; MacIntosh et al., 2014).

The quantification of cortical activation was a theoretical analysis based on the functional separation model of brain regions, while in reality cortical regions appeared as a brain network closely related in structure and function. The exercise was traditionally considered to be a process involving motor-related brain regions, such as the primary motor and premotor areas. However, the movement also involves many non-motor

regions (Rizzolatti et al., 2014). In previous studies, the focus on the activation of brain regions and cortical activation changes during exercise was one-sided. The brain functional network method based on quantifying the number and strength of brain connectivity might have more authenticity.

Our FC results showed that MC-related brain networks first undergo specific changes at the early stage of exercise, such as a significant increase in the information exchange between bilateral MCs. Recent neuroimaging studies have shown that task-evoked functional connectivity was thought to have transient interactions between specific brain regions related to specific task performance (Moore et al., 2022), and exercise could enhance connectivity in sensorimotor-related brain networks (Rajab et al., 2014). We believe that this increase in the level of homologous interbrain interaction was related to the efficiency of effective information transmission, which might be beneficial to further strengthen the control and planning of movement, and this notion has been confirmed by human and rodent studies (Venezia et al., 2017; Moore and Loprinzi, 2021).

As exercise intensity increases, the connectivity between bilateral MCs and other regions began to strengthen, such as bilateral OCs. These results suggested that race-walking could induce enhanced synchrony of neural activation in bilateral MC and OC. On the one hand, this result was consistent with the conclusion that motor performance depended more on bilateral MCs when tasks were more demanding (Verstynen and Ivry, 2011). On the other hand, performing more complex motor tasks required higher levels of visuomotor coordinated responses, and OC might play a role in the integration of body parts perception and sensorimotor functions (Astafiev et al., 2004).

In addition, the connectivity between PFC and MC changed most obviously in the sprint stage, and the main difference between the sprint stage and the starting stage also existed in these regions. This phenomenon was also confirmed by a recent study, which showed that increased exercise intensity could induce positive connectivity between the frontal network system and other cortices, especially between the PFC and the parietal lobe (Voss et al., 2020). The PFC and MC were important components of the fronto-parietal motor control network, which involve cognitive and control functions. Generally, PFC is a major hub of default mode network and executive control network (Buckner et al., 2008), and had basic functions such as imagination and emotion processing. Recent neuroimaging studies had shown that apart from being important in cognitive function, PFC accomplishes motion planning, organization, regulation, speed, and direction of motion (Hussar and Pasternak, 2013; Nee and D'Esposito, 2016). Emerging evidence from human behavioral experiments suggested that acute exercise was associated with improved performance in the PFC, which determines executive ability during motor tasks (Astafiev et al., 2004; Guiney and Machado, 2013). Therefore, we had reasonable speculation that when exercise intensity reached a certain level, the strength of functional connectivity between the prefrontal lobe and the motor region was the main neural mechanism that affected exercise ability and performance.

It should be noted that only right-handed participants were selected for this study. Studies have shown that handedness could affect individual brain function, including activation regions and network connectivity (Lee et al., 2019; Nair et al., 2019), so the conclusions of this study might not be fully applicable to left-handed athletes. In addition, our study has several limitations. Firstly, short-distance channels were not used in the present study, which might be one of the most effective methods to purify the signal. The fNIRS signal mainly contains evoked components and non-evoked components (Scholkmann et al., 2014). We currently use PCA, ICA and an effective preprocessing method could remove non-evoked components and part of the evoked components (cannot distinguish evoked cerebral functional brain activity from evoked cerebral systemic activity). Therefore, short-distance channels should be used as a standardized step in future research. Another limitation is that we did not use wearable tools to monitor participants' peripheral skeletal muscle data during race-walking, such as electromyography. We believe that because the fNIRS was implemented continuously throughout the experiment, the wearing of other monitoring devices for participants will increase the physiological burden, which could cause the negative effects on the brain network. Therefore, the focus of this study was to investigate changes in brain networks, rather than central-peripheral or neuromuscular coupling during race-walking. Thirdly, due to the characteristics and limitations of fNIRS, we only monitored cortical hemodynamic changes during race-walking. However, some subcortical regions, such as the insula, thalamus, and basal ganglia, are also involved in the neural control of motor performance (Moore et al., 2022). Therefore, more interesting results might be obtained by combining deep neuroimaging tools based on the methods in this study.

Overall, this network connectivity-based study confirmed that hemodynamic changes at different exercise intensities reflected different brain network-specific characteristics. Spontaneous neural activity in the PFC, MC, and OC responded differently to exercise intensity, and more extensive brain activation might increase information processing speed. In brain network connectivity, the increase in exercise intensity could improve the functional interaction between brain regions, which will be beneficial to integratng neural signals including proprioception, motor control and motor planning. It might be an important factor for athletes to maintain continuous motor coordination and control of activities under high intensity. This study extended the understanding of the brain networks involved in different exercise intensities, and it could be used as a sensitive and effective neural parameter to evaluate the effects of exercise.

Data availability statement

The raw data supporting the conclusions of this article will be made available by the authors, without undue reservation.

Ethics statement

The studies involving human participants were reviewed and approved by the Institutional Animal Ethical Committee of the Capital University of Physical Education and Sports, Beijing, China. Written informed consent to participate in this study was provided by the participants' legal guardian/next of kin. Written informed consent was obtained from the individual(s), and minor(s)' legal guardian/next of kin, for the publication of any potentially identifiable images or data included in this article.

Author contributions

QS, XC, RZ, JY, and HW worked together to complete the manuscript. QS, JY, and HW contributed to the conception and design of the study. QS and JY carried out the experiments. QS performed the data analyses and wrote the manuscript. QS and RZ provided statistical assistance and support. XC, JY, and HW provided opinions on grammar and rhetoric. All authors contributed to manuscript revision, read, and approved the submitted version.

Funding

This project was supported by the State Key R&D Program (Grant no. 2018YFF0300603) "Key Technology for Improving the Performance of Winter Paralympic Athlete" and (Grant no. PXM2020_014206_000016) "Research on key techniques of physical function characteristics of athletes in wheelchair curling, cross-country skiing and biathlon in Winter Paralympic Games".

Conflict of interest

The authors declare that the research was conducted in the absence of any commercial or financial relationships that could be construed as a potential conflict of interest.

Publisher's note

All claims expressed in this article are solely those of the authors and do not necessarily represent those of their affiliated organizations, or those of the publisher, the editors and the reviewers. Any product that may be evaluated in this article, or claim that may be made by its manufacturer, is not guaranteed or endorsed by the publisher.

References

Albertus, Y. (2008). *Critical analysis of techniques for normalising electromyographic data: From laboratory to clinical research*. Cape Town: University of Cape Town.

Amann, M., Eldridge, M. W., Lovering, A. T., Stickland, M. K., Pegelow, D. F., and Dempsey, J. A. (2006). Arterial oxygenation influences central motor output and exercise performance via effects on peripheral locomotor muscle fatigue in humans. *J. Physiol.* 575, 937–952. doi: 10.1113/jphysiol.2006.113936

Astafiev, S. V., Stanley, C. M., Shulman, G. L., and Corbetta, M. (2004). Extrastriate body area in human occipital cortex responds to the performance of motor actions. *Nat. Neurosci.* 7, 542–548. doi: 10.1038/nn1241

Bandrivskyy, A., Bernjak, A., Mcclintock, P., and Stefanovska, A. (2004). Wavelet phase coherence analysis: Application to skin temperature and blood flow. *Cardiovasc. Eng.* 4, 89–93. doi: 10.1023/B:CARE.0000025126.63253.43

Basso, J. C., and Suzuki, W. A. (2017). The effects of acute exercise on mood, cognition, neurophysiology, and neurochemical pathways: A review. *Brain Plast.* 2, 127–152. doi: 10.3233/BPL-160040

Brümmer, V., Schneider, S., Abel, T., Vogt, T., and Strueder, H. K. (2011). Brain cortical activity is influenced by exercise mode and intensity. *Med. Sci. Sports Exerc.* 43, 1863–1872. doi: 10.1249/MSS.0b013e3182172a6f

Büchel, D., Sandbakk, Ø., and Baumeister, J. (2021). Exploring intensity-dependent modulations in EEG resting-state network efficiency induced by exercise. *Eur. J. Appl. Physiol.* 121, 2423–2435. doi: 10.1007/s00421-021-04712-6

Buckner, R. L., Andrews-Hanna, J. R., and Schacter, D. L. (2008). "The brain's default network–anatomy, function, and relevance to disease," in *Year in cognitive neuroscience 2008*, eds A. Kingstone and M. B. Miller (Oxford: Blackwell Publishing), 1–38. doi: 10.1196/annals.1440.011

Chang, Y.-K., Labban, J. D., Gapin, J. I., and Etnier, J. L. (2012). The effects of acute exercise on cognitive performance: A meta-analysis. *Brain Res.* 1453, 87–101. doi: 10.1016/j.brainres.2012.02.068

Chang-Hwan, I. (2010). Estimation of effective connectivity between cortical areas using near-infrared spectroscopy (NIRS). *Front. Neurosci.* 4, 5730–5739. doi: 10.3389/conf.fnins.2010.06.00435

Chung, M. H., Martins, B., Privratsky, A., James, G. A., Kilts, C. D., Bush, K. A., et al. (2018). Individual differences in rate of acquiring stable neural representations of tasks in fMRI. *PLoS One* 13:e0207352. doi: 10.1371/journal.pone.0207352

Cronin, N. J., Hanley, B., and Bissas, A. (2016). Mechanical and neural function of triceps surae in elite racewalking. *J. Appl. Physiol.* 121, 101–105. doi: 10.1152/japplphysiol.00310.2016

Dashtestani, H., Zaragoza, R., Pirsiavash, H., Knutson, K. M., Kermanian, R., Cui, J., et al. (2018). Canonical correlation analysis of brain prefrontal activity measured by functional near infra-red spectroscopy (fNIRS) during a moral judgment task. *Behav. Brain Res.* 59, 73–80. doi: 10.1016/j.bbr.2018.10.022

D'Esposito, M., Postle, B. R., and Rypma, B. (2000). Prefrontal cortical contributions to working memory: Evidence from event-related fMRI studies. *Exec. Control Front. Lobe Curr. Issues* 133, 3–11. doi: 10.1007/978-3-642-59794-7_2

Fang, L., Huilin, Z., Jie, X., Qianqian, G., Huan, G., Shijing, W., et al. (2018). Lie detection using fNIRS monitoring of inhibition-related brain regions discriminates infrequent but not frequent liars. *Front. Hum. Neurosci.* 12:71. doi: 10.3389/fnhum.2018.00071

Fantini, S., Frederick, B., and Sassaroli, A. (2018). Perspective: Prospects of non-invasive sensing of the human brain with diffuse optical imaging. *APL Photonics* 3:110901. doi: 10.1063/1.5038571

Franceschini, M. A., Fantini, S., Thomspon, J. H., Culver, J. P., and Boas, D. A. (2003). Hemodynamic evoked response of the sensorimotor cortex measured noninvasively with near-infrared optical imaging. *Psychophysiology* 40, 548–560. doi: 10.1111/1469-8986.00057

Ge, R., Wang, Z., Yuan, X., Li, Q., Gao, Y., Liu, H., et al. (2021). The effects of two game interaction modes on cortical activation in subjects of different ages: A functional near-infrared spectroscopy study. *IEEE Access* 9, 11405–11415.

Gomez-Ezeiza, J., Santos-Concejero, J., Torres-Unda, J., Hanley, B., and Tam, N. (2019). Muscle activation patterns correlate with race walking economy in elite race walkers: A waveform analysis. *Int. J. Sports Physiol. Perform.* 14, 1250–1255. doi: 10.1123/ijspp.2018-0851

Guiney, H., and Machado, L. (2013). Benefits of regular aerobic exercise for executive functioning in healthy populations. *Psychon. Bull. Rev.* 20, 73–86. doi: 10.3758/s13423-012-0345-4

Herd, S. A., Banich, M. T., and O'reilly, R. C. (2006). Neural mechanisms of cognitive control: An integrative model of Stroop task performance and fMRI data. *J. Cogn. Neurosci.* 18, 22–32. doi: 10.1162/089892906775250012

Hernandez, M. E., Holtzer, R., Chaparro, G., Jean, K., Balto, J. M., Sandroff, B. M., et al. (2016). Brain activation changes during locomotion in middle-aged to older adults with multiple sclerosis. *J. Neurol. Sci.* 370, 277–283. doi: 10.1016/j.jns.2016.10.002

Herold, F., Wiegel, P., Scholkmann, F., Thiers, A., Hamacher, D., and Schega, L. (2017). Functional near-infrared spectroscopy in movement science: A systematic review on cortical activity in postural and walking tasks. *Neurophotonics* 4:041403. doi: 10.1117/1.NPh.4.4.041403

Holtzer, R., Schoen, C., Demetriou, E., Mahoney, J. R., Izzetoglu, M., Wang, C., et al. (2017). Stress and gender effects on prefrontal cortex oxygenation levels assessed during single and dual-task walking conditions. *Eur. J. Neurosci.* 45, 660–670. doi: 10.1111/ejn.13518

Holtzer, R., Verghese, J., Allali, G., Izzetoglu, M., Wang, C., and Mahoney, J. R. (2015). Neurological gait abnormalities moderate the functional brain signature of the posture first hypothesis. *Brain Topogr.* 29, 334–343. doi: 10.1007/s10548-015-0465-z

Holtzer, R., Yuan, J., Verghese, J., Mahoney, J. R., Izzetoglu, M., and Wang, C. (2016). Interactions of subjective and objective measures of fatigue defined in the context of brain control of locomotion. *J. Gerontol. A Biol. Sci. Med. Sci.* 72, 417–423. doi: 10.1093/gerona/glw167

Hu, X., Zhuang, C., Wang, F., Liu, Y. J., Im, C. H., and Zhang, D. (2019). fNIRS evidence for recognizably different positive emotions. *Front. Hum. Neurosci.* 13:120. doi: 10.3389/fnhum.2019.00120

Hussar, C. R., and Pasternak, T. (2013). Common rules guide comparisons of speed and direction of motion in the dorsolateral prefrontal cortex. *J. Neurosci.* 33, 972–986. doi: 10.1523/JNEUROSCI.4075-12.2013

Jobsis, F. F. (1977). Non-invasive, infra-red monitoring of cerebral O2 sufficiency, blood volume, HbO2-Hb shifts and bloodflow. *Acta Neurol. Scand.* 56, 452–453.

Jung, R., Moser, M., Baucsek, S., Dern, S., and Schneider, S. (2015). Activation patterns of different brain areas during incremental exercise measured by near-infrared spectroscopy. *Exp. Brain Res.* 233, 1175–1180. doi: 10.1007/s00221-015-4201-4

Kamijo, K., Nishihira, Y., Hatta, A., Kaneda, T., Wasaka, T., Kida, T., et al. (2004). Differential influences of exercise intensity on information processing in the central nervous system. *Eur. J. Appl. Physiol.* 92, 305–311. doi: 10.1007/s00421-004-1097-2

Katz, A. M. (2010). *Physiology of the heart*. Philadelphia, PA: Lippincott Williams & Wilkins.

Kim, H. Y., Seo, K., Jeon, H. J., Lee, U., and Lee, H. (2017). Application of functional near-infrared spectroscopy to the study of brain function in humans and animal models. *Mol. Cells* 40, 523–532. doi: 10.14348/molcells.2017.0153

Kojima, S., Morishita, S., Hotta, K., Qin, W., Usui, N., and Tsubaki, A. (2022). Temporal changes in cortical oxygenation in the motor-related areas and bilateral prefrontal cortex based on exercise intensity and respiratory metabolism during incremental exercise in male subjects: A near-Infrared spectroscopy study. *Front. Physiol.* 13:794473. doi: 10.3389/fphys.2022.794473

Kolomiets, O. I., Petrushkina, N. P., Bykov, E. V., and Yakubovskaya, I. A. (2017). Functional state characteristics of central nervous system among sportsmen with different orientation of the training process. *Psychol. Med. Biol. Probl. Phys. Cult. Sports* 12, 170–175.

Lee, S. H., Jin, S. H., and An, J. (2019). The difference in cortical activation pattern for complex motor skills: A functional near-infrared spectroscopy study. *Sci. Rep.* 9:14066. doi: 10.1038/s41598-019-50644-9

Levine, B. D. (2008). what do we know, and what do we still need to know? *J. Physiol.* 586, 25–34. doi: 10.1113/jphysiol.2007.147629

Li, Y., Song, F., Liu, Y., Wang, Y., and Ma, X. (2021). Relevance of emotional conflict and gender differences in the cognitive tasks of digital interface layouts using NIRS technology. *IEEE Access* 9, 1. doi: 10.1109/ACCESS.2020.3048737

Lin, M. I., and Lin, K. H. (2016). Walking while performing working memory tasks changes the prefrontal cortex hemodynamic activations and gait kinematics. *Front. Behav. Neurosci.* 10:92. doi: 10.3389/fnbeh.2016.00092

MacIntosh, B. J., Crane, D. E., Sage, M. D., Rajab, A. S., Donahue, M. J., Mcilroy, W. E., et al. (2014). Impact of a single bout of aerobic exercise on regional brain perfusion and activation responses in healthy young adults. *PLoS One* 9:e85163. doi: 10.1371/journal.pone.0085163

Medvedev, A. V. (2014). Does the resting state connectivity have hemispheric asymmetry? A near-infrared spectroscopy study. *Neuroimage* 85, 400–407. doi: 10.1016/j.neuroimage.2013.05.092

Miller, E. K., and Cohen, J. D. (2001). An integrative theory of prefrontal cortex function. *Annu. Rev. Neurosci.* 24, 167–202. doi: 10.1146/annurev.neuro.24.1.167

Miller, E. K., Li, L., and Desimone, R. (1993). Activity of neurons in anterior inferior temporal cortex during a short-term memory task. *J. Neurosci.* 13, 1460–1478. doi: 10.1523/JNEUROSCI.13-04-01460.1993

Moore, D., Jung, M., Hillman, C. H., Kang, M., and Loprinzi, P. D. (2022). Interrelationships between exercise, functional connectivity, and cognition among healthy adults: A systematic review. *Psychophysiology* 59:e14014. doi: 10.1111/psyp.14014

Moore, D., and Loprinzi, P. D. (2021). Exercise influences episodic memory via changes in hippocampal neurocircuitry and long-term potentiation. *Eur. J. Neurosci.* 54, 6960–6971. doi: 10.1111/ejn.14728

Mueller, P., Duderstadt, Y., Lessmann, V., and Mueller, N. G. (2020). Lactate and BDNF: Key mediators of exercise induced neuroplasticity? *J. Clin. Med.* 9:1136. doi: 10.3390/jcm9041136

Nair, S., Nenert, R. E., Allendorfer, J. B., Goodman, A. M., Vannest, J., Mirman, D., et al. (2019). Sex, age, and handedness modulate the neural correlates of active learning. *Front. Neurosci.* 13:961. doi: 10.3389/fnins.2019.00961

Naseer, N., and Hong, K.-S. (2015). fNIRS-based brain-computer interfaces: A review. *Front. Hum. Neurosci.* 9:3. doi: 10.3389/fnhum.2015.00003

Naseer, N., Hong, M. J., and Hong, K.-S. (2014). Online binary decision decoding using functional near-infrared spectroscopy for the development of brain-computer interface. *Exp. Brain Res.* 232, 555–564. doi: 10.1007/s00221-013-3764-1

Nee, D. E., and D'Esposito, M. (2016). The hierarchical organization of the lateral prefrontal cortex. *Elife* 5:e12112. doi: 10.7554/eLife.12112

Noakes, T. D. (2011). Time to move beyond a brainless exercise physiology: The evidence for complex regulation of human exercise performance. *Appl. Physiol. Nutr. Metab.* 36, 23–35. doi: 10.1139/H10-082

Radel, R., Brisswalter, J., and Perrey, S. (2017). Saving mental effort to maintain physical effort: A shift of activity within the prefrontal cortex in anticipation of prolonged exercise. *Cogn. Affect. Behav. Neurosci.* 17, 305–314. doi: 10.3758/s13415-016-0480-x

Rae, D. E., Noakes, T. D., San Juan, A. F., Pérez, M., Nogales-Gadea, G., Ruiz, J. R., et al. (2010). Excessive skeletal muscle recruitment during strenuous exercise in McArdle patients. *Eur. J. Appl. Physiol.* 110, 1047–1055. doi: 10.1007/s00421-010-1585-5

Raichlen, D. A., Bharadwaj, P. K., Fitzhugh, M. C., Haws, K. A., Torre, G. A., Trouard, T. P., et al. (2016). Differences in resting state functional connectivity between young adult endurance athletes and healthy controls. *Front. Hum. Neurosci.* 10:610. doi: 10.3389/fnhum.2016.00610

Rajab, A. S., Crane, D. E., Middleton, L. E., Robertson, A. D., Hampson, M., and Macintosh, B. J. (2014). A single session of exercise increases connectivity in sensorimotor-related brain networks: A resting-state fMRI study in young healthy adults. *Front. Hum. Neurosci.* 8:625. doi: 10.3389/fnhum.2014.00625

Rasmussen, P., Dawson, E. A., Nybo, L., Van Lieshout, J. J., Secher, N. H., and Gjedde, A. (2007). Capillary-oxygenation-level-dependent near-infrared spectrometry in frontal lobe of humans. *J. Cereb. Blood Flow Metab.* 27, 1082–1093. doi: 10.1038/sj.jcbfm.9600416

Reis, V. M., Van Den Tillaar, R., and Marques, M. C. (2011). Higher precision of heart rate compared with VO_2 to predict exercise intensity in endurance-trained runners. *J. Sports Sci. Med.* 10, 164–168.

Rizzolatti, G., Cattaneo, L., Fabbri-Destro, M., and Rozzi, S. (2014). Cortical mechanisms underlying the organization of goal-directed actions and mirror neuron-based action understanding. *Physiol. Rev.* 94, 655–706. doi: 10.1152/physrev.00009.2013

Robertson, C. V., and Marino, F. E. (2015). Prefrontal and motor cortex EEG responses and their relationship to ventilatory thresholds during exhaustive incremental exercise. *Eur. J. Appl. Physiol.* 115, 1939–1948. doi: 10.1007/s00421-015-3177-x

Rupp, T., and Perrey, S. (2008). Prefrontal cortex oxygenation and neuromuscular responses to exhaustive exercise. *Eur. J. Appl. Physiol.* 102, 153–163. doi: 10.1007/s00421-007-0568-7

Schmitt, A., Upadhyay, N., Martin, J. A., Rojas, S., Strüder, H. K., and Boecker, H. (2019). Modulation of distinct intrinsic resting state brain networks by acute exercise bouts of differing intensity. *Brain Plast.* 5, 39–55. doi: 10.3233/BPL-190081

Schneider, S., Rouffet, D., Billaut, F., and Strüder, H. (2013). Cortical current density oscillations in the motor cortex are correlated with muscular activity during pedaling exercise. *Neuroscience* 228, 309–314. doi: 10.1016/j.neuroscience.2012.10.037

Scholkmann, F., Kleiser, S., Metz, A. J., Zimmermann, R., Pavia, J. M., Wolf, U., et al. (2014). A review on continuous wave functional near-infrared spectroscopy and imaging instrumentation and methodology. *Neuroimage* 85, 6–27. doi: 10.1016/j.neuroimage.2013.05.004

Shephard, R. J. (2009). Is it time to retire the 'central governor'? *Sports Med.* 39, 709–721. doi: 10.2165/11315130-000000000-00000

Stephan, K. E., Kasper, L., Brodersen, K. H., and Mathys, C. (2009). Functional and effective connectivity. *Klin. Neurophysiol.* 40, 222–232. doi: 10.1055/s-0029-1243196

Sulpizio, S., Doi, H., Bornstein, M. H., Cui, J., Esposito, G., and Shinohara, K. (2018). fNIRS reveals enhanced brain activation to female (versus male) infant directed speech (relative to adult directed speech) in young human infants. *Infant Behav. Dev.* 52, 89–96. doi: 10.1016/j.infbeh.2018.05.009

Svensson, M., Lexell, J., and Deierborg, T. (2015). Effects of physical exercise on neuroinflammation, neuroplasticity, neurodegeneration, and behavior: What we can learn from animal models in clinical settings. *Neurorehabil. Neural Repair* 29, 577–589. doi: 10.1177/1545968314562108

Tachtsidis, I., and Scholkmann, F. (2016). False positives and false negatives in functional near-infrared spectroscopy: Issues, challenges, and the way forward. *Neurophotonics* 3:031405. doi: 10.1117/1.NPh.3.3.031405

Tucker, R., Rauch, L., Harley, Y. X., and Noakes, T. D. (2004). Impaired exercise performance in the heat is associated with an anticipatory reduction in skeletal muscle recruitment. *Pflügers Arch.* 448, 422–430. doi: 10.1007/s00424-004-1267-4

van de Ven, V. G., Formisano, E., Prvulovic, D., Roeder, C. H., and Linden, D. E. (2004). Functional connectivity as revealed by spatial independent component analysis of fMRI measurements during rest. *Hum. Brain Mapp.* 22, 165–178. doi: 10.1002/hbm.20022

Venezia, A. C., Quinlan, E., and Roth, S. M. (2017). A single bout of exercise increases hippocampal Bdnf: Influence of chronic exercise and noradrenaline. *Genes Brain Behav.* 16, 800–811. doi: 10.1111/gbb.12394

Verghese, J., Wang, C., Ayers, E., Izzetoglu, M., and Holtzer, R. (2017). Brain activation in high-functioning older adults and falls. *Neurology* 88, 191–197. doi: 10.1212/WNL.0000000000003421

Verstynen, T., and Ivry, R. B. (2011). Network dynamics mediating ipsilateral motor cortex activity during unimanual actions. *J. Cogn. Neurosci.* 23, 2468–2480. doi: 10.1162/jocn.2011.21612

Vilela, T. C., Muller, A. P., Damiani, A. P., Macan, T. P., Da Silva, S., Canteiro, P. B., et al. (2017). Strength and aerobic exercises improve spatial memory in aging rats through stimulating distinct neuroplasticity mechanisms. *Mol. Neurobiol.* 54, 7928–7937. doi: 10.1007/s12035-016-0272-x

Vints, W. A. J., Levin, O., Fujiyama, H., Verbunt, J., and Masiulis, N. (2022). Exerkines and long-term synaptic potentiation: Mechanisms of exercise-induced neuroplasticity. *Front. Neuroendocrinol.* 66:100993. doi: 10.1016/j.yfrne.2022.100993

Voss, M. W., Weng, T. B., Narayana-Kumanan, K., Cole, R. C., Wharff, C., Reist, L., et al. (2020). Acute exercise effects predict training change in cognition and connectivity. *Med. Sci. Sports Exerc.* 52, 131–140. doi: 10.1249/MSS.0000000000002115

Xie, H., Xu, G., Huo, C., Li, W., Zhao, H., Lv, Z., et al. (2021). Brain function changes induced by intermittent sequential pneumatic compression in patients with stroke as assessed by functional near-infrared spectroscopy. *Phys. Ther.* 101:pzab140. doi: 10.1093/ptj/pzab140

Xie, H., Zhang, M., Huo, C., Xu, G., Li, Z., and Fan, Y. (2019). Tai Chi Chuan exercise related change in brain function as assessed by functional near-infrared spectroscopy. *Sci. Rep.* 9:13198. doi: 10.1038/s41598-019-49401-9

Yücel, M. A., Selb, J. J., Huppert, T. J., Franceschini, M. A., and Boas, D. A. (2017). Functional near infrared spectroscopy: Enabling routine functional brain imaging. *Curr. Opin. Biomed. Eng.* 4, 78–86. doi: 10.1016/j.cobme.2017.09.011

Zaman, N. I. U., Salleh, M. Z., Marmaya, N. H., Hasan, H., Muhammad, M., Bakar, S. H. A., et al. (2021). The effects of exercise on the psycho-cognitive function of brain-derived neurotrophic factor (BDNF) in the young adults. *J. Cogn. Sci. Hum. Dev.* 7, 33–56. doi: 10.33736/jcshd.2767.2021

Zhang, H., Zhang, Y.-J., Lu, C.-M., Ma, S.-Y., Zang, Y.-F., and Zhu, C.-Z. (2010). Functional connectivity as revealed by independent component analysis of resting-state fNIRS measurements. *Neuroimage* 51, 1150–1161. doi: 10.1016/j.neuroimage.2010.02.080

Zhang, N., Yuan, X., Li, Q., Wang, Z., Gu, X., Zang, J., et al. (2021). The effects of age on brain cortical activation and functional connectivity during video game-based finger-to-thumb opposition movement: A functional near-infrared spectroscopy study. *Neurosci. Lett.* 746:135668. doi: 10.1016/j.neulet.2021.135668

Zhang, Q., Zhang, P., Song, L., Yang, Y., Yuan, S., Chen, Y., et al. (2019). Brain activation of elite race walkers in action observation, motor imagery, and motor execution tasks: A pilot study. *Front. Hum. Neurosci.* 13:80. doi: 10.3389/fnhum.2019.00080

Zhang, S., Peng, C., Yang, Y., Wang, D., and Li, D. (2021). Resting-state brain networks in neonatal hypoxic-ischemic brain damage: A functional near-infrared spectroscopy study. *Neurophotonics* 8:025007. doi: 10.1117/1.NPh.8.2.025007

frontiers | Frontiers in Human Neuroscience

TYPE Original Research
PUBLISHED 08 November 2022
DOI 10.3389/fnhum.2022.1011997

OPEN ACCESS

EDITED BY
Pieter Meyns,
University of Hasselt, Belgium

REVIEWED BY
Kyle Bills,
Noorda College of Osteopathic Medicine, United States
William Ray Reed,
University of Alabama at Birmingham, United States

*CORRESPONDENCE
Shannon Schueren
shannon@schueren.com

SPECIALTY SECTION
This article was submitted to Motor Neuroscience, a section of the journal Frontiers in Human Neuroscience

RECEIVED 04 August 2022
ACCEPTED 17 October 2022
PUBLISHED 08 November 2022

CITATION
Schueren S, Hunger H, Pham H, Smith DL, Layne C and Malaya CA (2022) Immediate effect of lower extremity joint manipulation on a lower extremity somatosensory illusion: a randomized, controlled crossover clinical pilot study.
Front. Hum. Neurosci. 16:1011997.
doi: 10.3389/fnhum.2022.1011997

Immediate effect of lower extremity joint manipulation on a lower extremity somatosensory illusion: a randomized, controlled crossover clinical pilot study

Shannon Schueren[1]*, Hugh Hunger[1], Huong Pham[1], Dean L. Smith[2], Charles Layne[3] and Christopher A. Malaya[1,3]

[1]Research Center, Parker University, Dallas, TX, United States, [2]Department of Kinesiology and Health, Miami University, Oxford, OH, United States, [3]Department of Health and Human Performance, Center for Neuromotor and Biomechanics Research, University of Houston, Houston, TX, United States

Objective: This study explored the influence of lower extremity manipulation on the postural after-effects of standing on an inclined surface.

Methods: Eight healthy individuals (28.0 ± 4.1 years) were recruited for this open-label, crossover study. Participants stood on an incline board for 3 min to develop a known form of somatosensory illusion. After randomization to either a lower-extremity joint manipulation or no intervention, participants immediately stood on a force plate for 3 min with eyes closed. After a 24-h washout period, participants completed the remaining condition. Center of pressure (CoP) position data was measured by a force plate and evaluated using statistical parametric mapping. Pathlength, mean velocity, and RMS were calculated for significant time periods and compared with corrected paired *t*-tests.

Results: Parametric maps revealed that CoP position of control and intervention conditions differed significantly for two time periods (70–86 s—control: 0.17 ± 1.86 cm/intervention: −1.36 ± 1.54 cm; 141–177 s—control: −0.35 ± 1.61 cm/intervention: −1.93 ± 1.48 cm). CoP pathlength was also significantly decreased for the second period (control: 6.11 ± 4.81 cm/intervention: 3.62 ± 1.92 cm).

Conclusion: These findings suggest that extremity manipulation may be a useful intervention for populations where CoP stability is an issue. This study contributes to the growing body of evidence that manipulation of the extremities can drive global postural changes, as well as influence standing behavior. Further, it suggests these global changes may be driven by alterations in central integration.

Clinical Trial Registration: ClinicalTrials.gov, NCT Number: NCT05226715.

KEYWORDS

chiropractic manipulation, motor control, postural balance, somatosensory illusion, extremities

Introduction

Postural control has been defined as the act of maintaining, achieving, or restoring a state of balance during any posture or activity (Pollock et al., 2000). This requires an individual to regulate their body position and orientation, as well as respond to external perturbations (Maki and McIlroy, 1997; Shumway-Cook and Woollacott, 2017). Maintaining postural orientation is a complex task requiring the integration of the somatosensory, vestibular, and visual systems to orient the body with regards to the surface underfoot (Smart and Smith, 2001). A study by Marshall and Murphy (2010) found that altered paraspinal motor responses in participants with low back pain correlated with poor balance. Other studies have found alterations in kinesthetic sense (Heikka and Astrom, 1996) and standing balance (Sjostrom et al., 2003), as well as with pain following spinal injury (Brumagne et al., 2000; Descarreaux et al., 2005). These alterations have been shown to be influenced by decreases in joint position sense (Treleaven et al., 2003, 2006). Joint manipulation has previously been found to increase joint position sense (Gong, 2013) and maybe a valuable therapy in the treatment of kinesthetic balance disorders.

Previous investigations of spinal manipulation have found neurologically driven influences on the central nervous system including changes in cortical facilitation and sensorimotor integration, as well inhibition of motor responses (Haavik-Taylor and Murphy, 2007; Taylor and Murphy, 2008; Haavik et al., 2016). Changes in peripheral proprioception and muscle activations have also been reported (Gong, 2013; Kingett et al., 2019). Some researchers have posited that these changes are driven by an afferent barrage of peripheral somatosensory information affecting central integrative processing methods (Taylor and Murphy, 2008; Savva et al., 2014).

While there is mounting evidence for a central, neurologically active component of spinal manipulation, it is unclear if these effects are also present during the manipulation of joints of the extremities. Studies by Malaya et al. (2020, 2021) have found task-based and postural changes from manipulation of the upper and lower extremities. The nature of these changes is not easily explainable as joint-localized phenomena—despite joint-specific application—and has been suggested to be centrally mediated, similar to the effects of spinal manipulation (Malaya et al., 2021). However, the relative contributions of central and peripheral mechanisms to the effects of extremity manipulation are still unknown.

Standing on a toes-up inclined surface has been seen to facilitate the development of a lasting somatosensory illusion; specifically, after stepping onto flat ground and closing their eyes, many individuals will adopt a forward lean proportional to the degree of incline experienced during the development of the illusion (Kluzik et al., 2005). This after-effect occurs regardless of the degree of incline, the direction of incline (anterior, posterior, lateral), static standing or stepping on an incline, and will still be seen in the forward lean of the trunk and head when the individual's legs are blocked from movement (Kluzik et al., 2007a). Both the trunk and head lean seen with leg blocking in the post-incline period, as well as several EMG studies performed by Kluzik et al. (2007b) confirm that the lean adaptation seen in the post-incline period is not explainable by tonic peripheral musculature contraction; rather, the leaning appears to be a central postural adaptation that orients relative to the surface (Kluzik et al., 2007a; Young and Layne, 2020; Young et al., 2020).

This pilot study aimed to explore the influence of lower extremity manipulation on the postural after-effects of standing on an inclined surface. Previous studies support the idea that these after-effects (e.g., illusionary misperceptions) are of central nervous system origin (Kluzik et al., 2005, 2007a,b; Wright, 2011). If manipulation of the extremity joints can modulate or influence a centrally mediated illusion, it is possible that joint manipulation also exerts an influence on the central nervous system. Understanding the mechanisms behind extremity-based joint manipulation and its potential effects on postural control could have broad implications for rehabilitation in clinical populations in which postural instability and falls are a health risk.

Materials and methods

Participants

This study recruited a sample of eight healthy individuals (25% female) between the ages of 18 and 35 (28.0 ± 4.1 years) over a 3-week period prior to study date (see **Table 1**). Participants had no documented surgeries, neuromusculoskeletal injuries, or systemic diseases that could affect their ability to stand on an incline for 3 min with their eyes closed. Participants were not knowingly pregnant and weighed less than the force plate operating limit of 440 lbs. Written informed consent was obtained from each participant prior to the start of experimental procedures. Approval to conduct this study was granted by the Institutional Review Board at Parker University (A-00222), in accordance with the Declaration of Helsinki. No participants were lost to follow-up and all collected

TABLE 1 Participant details.

Participant ID	Age (years)	Sex	Height (ft/in)	Weight (lbs)
1	34	Male	5′9″	158
2	29	Female	5′7″	150
3	24	Male	6′0″	165
4	32	Male	5′7″	160
5	29	Female	5′2″	107
6	24	Male	6′0″	200
7	34	Male	6′1″	195
8	26	Male	5′11″	170

data were used in the analysis. There were no adverse events or unintended effects during the course of the study.

Registered at ClinicalTrials.gov, NCT Number: NCT05226715.

Study design

This study was an open-label, controlled, crossover clinical pilot. Participants were randomized into two different groups using block randomization *via* a randomized number generator by the treating practitioner. All other study coordinators were blinded to the intervention each participant received. Participants were asked to stand on a force plate with eyes closed for 3 min so that baseline center of pressure (CoP) could be obtained. Immediately following baseline CoP measurement Group 1 received a bilateral, lower-extremity manipulation series (described below) in the supine position (intervention) on the first day, and, after a 24-h washout period, they underwent all procedures leading up to the intervention, without the manipulation series itself taking place (control condition). Group 2 performed the control condition on the first day, and the intervention condition on the second day after the same 24-h washout period. The washout period was chosen in line with previous work by Malaya et al. (2020, 2021; see **Figure 1**).

CoP was assessed on a force plate after the development of the incline illusion and immediately after receiving either the intervention or control condition for all participants. All testing took place over two consecutive days at Parker University.

The lower-extremity manipulation series consisted of a single high velocity, low amplitude manipulation bilaterally to the coxofemoral, tibiofemoral, and talotibial joints from proximal to distal in the supine position (as detailed in Malaya et al., 2020, 2021). Coxofemoral manipulation was performed in a long-lever superior to inferior thrust with bilateral web contacts on the distal thigh. Tibiofemoral manipulation was a long axis-distraction performed with an index contact on the distal tibia above the malleoli with a 5–10 degree knee angle. Talotibial manipulation was performed using a bilateral medial hand contact with thrust in the superior-to-inferior, posterior-to-anterior direction. All manipulations were performed bilaterally for each participant and by an experienced licensed chiropractor with expertise in extremity manipulation. The control condition required participants to lay supine on a chiropractic bench for 30 s without manipulation (see **Figure 2**). No adverse events were reported.

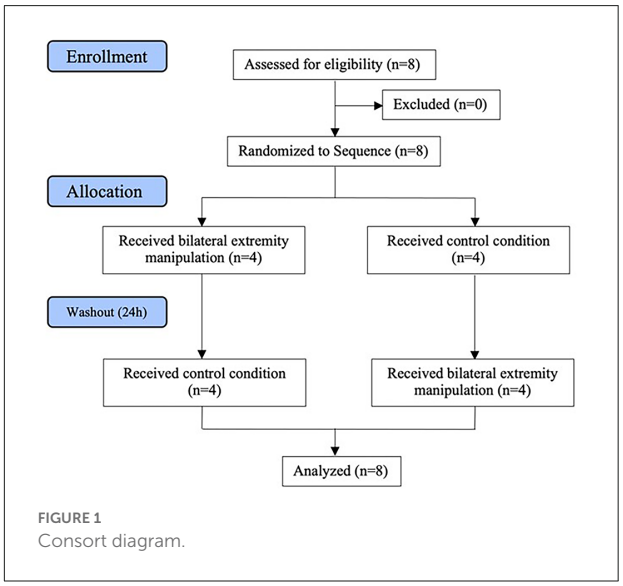

FIGURE 1
Consort diagram.

Development of the incline illusion

Participants were asked to stand on a 15° inclined, toes-up ankle stretching board for 3 min with their eyes closed. Previous work on this topic has established that eyes-closed standing on an incline board for 2.5 min can facilitate the development of an illusory leaning after-effect during subsequent standing on flat ground with closed eyes (Kluzik et al., 2005, 2007b).

Illusion response testing

Immediately after receiving the control or intervention (within 10 s), participants were asked to step off of the incline board and stand on a force plate for an additional 3 min. Participants were instructed to stand quietly, with their arms at their sides and eyes closed, and not to resist any tendency to lean in accordance with previous studies by Kluzik et al. (2005) which told participants to "not pay attention to your posture."

Data collection

Anterior to posterior CoP data were captured at 50 Hz with a BTracks^{TM} (Balance Tracking Systems) force plate using the Explore Balance software application (Balance Tracking Systems, version 2.0.4). All CoP data were low-pass filtered at 0.1 Hz with a 2nd order Butterworth filter to isolate slow postural changes and eliminate any fast fluctuations from stabilizing corrections (Gurfinkel et al., 1995; Fransson et al., 2002; Kluzik et al., 2005). Data were down-sampled in MATLAB using the resample function to achieve a total of 150 points, each representing a 1.2 s step in time (see Guthrie and Buchwald, 1991). CoP time series data from the control and intervention conditions were then compared directly using the statistical methods detailed below. CoP data were also used to calculate pathlength, mean velocity, and the root mean square of the lean behavior. In this study, pathlength is the cumulative distance traveled by

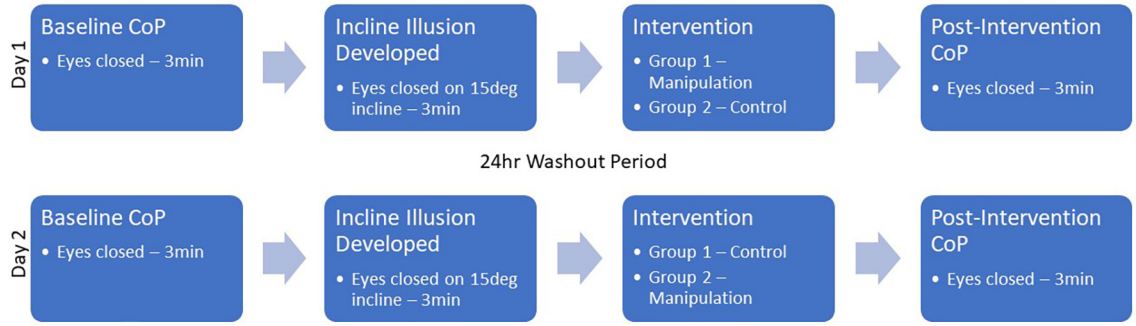

FIGURE 2
Study design.

each participant's CoP on the force plate (Paillard and Noé, 2015). RMS is a measure of the magnitude of movement that each participant's CoP varies with respect to the mean location (Paillard and Noé, 2015). All measures were calculated with a custom MATLAB script (MATLAB R2018b:9.5.0.944444).

Data analysis

Power analysis

A *post hoc* power analysis using G*Power (v.3.1) for a sample size of eight participants yielded an effect size of 1.47 with a power of 0.94 at an α of 0.05.

Primary outcome

Differences between the control and intervention CoP time series were evaluated by creating a new series comprised of two-tailed *t*-tests for each time point shared between conditions (see **Figure 3**). Autocorrelation values of 0.915 were found for the data according to the methods outlined in Guthrie and Buchwald (1991). In line with previous studies utilizing this analysis, when the value of the *t*-series exceeded our set significance of 0.05 for at least 12 subsequent points (given a series of 150 points with autocorrelation of 0.915), the difference was considered significant (Guthrie and Buchwald, 1991; Urakawa et al., 2017, 2018). This analysis was conducted using a custom MATLAB script (MATLAB R2018b:9.5.0.944444).

Secondary outcomes

Paired *t*-tests were used to compare pathlength, mean velocity, and RMS between the control and intervention conditions for significant time periods. Statistical significance

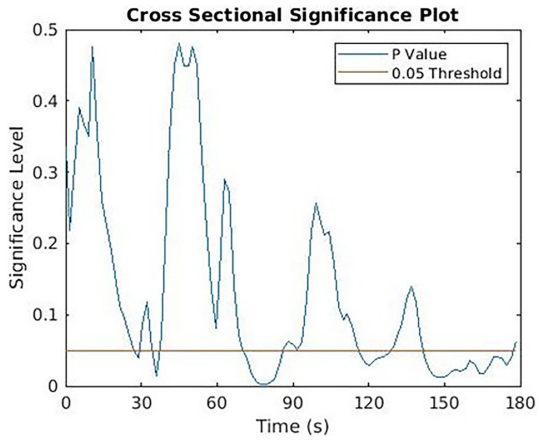

FIGURE 3
Cross sectional significance plot.

was set at 0.05 and a Bonferroni correction for six pairwise comparisons was applied to account for any error from multiple comparisons ($p < 0.05/6 = 0.0083$). All calculations denote measures in the anteroposterior direction. All analyses were conducted using MATLAB (MATLAB R2018b:9.5.0.944444).

Results

Overall, five separate time periods on the force plate contained values below our significance threshold of 0.05 (**Figure 3**). Of these original five, only two time periods had 12 or more continuous points below the significance level and could be considered statistically significant (**Table 2**). Pathlength, mean velocity, and RMS were calculated for the significant time periods and compared across conditions using Bonferroni corrected paired *t*-tests (**Table 3**).

10.3389/fnhum.2022.1011997

TABLE 2 Significance and center of pressure (CoP) comparisons of time periods on force plate.

Time range (s)	Consecutive points below	Control CoP mean ± Std (cm)	Intervention CoP mean ± Std (cm)
27.6–30	2	0.52 ± 1.81	−0.09 ± 1.73
34.8–38.4	3	0.42 ± 1.75	−0.18 ± 1.27
70.8–86.4	13*	0.17 ± 1.86	−1.36 ± 1.54
116.4–129.6	11	−0.15 ± 1.86	−1.81 ± 1.79
141.6–177.6	30*	−0.35 ± 1.61	−1.93 ± 1.48

When the value of the *t*-series exceeded our set significance of 0.05 (denoted by *) for at least 12 subsequent points (given a series of 150 points with an autocorrelation of 0.9150), the difference was considered significant.

TABLE 3 Paired *t*-tests for pathlength, mean velocity, and RMS of significant time periods.

Time range (s)	Pathlength mean ± Std (cm)		Mean velocity mean ± Std (cm/s)		RMS mean ± Std (cm)	
	Control	Intervention	Control	Intervention	Control	Intervention
70.8–86.4	1.92 ± 1.37	1.94 ± 0.99	0.04 ± 0.19	0.01 ± 0.23	1.36 ± 1.34	1.67 ± 1.25
141.6–177.6	6.11 ± 4.81*	3.62 ± 1.92*	0.02 ± 0.28	0.00 ± 0.14	1.44 ± 0.85	2.14 ± 1.23

*Denotes a statistically significant difference between respective control and intervention conditions as determined by corrected paired *t*-test ($p < 0.0083$).

A comparison of mean CoP position waveforms suggests that both groups initially exhibited an anterior sway compared to initial CoP positioning due to the incline illusion (see Figure 4). The control group displayed a slow posterior drift towards the initial CoP position after about 30 s from the initial recording, increasing in magnitude at 60 s and moving posteriorly beyond the initial position at about 120 s (see Figure 4). The intervention group displayed posterior motion earlier than the control group, after about 15 s from the initial recording, and exhibited a larger magnitude posterior shift comparatively. This group moved posteriorly beyond the initial position after about 30 s and remained almost 2 cm posterior for the remaining 2.5 min of the trial.

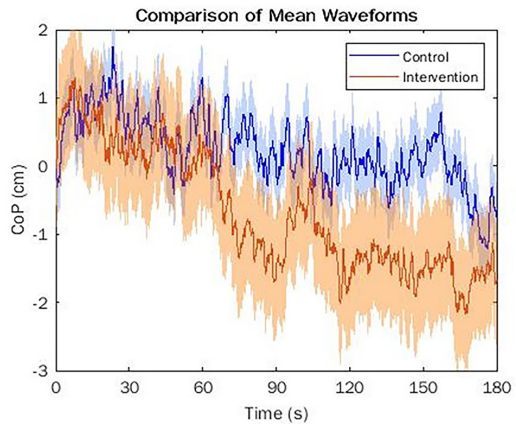

FIGURE 4
This figure details the mean waveforms of both the control (blue) and the intervention (orange) conditions for the center of pressure (CoP) position with two standard deviation range highlighted for each (shaded blue and shaded orange, respectively). Zero indicates the initial position. Negative values denote a CoP position posterior to initial position and positive values indicate a CoP position anterior to the initial position.

Discussion

This study investigated the influence of joint manipulation of the lower-extremities on the development and presence of a centrally mediated, somatosensory-based incline illusion. Bilateral manipulation of the coxofemoral, tibiofemoral, and talotibial joints appears to alter CoP position during an incline illusion compared to a control condition. These differences in CoP (based on CoP time series data) appeared at two intervals in the middle (70–86 s) and late-stage (141–178 s) of a 3-min illusion de-adaptation period. Further, participants in the manipulation group moved less overall (as measured by pathlength) during the final period. They also exhibited lower amplitude movements during the final period, though this was not significant after a correction for multiple comparisons.

Previous research has found changes in movement times (Smith et al., 2006), joint position sense (Haavik and Murphy, 2011), and range of motion (Silva et al., 2019) after spinal manipulation. Despite the local application of stimulus in spinal manipulation (i.e., the spine), larger behavioral and neurophysiological effects have been seen. This has led to postulations that these non-local changes are driven by downstream cortical stimulation, rather than spinal or local influences (Haavik et al., 2016). Studies by Malaya et al. (2020, 2021) have found similarly non-local effects of upper and lower-extremity manipulation across a variety of tasks; in particular, upper and lower-extremity manipulation appears to influence postural sway, dynamic and standing stability, as well as the overall rhythmicity of movements across both upper and lower-extremity tasking.

This study found that manipulation of the lower-extremities influenced both CoP position and overall movement distance during a centrally mediated somatosensory illusion. Sensory processing mechanisms are thought to be stored as global kinematic coordinates within the dorsospino cerebellar tract with reference specifically to whole-limb coordination as opposed to joint specific references (Bosco and Poppele, 2001). This is the hypothesized mechanism by Kluzik et al. (2007b) for the observed trunk and head lean while the legs were blocked in their post-incline illusion. An afferent barrage of somatosensory information *via* Ia afferents could explain how extremity manipulation alters centrally adapted postural control (Taylor and Murphy, 2008).

Previous studies by Pickar (2002) and Pickar and Bolton (2012) have suggested that spinal and extremity joint manipulations influence perceptual attenuation of joint position sense, leading to greater afferentation from peripheral receptors. The findings of this study support this line of thinking in that alterations in CoP during a centrally-mediated illusion were moderated by peripherally-based joint manipulations. It is possible these effects could point towards alterations in whole-limb reference frames in global kinematic coordinates within the dorsospino cerebellar tract; however, that is beyond the scope of this study. This study contributes to the growing evidence that manipulation of the extremities drives non-local changes in behavior and furthers this concept by suggesting these changes may be driven by alterations in central postural adaptations.

This study furthers our understanding of the influence of extremity manipulation on postural behaviors; however, several important questions remain unanswered. The time course of these postural changes is still unknown. While this study suggests the influence of extremity manipulation can extend to at least 2.5 min, concerted work is needed to fully understand the temporal extent of manipulative interventions. Further, the ability of extremity manipulation to influence CoP position implicates it as a potential therapy for clinical populations in which CoP instability and falls are a major health risk, such as the elderly (Daley and Spinks, 2000; Thomas et al., 2019).

There are several limitations to this study that impact the interpretation of these results. First, given the large standard deviations across CoP measures (and previous work utilizing incline illusions, see Kluzik et al., 2007a), it is likely that the participants of this study could be separated into "responders" and "non-responders" to the incline illusion, and quite possibly, to manipulation in general. To be more specific, it is possible that some participants were influenced by the incline illusion, and some were not. Similarly, some participants may have been influenced by manipulation, and some may not have been. However, this study was only interested in eliciting the presence or absence of a group effect, rather than individual variations to response; future work has been planned to specifically investigate this. This pilot study also has a small sample size. While the significant findings above suggest that the effects of lower-extremity manipulation are robust enough to elicit a significant group effect, a reproduction of this study should recruit more participants and examine individual responses and variation, in addition to group effects. Our authors decided against physical touching or sham manipulation in order to minimize any additional changes to peripheral muscle spindles outside of the development of the incline illusion. No consensus has been made on the gold-standard control or "sham" manipulation in the relevant literature. Future studies may address the effect of physically touching the hip/knee/foot as a sham/control manipulation. That being said, as several functional imaging studies have established central mechanisms for postural control (Duclos et al., 2007; Wright, 2011), the present authors felt that establishing extremity-manipulation's effect on an established centrally-mediated postural illusion was an acceptable starting place for further research into this area. Future studies should explore the use of EEG during the development of the incline illusion and post-incline postural adaptation to gain a better understanding of the specific effect manipulation has on centrally-mediated postural adaptations as well as other central processing mechanisms.

Conclusion

Participants in this study were adapted to a centrally mediated somatosensory illusion. After receiving bilateral lower-extremity manipulations, participants exhibited significantly different center of pressure positions and decreased pathlength as compared to controls. The results of this study show that extremity-manipulation alters a centrally-mediated postural illusion, and adds to the body of evidence suggesting that extremity-manipulation has central effects similar to that of spinal manipulation. Further, extremity manipulation may be a useful intervention in clinical populations where the center of pressure instability can lead to falls and injury.

Data availability statement

The raw data supporting the conclusions of this article will be made available by the authors, without undue reservation.

Ethics statement

The studies involving human participants were reviewed and approved by Parker University Institutional Review Board. The

patients/participants provided their written informed consent to participate in this study.

Author contributions

SS designed the research, collected data, interpreted the results, drafted and revised the manuscript. HH and HP participated in designing the research and collecting data. CM designed the research, collected data, interpreted results, performed statistical analysis, drafted and revised the manuscript. DS and CL revised the manuscript. All authors contributed to the article and approved the submitted version.

Conflict of interest

The authors declare that the research was conducted in the absence of any commercial or financial relationships that could be construed as a potential conflict of interest.

Publisher's note

References

Bosco, G., and Poppele, R. E. (2001). Proprioception from a spinocerebellar perspective. *Physiol. Rev.* 81, 539–568. doi: 10.1152/physrev.2001.81.2.539

Brumagne, S., Cordo, P., Lysens, R., Verschueren, S., and Swinnen, S. (2000). The role of paraspinal muscle spindles in lumbosacral position sense in individuals with and without low back pain. *Spine (Phila Pa 1976)* 25, 989–994. doi: 10.1097/00007632-200004150-00015

Daley, M. J., and Spinks, W. L. (2000). Exercise, mobility and aging. *Sports Med.* 29, 1–2. doi: 10.2165/00007256-200029010-00001

Descarreaux, M., Blouin, J. S., and Teasdale, N. (2005). Repositioning accuracy and movement parameters in low back pain subjects and healthy control subjects. *Eur. Spine J.* 14, 185–191. doi: 10.1007/s00586-004-0833-y

Duclos, C., Roll, R., Kavounoudias, A., and Roll, J. P. (2007). Cerebral correlates of the "Kohnstamm phenomenon": an fMRI study. *Neuroimage* 34, 774–783. doi: 10.1016/j.neuroimage.2006.06.050

Fransson, P.-A., Tjernstrom, F., Hafstrom, A., Magnusson, M., and Johansson, R. (2002). Analysis of short- and long-term effects of adaptation in human postural control. *Biol. Cybern.* 86, 355–365. doi: 10.1007/s00422-001-0305-y

Gong, W. (2013). Effects of cervical joint manipulation on joint position sense of normal adults. *J. Phys. Ther. Sci.* 25, 721–723. doi: 10.1589/jpts.25.721

Gurfinkel, V. S., Ivanenko, Y. P., Levik, Y. S., and Babakova, I. A. (1995). Kinesthetic reference for human orthograde posture. *Neuroscience* 68, 229–243. doi: 10.1016/0306-4522(95)00136-7

Guthrie, D., and Buchwald, J. S. (1991). Significance testing of difference potentials. *Psychophysiology* 28, 240–244. doi: 10.1111/j.1469-8986.1991.tb00417.x

Haavik, H., and Murphy, B. (2011). Subclinical neck pain and the effects of cervical manipulation on elbow joint position sense. *J. Manipulative Physiol. Ther.* 34, 88–97. doi: 10.1016/j.jmpt.2010.12.009

Haavik, H., Niazi, I. K., Jochumsen, M., Sherwin, D., Flavel, S., Türker, K. S., et al. (2016). Impact of spinal manipulation on cortical drive to upper and lower limb muscles. *Brain Sci.* 7:2. doi: 10.3390/brainsci7010002

Haavik-Taylor, H., and Murphy, B. (2007). Cervical spine manipulation alters sensorimotor integration: a somatosensory evoked potential study. *Clin. Neurophysiol.* 118, 391–402. doi: 10.1016/j.clinph.2006.09.014

Heikka, H., and Astrom, P. G. (1996). Cervicocephalic kinesthetic sensibility in patients with whiplash injury. *Scand. J. Rehabil. Med.* 28, 133–138.

Kingett, M., Holt, K., Niazi, I. K., Nedergaard, R. W., Lee, M., Haavik, H., et al. (2019). Increased voluntary activation of the elbow flexors following a single session of spinal manipulation in a subclinical neck pain population. *Brain Sci.* 9:136. doi: 10.3390/brainsci9060136

Kluzik, J., Fay, B. H., and Robert, J. P. (2007a). Postural after-effects of stepping on an inclined surface. *Neurosci. Lett.* 413, 93–98. doi: 10.1016/j.neulet.2006.11.034

Kluzik, J., Peterka, R. J., and Horak, F. B. (2007b). Adaptation of postural orientation to changes in surface inclination. *Exp. Brain Res.* 178, 1–17. doi: 10.1007/s00221-006-0715-0

Kluzik, J., Horak, F. B., and Peterka, R. J. (2005). Differences in preferred reference frames for postural orientation shown by after-effects of stance on an inclined surface. *Exp. Brain Res.* 162, 474–489. doi: 10.1007/s00221-004-2124-6

Maki, B. E., and McIlroy, W. E. (1997). The role of limb movements in maintaining upright stance: the "change-in-support" strategy. *Phys. Ther.* 77, 488–507. doi: 10.1093/ptj/77.5.488

Malaya, C. A., Haworth, J., Pohlman, K. A., Powell, C., and Smith, D. L. (2020). Impact of extremity manipulation on postural sway characteristics: a preliminary, randomized crossover study. *J. Manipulative Physiol. Ther.* 43, 457–468. doi: 10.1016/j.jmpt.2019.02.014

Malaya, C. A., Haworth, J., Pohlman, K. A., and Smith, D. L. (2021). Immediate impact of extremity manipulation on dual task performance: a randomized, crossover clinical trial. *Chiropr. Man. Ther.* 29:6. doi: 10.1186/s12998-021-00366-5

Marshall, P., and Murphy, B. (2010). Delayed abdominal muscle onsets and self-report measures of pain and disability in chronic low back pain. *J. Electromyogr. Kinesiol.* 20, 833–839. doi: 10.1016/j.jelekin.2009.09.005

Paillard, T., and Noé, F. (2015). Techniques and methods for testing the postural function in healthy and pathological subjects. *Biomed. Res. Int.* 2015:891390. doi: 10.1155/2015/891390

Pickar, J. G. (2002). Neurophysiological effects of spinal manipulation. *Spine J.* 2, 357–371. doi: 10.1016/s1529-9430(02)00400-x

Pickar, J. G., and Bolton, P. S. (2012). Spinal manipulative therapy and somatosensory activation. *J. Electromyogr. Kinesiol.* 22, 785–794. doi: 10.1016/j.jelekin.2012.01.015

Pollock, A. S., Durward, B. R., Rowe, P. J., and Paul, J. P. (2000). "What is balance?" *Clin. Rehabil.* 4, 402–406. doi: 10.1191/0269215500cr342oa

Savva, C., Giakas, G., and Efstathiou, M. (2014). The role of the descending inhibitory pain mechanism in musculoskeletal pain following high-velocity, low amplitude thrust manipulation: a review of the literature. *J. Back Musculoskelet. Rehabil.* 27, 377–382. doi: 10.3233/BMR-140472

Shumway-Cook, A., and Woollacott, M. H. (2017). *Motor Control: Translating Research Into Clinical Practice*. Philadelphia, PA: Wolters Kluwer.

Silva, A. C. D., Santos, G. M., Marques, C. M. G., and Marques, J. L. B. (2019). Immediate effects of spinal manipulation on shoulder motion range and pain in individuals with shoulder pain: a randomized trial. *J. Chiropr. Med.* 18, 19–26. doi: 10.1016/j.jcm.2018.10.001

Sjostrom, H., Allum, J., Carpenter, M. G., Adkin, A. L., Honegger, F., and Ettlin, T. (2003). Trunk sway measures of postural stability during clinical balance tests in patients with chronic whiplash injury symptoms. *Spine* 28, 1725–1734. doi: 10.1097/01.BRS.0000083170.34304.A3

Smart, L. J. Jr., and Smith, D. L. (2001). Postural dynamics: clinical and empirical implications. *J. Manipulative Physiol. Ther.* 24, 340–349. doi: 10.1067/mmt.2001.115262

Smith, D. L., Dainoff, M. J., and Smith, J. P. (2006). The effect of chiropractic adjustments on movement time: a pilot study using Fitts law. *J. Manipulative Physiol. Ther.* 29, 257–266. doi: 10.1016/j.jmpt.2006.03.009

Taylor, H. H., and Murphy, B. (2008). Altered sensorimotor integration with cervical spine manipulation. *J. Manipulative Physiol. Ther.* 31, 115–126. doi: 10.1016/j.jmpt.2007.12.011

Thomas, E., Battaglia, G., Patti, A., Brusa, J., Leonardi, V., Palma, A., et al. (2019). Physical activity programs for balance and fall prevention in elderly: a systematic review. *Medicine (Baltimore)* 98:e16218. doi: 10.1097/MD.0000000000016218

Treleaven, J., Jull, G., and LowChoy, N. (2006). The relationship of cervical joint position error to balance and eye movement disturbances in persistent whiplash. *Man. Ther.* 11, 99–106. doi: 10.1016/j.math.2005.04.003

Treleaven, J., Jull, G., and Sterling, M. (2003). Dizziness and unsteadiness following whiplash injury: characteristic features and relationship with cervical joint position error. *J. Rehabil. Med.* 35, 36–43. doi: 10.1080/16501970306109

Urakawa, T., Bunya, M., and Araki, O. (2017). Involvement of the visual change detection process in facilitating perceptual alternation in the bistable image. *Cogn. Neurodyn.* 11, 307–318. doi: 10.1007/s11571-017-9430-8

Urakawa, T., Nagano, K., Matsumoto, Y., and Araki, O. (2018). Enhancement of a genuine visual mismatch negativity correlates with the facilitation of perceptual alternation of a bistable image. *Neuroreport* 29, 1104–1108. doi: 10.1097/WNR.0000000000001079

Wright, W. G. (2011). Tonic postural lean after-effects influenced by support surface stability and dynamics. *Hum. Mov. Sci.* 30, 238–248. doi: 10.1016/j.humov.2010.05.006

Young, D. R., and Layne, C. S. (2020). Effects of shank vibration on lean after-effect. *J. Motil. Behav.* 53, 611–621. doi: 10.1080/00222895.2020.1815640

Young, D. R., Parikh, P. J., and Layne, C. S. (2020). Non-invasive brain stimulation of the posterior parietal cortex alters postural adaptation. *Front. Hum. Neurosci.* 14:248. doi: 10.3389/fnhum.2020.00248

frontiers | Frontiers in Human Neuroscience

TYPE Mini Review
PUBLISHED 11 November 2022
DOI 10.3389/fnhum.2022.1037410

OPEN ACCESS

EDITED BY
Giovanni Mirabella,
University of Brescia, Italy

REVIEWED BY
Luca Falciati,
University of Brescia, Italy
Sara Parmigiani,
University of Milan, Italy

*CORRESPONDENCE
Helene M. Sisti
hsisti@norwich.edu

SPECIALTY SECTION
This article was submitted to Motor Neuroscience, a section of the journal Frontiers in Human Neuroscience

RECEIVED 05 September 2022
ACCEPTED 18 October 2022
PUBLISHED 11 November 2022

CITATION
Sisti HM, Beebe A, Bishop M and Gabrielsson E (2022) A brief review of motor imagery and bimanual coordination.
Front. Hum. Neurosci. 16:1037410.
doi: 10.3389/fnhum.2022.1037410

A brief review of motor imagery and bimanual coordination

Helene M. Sisti*, Annika Beebe, Mercedes Bishop and Elias Gabrielsson

Department of Psychology, Norwich University, Northfield, VT, United States

Motor imagery is increasingly being used in clinical settings, such as in neurorehabilitation and brain computer interface (BCI). In stroke, patients lose upper limb function and must re-learn bimanual coordination skills necessary for the activities of daily living. Physiotherapists integrate motor imagery with physical rehabilitation to accelerate recovery. In BCIs, users are often asked to imagine a movement, often with sparse instructions. The EEG pattern that coincides with this cognitive task is captured, then used to execute an external command, such as operating a neuroprosthetic device. As such, BCIs are dependent on the efficient and reliable interpretation of motor imagery. While motor imagery improves patient outcome and informs BCI research, the cognitive and neurophysiological mechanisms which underlie it are not clear. Certain types of motor imagery techniques are more effective than others. For instance, focusing on kinesthetic cues and adopting a first-person perspective are more effective than focusing on visual cues and adopting a third-person perspective. As motor imagery becomes more dominant in neurorehabilitation and BCIs, it is important to elucidate what makes these techniques effective. The purpose of this review is to examine the research to date that focuses on both motor imagery and bimanual coordination. An assessment of current research on these two themes may serve as a useful platform for scientists and clinicians seeking to use motor imagery to help improve bimanual coordination, either through augmenting physical therapy or developing more effective BCIs.

KEYWORDS

motor imagery (MI), bimanual coordination, brain computer interface (BCI), neurorehabilitation, motor control, EEG, neuroplasticity, learning

Introduction

The rationale for this brief review was borne out of two observations: (1) brain computer interface (BCI) applications depend largely on motor imagery (Wolpaw and Wolpaw, 2012; McFarland and Wolpaw, 2018) (2) patient outcome can be improved when physical therapy is augmented with motor imagery (Mulder, 2007; Deutsch et al., 2012). Motor imagery is defined as the mental simulation of a movement in the absence of any overt movement (Decety, 1996; Jeannerod, 1999; Neuper et al., 2005).

While the benefits of motor imagery have been recognized by athletes for decades, its advantages in clinical and rehabilitative settings, as well as its integration with BCI, is much more recent (Warner and McNeill, 1988; de Vries and Mulder, 2007). In BCI, individuals learn to control an external device, such as a neuroprosthetic device or more commonly, a computer cursor, by regulating their brain activity. Early demonstrations of this type of control were observed when individuals modulated their mu rhythm in the sensorimotor cortex (Wolpaw et al., 1991; McFarland et al., 2000; Neuper et al., 2009). More recent studies have demonstrated that BCI control is not limited to the mu rhythm, comprised of alpha and beta frequencies, but also occurs in several other ranges, including delta, theta, (Babiloni et al., 2017) and gamma rhythms (Babiloni et al., 2016). When a user learns to replicate this pattern, and conversely, the BCI accurately extracts and classifies the signature wave properties, then the individual acquires BCI control (McFarland and Wolpaw, 2018). This phenomenon requires multiple practice sessions to develop and is not present in all users (Vidaurre and Blankertz, 2010; Lotte and Jeunet, 2015; Thompson, 2019). It is important to acknowledge that movement execution and observation, which are closely related to motor imagery, have a complex underpinning. The neural dynamics that underlie movement execution and action observation overlap, and while they are highly relevant, they are beyond the scope of this brief review.

The majority of research in BCI has grown out of the machine learning perspective, i.e., developing computational algorithms that reliably interpret EEG signals (Aricò et al., 2018; McFarland and Wolpaw, 2018), while much less research has been dedicated to the nature of the user's cognitive state. Further, stroke, and other neurodegenerative diseases such as multiple sclerosis, typically result in the loss of bimanual coordination. Many of the activities of daily living depend on successful bimanual coordination, such as buttoning a shirt or opening a tube of toothpaste. Therefore, a greater understanding of the use of motor imagery in bimanual coordination skills may help accelerate patient recovery and inform future research. The aim of this review is to bring together two themes, motor imagery and bimanual coordination, that are not often considered together, and to examine them in the context of their capacity to enhance neurorehabilitation and BCI development.

Review criteria

This review was conducted using two scientific databases, PubMed and Scopus, with the keywords, motor imagery AND bimanual coordination. We adopted '*motor* imagery' in favor or '*mental* imagery' because the former is specific to movement and motor skills (Collet and Guillot, 2010), whereas the latter is a broader term that includes general cognitive tasks and does not necessarily require any movement. For example, mental rotation of a three-dimensional object, memory retrieval, and mental arithmetic would not be categorized as motor imagery. Bimanual coordination includes a diverse range of skills which depend upon simultaneous use of the left and right hands (Ivry et al., 2004; Swinnen and Wenderoth, 2004). The PubMed database retrieved 11 results and Scopus retrieved 17. All of PubMed's results were duplicates of Scopus. Studies that focused on gait abnormalities in diseased populations (Vercruysse et al., 2012) or included TMS (Levin et al., 2004; Wang et al., 2015, 2016) were excluded.

Movement topology

Bimanual coordination tasks range in complexity from those as simple as clapping, which an infant performs almost reflexively, to others that require a lifetime of practice, such as a concert pianist performing a difficult sonata. In the 16 research articles, the types of bimanual movements tested ranged from simple, laboratory tasks, such as bimanual sequence learning (Debarnot et al., 2012) and finger-thumb opposition task (Nair et al., 2003) to those high in ecological validity, such as tying shoelaces, buttoning a shirt (Szameitat et al., 2012) or mimicking piano playing (Riquelme-Ros et al., 2020). The simultaneous circle and line drawing task was used across a large range of ages and developmental stages (Piedimonte et al., 2014) in autistic spectrum conditions (Piedimonte et al., 2018) and in stroke patients (Morioka et al., 2019). The simultaneous circle-line drawing task is used as a method for investigating the bimanual coupling effect (Franz et al., 1991). That is, when a person attempts to draw a circle with one hand and a line with the other, the line starts to resemble a circle. The extent to which the linear trajectory takes the shape of a circle can be quantified using the 'ovalization index' (OI) (Garbarini et al., 2012; Piedimonte et al., 2014). This OI is thereby a quantitative measure of the degree of neural cross-talk. In other words, as the line being drawn with one hand, starts to resemble the circle being drawn by the other (or vice cersa), interference across the two hemispheres can be inferred (Franz et al., 1991; Garbarini et al., 2012; Piedimonte et al., 2014). This model was used in healthy (Piedimonte et al., 2014), autistic (Piedimonte et al., 2018), and stroke patients (Morioka et al., 2019). Morioka et al. (2019) noted that use-dependent plasticity is an important factor to consider in stroke patients. When movement execution becomes difficult or impossible due to a brain lesion, usually a contralateral one, the patient may stop even thinking about the movement. This type of motor neglect could contribute to a decline in motor representation. By asking patients to draw a line or circle with a paralyzed limb, some degree of motor planning was occurring. Therefore, even if movement execution was not observed, the motor representation was presumably being reactivated (Morioka et al., 2019). In their study, King et al. (2022) used a desktop pedal exerciser designed for the hands. They noted that bilateral arm training for the use of motor imagery in BCI is receiving increased attention because unlike unimanual

motion, it enables (a) motor cortex disinhibition of the injured hemisphere, (b) enhanced paths from the contralesional region to recruitment, and (c) upregulation of descending motor neuron commands to propriospinal neurons (Whitall et al., 2011; Lee et al., 2016).

It is important to consider seminal research on bimanual coordination constraints. Haken et al. (1985) compared left and right hand movements to a coupled non-linear oscillator. In so doing, they developed what came to be known as the HKB model, which could make robust predictions concerning a range of bimanual coordination patterns (for full review, see Kelso, 2021). One of the implications of this model was that it brought to light the importance of movement topology (McGinnis and Newell, 1982; Schmidt and Lee, 2018). Briefly, when the left and right hands move in a symmetric or mirror-like pattern along the midline, they are easier to perform than when they are required to move in the same direction, i.e., in a parallel, asymmetric pattern (Swinnen, 2002). Further, the model accurately predicted that if individuals were asked to perform the less favorable, asymmetric movements at faster and faster rates, then bimanual coordination would be compromised; movements would start to transition to the intrinsically favorable mirror symmetric patterns (Swinnen and Wenderoth, 2004). Notably, bimanual coordination movements that were reliably predicted using *discrete* bimanual skills, such as finger tapping, could not be uniformly applied to those that required *continuous* bimanual skills, such as dial rotation (Sisti et al., 2011). For instance, in finger-tapping, some combinations can be learned at a faster rate others (Summers, 2002); integer ratios, where two taps of the hand occur for every one tap of the other (2:1) are easier to learn compared with non-integer ratios, three taps of one hand for every two taps of the other hand (3:2). However, when subjects are asked to perform a similar combination but with a continuous motor skill instead of a discrete one, this difference disappears and the relative velocity between the two hands becomes the predictive parameter (Sisti et al., 2011). When shifting from behavioral and musculoskeletal perspectives to one that is neurophysiological, the importance of movement topology is especially clear. That is, movement direction is uniquely encoded by neuronal populations (Georgopoulos et al., 1986). Therefore, there is both behavioral and neuronal evidence for the importance of considering movement topology in the context of developing BCI systems and neurorehabilitation strategies that enhance bimanual coordination.

Motor imagery and Bernstein's degree of freedom problem

Dahm and Rieger (2016a) point out that a variety of motor coordination constraints, such as Fitts' Law, are also present in motor imagery (Fitts, 1954; Cerritelli et al., 2011; Dahm and Rieger, 2016a). They included three motor imagery conditions of a bimanual coordination task in order to determine the extent of cognitive constraints (Dahm and Rieger, 2016a). The study built on accumulating evidence for the role of cognitive and perceptual constraints in bimanual coordination (Mechsner et al., 2001). Briefly, participants learned target reaching tasks in which congruent and incongruent targets (X to O, vs. O to O) were included and required both symmetric and parallel movements to perform successfully. Both real and imagined movements were timed, and the three experimental conditions included were based on the phase of movement, i.e., initiation, termination, and the entire duration of the movement (Dahm and Rieger, 2016a). Participants engaged in kinesthetic imagery. Ease of imagery, vividness of imagery and concentration were all assessed using a Likert scale. It was noted that task-dependent processes occur in which several types of motor imagery may be differentially engaged. For instance, while drawing is a unimanual motor task, it relies heavily on visual cues, however, movements such as rowing or reaching may be more dependent on kinesthetic cues (Dahm and Rieger, 2016a). Further, components of the movement, such as initiation and termination, are important considerations. In another study, they examined whether bimanual coordination constraints are present in motor imagery (Dahm and Rieger, 2016b). They used three tasks to compare different versions of the mental chronometry paradigm, in which the time it takes to complete a motor imagery task is measured. The key finding was that bimanual coordination constraints were also present in motor imagery, i.e., imagined symmetric movements resulted in shorter inter-response intervals and greater accuracy than parallel movements (Dahm and Rieger, 2016b).

Szameitat et al. (2012) also included a kinesthetic first person perspective. Further, they instructed participants to "engage intensely" and with "high frequency" for the duration of a set time trial. Self-reported assessment of how vividly participants could imagine the movement was completed using a 7-point Likert scale. Szameitat et al. (2012) captured potential movement during imagery by having participants hold a force sensitive grip in each hand. Interestingly, the only condition that detected a significant increase from baseline was the most difficult one, i.e., imagination of a complex movement using the non-dominant hand.

The Russian neurophysiologist, Nikolai Bernstein (1967) first described what would come to be known as the degrees of freedom problem (1967). That is, redundant solutions exist for any given motor skill. When Bernstein's degrees of freedom problem is considered in the context of motor imagery, redundant solutions multiply. In addition, there is the obvious issue that while behavior is directly observable, cognition is only indirectly observed. This highlights the need for specifying type of motor imagery, explicit *a priori* instructions as well as qualitative and quantitative *post hoc* assessments. The majority of papers reviewed included the favorable kinesthetic, first-person perspective, which emphasizes internal, proprioceptive sensations (see **Table 1**).

Brain mapping approaches: Region of interest and functional connectivity

The first demonstration of the neuroanatomical correlates of imagined bimanual coordination skills was reported by Szameitat et al. (2012). Their prediction, and substantiation, that the neural activity of a specific cortical region of interest would not be selectively increased, rather connectivity would change, was built on the previous research of Puttemans et al. (2005). They reported that when skills are learned to the point that they become automatic, they are said to be overlearned, and in this case the neuroanatomical correlates are *sub*cortical, and not cortical. In the early stages when attentional resources and cognitive demands are high, cortical

TABLE 1 A subset of articles from the literature review that focused on neurologically health adults.

References	Movement type	Motor imagery	Neuro-imaging technique	Population studied	Key points
Riquelme-Ros et al., 2020	Drumming of the fingers, swinging wrist up and down; mimicked piano playing – Imagined only	Not specified	EEG	Expert piano players (n = 4; 2 males, 2 females, mean 24.5 years) vs. controls (n = 4; 2 males, 2 females, mean 32.75 years)	-The Common Spatial Patterns (CSP) machine learning algorithm was applied to *feature extraction* and Linear Discriminant Analysis (LDA) machine learning algorithm was applied to *classification* using 8 electrode cap. -Expert pianists achieved higher level of BCI control (75%) compared with non- pianists (63%) using motor imagery.
Dahm and Rieger, 2016a	Target task including reaching in response to a cue; reaction time, movement time, and movement preparation time were captured	Kinesthetic imagery at each phase of the movement, pressing and holding the start button, reaching for the target and pressing the target	Cognition and behavior only	Healthy adults (n = 23, mean age 24.5 years)	-Bimanual coordination constraints are present in motor imagery. -Functional equivalence between real and imagined movement is present even for short reaction times to stimuli. -Task-dependent differences occur in motor imagery; some rely more heavily on kinesthetic representation whereas others rely more heavily on a visual representation. -Different subcomponents of movement are not equally vivid during motor imagery.
Sallard et al., 2014	Unimanual and bimanual finger tapping	Not specified	EEG	Young (n = 29; 14 males, 15 females; age range 19-29 years) vs. Old (n = 27; healthy adults, 12 males 15 females; age range 60–83)	-Main effect of tapping condition in both low and high beta bands, with lower power in bimanual than unimanual in both age groups. -Bimanual advantage is absent in the elderly; Motor imagery was not included in the methods, rather in the interpretation of the results. -Elderly may rely more on visual imagery compared with kinesthetic imagery due to reduced kinesthetic reafferences.
Debarnot et al., 2012	Simple and complex unimanual and bimanual finger sequence learning	Kinesthetic, internal visual	Cognition and behavior only	Healthy adults (n = 48, gender not reported, mean age 27.8 years	-Sleep following Motor Imagery training improved performance compared to same passage of time with no sleep (daytime interval). -Strongest performance gains were obtained for the most challenging task; this finding illustrates that similar to learning a physical motor skill, sleep enhances memory consolidation of MI, and the effect is enhanced as the difficulty of the skill increases.
Szameitat et al., 2012	Everyday tasks such as tying shoelaces, buttoning a shirt	Kinesthetic first person	fMRI	Neurologically healthy adults (n = 17, 6 male, 11 female, aged 19-31; mean 22 years)	-High in ecological validity; results consistent with laboratory models of bimanual coordination. -Detected changes in functional connectivity within and between cerebral hemispheres. -Highlighted importance of multivariate network analysis rather than region-of-interest approach.
Nair et al., 2003	Unimanual and bimanual finger to thumb opposition task	Not specified	fMRI	Neurologically healthy adults (n = 8; 3 males and 5 females; ages 25–40)	-Sensorimotor cortex, supplementary motor area (SMA), superior parietal lobule and cerebellum were identified when the tasks involved both planning and execution. -Cerebellar activity present during actual, but not imagined, movement; thereby supporting motor control theory that the cerebellum monitors cortical output and provides corrective information to the motor cortex primarily during physical, executed movement. -Subjects reported that imagining the bimanual sequence movement was the most difficult of the tasks performed.

Clinical populations, such as Parkinson's disease, cerebral palsy or autistic spectrum disorder, are beyond the scope of this brief review.

regions are engaged; however during later stages of learning, cortical activation dissipates and subcortical activations become dominant (Puttemans et al., 2005). Szameitat et al. (2012) found changes in functional found changes in functional connectivity between parietal and premotor areas within and between hemispheres. This was in contrast to the lack of effect of any change in neural activation of a specific cortical region. This distinction is noteworthy because EEG captures cortical changes, while activity changes in subcortical structures depend on how well the "source localization" problem is addressed.

Coordinating the left and right hands depends on the primary and premotor cortices (M1 and PMC) and supplementary motor area (SMA) in the cortex, the cerebellum, and subcortically, the cingulate motor area and basal ganglia (Swinnen and Wenderoth, 2004; Jantzen et al., 2008; Rueda-Delgado et al., 2014). These areas are also active in unimanual movements (Cabibel et al., 2020). As task demands increase, the network extends beyond these regions to encompass prefrontal, parietal, and temporal areas (Swinnen and Wenderoth, 2004; Rueda-Delgado et al., 2014). While contralateral motor control has long been established, recent studies have highlighted the important contributions of ipsilateral motor control as well (Bundy and Leuthardt, 2019). Several studies have shown that the sensorimotor areas of the ipsilateral hemisphere are also activated (Bundy and Leuthardt, 2019), though its role is not yet clear. Some sustain that the ipsilateral activation contributes to the planning and execution of contralateral limb movements as the kinematic and movement parameters of the contralateral limb can be decoded from signals recorded in the ipsilateral hemisphere in monkeys (Ames and Churchland, 2019) and in humans (Bundy et al., 2018). Furthermore, the two hemispheres seem to have different roles in terms of praxis, independently from handedness. In fact, lesions of the left hemisphere lead to apraxia, i.e., the impairments in the production of complex movement in the absence of muscle deficits, much more often than right hemisphere damages (Haaland, 2006). Notably, a study showed that the ipsilateral cortical representation of reaching arm movements strikingly differs between the left and right hemispheres (Merrick et al., 2022). Finally, Mancini and Mirabella (2021) found left dominance in reactive inhibitory control. Inhibitory control is a pillar of motor control (Mirabella, 2014), and very likely, implementing inhibitory control in BCI could greatly help in restoring naturalistic behaviors (Mirabella and Lebedev, 2017).

Conclusion

-Developing effective BCI systems and neurorehabilitation strategies may depend on careful consideration of the type of bimanual movements individuals are being asked to learn.

-Skills that have been learned so well that they become automatic rely more heavily on subcortical structures and less so on cortical structures. EEG captures only surface cortical changes, and not subcortical ones. Although activity from deeper brain structures may be inferred as the "source localization" problem is resolved, EEG does not have the spatial resolution of fMRI. Therefore, movement topology and learning factors must be considered. For instance, the inclusion of more complex bimanual patterns may reveal cortical activation patterns that are distinct from simpler bimanual coordination patterns that require little training to learn.

-Assessing the vividness of a person's motor imagery skills using both qualitative and quantitative measures, such as R-VMIQ and mental chronometry, may account for unexplained variance, thereby leading to more effective classifiers in BCI and better MI intervention strategies in clinical settings.

Author contributions

HS conceived the topic, led the literature search, prepared the manuscript, and final table. AB, MB, and EG conducted the literature searches, retrieved full-text articles, and prepared earlier versions of the table. All authors contributed to the article and approved the submitted version.

Funding

This project was supported by an Institutional Development Award (IDeA) from the National Institute of General Medical Sciences of the National Institutes of Health under grant no. P20GM103449. Its contents are solely the responsibility of the authors and do not necessarily represent the official views of NIGMS or NIH. Research was also supported by our collaborators at the National Center for Adaptive Neurotechnologies, under grant no. P41 EB018783 (NIH, NIBIB).

Conflict of interest

The authors declare that the research was conducted in the absence of any commercial or financial relationships that could be construed as a potential conflict of interest.

Publisher's note

References

Ames, K. C., and Churchland, M. M. (2019). Motor cortex signals for each arm are mixed across hemispheres and neurons yet partitioned within the population response. *Elife* 8:e46159. doi: 10.7554/eLife.46159.027

Aricò, P., Borghini, G., Di Flumeri, G., Sciaraffa, N., and Babiloni, F. (2018). Passive BCI beyond the lab: Current trends and future directions. *Physiol. Meas.* 39:08TR02. doi: 10.1088/1361-6579/aad57e

Babiloni, C., Del Percio, C., Lopez, S., Di Gennaro, G., Quarato, P. P., Pavone, L., et al. (2017). Frontal functional connectivity of electrocorticographic delta and theta rhythms during action execution versus action observation in humans. *Front. Behav. Neurosci.* 11:20. doi: 10.3389/fnbeh.2017.00020

Babiloni, C., Del Percio, C., Vecchio, F., Sebastiano, F., Di Gennaro, G., Quarato, P. P., et al. (2016). Alpha, beta and gamma electrocorticographic rhythms in somatosensory, motor, premotor and prefrontal cortical areas differ in movement execution and observation in humans. *Clin. Neurophysiol.* 127, 641–654. doi: 10.1016/j.clinph.2015.04.068

Bernstein, N. A. (1967). *The co-ordination and regulation of movements*. Oxford: Pergamon Press.

Bundy, D. T., and Leuthardt, E. C. (2019). The cortical physiology of ipsilateral limb movements. *Trends Neurosci.* 42, 825–839.

Bundy, D. T., Szrama, N., Pahwa, M., and Leuthardt, E. C. (2018). Unilateral, 3D arm movement kinematics are encoded in ipsilateral human cortex. *J. Neurosci.* 38, 10042–10056. doi: 10.1523/JNEUROSCI.0015-18.2018

Cabibel, V., Hordacre, B., and Perrey, S. (2020). Implication of the ipsilateral motor network in unilateral voluntary muscle contraction: The cross-activation phenomenon. *J. Neurophysiol.* 123, 2090–2098. doi: 10.1152/jn.00064.2020

Cerritelli, C., Guillot, A., Lebon, F., MacIntyre, T., and Moran, A. (2011). Measuring motor imagery using psychometric, behavioral, and psychophysiological tools. *Exerc. Sport Sci. Rev.* 39, 85–92. doi: 10.1097/JES.0b013e31820ac5e0

Collet, C., and Guillot, A. (2010). "Autonomic nervous system activities during imagined movements," in *The neurophysiological foundations of mental and motor imagery*, eds A. Guillot and C. Collet (New York, NY: Oxford University Press), 95–108. doi: 10.1093/acprof:oso/9780199546251.003.0007

Dahm, S. F., and Rieger, M. (2016a). Cognitive constraints on motor imagery. *Psychol. Res.* 80, 235–247. doi: 10.1007/s00426-015-0656-y

Dahm, S. F., and Rieger, M. (2016b). Is there symmetry in motor imagery? Exploring different versions of the mental chronometry paradigm. *Atten. Percept. Psychophys.* 78, 1794–1805. doi: 10.3758/s13414-016-1112-9

de Vries, S., and Mulder, T. (2007). Motor imagery and stroke rehabilitation: A critical discussion. *J. Rehabil. Med.* 39, 5–13. doi: 10.2340/16501977-0020

Debarnot, U., Castellani, E., and Guillot, A. (2012). Selective delayed gains following motor imagery of complex movements. *Arch. Ital. Biol.* 150, 238–250. doi: 10.4449/aib.v150i4.1394

Decety, J. (1996). The neurophysiological basis of motor imagery. *Behav. Brain Res.* 77, 45–52. doi: 10.1016/0166-4328(95)00225-1

Deutsch, J., Maidan, I., and Dickstein, R. (2012). Patient-centered integrated motor imagery delivered in the home with telerehabilitation to improve walking after stroke. *Phys. Ther.* 92, 1065–1077. doi: 10.2522/ptj.20110277

Fitts, P. M. (1954). The information capacity of the human motor system in controlling the amplitude of movement. *J. Exp. Psychol.* 47, 381–391. doi: 10.1037/h0055392

Franz, E. A., Zelaznik, H. N., and McCabe, G. (1991). Spatial topological constraints in a bimanual task. *Acta Psychol.* 77, 137–151. doi: 10.1016/0001-6918(91)90028-x

Garbarini, F., Rabuffetti, M., Piedimonte, A., Pia, L., Ferrarin, M., Frassinetti, F., et al. (2012). 'Moving' a paralysed hand: Bimanual coupling effect in patients with anosognosia for hemiplegia. *Brain* 135, 1486–1497. doi: 10.1093/brain/aws015

Georgopoulos, A. P., Schwartz, A. B., and Kettner, R. E. (1986). Neuronal population coding of movement direction. *Science* 233, 1416–1419. doi: 10.1126/science.3749885

Haaland, K. Y. (2006). Left hemisphere dominance for movement. *Clin. Neuropsychol.* 20, 609–622. doi: 10.1080/13854040590967577

Haken, H., Kelso, J. A., and Bunz, H. (1985). A theoretical model of phase transitions in human hand movements. *Biol. Cybern.* 51, 347–356. doi: 10.1007/BF00336922

Ivry, R., Diedrichsen, J., Spencer, R., Hazeltine, E., and Semjen, A. (2004). "A cognitive neuroscience perspective on bimanual coordination and interference," in *Neuro-behavioral determinants of interlimb coordination*, eds S. P. Swinnen and J. Duysens (Boston, MA: Springer), 259–295.

Jantzen, K. J., Oullier, O., and Scott Kelso, J. A. (2008). Neuroimaging coordination dynamics in the sport sciences. *Methods* 45, 325–335. doi: 10.1016/j.ymeth.2008.06.001

Jeannerod, V. (1999). Mental imaging of motor activity in humans. *Curr. Opin. Neurobiol.* 9, 735–739.

Kelso, J. A. (2021). The Haken–Kelso–Bunz (HKB) model: From matter to movement to mind. *Biol. Cybern.* 115, 305–322. doi: 10.1007/s00422-021-00890-w

King, J. T., John, A. R., Wang, Y. K., Shih, C. K., Zhang, D., Huang, K. C., et al. (2022). Brain connectivity changes during bimanual and rotated motor imagery. *IEEE J. Transl. Eng. Health Med.* 10:2100408. doi: 10.1109/jtehm.2022.3167552

Lee, S., Kim, Y., and Lee, B. H. (2016). Effect of virtual reality-based bilateral upper extremity training on upper extremity function after stroke: A randomized controlled clinical trial. *Occup. Ther. Int.* 23, 357–368. doi: 10.1002/oti.1437

Levin, O., Steyvers, M., Wenderoth, N., Li, Y., and Swinnen, S. P. (2004). Dynamical changes in corticospinal excitability during imagery of unimanual and bimanual wrist movements in humans: A transcranial magnetic stimulation study. *Neurosci. Lett.* 359, 185–189. doi: 10.1016/j.neulet.2004.01.070

Lotte, F., and Jeunet, C. (2015). "'Towards improved BCI based on human learning principles," in *Proceedings of the 3rd international winter conference on brain-computer interface*, (Gangwon: IEEE), 1–4. doi: 10.1109/IWW-BCI.2015.7073024

Mancini, C., and Mirabella, G. (2021). Handedness does not impact inhibitory control, but movement execution and reactive inhibition are more under a left-hemisphere control. *Symmetry* 13:1602.

McFarland, D. J., Miner, L. A., Vaughan, T. M., and Wolpaw, J. R. (2000). Mu and beta rhythm topographies during motor imagery and actual movements. *Brain Topogr.* 12, 177–186. doi: 10.1023/a:1023437823106

McFarland, D. J., and Wolpaw, J. R. (2018). Brain–computer interface use is a skill that user and system acquire together. *PLoS Biol.* 16:e2006719. doi: 10.1371/journal.pbio.2006719

McGinnis, P. M., and Newell, K. M. (1982). Topological dynamics: A framework for describing movement and its constraints. *Hum. Mov. Sci.* 1, 289–305.

Mechsner, F., Kerzel, D., Knoblich, G., and Prinz, W. (2001). Perceptual basis of bimanual coordination. *Nature* 414, 69–73. doi: 10.1038/35102060

Merrick, C. M., Dixon, T. C., Breska, A., Lin, J., Chang, E. F., King-Stephens, D., et al. (2022). Left hemisphere dominance for bilateral kinematic encoding in the human brain. *Elife* 11:e69977. doi: 10.7554/eLife.69977

Mirabella, G. (2014). Should I stay or should I go? Conceptual underpinnings of goal-directed actions. *Front. Syst. Neurosci.* 8:206. doi: 10.3389/fnsys.2014.00206

Mirabella, G., and Lebedev, M. À (2017). Interfacing to the brain's motor decisions. *J. Neurophysiol.* 117, 1305–1319. doi: 10.1152/jn.00051.2016

Morioka, S., Osumi, M., Nishi, Y., Ishigaki, T., Ishibashi, R., Sakauchi, T., et al. (2019). Motor-imagery ability and function of hemiplegic upper limb in stroke patients. *Ann. Clin. Transl. Neurol.* 6, 596–604.

Mulder, T. (2007). Motor imagery and action observation: Cognitive tools for rehabilitation. *J. Neural Transm.* 114, 1265–1278. doi: 10.1007/s00702-007-0763-z

Nair, D. G., Purcott, K. L., Fuchs, A., Steinberg, F., and Kelso, J. A. (2003). Cortical and cerebellar activity of the human brain during imagined and executed unimanual and bimanual action sequences: A functional MRI study. *Brain Res. Cogn. Brain Res.* 15, 250–260. doi: 10.1016/s0926-6410(02)00197-0

Neuper, C., Scherer, R., Reiner, M., and Pfurtscheller, G. (2005). Imagery of motor actions: Differential effects of kinesthetic and visual-motor mode of imagery in single-trial EEG. *Brain Res. Cogn. Brain Res.* 25, 668–677. doi: 10.1016/j.cogbrainres.2005.08.014

Neuper, C., Scherer, R., Wriessnegger, S., and Pfurtscheller, G. (2009). Motor imagery and action observation: Modulation of sensorimotor brain rhythms during mental control of a brain–computer interface. *Clin. Neurophysiol.* 120, 239–247. doi: 10.1016/j.clinph.2008.11.015

Piedimonte, A., Conson, M., Frolli, A., Bari, S., Della Gatta, F., Rabuffetti, M., et al. (2018). Dissociation between executed and imagined bimanual movements in autism spectrum conditions. *Autism Res.* 11, 376–384. doi: 10.1002/aur.1902

Piedimonte, A., Garbarini, F., Rabuffetti, M., Pia, L., and Berti, A. (2014). Executed and imagined bimanual movements: A study across different ages. *Dev. Psychol.* 50, 1073–1080. doi: 10.1037/a0034482

Puttemans, V., Wenderoth, N., and Swinnen, S. P. (2005). Changes in brain activation during the acquisition of a multifrequency bimanual coordination task: From the cognitive stage to advanced levels of automaticity. *J. Neurosci.* 25, 4270–4278. doi: 10.1523/jneurosci.3866-04.2005

Riquelme-Ros, J. V., Rodriguez-Bermudez, G., Rodriguez-Rodriguez, I., Rodriguez, J. V., and Molina-Garcia-Pardo, J. M. (2020). On the better performance of pianists with motor imagery-based brain-computer interface systems. *Sensors* 20:4452. doi: 10.3390/s20164452

Rueda-Delgado, L. M., Solesio-Jofre, E., Serrien, D. J., Mantini, D., Daffertshofer, A., and Swinnen, S. P. (2014). Understanding bimanual coordination across small time scales from an electrophysiological perspective. *Neurosci. Biobehav. Rev.* 47, 614–635. doi: 10.1016/j.neubiorev.2014.10.003

Sallard, E., Spierer, L., Ludwig, C., Deiber, M. P., and Barral, J. (2014). Age-related changes in the bimanual advantage and in brain oscillatory activity during tapping movements suggest a decline in processing sensory reafference. *Exper. Brain Res.* 232, 469–479. doi: 10.1007/s00221-013-3754-3

Schmidt, R. A., and Lee, T. D. (2018). *Motor control and learning: A behavioral emphasis*. Champaign, IL: Human Kinetics.

Sisti, H. M., Geurts, M., Clerckx, R., Gooijers, J., Coxon, J. P., Heitger, M. H., et al. (2011). Testing multiple coordination constraints with a novel bimanual visuomotor task. *PLoS One* 6:e23619. doi: 10.1371/journal.pone.0023619

Summers, J. (2002). Practice and training in bimanual coordination tasks: Strategies and constraints. *Brain Cogn.* 48, 166–178.

Swinnen, S. P. (2002). Intermanual coordination: From behavioural principles to neural-network interactions. *Nat. Rev. Neurosci.* 3, 348–359. doi: 10.1038/nrn807

Swinnen, S. P., and Wenderoth, N. (2004). Two hands, one brain: Cognitive neuroscience of bimanual skill. *Trends Cogn. Sci.* 8, 18–25.

Szameitat, A. J., McNamara, A., Shen, S., and Sterr, A. (2012). Neural activation and functional connectivity during motor imagery of bimanual everyday actions. *PLoS One* 7:e38506. doi: 10.1371/journal.pone.0038506

Thompson, M. C. (2019). Critiquing the concept of BCI illiteracy. *Sci. Eng. Ethics* 25, 1217–1233. doi: 10.1007/s11948-018-0061-1

Vercruysse, S., Spildooren, J., Heremans, E., Vandenbossche, J., Wenderoth, N., Swinnen, S. P., et al. (2012). Abnormalities and cue dependence of rhythmical upper-limb movements in Parkinson patients with freezing of gait. *Neurorehabil. Neural Repair* 26, 636–645. doi: 10.1177/1545968311431964

Vidaurre, C., and Blankertz, B. (2010). Towards a cure for BCI illiteracy. *Brain Topogr.* 23, 194–198. doi: 10.1007/s10548-009-0121-6

Wang, K., Wang, Z., Zhou, P., Qi, H., He, F., Liu, S., et al. (2015). "MEP analysis of hand motor imagery with bimanual coordination under transcranial magnetic stimulation," in *Proceedings of the IEEE 7th international conference on awareness science and technology (iCAST)*, Qinhuangdao. 111–114. doi: 10.1109/ICAwST.2015.7314030

Wang, K., Wang, Z., Zhou, P., Qi, H., He, F., Liu, S., et al. (2016). MEP analysis of hand motor imagery with bimanual coordination under transcranial magnetic stimulation. *J. Adv. Comput. Intell. Intell. Inform.* 20, 462–466.

Warner, L., and McNeill, M. E. (1988). Mental imagery and its potential for physical therapy. *Phys. Ther.* 68, 516–521. doi: 10.1093/ptj/68.4.516

Whitall, J., Waller, S. M., Sorkin, J. D., Forrester, L. W., Macko, R. F., Hanley, D. F., et al. (2011). Bilateral and unilateral arm training improve motor function through differing neuroplastic mechanisms: A single-blinded randomized controlled trial. *Neurorehabil. Neural Repair* 25, 118–129. doi: 10.1177/1545968310380685

Wolpaw, J. R., McFarland, D. J., Neat, G. W., and Forneris, C. A. (1991). An EEG-based brain-computer interface for cursor control. *Electroencephalogr. Clin. Neurophysiol.* 78, 252–259. doi: 10.1016/0013-4694(91)90040-b

Wolpaw, J. R., and Wolpaw, E. W. (2012). *Brain-computer interfaces: Principles and practice*. New York, NY: Oxford University Press.

frontiers | Frontiers in Human Neuroscience

TYPE Original Research
PUBLISHED 08 December 2022
DOI 10.3389/fnhum.2022.1028700

OPEN ACCESS

EDITED BY
Daniela De Bartolo,
Santa Lucia Foundation (IRCCS), Italy

REVIEWED BY
Virginia López-Alonso,
University of A Coruña, Spain
Thomas A. Stoffregen,
University of Minnesota Twin Cities, United States
Žiga Kozinc,
University of Primorska, Slovenia

*CORRESPONDENCE
Koichi Hiraoka
hiraoka@omu.ac.jp

SPECIALTY SECTION
This article was submitted to Motor Neuroscience, a section of the journal Frontiers in Human Neuroscience

RECEIVED 26 August 2022
ACCEPTED 11 November 2022
PUBLISHED 08 December 2022

CITATION
Hamada N, Kunimura H, Matsuoka M, Oda H and Hiraoka K (2022) Advanced cueing of auditory stimulus to the head induces body sway in the direction opposite to the stimulus site during quiet stance in male participants. *Front. Hum. Neurosci.* 16:1028700. doi: 10.3389/fnhum.2022.1028700

Advanced cueing of auditory stimulus to the head induces body sway in the direction opposite to the stimulus site during quiet stance in male participants

Naoki Hamada[1], Hiroshi Kunimura[1], Masakazu Matsuoka[1], Hitoshi Oda[2] and Koichi Hiraoka[1]*

[1]Department of Rehabilitation Science, School of Medicine, Osaka Metropolitan University, Habikino, Japan, [2]Graduate School of Comprehensive Rehabilitation, Osaka Prefecture University, Habikino, Japan

Under certain conditions, a tactile stimulus to the head induces the movement of the head away from the stimulus, and this is thought to be caused by a defense mechanism. In this study, we tested our hypothesis that predicting the stimulus site of the head in a quiet stance activates the defense mechanism, causing a body to sway to keep the head away from the stimulus. Fourteen healthy male participants aged 31.2 ± 6.8 years participated in this study. A visual cue predicting the forthcoming stimulus site (forehead, left side of the head, right side of the head, or back of the head) was given. Four seconds after this cue, an auditory or electrical tactile stimulus was given at the site predicted by the cue. The cue predicting the tactile stimulus site of the head did not induce a body sway. The cue predicting the auditory stimulus to the back of the head induced a forward body sway, and the cue predicting the stimulus to the forehead induced a backward body sway. The cue predicting the auditory stimulus to the left side of the head induced a rightward body sway, and the cue predicting the stimulus to the right side of the head induced a leftward body sway. These findings support our hypothesis that predicting the auditory stimulus site of the head induces a body sway in a quiet stance to keep the head away from the stimulus. The right gastrocnemius muscle contributes to the control of the body sway in the anterior–posterior axis related to this defense mechanism.

KEYWORDS

defense mechanism, postural control, auditory stimulus, tactile stimulus, center of pressure, electromyography

Introduction

We frequently observed the head of the participants moving forward in a quiet stance when a coil, attached to a magnetic stimulator, was placed over the back of the head for transcranial magnetic stimulation (TMS). The participants could have predicted the forthcoming TMS when the coil was placed over the back of the head. Predicting the perturbation changed the motor response to the perturbation (Caudron et al., 2008; Jacobs et al., 2008; Matsuoka et al., 2020) and influenced the vestibular function when the participants were in the stance (Guerraz and Day, 2005). Previous findings are consistent with the hypothesis that postural control in a quiet stance is influenced by predicting the forthcoming stimulus. Based on this view, a forward sway of the body induced by placing the coil at the back of the head is likely due to predicting forthcoming TMS at this site. When TMS is given, the coil produces a clicking sound. The clicking sound of TMS elicits a large auditory-evoked potential, indicating that the clicking sound activates the auditory cognitive process (Nikouline et al., 1999; Tiitinen et al., 1999). Accordingly, the forward sway of the head induced by placing the TMS coil over the back of the head may be explained by a view that humans move the head forward due to the prediction of the clicking sound.

This event, the forward sway of the body induced by the prediction of the clicking sound over the back of the head, may be explained by a defense mechanism. Mammalians move their body to keep them away from physical offense (Graziano and Cooke, 2006). The startle response induced by a loud sound and the withdrawal reflex induced by the noxious tactile stimulus are typical examples of the defense response (Sherrington, 1910; Landis and Hunt, 1939; Pfeiffer, 1962; Koch, 1999; Yeomans et al., 2002; Graziano and Cooke, 2006; Davis et al., 2009; Jure, 2020). These defense responses have been thought to play a role in constructing safety margins around the body for keeping the body away from the noxious stimulus.

Mammalians, including humans, respond to the stimulus given within defensive peripersonal space (flight zone), defined as the space directly surrounding the body at a grasping distance (Rizzolatti et al., 1997; Vagnoni and Longo, 2019; Rabellino et al., 2020). The cortically mediated excitatory long-loop reflex was facilitated when the stimulated hand was within the defensive peripersonal space (Versace et al., 2019). The blink reflex was found to be facilitated when a stimulated hand (electrical stimulation to the median nerve at the wrist) was close to the face, called the hand–blink reflex in humans (Sambo et al., 2012; Biggio et al., 2019). Those findings indicate that the defense mechanism is activated particularly when the tactile stimulus is close to the head. When tactile stimulation (air puff) was given to the head, the monkeys moved their heads away from the stimulus (Cooke et al., 2003). This finding indicates that tactile stimulus to the head activates the defense mechanism to keep the body away from the stimulus. Postural control is sensitive to the motion of the audible environment (Stoffregen et al., 2009). There is auditory peripersonal space around the head in humans (Ladavas et al., 2001). Those findings indicate that the defense mechanism is likely activated not only by a tactile stimulus but also by an auditory stimulus. Based on this view, we hypothesized that predicting the stimulus site of the head induces a body sway to keep the head away from the stimulus mediated by the defense mechanism (Hypothesis 1). We tested this hypothesis by investigating the effect of predicting forthcoming auditory or tactile stimulus sites of the head-on-body sway in a quiet stance.

In a quiet stance, ankle muscles control the body's sway (Winter et al., 1998; Warnica et al., 2014). Accordingly, the body sway induced by predicting the stimulus site must be associated with a change in ankle muscle activity. More specifically, anterior–posterior body sway is mainly controlled by the ankles (Winter, 1993). Based on this finding, the ankle muscles likely respond to the prediction of the stimulus site particularly in the sagittal plane (forehead or back of the head), if the deviation of the body is mediated by the defense mechanism (Hypothesis 2). This hypothesis was also examined in the present study.

The amount of body sway also reflects the postural control in a quiet stance. A static sound cue was found to decrease the amount of body sway in stance (Gandemer et al., 2017). A rotating sound cue was found to decrease the amount of body sway in stance (Gandemer et al., 2014). Auditory stimulus reduced the amount of body sway in stance (Agaeva and Altman, 2005; Ross and Balasubramaniam, 2015; Ross et al., 2016). Predicting the sound stimulus may activate the mechanism that is the same as the mechanism underlying those previous findings. When humans maintained their stance on an elevated ground surface, the COP displacement decreased, indicating that postural threat decreases body sway in a quiet stance (Carpenter et al., 2001; Brown et al., 2006). These previous findings are explained by the view that emotional stress decreases the amount of body sway in a stance. Predicting the stimulus to the head likely induces emotional stress, and thus, may decrease the amount of the body sway. Based on those, we hypothesized that predicting the sound and/or tactile stimulus decreases the amount of body sway in a quiet stance (Hypothesis 3).

Methods

Participants

A total of 14 healthy male participants aged 31.2 ± 6.8 years participated in this study. There are gender differences in

physical characteristics, motor performance (Hamill et al., 1977; Thomas and French, 1985), and postural control (Gribble et al., 2009). The inter-individual variability of measures representing postural control in female participants is greater than that in male participants (Kahraman et al., 2018). Based on those previous findings, to exclude the variability of postural responses caused by gender differences, and to minimize the inter-individual variability of postural control, only male participants were recruited. All the participants were right-footed according to the revised version of the Waterloo Footedness Questionnaire (Elias et al., 1998; Zverev, 2006). The participants did not have a history of orthopedic or neurological disorders. The experimental protocol was explained, and the participants gave their written informed consent to participate in this experiment. All the procedures were approved by the Ethics Committee of Osaka Prefecture University.

Apparatus

A gravicorder was used to measure the center of pressure (COP) (Static Sensograph, 1G06, NEC Sanei, Tokyo). A speaker producing sound with 45 dB of sound pressure was placed around the head for the trial block investigating the effect of the predicted auditory stimulus site of the head (auditory stimulus trial block). Electrical stimulus electrodes, providing an electrical tactile stimulus, were placed over the skin at the forehead (5 cm caudal to the nasion), inion, or the left or right mastoid in the tactile stimulus trial block. The loci of the nasion, inion, and mastoids were determined via palpation over the skin. The distance between the two electrodes placed at each site was 1 cm. A display showing pictures predicting the presence and site of the stimulus (S-12140, Takei kiki, Tokyo, Japan) was placed 1 m in front of the participants. The participants wore liquid crystal goggles (T.K.K.2275, Takei Kiki, Tokyo, Japan). The goggles were either opaque for visual occlusion or transparent to allow vision. Electrodes recording the electromyographic (EMG) activity in the left gastrocnemius medius (GM), right GM, left tibialis anterior (TA), and right TA muscles were placed over the belly of the muscles. The inter-electrode distance in each muscle was 2 cm. The EMG signals were amplified with a pass-band filter from 15 Hz to 1 kHz using amplifiers (MEG 5200, Nihon Kohden, Tokyo). Analog signals from the gravicorder and EMG amplifiers were digitized using an A/D converter (PowerLab/8SP and 2sp; ADInstruments, Colorado Spring, CO, USA) at a sampling rate of 2 kHz, and the digitized signals were stored in a personal computer.

Procedure

The participants maintained the stance with the feet together over the gravicorder. Before beginning each trial, the liquid crystal goggles were opaque so that their vision was occluded. An experimenter monitored the COP and initiated the trial when the COP was stable. The goggles became transparent in the time window between 0 and 2.2 s after the beginning of the trial (Figure 1A). The goggles were opaque after this time until the time at which the stimulus was given so that the influence of the visual information other than the visual cue was minimum. A picture depicting a bird's-eye view of the head was presented on the display in the time window between 2 and 2.2 s after the beginning of the trial. In this picture, an arrow predicting the stimulus site was given in the trials with the stimulation (Figure 1B). The bird's-eye view of the head was presented, but the arrow was not presented in the trials without the stimulation (N condition). The meaning of this arrow was explained to the participants before beginning the experiment. The goggles were again opaque after this moment until the end of the trial.

An auditory stimulus was given 4 s after the onset of the visual cue in the auditory stimulus trial block (Figure 1A). The auditory stimulus was given with a speaker placed at the site, where the arrow in the picture of the visual cue was predicted. The speaker was 5 cm away from the stimulus site of the head. An electrical tactile stimulus was given 4 s after the onset of the visual cue in the tactile stimulus trial block. In the tactile stimulus trial block, an electrical stimulus was given. The intensity of the stimulus was 1.5 times the intensity of the tactile perceptual threshold. The stimulus intensity increased from the subthreshold to the suprathreshold level in an increment of 0.47 V every 1 s, and the least intensity at which the participants perceived the stimulus was considered to be the stimulus intensity at the tactile perceptual threshold. The tactile stimulus trial block was conducted 20 min after the auditory stimulus trial block. The stimulus was given at one of the four sites (forehead [F], back of the head [B], or left [L] or right side of the head [R]). Each trial lasted 6 s. The stimulus at each site was given in 10 trials. No stimulus was given in the 10 trials of the N condition. Thus, 50 trials were conducted in each trial block. One of these five conditions was randomly assigned in each trial.

Data analysis

The COP in the medial–lateral axis was called COPx, and that in the anterior–posterior axis was called COPy. The mean COP position was calculated at each 1 s. The positive value of the COPx position indicates the rightward deviation of the COP, and that of the COPy position indicates the forward deviation of the COP. The mean and standard deviation of the COP were calculated at every 1 s (5–4, 4–3, 3–2, 2–1, and 1–0 s before the stimulus onset). The standard deviation of the COP represented the amount of the body sway at each 1 s. The EMG trace in each trial was rectified, and the amplitude of the rectified EMG trace was averaged at each 1 s.

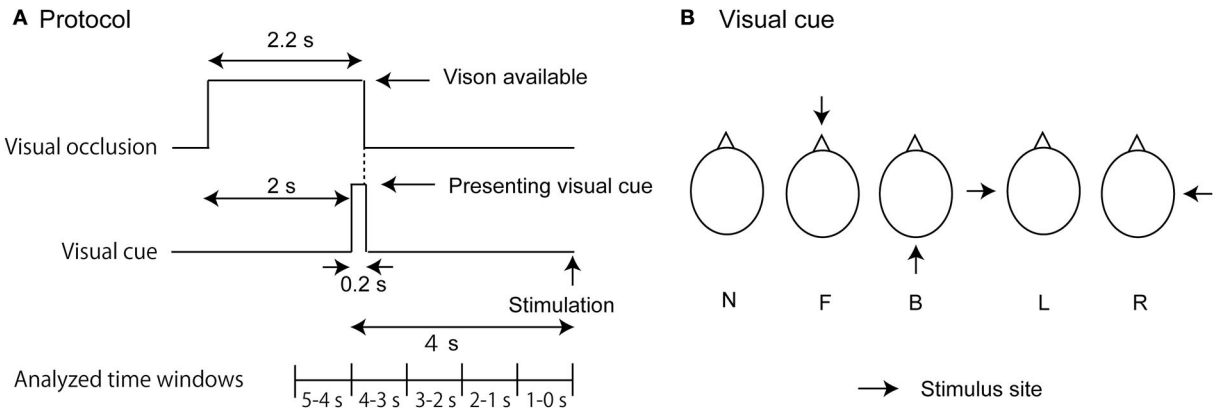

FIGURE 1
Experimental design. The time protocol in each trial is shown in **(A)**. Visual cues indicating a bird's-eye view of the stimulus site are shown in **(B)**. In **(B)**, each abbreviation indicates the stimulus condition: L, L condition (cue predicting the stimulus to the left side of the head); R, R condition (cue predicting the stimulus to the right side of the head); F, F condition (cue predicting the stimulus to the forehead); and B, B condition (cue predicting the stimulus to the back of the head).

A repeated-measures two-way ANOVA was conducted to test the main effects on all measures: time (five levels; 5–4, 4–3, 3–2, 2–1, and 1–0 s before the stimulus onset) and stimulation (five levels; N, F, B, L, and R conditions). The Greenhouse–Geisser correction was conducted on the results whenever Mauchly's test of sphericity was significant. If there was a significant interaction between the main effects, then a test of the simple main effect was conducted. If there was a significant main effect or simple main effect, then a multiple comparison test (Bonferroni's test) followed it. The alpha level was 0.05. Excel Toukei 2010 ver. 1.13 (Social Survey Research Information, Tokyo) was used for the statistical analysis. The data in the results were expressed as the mean and standard error of the mean. The data, normalized by subtracting the average value at 1–0 s before the onset of the visual cue (5–4 s before the stimulus) from the values averaged at every 1 s in the time window between 4 and 0 s before the stimulus, were used to depict the mean and error bars of the figures.

Results

COP position

Auditory stimulus trial block

The effect of predicting the auditory stimulus site on the COPx position is shown in Figure 2A. There was a significant interaction between the main effects [$F_{(16,208)} = 2.338$, $p = 0.003$]. The test of the simple main effect revealed a significant effect of time in the L condition [$F_{[4,260]} = 8.172$, $p < 0.001$]. The COPx position significantly deviated to the rightward direction at 3–0 s before the stimulus compared with the 5–4 s before the stimulus (1–0 s before the visual cue) in the L condition ($p < 0.05$). The COPx position significantly deviated to the rightward direction at 2–0 s before the stimulus compared with the 4–3 s before the stimulus in the L condition ($p < 0.05$). The COPx position significantly deviated to the rightward direction at 2–0 s before the stimulus compared with the 3–2 s before the stimulus in the L condition ($p < 0.05$). The test of the simple main effect revealed a significant effect of the stimulus at 2–1 s [$F_{[4,260]} = 3.271$, $p = 0.012$] and at 1–0 s [$F_{[4,260]} = 6.553$, $p < 0.001$] before the stimulus. As shown in Figures 2A,B, the COPx position was significantly deviated rightward in the L condition compared with the N condition at 2–0 s before the stimulus but deviated leftward compared with the N condition in the R condition at 1–0 s before the stimulus ($p < 0.05$). The COPx position significantly deviated rightward in the F condition compared with the N condition at 1–0 s before the stimulus ($p < 0.05$). The COPx position in the L condition for individual participants is shown in Figure 3.

The effect of predicting the auditory stimulus site on the COPy position is shown in Figure 2C. There was a significant interaction between the main effects [$F_{(4.727,61.451)} = 5.611$, $p < 0.001$]. The test of the simple main effect revealed a significant effect of time in the B [$F_{(4,260)} = 4.522$, $p = 0.002$], F [$F_{(4,260)} = 8.193$, $p < 0.001$], and L conditions [$F_{(4,260)} = 2.711$, $p = 0.031$]. The COPy position deviated backward at 2–0 s before the stimulus compared with that at 5–2 s before the stimulus and at 1–0 s before the stimulus compared with that at 2–1 s before the stimulus in the F condition ($p < 0.05$). The COPy position deviated forward at 2–0 s before the stimulus compared with that at 5–2 s before the stimulus in the B condition ($p < 0.05$). The COPy position deviated forward at 2–1 s before the stimulus compared with that at 5–2 s before the stimulus, and at 1–0 s before the stimulus compared with that at 5–3 s before the stimulus in the L condition ($p < 0.05$). The test of the simple

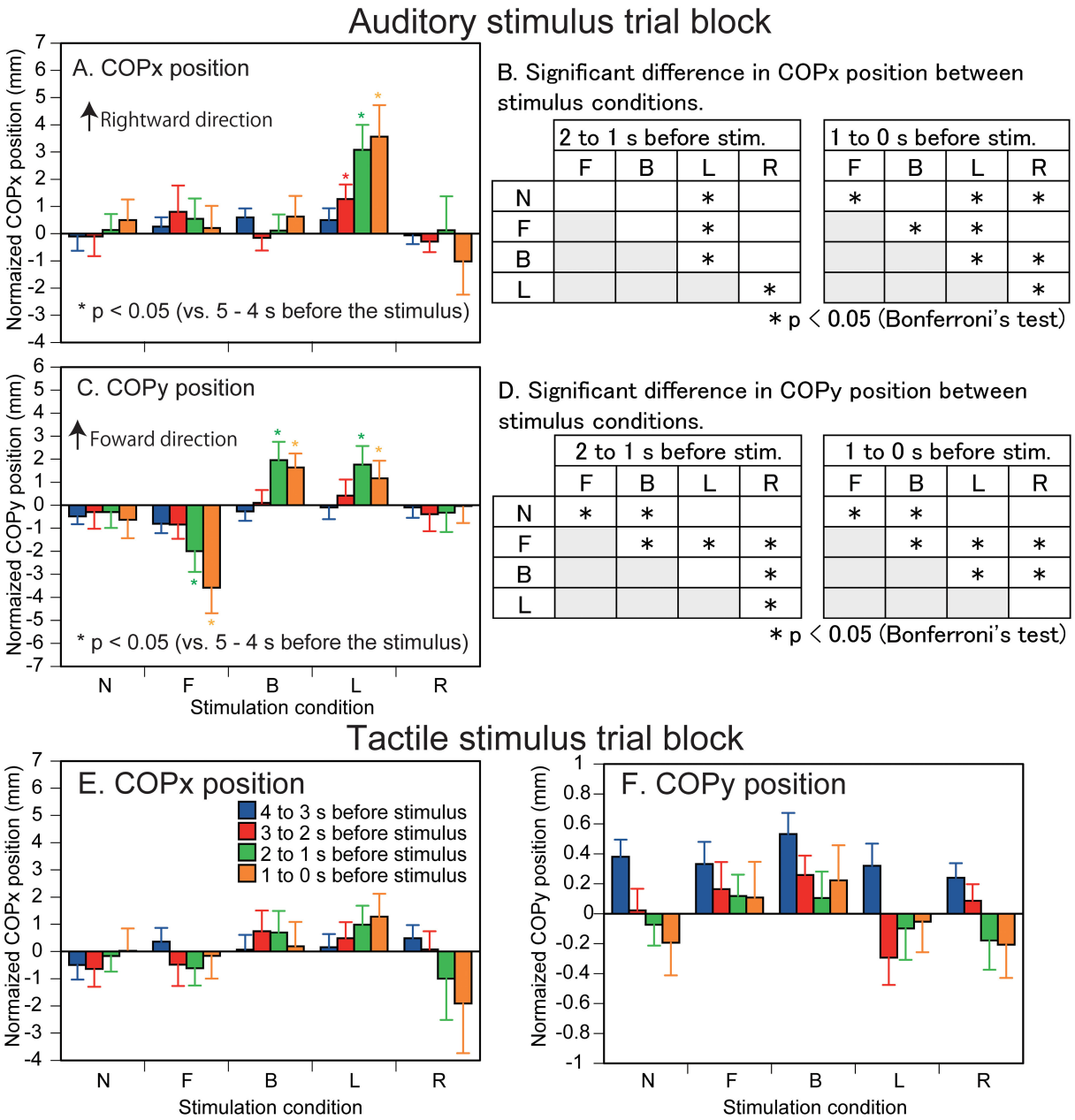

FIGURE 2
Effect of predicting the auditory **(A–D)** and tactile stimulus site **(E,F)** on the COP position. Bars indicate the mean, and error bars indicate standard errors of the mean **(A,C,E,F)**. The data are normalized by subtracting the average value at 1–0 s before the onset of the visual cue (5–4 s before the stimulus) from the values averaged at every 1 s in the time window between 4 and 0 s before the stimulus. Asterisks indicate significant differences in the COP position compared with the COP position at the time 5–4 s before the stimulus (1–0 s before the visual cue) in the same condition. Results of Bonferroni's test examining the difference between the stimulus conditions are shown in **B** and **D**. N, trials with the cue predicting non-stimulation; F, trials with the cue predicting the stimulus to the forehead; B, trials with the cue predicting the stimulus to the back of the head; L, trials with the cue predicting the stimulus to the left side of the head; R, trials with the cue predicting the stimulus to the right side of the head.

main effect revealed a significant simple main effect of the stimulus at 2–1 s [$F_{(4,260)} = 4.264$, $p = 0.002$] and at 1–0 s [$F_{(4,260)} = 8.043$, $p < 0.001$] before the stimulus. As shown in Figure 2D, the COPy position in the F condition significantly deviated backward compared with the N condition 2–0 s before the stimulus ($p < 0.05$). The COPy position in the B condition significantly deviated forward compared with the N condition 2–0 s before the stimulus ($p < 0.05$).

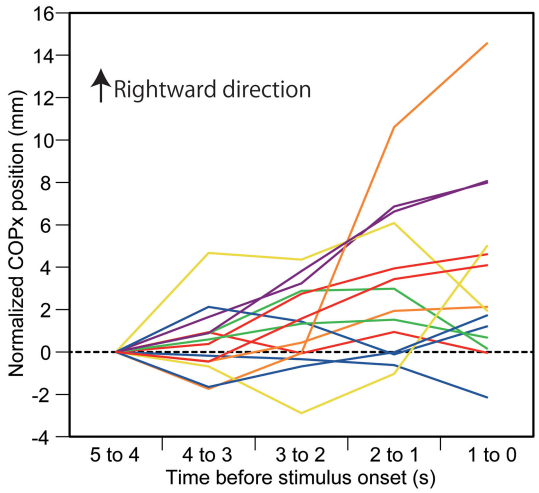

FIGURE 3
Individual data on the COPx position in auditory stimulus trial block. Each line indicates the COPx position in each participant. The data are normalized by subtracting the average value at 1–0 s before the onset of the visual cue (5–4 s before the stimulus) from the values averaged at every 1 s in the time window between 4 and 0 s before the stimulus.

Tactile stimulus trial block

The COPx position is shown in Figure 2E. There was neither a significant main effect of time [$F_{(1.905,24.77)} = 0.058$, $p = 0.937$] nor stimulus [$F_{[2.129,27.675]} = 0.442$, $p = 0.660$] without significant interaction between the main effects [$F_{(16,208)} = 1.409$, $p = 0.140$]. The COPy position is shown in Figure 2F. There was neither a significant main effect of time [$F_{(2.207,28.691)} = 1.790$, $p = 0.182$] nor stimulus [$F_{(4,52)} = 2.445$, $p = 0.058$] without significant interaction between the main effects [$F_{(3.404,44.250)} = 1.652$, $p = 0.186$].

COP displacement

Auditory stimulus trial block

The standard deviation of the COPx is shown in Figure 4A. There was no significant interaction between the time and stimulus [$F_{(16,208)} = 1.301$, $p = 0.199$]. There was a significant effect of the stimulus [$F_{(2.348,30.523)} = 3.536$, $p = 0.035$]. The standard deviation of the COPx in the R condition was significantly greater than that in the B condition ($p < 0.05$). There was a significant effect of the time [$F_{(1.823,23.694)} = 5.530$, $p = 0.012$]. The standard deviation of the COPx at 4–3 s before the stimulus was significantly smaller than that at 3–0 s before the stimulus ($p < 0.05$).

The standard deviation of the COPy is shown in Figure 4C. There was no significant interaction between the main effects [$F_{(16,208)} = 0.566$, $p = 0.907$]. There was no significant effect of the stimulus [$F_{(4,52)} = 1.456$, $p = 0.229$]. There was a significant main effect of time [$F_{(2.049,26.634)} = 11.515$, $p < 0.001$]. The standard deviation of the COPx at 4–3 s before the stimulus was significantly smaller than that at the other times ($p < 0.05$).

Tactile stimulus trial block

The standard deviation of the COPx is shown in Figure 4B. There was no significant interaction between the time and stimulus [$F_{(16,208)} = 0.999$, $p = 0.459$]. There was a significant main effect of time [$F_{(1.856,24.133)} = 4.215$, $p = 0.029$]. The standard deviation of the COPx at 4–3 s before the stimulus was significantly smaller than that at 5–4 and 2–0 s before the stimulus ($p < 0.05$). There was no significant main effect of the stimulus [$F_{(2.021,26.267)} = 1.006$, $p = 0.380$].

The standard deviation of the COPy is shown in Figure 4D. There was no significant interaction between the time and stimulus regarding the standard deviation [$F_{(16,208)} = 0.643$, $p = 0.847$]. There was a significant main effect of time [$F_{(2.156,28.032)} = 7.237$, $p = 0.002$]. The standard deviation of the COPx at 4–3 s before the stimulus was significantly smaller than that at 3–0 s before the stimulus ($p < 0.05$). There was no significant main effect of the stimulus [$F_{(4,52)} = 2.266$, $p = 0.075$].

EMG

Muscles with a significant interaction between the main effects

The EMG amplitude of the left GM in the auditory stimulus trial block is shown in Figure 5A. There was a significant interaction between the main effects [$F_{(16,208)} = 1.847$, $p = 0.027$]. The test of the simple main effect revealed a significant effect of time in the B condition [$F_{(4,260)} = 3.498$, $p = 0.008$]. The EMG amplitude at 3–0 s before the stimulus was significantly greater than that at 5–3 s before the stimulus in the B condition ($p < 0.001$). The test of the simple main effect did not reveal a significant effect of the stimulus in each time window.

The EMG amplitude of the right GM in the auditory stimulus trial block is shown in Figure 5B. There was a significant interaction between the main effects [$F_{(16,208)} = 1.827$, $p = 0.029$]. The test of the simple main effect revealed a significant effect of time in the L condition [$F_{(4,260)} = 2.554$, $p = 0.039$]. The EMG amplitude at 3–0 s before the stimulus was significantly greater than that at 5–3 s before the stimulus in the L condition ($p < 0.05$). The test of the simple main effect revealed a significant effect of the stimulus at 2–1 s [$F_{(4,260)} = 2.764$, $p = 0.028$] and 1–0 s [$F_{(4,260)} = 2.731$, $p = 0.030$] before the stimulus. As shown in Figure 5C, The EMG amplitude at 2–1 s before the stimulus in the B condition and that at 1–0 s before the stimulus in the L condition was greater than that in the N

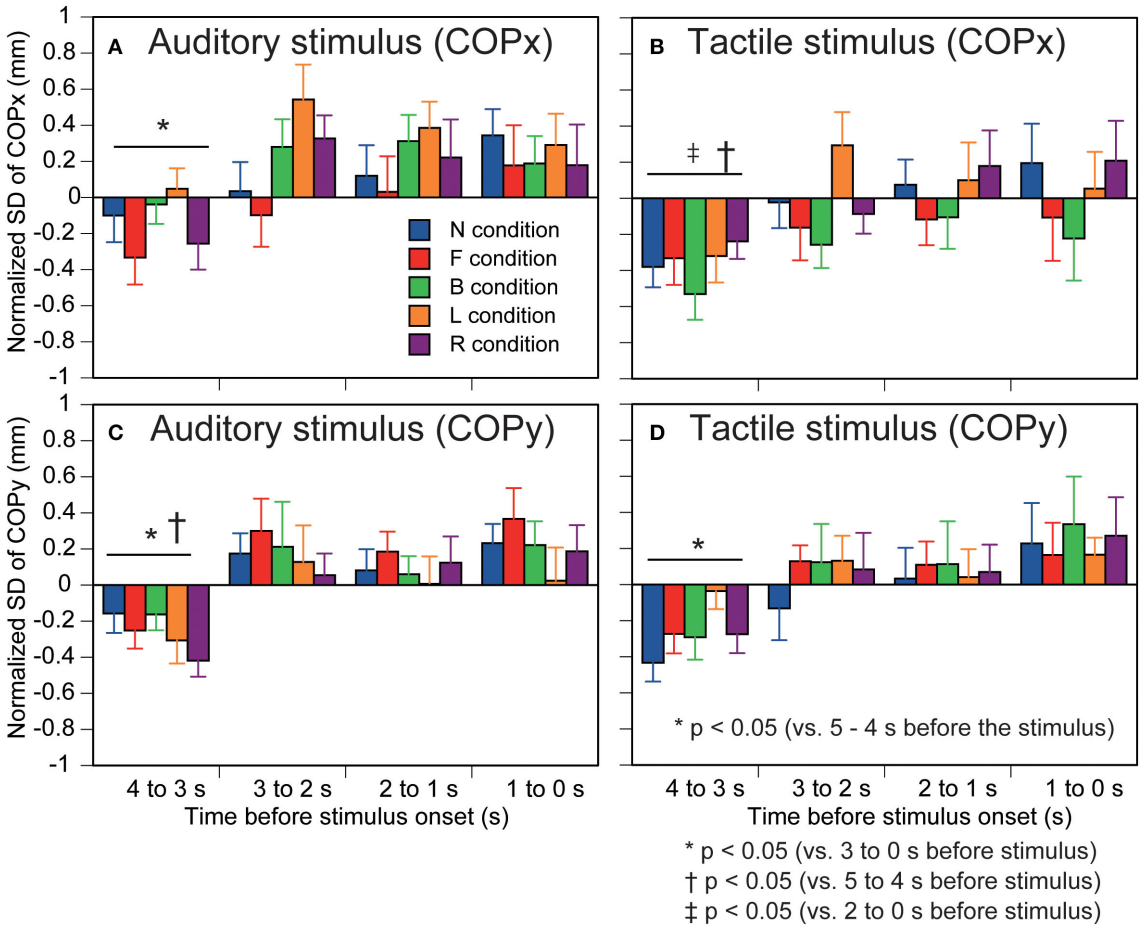

FIGURE 4
Effect of predicting the auditory or tactile stimulus on the standard deviation of COP. Auditory stimulus trial blocks are in the left panels **(A,C)** and tactile stimulus trial blocks are in the right panels **(B,D)**. The upper panels are COPx **(A,B)** and lower panels are COPy **(C,D)**. Bars indicate the mean, and error bars indicate standard errors of the mean. The data are normalized by subtracting the average value at 1–0 s before the onset of the visual cue (5–4 s before the stimulus) from the values averaged at each 1 s in the time window between 4 and 0 s before the stimulus. N, trials with the cue predicting non-stimulation; F, trials with the cue predicting the stimulus to the forehead; B, trials with the cue predicting the stimulus to the back of the head; L, trials with the cue predicting the stimulus to the left side of the head; R, trials with the cue predicting the stimulus to the right side of the head. Effect of predicting the auditory or tactile stimulus on the standard deviation of COP. Auditory stimulus trial blocks are in the left panels **(A,C)** and tactile stimulus trial blocks are in the right panels **(B,D)**. The upper panels are COPx **(A,B)** and lower panels are COPy **(C,D)**. Bars indicate the mean, and error bars indicate standard errors of the mean. The data are normalized by subtracting the average value at 1–0 s before the onset of the visual cue (5–4 s before the stimulus) from the values averaged at each 1 s in the time window between 4 and 0 s before the stimulus. N, trials with the cue predicting non-stimulation; F, trials with the cue predicting the stimulus to the forehead; B, trials with the cue predicting the stimulus to the back of the head; L, trials with the cue predicting the stimulus to the left side of the head; R, trials with the cue predicting the stimulus to the right side of the head.

condition. The EMG amplitude at 2–0 s before the stimulus in the F condition was smaller than that in the N condition.

The EMG amplitude of the left TA in the tactile stimulus trial block is shown in Figure 5D. There was a significant interaction between the main effects [$F_{(16,208)} = 1.901$, $p = 0.022$]. The test of the simple main effect revealed a significant effect of time in the B [$F_{(4,260)} = 3.405$, $p = 0.010$], F [$F_{(4,260)} = 3.278$, $p = 0.012$], L [$F_{(4,260)} = 5.854$, $p < 0.001$], and R [$F_{(4,260)} = 9.402$, $p < 0.001$] conditions. The EMG amplitude at 5–4 s before the stimulus was significantly smaller than that at the other times, and that at 4–2 s before the stimulus was significantly smaller than that at 2–0 s before the stimulus in the B condition ($p < 0.05$). The EMG amplitude at 5–3 s before the stimulus was significantly smaller than that at 3–0 s before the stimulus (1–0 s before the visual cue) in the F condition ($p < 0.05$). The EMG amplitude at 5–4 s before the stimulus (1–0 s before the visual cue) was significantly smaller than that at 4–0 s before the stimulus, and that at 4–3 s before the stimulus was smaller than 3–2 and 1–0 s before the stimulus in the L condition ($p < 0.05$). The EMG amplitude at 5–4 s before the stimulus (1–0 s before the visual cue) was significantly smaller than that at 3–0 s before the stimulus, and that at 4–2 s before

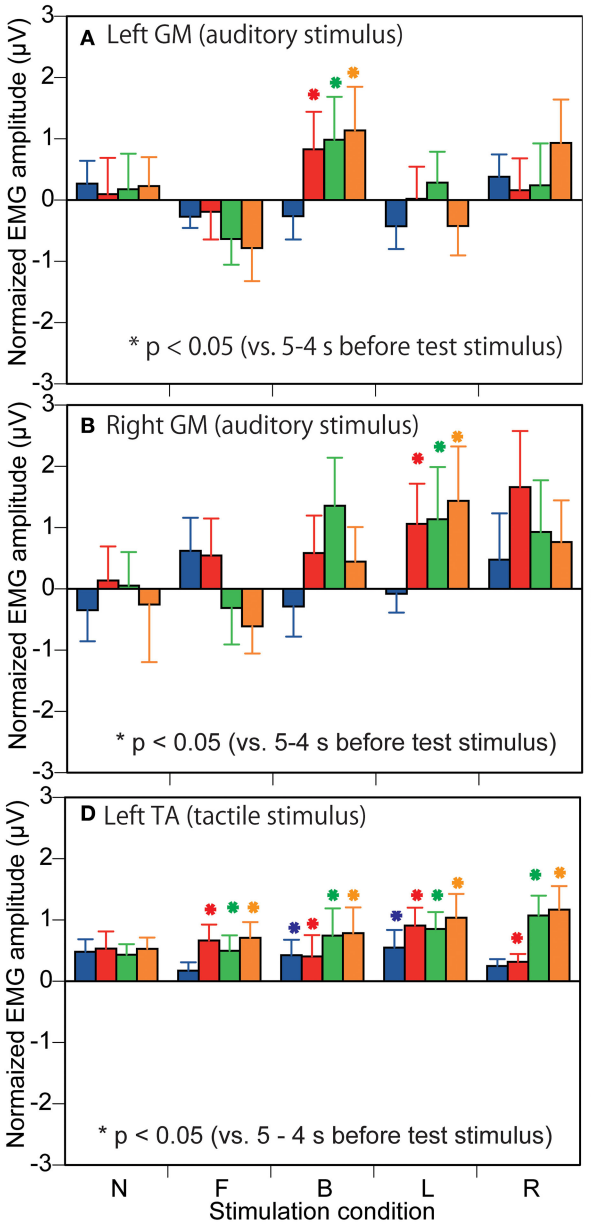

EMG; electrohyographic
TA; tibialis anterior muscle
GM; gastrocnemius medius muscle

- 4 to 3 s before stimulus
- 3 to 2 s before stimulus
- 2 to 1 s before stimulus
- 1 to 0 s before stimulus

C

Significant difference in right GM–EMG amplitude between stimulus conditions.

	2 to 1 s before stim.				1 to 0 s before stim.			
	F	B	L	R	F	B	L	R
N	*	*			*		*	
F		*	*	*		*	*	*
B				*				
L								*

* p < 0.05 (Bonferroni's test)

E

Significant difference in left TA–EMG amplitude between stimulus conditions.

	2 to 1 s before stim.				1 to 0 s before stim.			
	F	B	L	R	F	B	L	R
N		*	*	*	*	*	*	*
F		*		*				*
B								
L								

* p < 0.05 (Bonferroni's test)

FIGURE 5
Effect of predicting the stimulus site on the EMG amplitude in the muscles in which a significant interaction between the main effects is revealed. The data are normalized by subtracting the average value at 1–0 s before the onset of the visual cue (5–4 s before the stimulus) from the values averaged at each 1 s in the time window between 4 and 0 s before the stimulus. Bars indicate the mean, and error bars indicate standard errors of the mean in the left panels **(A,B,D)**. Asterisks indicate significant differences from mean amplitude at the time 5–4 s before the stimulus (1–0 s before the visual cue) in the same condition in the left panels **(A,B,D)**. The results of Bonferroni test for the right GM amplitude in the auditory trial block are shown in panel **(C)** and those for the left TA in the tactile stimulus trial block are shown in panel **(E)**. N, trials with the cue predicting non-stimulation; F, trials with the cue predicting the stimulus to the forehead; B, trials with the cue predicting the stimulus to the back of the head; L, trials with the cue predicting the stimulus to the left side of the head; R, trials with the cue predicting the stimulus to the right side of the head. EMG, electromyography.

the stimulus was significantly smaller than 2–0 s before the stimulus in the R condition ($p < 0.05$). The test of the simple main effect revealed a significant effect of the stimulus at 2–1 s [$F_{(4,260)} = 3.190$, $p = 0.014$] and at 1–0 s [$F_{(4,260)} = 3.001$, $p = 0.019$] before the stimulus. As shown in Figure 5E, the EMG amplitude in the B, L, and R conditions at 2–1 s before stimulation was significantly greater than that in the N condition and the EMG amplitude at 1–0 s before stimulation in the F, B, L, and R conditions was significantly greater than that in the N condition.

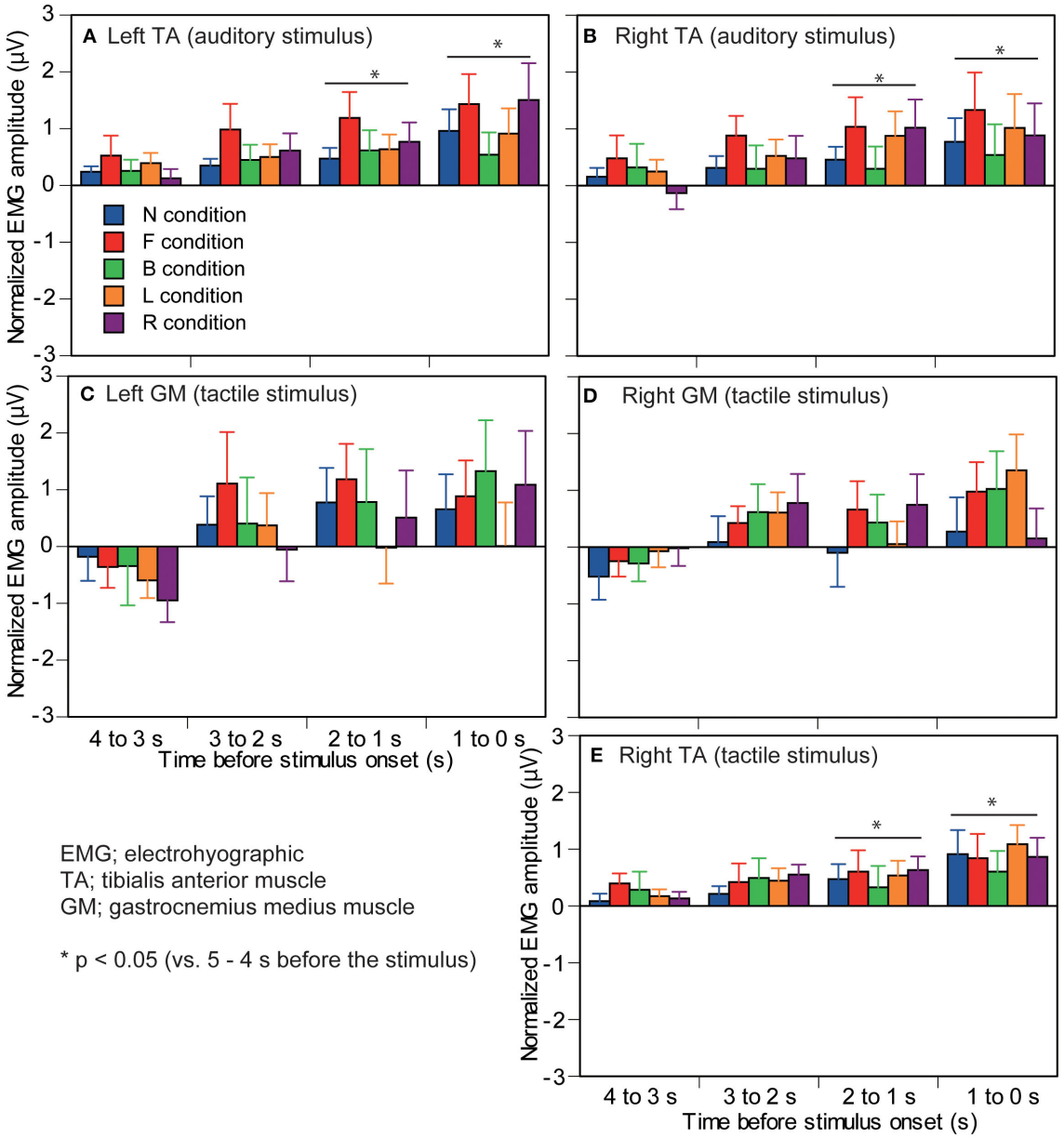

FIGURE 6
Effect of predicting the stimulus site on the EMG amplitude in which significant interaction between the main effects is not found. The left panels are the muscles in the left ankle **(A,C)** and the right panels are the muscles in the right ankle **(B,D,E)**. Upmost panels are the muscles in the auditory stimulus trial block **(A,B)**, and the other panels are the muscles in the tactile stimulus trial block **(C–E)**. The data are normalized by subtracting the average value at 1–0 s before the onset of the visual cue (5–4 s before the stimulus) from the values averaged at each 1 s in the time window between 4 and 0 s before the stimulus. Bars indicate the mean, and error bars indicate standard errors of the mean. Asterisks indicate significant differences from mean amplitude at the time 5–4 s before the stimulus (1–0 s before the visual cue) in the same condition. N, trials with the cue predicting non-stimulation; F, trials with the cue predicting the stimulus to the forehead; B, trials with the cue predicting the stimulus to the back of the head; L, trials with the cue predicting the stimulus to the left side of the head; R, trials with the cue predicting the stimulus to the right side of the head. EMG, electromyography.

Muscles without significant interaction between the main effects

The EMG amplitude of the left TA in the auditory stimulus trial block is shown in Figure 6A. There was no significant interaction between the main effects [$F_{(16,208)} = 1.458$, $p = 0.118$]. There was a significant main effect of time [$F_{(1.528,19.861)} = 5.689$, $p = 0.016$]. The EMG amplitude at 5–4 s before the stimulus (1–0 s before the visual cue) was significantly smaller than that at 2–0 s before the stimulus. The EMG amplitude at 1–0 s before the stimulus was significantly greater than that at 4–3 s

before the stimulus. There was no significant main effect of the stimulus [$F_{(2.221,28.874)} = 3.146$, $p = 0.053$].

The EMG amplitude of the right TA in the auditory stimulus trial block is shown in Figure 6B. There was no significant interaction between the main effects [$F_{(16,208)} = 0.695$, $p = 0.798$]. There was a significant main effect of time [$F_{(1.402,18.226)} = 5.384$, $p = 0.023$]. The EMG amplitude at 5–4 s before the stimulus was significantly smaller than that at 2–0 s before the stimulus ($p < 0.05$). The EMG amplitude at 4–3 s before the stimulus was significantly smaller than that at 1–0 s before the stimulus ($p < 0.05$). There was no significant main effect of the stimulus [$F_{(2.045,26.579)} = 1.111$, $p = 0.345$].

The EMG amplitude of the left GM in the tactile stimulus trial block is shown in Figure 6C. There was no significant interaction between the main effects [$F_{(16,208)} = 0.625$, $p = 0.861$]. There was a significant main effect of time [$F_{(4,52)} = 4.109$, $p = 0.006$]. The EMG amplitude at 4–3 s before the stimulus was significantly smaller than that at 2–0 s before the stimulus ($p < 0.05$). There was no significant main effect of the stimulus [$F_{(4,52)} = 1.447$, $p = 0.232$].

The EMG amplitude of the right GM in the tactile stimulus trial block is shown in Figure 6D. There was no significant interaction between the main effects [$F_{(16,208)} = 1.026$, $p = 0.431$]. There was neither a significant main effect of the stimulus [$F_{(1.833,23.835)} = 1.641$, $p = 0.216$] nor of time [$F_{(2.173,28.254)} = 3.043$, $p = 0.060$].

The EMG amplitude of the right TA in the tactile stimulus trial block is shown in Figure 6E. There was no significant interaction between the main effects [$F_{(16,208)} = 0.455$, $p = 0.965$]. There was a significant main effect of time [$F_{(1.685,21.907)} = 9.170$, $p = 0.002$]. The EMG amplitude at 5–4 s before the stimulus was significantly smaller than that at 2–0 s before the stimulus ($p < 0.05$). The EMG amplitude at 4–3 s before the stimulus was significantly smaller than that at 1–0 s before the stimulus ($p < 0.05$). There was no significant main effect of the stimulus [$F_{(4,52)} = 0.826$, $p = 0.515$].

Discussion

Predicting auditory stimulus and body sway

There are defense mechanisms that keep the body away from the stimulus (Graziano and Cooke, 2006). The withdrawal reflex elicited by a noxious tactile stimulus and the startle response induced by the loud auditory stimulus are typical defense responses in humans (Sherrington, 1910; Landis and Hunt, 1939; Schouenborg et al., 1995; Clarke and Harris, 2004). Such defense mechanisms are activated even when tactile stimulation is given to the head; when tactile stimulation (air puff) was given to the head, monkeys moved their heads away from the stimulus (Cooke et al., 2003). Based on these findings, we hypothesized that the defense mechanisms may even be activated by predicting the forthcoming auditory stimulus site of the head in a quiet stance (Hypothesis 1). In this study, a visual cue predicting the auditory stimulus site induced a body sway in a direction contrary to the predicted stimulus site. This finding is in line with our Hypothesis 1 that predicting the auditory stimulus site of the head induces a body sway in the direction contrary to the predicted stimulus site to keep the head away from the stimulus and that this is mediated by the defense mechanism.

One alternative mechanism underlying the body sway induced by the prediction of the auditory stimulus site in a quiet stance is sound localization. The head was found to move to localize the sound direction (Wallach, 1939; Toyoda et al., 2011; Nojima et al., 2013; McAnally and Martin, 2014). Head movement reduced the front–back error of sound localization (Perrett and Noble, 1997; Iwaya et al., 2003). Based on these findings, one may speculate that the body sway induced by the prediction of the auditory stimulus site is partially explained by the head moving to improve sound localization. However, this view is unlikely to be true because keeping the head away from the auditory stimulus site does not seem to improve sound localization.

Asymmetrical body sway

One interesting finding regarding the effect of the prediction of the auditory stimulus on the body sway was that the body sway induced by the prediction of the auditory stimulus given to the left side of the head tended to be much greater than that induced by the prediction of the stimulus given to the right side of the head. Moreover, the COP position significantly deviated rightward by predicting the left head stimulus immediately before the stimulus compared with the COP position immediately before the visual cue, but a significant deviation of the COP position over time was absent when predicting the right head stimulus. Those findings may be explained by an approach-avoidance associative network; the left hemisphere is related to the approach-related thought and the right hemisphere is related to the avoidance-related thought (Fetterman et al., 2013). A monaural auditory stimulus in one ear was found to increase the regional cerebral blood flow in the primary auditory area contralateral to the auditory stimulus side (Hirano et al., 1997); the auditory-evoked magnetic field was larger in the auditory cortex contralateral to the auditory stimulus side (Pantev et al., 1986); and a monaural auditory stimulus predominantly activated the contralateral auditory centers (Scheffler et al., 1998; Schönwiesner et al., 2007). This means that auditory stimulus to the left ear causes greater auditory input to the right hemisphere. Accordingly, the different effects of the prediction of the left auditory stimulus and that of the right auditory stimulus may be explained by

a view that the body sways to keep the head away from the auditory stimulus site when the individual predicts auditory stimulus to the left side of the head because avoidance-related thought is processed in the right hemisphere, which receives its auditory input from the left ear.

Predicting auditory stimulus-induced muscle activity

There was a significant simple main effect of the stimulus site on the EMG amplitude in the right GM. This means that the time course of the change in the right GM activity is dependent on the prediction of the stimulus site of the head. This predicted site-dependent activity of the right GM was present immediately before the stimulus; predicting that the stimulus to the back of the head significantly increased the activity of the right GM, and that to the forehead significantly decreased the activity of the right GM at 2–0 s before the stimulus. The time window of the predicted site-dependent change in the activity of the right GM was the same as the time window of the predicted site-dependent change in body sway (i.e., at 2–0 s before the stimulus). These findings indicate that the activity of the right GM is related to the body sway induced by the prediction of the auditory stimulus site.

The GM is activated eccentrically when the stance leg leans forward in the late stance phase of gait (Perry, 1992). This means that the GM in the stance leg contracts eccentrically when the lower leg leans forward. Accordingly, the increase in the activity of the right GM and forward body sway induced by predicting the auditory stimulus to the back of the head and the decrease in the activity of the right GM and backward body sway induced by the prediction of the forward head fits well with the kinesiological mechanism, that is, eccentric contraction of the ankle extensor (i.e., GM) to support the body against the forward body sway and vice versa. Thus, the right GM is likely to be a key muscle supporting the forward-leaned body induced by the prediction of the auditory stimulus to the back of the head.

On the one hand, the EMG amplitude in the right GM was significantly increased with the prediction of the auditory stimulus to the left head, and a similar increased tendency was induced by the prediction of the auditory stimulus to the right head. On the other hand, the EMG amplitude in the right GM was significantly increased by predicting the auditory stimulus to the back of the head but was significantly decreased by predicting the auditory stimulus to the forehead. That is, the direction of the change in the right GM activity was dependent on the predicted site of the stimulus in the sagittal plane. The ankle mainly contributes to the control of the anterior–posterior body sway in a quiet stance, although the hip mainly contributes to the control of the medial–lateral body sway (Winter, 1993). Accordingly, the different directions of the change in the right GM activity induced by the prediction of the stimulus to the forehead and that induced by that to the back of the head likely reflect ankle control of the anterior–posterior body sway in a quiet stance. Thus, Hypothesis 2 was supported for the prediction of the auditory stimulus.

In the present study, the effect of predicting the auditory or tactile stimulus on GM activity was asymmetrical. The change in the right GM activity was dependent on the predicted site of the auditory stimulus, but the left GM activity was not. All the participants were right-footed. Thus, the finding may be explained by the view that the prediction of the auditory stimulus site is associated with the activity in the ankle extensor of the dominant leg. Nevertheless, this view must be handled with caution, because this view is not in line with the previous findings on the contribution of the dominant and non-dominant leg to the control of the postural task. The contribution of the leg to the postural control has been found to not be different between the dominant and non-dominant leg sides (Paillard and No, 2020; Schorderet et al., 2021).

Predicting tactile stimulus

A visual cue predicting the tactile stimulation site did not induce a body sway in the quiet stance. This finding was inconsistent with the finding on the prediction of the auditory stimulus site. In addition, the present finding on the prediction of the tactile stimulation site was not in line with a finding that tactile stimulus to the head activated the defense mechanism (Cooke et al., 2003). One explanation for the absence of an effect of predicting tactile stimulation on body sway is that the defense mechanism is not activated by the prediction of tactile stimulus to the head in a quiet stance.

In the present study, the order of the trial block was constant across the participants; the auditory stimulus trial block was first and the tactile stimulus trial block was second. Thus, the tactile stimulus trial block was preceded by the repetitive auditory stimuli. Habituation of the response occurs after the repetitive stimuli (Webster, 1971; Dimitrijevi et al., 1972). Thus, one may speculate that habituation induced by the repetitive auditory stimulus occurred in the second trial block (tactile stimulus trial block), and this may be a reason that the prediction of the tactile stimulus was not effective on the postural sway in quiet stance. However, in our opinion, this view is unlikely, because the interval between the trial blocks (20 min) was long enough to eliminate habituation. Moreover, because the stimulus modality was different between the two trial blocks, habituation induced by the repetitive auditory stimulation preceding the tactile stimulus trial block is likely minor.

There was a significant interaction between the main effects on the EMG amplitude in the left TA. The EMG amplitude increased immediately before the stimulus when the participants

predicted the tactile stimulus to the head no matter where the predicted stimulus site was. Even though the amount of the increase was significantly different between the stimulus sites, the direction of the change was the same across all the stimulus conditions. Thus, this increase is likely due to predicting the presence of the stimulus no matter where the stimulus is given. In the right TA, the activity level increased immediately before the stimulus (1 - 0 s before the stimulus) across all the stimulus conditions. This means that the activity level of the TA increases immediately before the stimulus no matter whether the stimulation is given or not. Taken together, the increase in the TA activity is not related to the defense mechanism, in which the direction of the change in the EMG activity must be dependent on the predicted stimulus site.

Amount of body sway

A static sound cue was found to decrease the amount of body sway in a stance (Gandemer et al., 2017). A rotating sound cue was also found to decrease the amount of body sway in a stance (Gandemer et al., 2014). Auditory stimulus reduced the amount of body sway in a stance (Agaeva and Altman, 2005; Ross and Balasubramaniam, 2015; Ross et al., 2016). When humans maintained their stance on an elevated ground surface, the COP displacement decreased, indicating that postural threat decreases body sway in a quiet stance (Carpenter et al., 2001; Brown et al., 2006). These previous findings are explained by the view that emotional stress decreases the amount of body sway in a stance. Predicting stimulus to the head likely induces emotional stress. This stress may raise the individual's alertness and influences the amount of body sway. According to these previous findings, we hypothesized that predicting the stimulus to the head decreases the amount of body sway (Hypothesis 3). However, this hypothesis was not supported; any significant change in the standard deviation of the COP was not revealed immediately before the stimulus.

The amount of the body sway (i.e., the SD of the COP) decreased immediately after the presentation of the visual cue (i.e., 4–3 s before the stimulus) compared with the time at 5–4 and/or 3–0 s before the stimulus. A visual cue was given at 4 s before the stimulus. Vision significantly contributes to head stabilization (Guitton et al., 1986). Thus, the finding is likely explained by the view that the freezing of the body to stabilize the head for viewing the visual cue lasted for 1 s immediately after the visual cue.

Limitations

The experiment was conducted only for male participants. Thus, we could not compare the gender difference in the present study. Further studies are needed on female participants. One may raise a question of why the effect of stimulus modality was not examined in the present study. To test the effect of the stimulus modality, a large sample size is required for three-way ANOVA. In the present study, the sample size was 14. Accordingly, the effect of the stimulus modality was not tested, because the sample size was not enough to conduct three-way ANOVA. These are the limitations of the present study.

Conclusion

A visual cue predicting an auditory stimulus to the back of the head induced a forward body sway, while the visual cue predicting an auditory stimulus to the forehead induced a backward body sway. The cue predicting the auditory stimulus to the left side of the head induced a rightward body sway, while the cue predicting the auditory stimulus to the right side of the head induced a leftward body sway. These findings support our hypothesis that predicting the auditory stimulus site of the head induces a body sway in the direction contrary to the predicted stimulus site to keep the head away from the stimulus, mediated by the defense mechanism. The right gastrocnemius muscle contributes to the control of the body sway in the anterior–posterior axis related to this defense mechanism.

Data availability statement

The original contributions presented in the study are included in the article/Supplementary material, further inquiries can be directed to the corresponding authors.

Ethics statement

The studies involving human participants were reviewed and approved by Ethics Committee of Osaka Prefecture University. The patients/participants provided their written informed consent to participate in this study.

Author contributions

NH and KH: study design, conducting experiment, data analysis, and writing manuscript. HK, MM, and HO: conducting experiment. All authors contributed to the article and approved the submitted version.

Conflict of interest

The authors declare that the research was conducted in the absence of any commercial or financial relationships

that could be construed as a potential conflict of interest.

Publisher's note

All claims expressed in this article are solely those of the authors and do not necessarily represent those of their affiliated organizations, or those of the publisher, the editors and the reviewers. Any product that may be evaluated in this article, or claim that may be made by its manufacturer, is not guaranteed or endorsed by the publisher.

Supplementary material

The Supplementary Material for this article can be found online at: https://www.frontiersin.org/articles/10.3389/fnhum.2022.1028700/full#supplementary-material

References

Agaeva, M., and Altman, Y. (2005). Effect of a sound stimulus on postural reactions. *Hum. Physiol.* 31, 511–514. doi: 10.1007/s10747-005-0090-4

Biggio, M., Bisio, A., Ruggeri, P., and Bove, M. (2019). Defensive peripersonal space is modified by a learnt protective posture. *Sci. Rep.* 9:6739. doi: 10.1038/s41598-019-43258-8

Brown, L. A., Polych, M. A., and Doan, J. B. (2006). The effect of anxiety on the regulation of upright standing among younger and older adults. *Gait Posture.* 24, 397–405. doi: 10.1016/j.gaitpost.2005.04.013

Carpenter, M. G., Frank, J. S., Silcher, C. P., and Peysar, G. W. (2001). The influence of postural threat on the control of upright stance. *Exp. Brain Res.* 138, 210–218. doi: 10.1007/s002210100681

Caudron, S., Boy, F., Forestier, N., and Guerraz, M. (2008). Influence of expectation on postural disturbance evoked by proprioceptive stimulation. *Exp Brain Res.* 184, 53–59. doi: 10.1007/s00221-007-1079-9

Clarke, R. W., and Harris, J. (2004). The organization of motor responses to noxious stimuli. *Brain Res Rev.* 46, 163–172. doi: 10.1016/j.brainresrev.2004.07.005

Cooke, D. F., Taylor, C. S., Moore, T., and Graziano, M. S. (2003). Complex movements evoked by microstimulation of the ventral intraparietal area. *Proc. Natl. Acad. Sci. U.S.A.* 100, 6163–6168. doi: 10.1073/pnas.1031751100

Davis, J. R., Campbell, A. D., Adkin, A. L., and Carpenter, M. G. (2009). The relationship between fear of falling and human postural control. *Gait Posture* 29, 275–279. doi: 10.1016/j.gaitpost.2008.09.006

Dimitrijevi,ć, M. R., Faganel, J., Gregori,ć, M., Nathan, P. W., and Trontelj, J. K. (1972). Habituation: effects of regular and stochastic stimulation. *J. Neurol. Neurosurg. Psychiat.* 35, 234–242. doi: 10.1136/jnnp.35.2.234

Elias, L. J., Bryden, M. P., and Bulman-Fleming, M. B. (1998). Footedness is a better predictor than is handedness of emotional lateralization. *Neuropsychologia* 36, 37–43. doi: 10.1016/S0028-3932(97)00107-3

Fetterman, A. K., Ode, S., and Robinson, M. D. (2013). For which side the bell tolls: The laterality of approach-avoidance associative networks. *Motiv. Emot.* 37, 33–38. doi: 10.1007/s11031-012-9306-5

Gandemer, L., Parseihian, G., Kronland-Martinet, R., and Bourdin, C. (2014). The influence of horizontally rotating sound on standing balance. *Exp. Brain Res.* 232, 3813–3820. doi: 10.1007/s00221-014-4066-y

Gandemer, L., Parseihian, G., Kronland-Martinet, R., and Bourdin, C. (2017). Spatial cues provided by sound improve postural stabilization: evidence of a spatial auditory map?. *Front Neurosci.* 11:357. doi: 10.3389/fnins.2017.00357

Graziano, M. S., and Cooke, D. F. (2006). Parieto-frontal interactions, personal space, and defensive behavior. *Neuropsychologia* 44, 845–859. doi: 10.1016/j.neuropsychologia.2005.09.009

Gribble, P. A., Robinson, R. H., Hertel, J., and Denegar, C. R. (2009). The effects of gender and fatigue on dynamic postural control. *J. Sport Rehab.* 18, 240–257. doi: 10.1123/jsr.18.2.240

Guerraz, M., and Day, B. L. (2005). Expectation and the vestibular control of balance. *J. Cogn. Neurosci.* 17, 463–469. doi: 10.1162/0898929053279540

Guitton, D., Kearney, R. E., Wereley, N., and Peterson, B. W. (1986). Visual, vestibular and voluntary contributions to human head stabilization. *Exp. Brain Res.* 64, 59–69. doi: 10.1007/BF00238201

Hamill, P. V., Drizd, T. A., Johnson, C. L., Reed, R. B., and Roche, A. F. (1977). *NCHS Growth Curves for Children Birth-18 Years.* Washington, DC: Department of Health Education and Welfare. doi: 10.1037/e405052004-001

Hirano, S., Naito, Y., Okazawa, H., Kojima, H., Honjo, I., Ishizu, K., et al. (1997). Cortical activation by monaural speech sound stimulation demonstrated by positron emission tomography. *Exp. Brain Res.* 113, 75–80. doi: 10.1007/BF02454143

Iwaya, Y., Suzuki, Y., and Kimura, D. (2003). Effects of head movement on front-back error in sound localization. *Acoust. Sci. Tech.* 24, 322–324. doi: 10.1250/ast.24.322

Jacobs, J. V., Fujiwara, K., Tomita, H., Furune, N., Kunita, K., and Horak, F. B. (2008). Changes in the activity of the cerebral cortex relate to postural response modification when warned of a perturbation. *Clin. Neurophysiol.* 119, 1431–1442. doi: 10.1016/j.clinph.2008.02.015

Jure, F. A. (2020). *Protective Mechanisms in Lower Limb to Noxious Stimuli: The Nociceptive Withdrawal Reflex.* Aalborg Universitetsforlag. Aalborg Universitet. Det Sundhedsvidenskabelige Fakultet.

Kahraman, B. O., Kahraman, T., Kalemci, O., and Sengul, Y. S. (2018). Gender differences in postural control in people with nonspecific chronic low back pain. *Gait Posture* 64, 147–151. doi: 10.1016/j.gaitpost.2018.06.026

Koch, M. (1999). The neurobiology of startle. *Prog. Neurobiol.* 59, 107–128. doi: 10.1016/S0301-0082(98)00098-7

Ladavas, E., Pavani, F., and Farne, A. (2001). Auditory peripersonal space in humans: a case of auditory-tactile extinction. *Neurocase* 7, 97–103. doi: 10.1093/neucas/7.2.97

Landis, C., and Hunt, W. A. (1939). *The Startle Pattern.* New York, NY: Farrar and Rinehart.

Matsuoka, M., Kunimura, H., and Hiraoka, K. (2020). Effect of time and direction preparation on ankle muscle response during backward translation of a support surface in stance. *Motor Control.* 24, 253–273. doi: 10.1123/mc.2019-0042

McAnally, K. I., and Martin, R. L. (2014). Sound localization with head movement: implications for 3-d audio displays. *Front. Neurosci.* 8:210. doi: 10.3389/fnins.2014.00210

Nikouline, V., Ruohonen, J., and Ilmoniemi, R. J. (1999). The role of the coil click in TMS assessed with simultaneous EEG. *Clin. Neurophysiol.* 110, 1325–1328. doi: 10.1016/S1388-2457(99)00070-X

Nojima, R., Morimoto, M., Sato, H., and Sato, H. (2013). Do spontaneous head movements occur during sound localization. *Acoust. Sci. Tech.* 34, 292–295. doi: 10.1250/ast.34.292

Paillard, T., and No,é, F. (2020). Does monopedal postural balance differ between the dominant leg and the non-dominant leg? A review. *Hum. Mov. Sci.* 74:102686. doi: 10.1016/j.humov.2020.102686

Pantev, C., Lütkenhöner, B., Hoke, M., and Lehnertz, K. (1986). Comparison between simultaneously recorded auditory-evoked magnetic fields and potentials elicited by ipsilateral, contralateral and binaural tone burst stimulation. *Audiology* 25, 54–61. doi: 10.3109/00206098609078369

Perrett, S., and Noble, W. (1997). The contribution of head motion cues to localization of low-pass noise. *Percept Psychophys.* 59, 1018–1026. doi: 10.3758/BF03205517

Perry, J. (1992). *Gait Analysis: Normal and Pathological, Function*. Thorofare, NJ: Slack.

Pfeiffer, W. (1962). The fright reaction of fish. *Biol Rev Camb Philos Soc*. 37, 495–511. doi: 10.1111/j.1469-185X.1962.tb01333.x

Rabellino, D., Frewen, P. A., McKinnon, M. C., and Lanius, R. A. (2020). Peripersonal space and bodily self-consciousness: implications for psychological trauma-related disorders. *Front. Neurosci*. 14:586605. doi: 10.3389/fnins.2020.586605

Rizzolatti, G., Fadiga, L., Fogassi, L., and Gallese, V. (1997). The space around us. *Science* 277, 190–191. doi: 10.1126/science.277.5323.190

Ross, J. M., and Balasubramaniam, R. (2015). Auditory white noise reduces postural fluctuations even in the absence of vision. *Exp Brain Res*. 233, 2357–2363. doi: 10.1007/s00221-015-4304-y

Ross, J. M., Will, O. J., McGann, Z., and Balasubramaniam, R. (2016). Auditory white noise reduces age-related fluctuations in balance. *Neurosci. Lett*. 630, 216–221. doi: 10.1016/j.neulet.2016.07.060

Sambo, C. F., Liang, M., Cruccu, G., and Iannetti, G. D. (2012). Defensive peripersonal space: the blink reflex evoked by hand stimulation is increased when the hand is near the face. *J. Neurophysiol*. 107, 880–889. doi: 10.1152/jn.00731.2011

Scheffler, K., Bilecen, D., Schmid, N., Tschopp, K., and Seelig, J. (1998). Auditory cortical responses in hearing subjects and unilateral deaf patients as detected by functional magnetic resonance imaging. *Cereb. Cortex* 8, 156–163. doi: 10.1093/cercor/8.2.156

Schönwiesner, M., Krumbholz, K., Rübsamen, R., Fink, G. R., and von Cramon, D. Y. (2007). Hemispheric asymmetry for auditory processing in the human auditory brain stem, thalamus, and cortex. *Cereb. Cortex*. 17, 492–499. doi: 10.1093/cercor/bhj165

Schorderet, C., Hilfiker, R., and Allet, L. (2021). The role of the dominant leg while assessing balance performance. A systematic review and meta-analysis. *Gait Posture* 84, 66–78. doi: 10.1016/j.gaitpost.2020.11.008

Schouenborg, J., Weng, H. R., Kalliomäki, J., and Holmberg, H. (1995). A survey of spinal dorsal horn neurones encoding the spatial organization of withdrawal reflexes in the rat. *Exp. Brain Res*. 106, 19–27. doi: 10.1007/BF00241353

Sherrington, C. S. (1910). Flexion-reflex of the limb, crossed extension-reflex, and reflex stepping and standing. *J. Physiol*. 40, 28–121. doi: 10.1113/jphysiol.1910.sp001362

Stoffregen, T. A., Villard, S., Kim, C., Ito, K., and Bardy, B. G. (2009). Coupling of head and body movement with motion of the audible environment. *J Exp Psychol*. 35, 1221–1231. doi: 10.1037/a0014251

Thomas, J. R., and French, K. E. (1985). Gender differences across age in motor performance: a meta-analysis. *Psychol Bull*. 98:260. doi: 10.1037/0033-2909.98.2.260

Tiitinen, H., Virtanen, J., Ilmoniemi, R. J., Kamppuri, J., Ollikainen, M., Ruohonen, J., et al. (1999). Separation of contamination caused by coil clicks from responses elicited by transcranial magnetic stimulation. *Clin. Neurophysiol*. 110, 982–985. doi: 10.1016/S1388-2457(99)00038-3

Toyoda, Y., Morikawa, D., and Hirahara, T. (2011). *Head Movements During Horizontal Sound Localization*. In INTER-NOISE and NOISE-CON Congress and Conference Proceedings (Vol. 2011, No. 6, pp. 1868-1873). Institute of Noise Control Engineering.

Vagnoni, E., and Longo, M. R. (2019). "Peripersonal space: its functions, plasticity, and neural basis," in *Spatial Senses* (Routledge), 199–225. doi: 10.4324/9781315146935-12

Versace, V., Campostrini, S., Sebastianelli, L., Saltuari, L., and Kofler, M. (2019). Modulation of exteroceptive electromyographic responses in defensive peripersonal space. *J. Neurophysiol*. 121, 1111–1124. doi: 10.1152/jn.00554.2018

Wallach, H. (1939). On sound localization. *J. Acoust. Soc. Am*. 10, 270–274. doi: 10.1121/1.1915985

Warnica, M. J., Weaver, T. B., Prentice, S. D., and Laing, A. C. (2014). The influence of ankle muscle activation on postural sway during quiet stance. *Gait Posture* 39, 1115–1121. doi: 10.1016/j.gaitpost.2014.01.019

Webster, W. R. (1971). The effects of repetitive stimulation on auditory evoked potentials. *Electroencephalogr. Clin. Neurophysiol*. 30, 318–330. doi: 10.1016/0013-4694(71)90115-5

Winter, D. A. (1993). Medial-lateral and anterior-posterior motor responses associated with center of pressure changes in quiet standing. *Neurosci. Res. Commun*. 12, 141–148.

Winter, D. A., Patla, A. E., Prince, F., Ishac, M., and Gielo-Perczak, K. (1998). Stiffness control of balance in quiet standing. *J. Neurophysiol*. 80, 1211–1221. doi: 10.1152/jn.1998.80.3.1211

Yeomans, J. S., Li, L., Scott, B. W., and Frankland, P. W. (2002). Tactile, acoustic and vestibular systems sum to elicit the startle reflex. *Neurosci. Biobehav. Rev*. 26, 1–11. doi: 10.1016/S0149-7634(01)00057-4

Zverev, Y. P. (2006). Spatial parameters of walking gait and footedness. *Ann. Hum. Biol*. 33, 161–176. doi: 10.1080/03014460500500222

frontiers | Frontiers in Human Neuroscience

TYPE Original Research
PUBLISHED 09 February 2023
DOI 10.3389/fnhum.2023.1089276

OPEN ACCESS

EDITED BY
Daniela De Bartolo,
Santa Lucia Foundation (IRCCS), Italy

REVIEWED BY
Enrica Laura Santarcangelo,
University of Pisa, Italy
Yumie Ono,
Meiji University, Japan

*CORRESPONDENCE
Hongliu Yu
yhl_usst@outlook.com

SPECIALTY SECTION
This article was submitted to Motor Neuroscience, a section of the journal Frontiers in Human Neuroscience

RECEIVED 04 November 2022
ACCEPTED 23 January 2023
PUBLISHED 09 February 2023

CITATION
Zheng J, Ma Q, He W, Huang Y, Shi P, Li S and Yu H (2023) Cognitive and motor cortex activation during robot-assisted multi-sensory interactive motor rehabilitation training: An fNIRS based pilot study.
Front. Hum. Neurosci. 17:1089276.
doi: 10.3389/fnhum.2023.1089276

Cognitive and motor cortex activation during robot-assisted multi-sensory interactive motor rehabilitation training: An fNIRS based pilot study

Jinyu Zheng[1], Qiqi Ma[1], Wanying He[1], Yanping Huang[1], Ping Shi[1,2,3], Sujiao Li[1,2,3] and Hongliu Yu[1,2,3]*

[1]Institute of Rehabilitation Engineering and Technology, University of Shanghai for Science and Technology, Shanghai, China, [2]Shanghai Engineering Research Center of Assistive Devices, Shanghai, China, [3]Key Laboratory of Neural-Functional Information and Rehabilitation Engineering of the Ministry of Civil Affairs, Shanghai, China

Objective: This study aimed to evaluate the effects of multiple virtual reality (VR) interaction modalities based on force-haptic feedback combined with visual or auditory feedback in different ways on cerebral cortical activation by functional near-infrared spectroscopy (fNIRS). Methods: A modular multi-sensory VR interaction system based on a planar upper-limb rehabilitation robot was developed. Twenty healthy participants completed active elbow flexion and extension training in four VR interaction patterns, including haptic (H), haptic + auditory (HA), haptic + visual (HV), and haptic + visual + auditory (HVA). Cortical activation changes in the sensorimotor cortex (SMC), premotor cortex (PMC), and prefrontal cortex (PFC) were measured.

Results: Four interaction patterns all had significant activation effects on the motor and cognitive regions of the cerebral cortex ($p < 0.05$). Among them, in the HVA interaction mode, the cortical activation of each ROI was the strongest, followed by HV, HA, and H. The connectivity between channels of SMC and bilateral PFC, as well as the connectivity between channels in PMC, was the strongest under HVA and HV conditions. Besides, the two-way ANOVA of visual and auditory feedback showed that it was difficult for auditory feedback to have a strong impact on activation without visual feedback. In addition, under the condition of visual feedback, the effect of fusion auditory feedback on the activation degree was significantly higher than that of no auditory feedback.

Conclusions: The interaction mode of visual, auditory, and haptic multi-sensory integration is conducive to stronger cortical activation and cognitive control. Besides, there is an interaction effect between visual and auditory feedback, thus improving the cortical activation level. This research enriches the research on activation and connectivity of cognitive and motor cortex in the process of modular multi-sensory interaction training of rehabilitation robots. These conclusions provide a theoretical basis for the optimal design of the interaction mode of the rehabilitation robot and the possible scheme of clinical VR rehabilitation.

KEYWORDS

rehabilitation robot, multi-sensory interactive, cognitive cortex, motor cortex, near-infrared spectroscopy

1. Introduction

In the past two decades, research and development of robot-assisted rehabilitation have accelerated dramatically as a promising rehabilitation therapy (Cao et al., 2020). It provides a standardized environment for more intensive and repetitive interventions, thereby reducing the stress and workload of therapists. The basic design principle of rehabilitation robots is to induce cerebral cortex activation by processing external stimuli (Kaplan, 1988). If feedback stimuli related to motor performance are synchronized with motor output, these not only enhance motivation but also promote plasticity in the motor cortex (Stefan, 2000). External stimuli can be expressed in many forms, including visual, auditory, and haptic stimuli, in motor learning applications (Deutsch et al., 2004).

Virtual reality (VR) based rehabilitation therapy can provide various feedback stimuli such as visual, auditory, and haptic stimuli. Currently, its application in the clinical medical field is becoming increasingly widespread; however, its rehabilitation effects remain unclear. It has been argued that excessive feedback may lead to patient dependence. However, it has also been suggested that multisensory stimulation is beneficial for improving patients' positive expectations and self-efficacy (Shamy, 2010). Therefore, to achieve the optimal training effect of robotic rehabilitation training, it is necessary to study the influence of the form and intensity of feedback stimuli on the method's training effects. By exploring the optimal interaction mode, a theoretical basis for a robotic interaction design can be provided. This is of great significance for the development of cranial nerve rehabilitation.

Currently, most studies compare several single-feedback stimuli such as visual and auditory stimuli. Wang et al. (2022) studied the effect of visual and auditory feedback based on the upper limb rehabilitation system on cortical activation. However, haptic feedback was not involved in this study. Haptic feedback is the most direct and necessary form of motion information for robots (Lieberman and Breazeal, 2007), it is indispensable. Research methods that combine other types of feedback in a variety of ways based on haptic feedback appear to be more applicable and comprehensive. Therefore, this study explored the effects of haptic feedback combined with visual or auditory feedback on cortical activation. By exploring the optimal feedback method, the rehabilitation efficiency of a rehabilitation robot can be improved.

The basic principle of neurological rehabilitation for stroke is brain plasticity. In the process of rehabilitation training, external sensory stimulation can promote neural activity, thereby promoting neural remodeling and functional recovery. This is also the significance of VR technology used in stroke rehabilitation. Therefore, studying the neural activity of the brain during rehabilitation training is the most intuitive way to reflect the training effect. Typically, the motor and cognitive cortices are activated during robot-assisted rehabilitation training. The premotor cortex (PMC) is involved in the planning and execution of motor tasks (Grafton et al., 1998). The sensorimotor cortex (SMC) is associated with task complexity and attention (control of attentional resources) during voluntary movements (Han et al., 2018). The PFC is mainly responsible for executive control processes related to working memory, coordinating other brain regions to accomplish goal-oriented behaviors, and plays an essential role in higher cognitive functions such as episodic memory and reasoning ability (Jacky et al., 2015, Carlen, 2017). Studies have shown that neural networks are active during complex executive processes and that the PFC is highly correlated with the posterior parietal cortex (Periánez et al., 2004). Therefore, the PMC, SMC, and PFC were selected as regions of interest (ROIs) in this study. During the training process, the cortical activation of the ROIs was measured to investigate the impact of different interaction modes on the training effect.

Currently, functional neuroimaging techniques that can be used to explore the activation of the cortex by external stimuli include positron emission tomography (PET), functional magnetic resonance imaging (fMRI), and functional near-infrared spectroscopy (fNIRS). Among these, fNIRS is non-invasive, has moderate spatial resolution, allows participants to perform body movements, is easy to wear, and has low sensitivity to motion artifacts. It is suitable for experiments with strong demands for interaction or brain activity detection in natural situations. Therefore, this research used fNIRS technology to study the corresponding ROIs in the cerebral cortex. The rationale is that neuronal activity induces hemodynamic responses through neurovascular coupling, which are related to changes in oxyhemoglobin (HbO) and deoxyhemoglobin (HbR) concentrations measured by fNIRS (Scholkmann et al., 2014). Therefore, neuronal activity can be studied by observing changes in hemoglobin concentration in cerebral blood flow.

The purpose of this study was to use fNIRS technology to detect the activation of the cerebral cortex under different VR interaction modes and to explore the optimal feedback mode to improve the effectiveness of rehabilitation training. A multimodal, VR, interactive training system based on an end effector rehabilitation robot was developed to provide modular visual, auditory, and haptic feedback. In this study, experimental conditions based on haptic feedback that combined visual and auditory stimuli in different forms were established, including haptic (H), haptic + auditory (HA), haptic + visual (HV), and haptic + visual + auditory (HVA). This research method was used to compare and study the potential differential effects of different VR interaction modes on the cerebral cortex and to explore a better interaction method. This provided a theoretical basis for optimizing the interaction design of rehabilitation robots.

2. Materials and methods

2.1. Equipment

2.1.1. VR interactive system of upper-limb rehabilitation robot

The end effector upper-limb rehabilitation robot ArmGuider was jointly developed by the University of Shanghai for Science and Technology and Shanghai ZD Medical Technology Co., Ltd., Shanghai, China. It is mainly composed of a working platform, linkage mechanism, power system, and display screen (**Figure 1**). The working platform is 1.20 meters long and 1.10 meters wide. The screen is 0.94 meters long and 0.53 meters wide. The robot offers multiple training modes and different speed and intensity levels. Moreover, it can realize trajectory training in the horizontal plane. The two-link system can transmit the interactive force between the power system and the end effector as a transmission component. During the training process, the patient's affected arm was secured to the end effector (**Figures 1C, D**). The patient applied a force or the force was driven by the end effector. The robot can adjust the strength of the assistance or resistance provided in real time according to the

force exerted by the user on the end effector to maintain a constant speed of movement or the patient's training motivation. The target disease for this rehabilitation robot is stroke with mild motor and cognitive impairment. Some previous studies have shown that for stroke patients with mild brain injury, the neural response of their cerebral cortex is similar to that of healthy people (Rehme et al., 2011, Rehme et al., 2012). Therefore, the cortical activity of healthy people can reflect the neural activity of patients with mild stroke to a certain extent, which provides a certain experimental basis for clinical treatment.

Several studies on robotic therapy devices have shown that continuous passive movement combined with active movement can promote motor recovery (Krebs et al., 2003, Hogan et al., 2006, Krebs, 2009). In this study, a novel passive-active combined training mode was adopted, as this mode allows for the adjustment of the interaction force according to the degree of patient participation to achieve the transformation of the active and passive modes. This innovative robotic training mode will assist therapists in delivering optimized therapy to restore upper extremity function in stroke patients with various needs and abilities (Blank et al., 2014). In addition, according to the characteristics of passive-active training, we designed a corresponding VR interaction system using the Unity 3D game engine. The virtual environment mainly uses natural scenery such as forests and grasslands as design elements (**Figure 1A**). The position of the end effector and the direction of the force were calculated in real-time and streamed to the virtual reality application. A butterfly net in a virtual environment then mapped the end effector. The butterfly flew according to a preset trajectory (**Figure 1A**) to represent the participants in the virtual environment and moved accordingly based on their actual movements.

In this study, auditory, visual, and haptic feedback were combined in a VR system. Haptic feedback involves the robot adjusting the force exerted on the end effector according to the active force exerted by the participant. To evaluate the patient's exercise ability, we introduced the concept of "engagement," that is, the proportion of the patient's active exertion in the force required to complete the task. Throughout the training process, user engagement was displayed on the screen in real-time. The main task of the participants was to control the butterfly net to catch the virtual butterfly by pushing the end effector. When the participant's engagement exceeded 30%, the butterfly in the virtual environment was "caught." Visual feedback refers to the real-time display of the motion trajectory and special effects of bonus points when the task was completed. Auditory feedback refers to the sound played when a task was completed. Typically, feedback strategies can be categorized according to when feedback is provided: during motor task execution [concurrent (online, real-time) feedback], or after (terminal feedback) motor task execution. In general, a visual concurrent feedback design is desirable to guide participants to optimal movements without relying on feedback. The reference trajectories provided additional information regarding the participants' range of motion. Therefore, concurrent feedback and terminal feedback were included in this study, and their effects on neural activity need to be further explored.

2.1.2. fNIRS system

In this study, a continuous-wave fNIRS system (Brite24, Artinis, Netherlands) was used to measure cortical activity. A system with wavelengths of 760 and 850 nm was used to record cortical activity at a sampling rate of 10 Hz. To test cortical neural activity in the cognitive and motor areas, we chose two 12-channel optode templates with a total of 18 optodes (10 light sources and 8 detectors) (**Figure 2**). The optodes were mounted on a holder on the NIRS cap. The distance between the sources and detectors was 3.0 cm. For accurate fixation, caps were available in large, medium, and small sizes to accommodate different head sizes. The international 10–20 system was used to locate the fNIRS optodes (Wang et al., 2018). Cz, Fz, and other symbol positions were marked on the caps according to the 10–20 system. For more accurate positioning, the cranial vertex (Cz) was set as a reference point for the positioning of the optodes. In addition, the Montreal Neurological Institute (MNI) 152 is the most widely used average brain template, created by averaging 152 brains co-registered with the Talairach brain (Peters, 1998) to eliminate differences in the shape and anatomy of different brains. Previous studies have established a correspondence between the MNI coordinate system and the 10–20 system (Jasper, 1958). At the same time, NIRS-SPM provides statistical parametric mapping tools for fNIRS (Collins et al., 1994). NIRS-SPM uses probabilistic registration of 3D spatial data of optodes and 10–20 landmark positions to transform functional images into the MNI space (**Figure 2**). The brain areas corresponding to each channel were then extrapolated from the reference points based on the MNI template (Okamoto et al., 2004). The ROIs based on the Brodmann area (BA) regions included the SMC (BA4), PMC (BA6), and PFC (BA8/9/46). The channels corresponding to each ROI were as follows: PFC: channels 1–12; SMC: channels 14, 15, 17, 19, 20, 21, and 23; and PMC: channels 13, 16, 18, 22, and 24.

2.2. Participants

Twenty healthy participants (five women; mean age, 24 ± 2.34) with no history of neurological, motor, or psychological disorders participated in this study. Auditory, visual, and cognitive abilities were tested during the experimental training before the experiment, and no impairments were found. All the participants were fully informed of the experimental procedures. In addition, to avoid the different effects on cortical activation that occur due to handedness, we tested the handedness of all participants using the Edinburgh Handedness Inventory to ensure the accuracy of the experimental results (Oldfield, 1969). The test results showed that all the participants were right-handed.

2.3. Procedure

In this study, the four experimental conditions were as follows: H, HA, HV, and HVA. As shown in **Figure 3**, under the H condition, the interactive interface was blank, and the participants could only feel the interactive force of the robot end effector without visual and auditory feedback. In the HA condition, interactive forces and prompt tones were provided, but no interactive interface was visible. Those in the HV and HVA conditions could see the interactive interface; however, the conditions differed in terms of whether a prompt tone was provided. In addition, the training speed was set to 0.12 m/s. The training trajectory was a straight line (length of 45 cm) in the Y-direction, as shown in **Figures 1C, D**. The trajectory allows for the training of elbow flexion and extension and strengthening of the biceps and triceps muscles. We measured the participants' cortical activity under the four conditions. A block

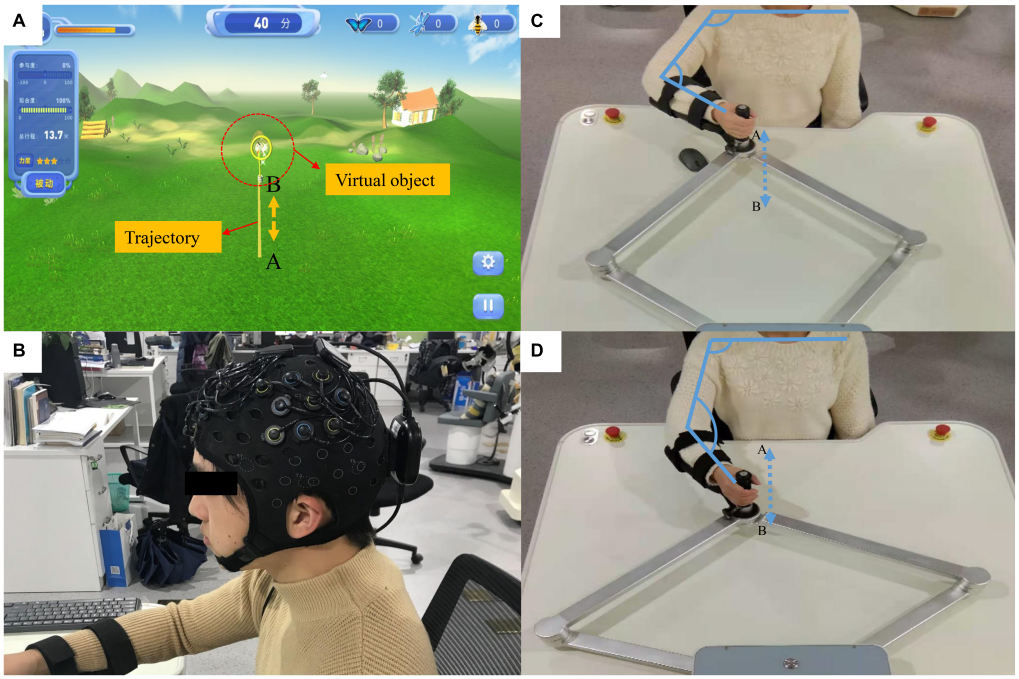

FIGURE 1
Rehabilitation robots and fNIRS equipment. **(A)** The virtual reality (VR) system; the yellow line (from A to B) represents the training trajectory while the butterfly net represents the virtual object mapping the robot's end effector. **(B)** The fNIRS equipment. **(C,D)** The actual movement process during the experiment. The participant's hand was fixed onto the end effector and they carried out a straight-line reciprocating motion from A to B. The actual distance from A to B is 0.45 meters.

paradigm design that repeats three cycles (with each cycle consisting of two phases, rest (40 s) to task (40 s)) was used for each task, as depicted in **Figure 3**. Therefore, a single measurement lasted 240 s. During the 40 s task phase, there are approximately five upper arm flexion and extension movements. The execution sequence of the four experimental conditions was assigned randomly by applying a random permutation function "randperm" in MATLABR2012b (MathWorks, Natick, MA, USA).

Cortical activation was measured using an fNIRS system. The ROIs were the SMC, PMC, and PFC, and the arrangement of the optodes is illustrated in **Figure 2**. As the signals of channels 1–7 were weak and unstable after pre-processing, these channels were removed. The channels corresponding to each ROI were as follows: PFC, channels 8, 9, 10, 11, and 12; SMC, channels 14, 15, 17, 19, 20, 21, and 23; and PMC, channels 13, 16, 18, 22, and 24. According to the modified Beer–Lambert law, we obtained the HbO and HbR values that followed changes in cortical concentration levels (Holper et al., 2009). The optodes were placed on the cap according to the template. According to the international 10–20 system, the cap was positioned on each participant's forehead by centering the specific mark on the bottom line of the optodes at the Fpz (10% of the distance between the Nasion and Inion). The same method was applied for Cz and Fz for validation. We then used the MNI template for probabilistic registration in the NIRS-SPM system (Collins et al., 1994). The luminous flux of each channel was adjusted to a better range to ensure the reliability of the experimental data.

The experiment was conducted in a quiet and stable-light environment. Before the experiment, the participants were asked to sit comfortably in a chair with their upper bodies upright. The heights of the working platform and chair were adjusted to a comfortable position. The participant's right forearm was fixed to the end effector. Moreover, the participants were trained on the robot for five minutes to familiarize themselves with the experimental procedure and operating methods. During the experiment, the participants were required to perform upper limb reciprocation between points A and B under different experimental conditions (**Figures 1C, D**). Participants were required to actively participate to achieve the highest possible engagement. In addition, auditory stimuli were presented to participants through loudspeakers. The participants were required to focus on the screen in all four experimental conditions, including on the blank background in the H and HA conditions, as shown in **Figure 3**. In addition, participants were instructed to relax their bodies during the experiment and avoid physical movements other than those of the right arm, including facial movements, frequent blinking, and looking around. One experimenter operated the robot and provided participants with verbal prompts including "start" and "rest," while another experimenter used the fNIRS system to monitor changes in cerebral cortex activity in real-time (Cope and Delpy, 1988).

2.4. Data analysis

2.4.1. Cortical activation imaging

The fNIRS equipment measured changes in the optical density of cerebral blood flow non-invasively. According to the modified Beer–Lambert law, the relative change in HbO concentration can be obtained by changing the optical density (Holper et al., 2009). We analyzed the fNIRS data using the software package NIRS-SPM (KAIST, Daejeon, South Korea) (Collins et al., 1994) implemented in MATLAB (MathWorks, Natick, MA, USA). Global drifts often occur

A

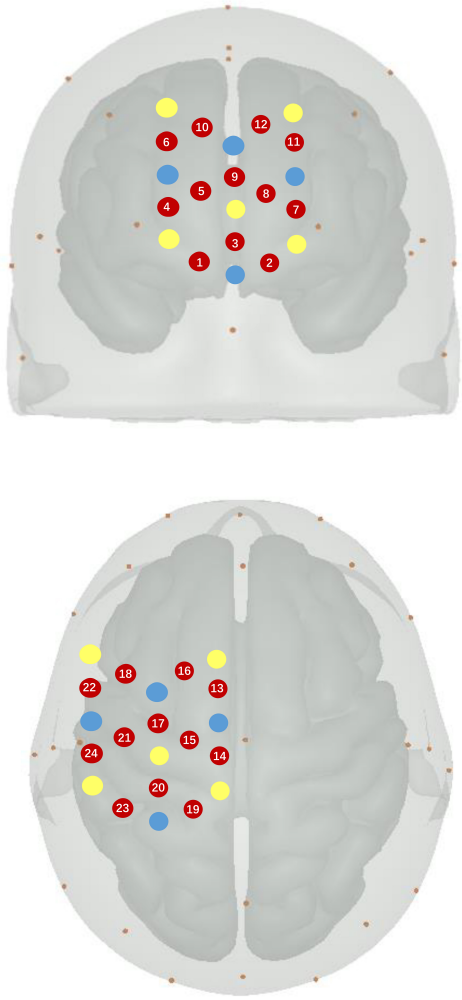

B

	MNI (x, y, z)			BA (%)
Ch 1	15	74	6	10 - Frontopolar area (94) 11 - Orbitofrontal area (6)
Ch 2	-15	73	5	10 - Frontopolar area (87) 11 - Orbitofrontal area (13)
Ch 3	4	68	21	10 - Frontopolar area (100)
Ch 4	30	67	15	10 - Frontopolar area (95) 46 - Dorsolateral prefrontal cortex (5)
Ch 5	17	65	30	9 - Dorsolateral prefrontal cortex (24) 10 - Frontopolar area (76)
Ch 6	32	54	33	9-46 - Dorsolateral prefrontal cortex (100)
Ch7	-29	66	12	10 - Frontopolar area (91) 11 - Orbitofrontal area (3) 46 - Dorsolateral prefrontal cortex (6)
Ch8	-12	65	29	9 - Dorsolateral prefrontal cortex (19) 10 - Frontopolar area (81)
Ch 9	1	53	43	9 - Dorsolateral prefrontal cortex (100)
Ch 10	15	48	51	8 - Includes Frontal eye fields (7) 9 - Dorsolateral prefrontal cortex (93)
Ch 11	-31	53	32	9-46 - Dorsolateral prefrontal cortex (100)
Ch 12	-15	46	51	8 - Includes Frontal eye fields (12) 9 - Dorsolateral prefrontal cortex (88)
Ch 13	-36	-4	66	4 - Primary Motor Cortex (3) 6 - Pre-Motor and Supplementary Motor Cortex (97)
Ch 14	-30	-27	74	3 - Primary Somatosensory Cortex (5) 4 - Primary Motor Cortex (75) 6 - Pre-Motor and Supplementary Motor Cortex (20)
Ch 15	-42	-20	68	3 - Primary Somatosensory Cortex (18) 4 - Primary Motor Cortex (64) 6 - Pre-Motor and Supplementary Motor Cortex (18)
Ch 16	-49	8	52	6 - Pre-Motor and Supplementary Motor Cortex (75) 9 - Dorsolateral prefrontal cortex (25)
Ch 17	-55	-12	54	3 - Primary Somatosensory Cortex (26) 4 - Primary Motor Cortex (43) 6 - Pre-Motor and Supplementary Motor Cortex (31)
Ch 18	-62	-1	36	3 - Primary Somatosensory Cortex (4) 4 - Primary Motor Cortex (20) 6 - Pre-Motor and Supplementary Motor Cortex (42) 43 - Subcentral area (34)
Ch 19	-35	-46	71	1-2-3 - Primary Somatosensory Cortex (49) 7 - Somatosensory Association Cortex (45) 40 - Supramarginal gyrus part of Wernicke's area (6)
Ch 20	-49	-32	64	1-2-3 - Primary Somatosensory Cortex (92) 4 - Primary Motor Cortex (8)
Ch 21	-60	-23	51	1-2-3- Primary Somatosensory Cortex (83) 4 - Primary Motor Cortex (10) 40 - Supramarginal gyrus part of Wernicke's area (7)
Ch 22	-67	-17	33	1-2-3 - Primary Somatosensory Cortex (65) 43 - Subcentral area (31) 48 - Retrosubicular area (4)
Ch 23	-53	-50	56	39 - Angular gyrus, part of Wernicke's area (3) 40 - Supramarginal gyrus part of Wernicke's area (97)
Ch 24	-63	-41	47	40 - Supramarginal gyrus part of Wernicke's area (100)

FIGURE 2
Localization of the fNIRS optodes, channels, MNI coordinates, and Brodmann correspondences. **(A)** Yellow, transmitters; blue, detectors; and red, channels. **(B)** Montreal Neurological Institute (MNI) coordinates for each channel (n = 24) with x, y, and z coordinates. The Brodmann area correspondences (number, name, and %) were extracted from the NIRS-SPM toolbox on the right.

due to breathing, cardiac, vaso-motion, or other experimental errors in fNIRS experiments. In this study, the hemodynamic response function (HRF) and wavelet-MDL were employed to eliminate the global trend and improve the signal-to-noise ratio (SNR) (Yu et al., 2011). Besides, the hemodynamic modality separation method was used to further remove the global trend (Yamada et al., 2012). Moreover, a generalized linear model (GLM) was used to analyze the fNIRS data by simulating the hypothetical HbO response under experimental conditions (Ye et al., 2009). After analyzing each participant's data, a group analysis was conducted on all participants' experimental data under the same experimental conditions, and a t-test was selected to obtain the activation diagram of each experimental condition.

2.4.2. Statistical analysis

The GLM model is a linear combination of predicted responses to different stimuli and error terms. By comparing the ideal and detected modes of the GLM, the β coefficient can be estimated by applying the least-squares method. The activation level of the cerebral cortex can then be obtained by statistical analysis of the β (Collins et al., 1994). Each channel corresponds to a β value that represents the activation level of the channel. The β value of the corresponding channel in each ROI was statistically analyzed as a parameter representing the activation level of this channel. In this study, the average of the β values of channels located in the same ROI was calculated and then a two-way repeated measures ANOVA was performed across different experimental conditions and different ROIs. In addition, a Greenhouse–Geisser (G–G) correction was applied when the spherical hypothesis was violated. The Bonferroni test was used for *post hoc* analysis, followed by ANOVA. Statistical analysis was performed using SPSS software for Windows (version 26.0; SPSS Inc., Chicago, IL, USA). If the p-value was less than 0.05, the null hypothesis of no difference was rejected.

2.4.3. Connectivity analysis

Connectivity analysis provides more information regarding dynamic network-level changes than that inferred from the extent and laterality of activation (Veldsman et al., 2015). This may be a complementary approach to understanding the neural reorganization patterns underlying stroke recovery (Grefkes and Fink, 2014). In this

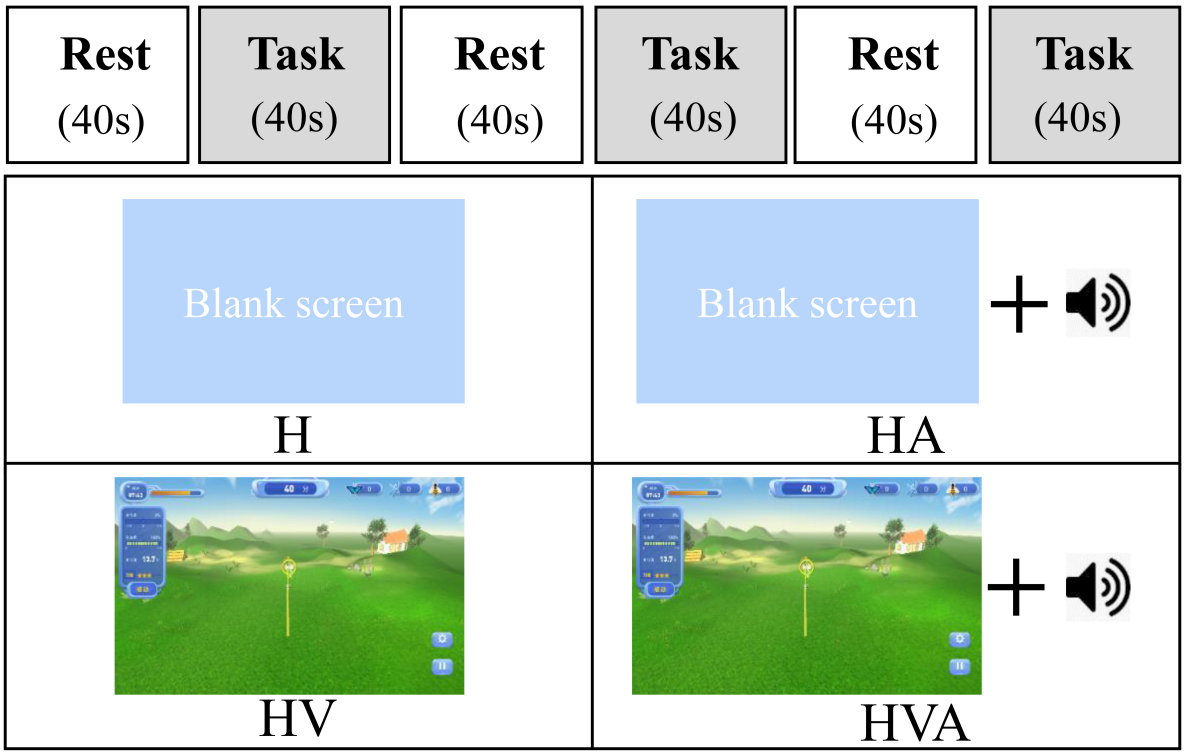

FIGURE 3
The experimental paradigm and the four different virtual reality (VR) training modes. The patients performed four cycling tasks, each starting with a 40 s rest period and a 40 s training period, which was repeated three times. The abbreviations in the figure represent haptic (H), haptic + auditory (HA), haptic + visual (HV), and haptic + visual + auditory (HVA).

study, the Pearson correlation coefficient was used to characterize the connectivity among the studied brain areas. The Pearson correlation coefficient was obtained by dividing the covariance by the standard deviation of the two variables (generally represented by r), with r represented by values between −1 and 1. As the linear relationship between the two variables increased, the correlation coefficient tended to be 1 or −1. The HbO concentration in the task phase was analyzed, and the sample size for each channel was 1200. Pearson correlation coefficients between each channel were calculated. The average of the analysis data for all participants was then computed. In order to compare the correlation coefficients more intuitively, statistical analysis was carried out. The average value of correlation coefficients of between channels located in the corresponding ROIs was calculated. Then, one-way ANOVA was performed among the experimental conditions, and the Bonferroni correction was conducted.

3. Results

This study investigated the cortical activation and functional connectivity among brain areas during different VR interaction modes using fNIRS technology. The engagement was calculated as the behavioral result. Optical imaging and statistical analysis of beta waves were performed for cortical activation analysis. In addition, Pearson's correlation analysis was applied to assess the connectivity among the ROIs.

The statistical analysis of engagement in four conditions is shown in Figure 4. During the experiment, the sensors of the robot recorded the active force exerted by the subject on the end effector. We calculated the ratio of the subject's active force to the total force required to complete the task to obtain the engagement, as the behavioral result. One-way ANOVAs were performed for the engagement of four conditions. As can be seen in Figure 4, the engagement was highest in the HVA group, followed by the HV, HA, and H groups, respectively. Among them, there were significant differences between the H and HVA, HA and HVA conditions ($p < 0.05$).

The time series data of concentration change of HbO and HHb are plotted in Figure 5. We randomly selected channel 8 and calculated the averaged fNIRS responses (of both HbO and HHb) that were superimposed across four conditions of all subjects. The solid line represents the mean of the concentration and the shade represents the error (mean ± SD) (n = 20). The three areas separated by dotted lines in the figure represent three trials, where the first 40 s of each trial are the task phase. In the figure, HbO and HHb under the same conditions are drawn in the same color. In the task phase, the HbO concentration change curve shows an upward trend, while the HHb concentration change curve shows a downward trend. It can be seen from the figure that the average concentration changes of HbO and HHb show good periodicity. When the concentration of HbO increases, the concentration of HHb decreases slightly.

The fNIRS cortical activation imaging scans during the four VR training modes are illustrated in Figure 6 ($p < 0.05$, uncorrected). The color bar represents the t-value. As shown in the figure, the SMC, PMC, and PFC regions showed significant activation ($p < 0.05$) under the four interaction modes. It is worth mentioning that the activation levels in both the cognitive and motor regions of the HV

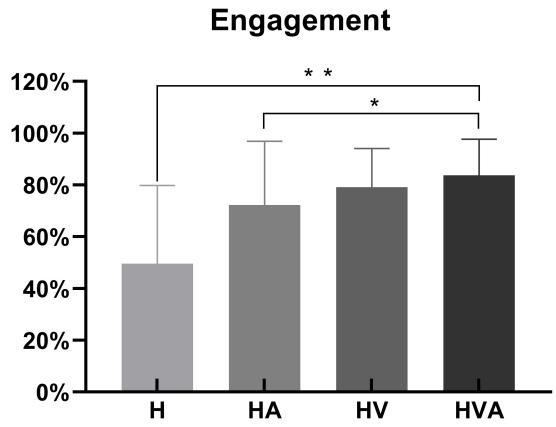

FIGURE 4
Statistical analysis of the engagement under four experimental conditions. *$p < 0.05$, **$p < 0.01$. The abbreviations in the figure represent haptic (H), haptic + auditory (HA), haptic + visual (HV), and haptic + visual + auditory (HVA).

and HVA groups were similar. Furthermore, compared to the H and HA groups, the activation area, and degree of the HVA and HV groups were stronger. Additionally, in the motor region, the activation area of the H group was broader than that of the HA group. Nevertheless, the degree of activation of the HA group was higher than that of the H group (**Figure 6**).

The statistical analysis of the regression coefficients (β) under four experimental conditions of three ROIs was shown in **Figure 7**. The results of repeated measures ANOVA showed that the main effect of experimental conditions was significant, $F = 27.4$, $p < 0.001$, $\eta^2 = 0.259$. The main effect of ROI was significant, $F = 5.705$, $p = 0.012$, $\eta^2 = 0.024$. The interaction between ROI and conditions was significant, $F = 4.686$, $p = 0.001$, $\eta^2 = 0.056$. The simple effect test of experimental conditions showed that in PFC, the simple effect of experimental conditions was significant, $F = 26.216$, $p < 0.001$, $\eta^2 = 0.251$. In SMC, the simple effect of experimental conditions was significant, $F = 27.701$, $p < 0.001$, $\eta^2 = 0.261$. In PMC, the simple effect of experimental conditions was significant, $F = 11.156$, $p < 0.001$, $\eta^2 = 0.125$. The simple effect test result of ROI shows that under the H condition, the simple effect of ROI was significant, $F = 8.440$, $p < 0.001$, $\eta^2 = 0.067$. Under HA condition, the simple effect of ROI was significant, $F = 9.155$, $p < 0.001$, $\eta^2 = 0.073$. Under the HV condition, the simple effect of ROI was not significant, $F = 0.243$, $p = 0.785$, $\eta^2 = 0.002$. Under the HVA condition, the simple effect of ROI was not significant, $F = 1.604$, $p = 0.203$, $\eta^2 = 0.014$. After multiple comparisons, it was found that under the H condition, the beta values of PFC, PMC, and SMC decreased in turn, and the beta values of PFC were significantly higher than SMC ($p < 0.001$). Under the HA condition, the beta values of PFC, SMC, and PMC decreased in turn, and the beta values of PFC and SMC were significantly higher than that of PMC ($p < 0.001$). Under the HV condition, the beta values of SMC, PFC, and PMC decreased in turn, without significant difference. Under the HVA condition, the beta values of PMC, SMC, and PFC decreased in turn, and there was no significant difference.

To investigate the effect of auditory feedback in the presence of visual feedback, we conducted a two-way ANOVA on the beta values of all ROIs under the condition of the presence or absence of visual and auditory feedback. The results of the intersubjective effect test showed that the test statistic of whether there was visual feedback or not was $F = 86.472$, $p < 0.001$, indicating that there was a significant difference in the effect of visual feedback on the activation level. The test statistic of auditory feedback was $F = 17.633$, $p < 0.001$, indicating that there was a significant difference in the influence of auditory

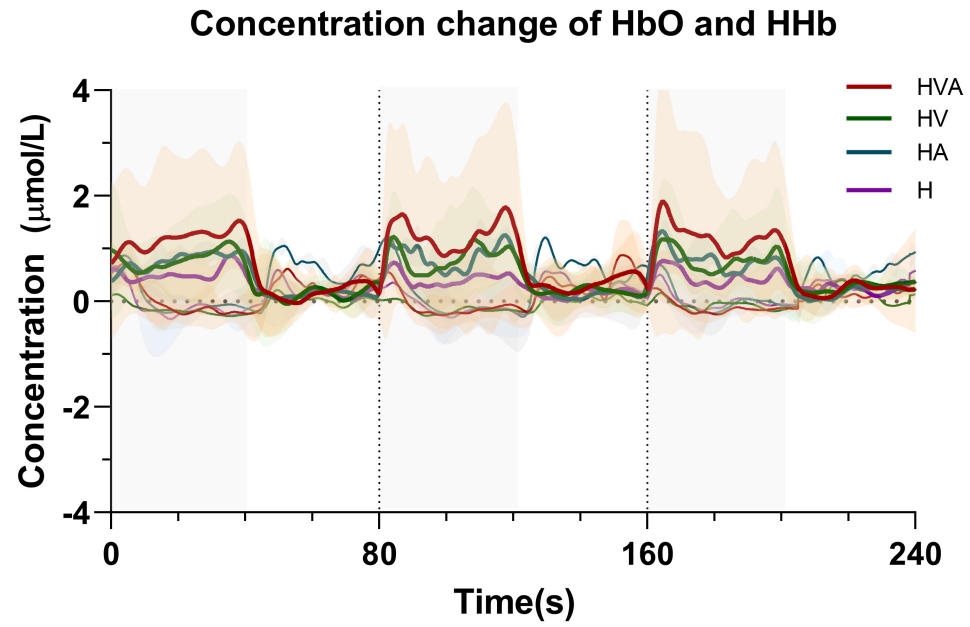

FIGURE 5
Time series of oxyhemoglobin (HbO) and HHb changes during the task. The solid line represents the mean of the concentration and the shade represents the error (mean ± SD) ($n = 20$). The three areas separated by dotted lines in the figure represent three trials, where the first 40 s of each trial are the task phase. The red, green, blue, and purple curves represent HVA, HV, HA, and H modes, respectively. Thicker lines represent HbO and thinner lines represent HHb. The abbreviations in the figure represent haptic (H), haptic + auditory (HA), haptic + visual (HV), and haptic + visual + auditory (HVA).

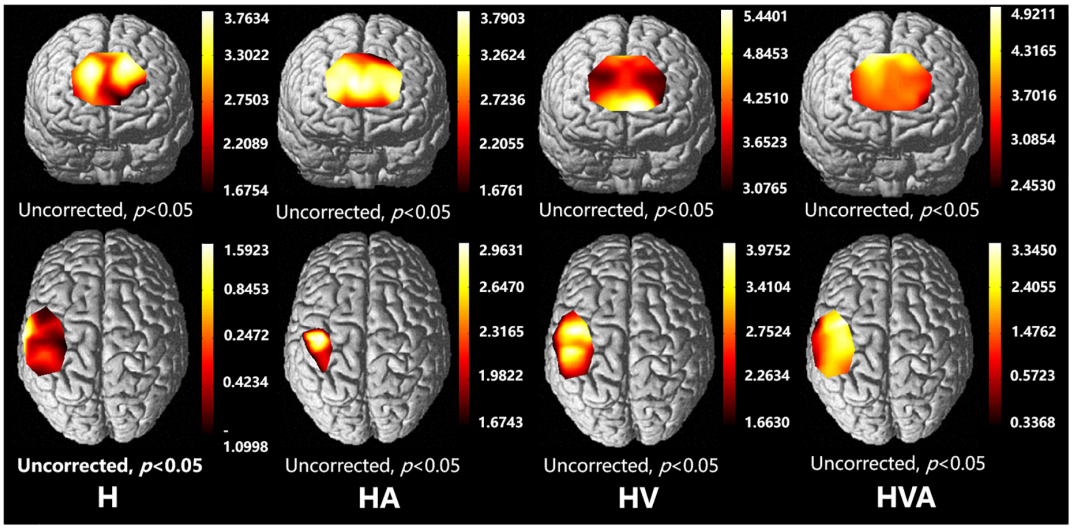

FIGURE 6
Optical imaging of cortical activities (group analysis). The abbreviations in the figure represent haptic (H), haptic + auditory (HA), haptic + visual (HV), and haptic + visual + auditory (HVA).

feedback on the activation level. The test statistic of whether there was visual feedback * whether there was auditory feedback was $F = 22.168$, $p < 0.001$, indicating that visual and auditory feedback have an interaction effect, which had a significant impact on the activation level. The result of the descriptive statistical analysis was shown in Figure 8. As can be seen from the figure, in the absence of visual feedback, the impact of auditory feedback on the activation level was similar, while in the presence of visual feedback, the impact of auditory feedback on the activation level was significantly improved.

The functional connectivity analysis of HbO among the ROIs is shown in Figure 6. Each pixel value in the 24 × 24 matrix corresponds to the value of the Pearson correlation coefficient, which represents the correlation between the two measurement channels. The channels were ordered according to the ROI to which they belong. The ROIs were distinguished by gaps forming a 9 × 9 matrix. The numbers marked in the figure are the mean values of the Pearson correlation coefficients among the channels in each ROI. It can be concluded that the correlation between the SMC and PMC was the strongest in the HVA training mode, whereas the strongest correlation between the PMC and PFC was found in the H training mode. The strongest correlation between the SMC and PFC was observed in the HVA and HV training modes. In addition, the correlations between the channels within the PFC and SMC were stronger in the H and HA modes. However, the correlation between the channels of the two ROIs was stronger under the HV and HVA modes.

The results of the statistical analysis of the correlation coefficients (r) are shown in Figure 10. As can be seen from the figure, the connectivity of bilateral PFC vs. PFC, and SMC vs. SMC was strong and similar under all experimental conditions. The connectivity of bilateral PFC vs. SMC, and PMC vs. PMC was stronger under HVA and HV conditions, and the connectivity of SMC vs. PMC

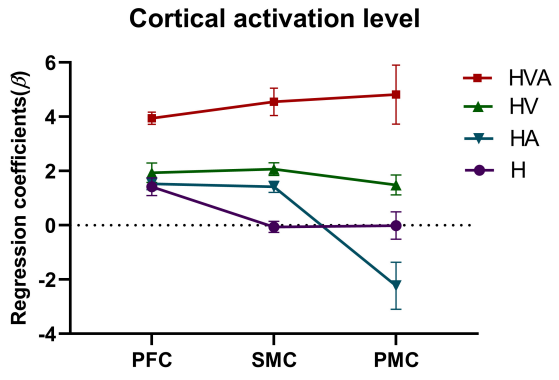

FIGURE 7
Statistical analysis of the regression coefficients (β) under four experimental conditions of three regions of interest (ROIs). SMC, sensorimotor cortex; PFC, prefrontal cortex; PMC, premotor cortex. The abbreviations in the figure represent haptic (H), haptic + auditory (HA), haptic + visual (HV), and haptic + visual + auditory (HVA).

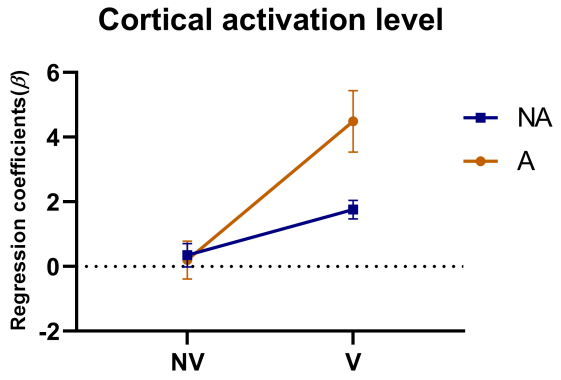

FIGURE 8
Statistical analysis of the regression coefficients (β) under the presence or absence of visual feedback or auditory feedback. A simple representation was given in the figure. NV, no visual feedback; V, visual feedback; NA, no auditory feedback; A, auditory feedback.

was strongest under HVA conditions. However, the connectivity of bilateral PFC vs. PMC was the strongest under H.

4. Discussion

This study aimed to investigate the effects of different VR interaction modes on the degree of cortical activation and connectivity among ROIs. We developed a modular VR interactive system based on an end-effector rehabilitative robot. Four different VR interaction modes (H, HA, HV, and HVA) were included in this study, the behavioral performance and cortical activation were measured using the robot and fNIRS equipment, respectively. The results showed that the behavioral performance under HVA was the best (**Figure 4**). The average concentration changes of HbO and HHb showed good periodicity. When the concentration of HbO increases, the concentration of HHb decreases slightly (**Figure 5**). The results showed that all four VR interaction modes had significant activation effects on the cerebral cortex, with the HVA condition inducing the strongest activation, encompassing the SMC, PMC, and PFC regions (**Figure 7**). Furthermore, the HVA mode also displayed a significant advantage in functional connectivity between SMC and PMC regions (**Figures 9**, **10**).

Previous research has shown that the visual perception of spatial information is more accurate, whereas the auditory perception of time information is even more accurate (Freides, 1974). Haptic perception can fulfill the relatively high requirements related to temporal and spatial information processing (Nesbitt, 2004), while visual feedback plays an essential role in therapeutic regimens for voluntary movements (Luara et al., 2016). These features can be powerful when employed with VR technology (Maciejasz et al., 2014). In addition, auditory feedback can redistribute one's perceptual and cognitive load and become the focus of attention (Eldridge, 2006, Secoli et al., 2011). However, the impact of auditory feedback is largely dependent on the intuitiveness and accuracy of the mapping interpretation, and it must be chosen carefully; therefore, auditory displays are less common than visual displays (Sigrist et al., 2013). It can be seen from the results of this study that in the absence of visual feedback, compared with the H mode, the HA mode had a smaller area of activation in the motor cortex (**Figure 6**), a weaker degree of cortical activation in PMC (**Figure 7**), and weaker connectivity between PFC and SMC, PFC and PMC (**Figures 9**, **10**). The results of two-way ANOVA of the existence of visual feedback and auditory feedback show that auditory feedback was difficult to show a strong effect on cortical activation level in the absence of visual feedback. However, in the presence of visual feedback, the improvement of activation level by fusion auditory feedback was significantly higher

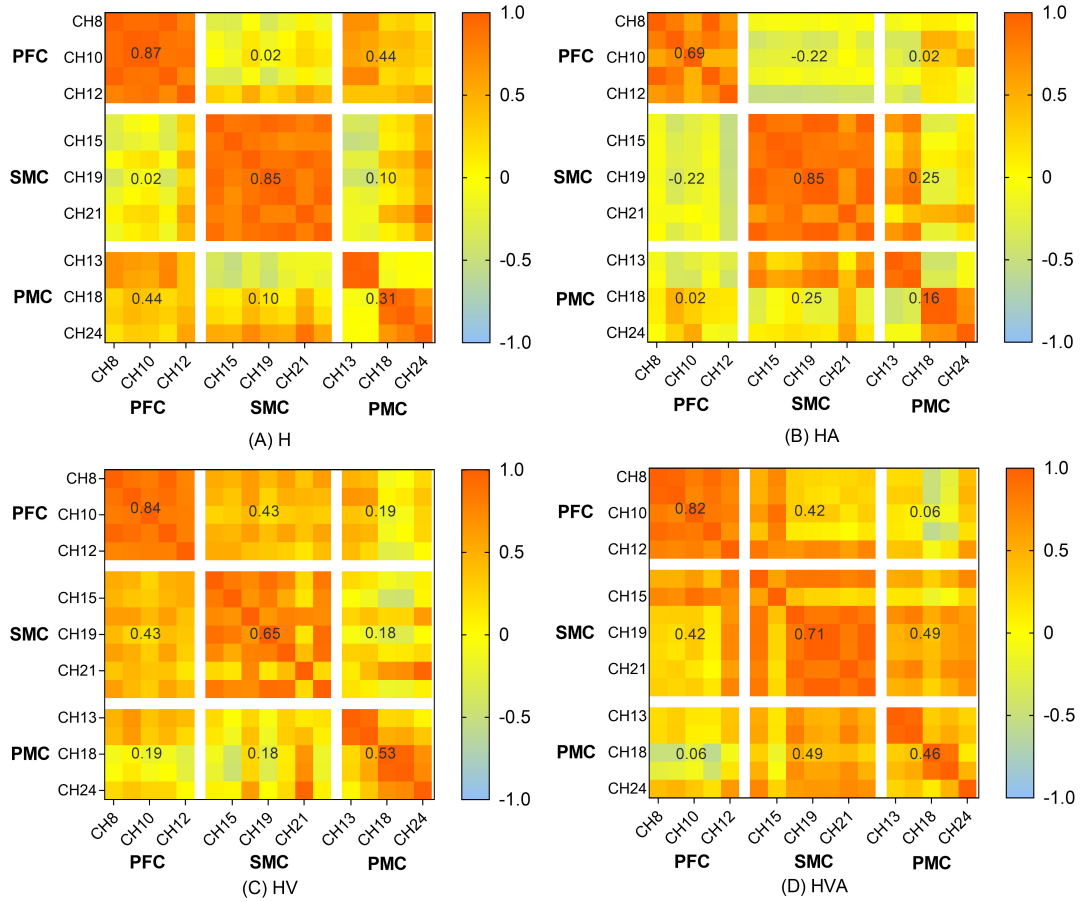

FIGURE 9
Heat map of the connectivity among the channels. The matrix map includes all channel pairs. Color bars indicate the value of *r*. The x and y axes representing the ROIs indicate the dorsolateral prefrontal cortex (PFC, channels 8–12), somatosensory area (SMC, channels 14, 15, 17, 19–21, and 23), and premotor cortex (PMC, channels 13, 16, 18, 22, and 24). The abbreviations in the figure represent haptic (H), haptic + auditory (HA), haptic + visual (HV), and haptic + visual + auditory (HVA).

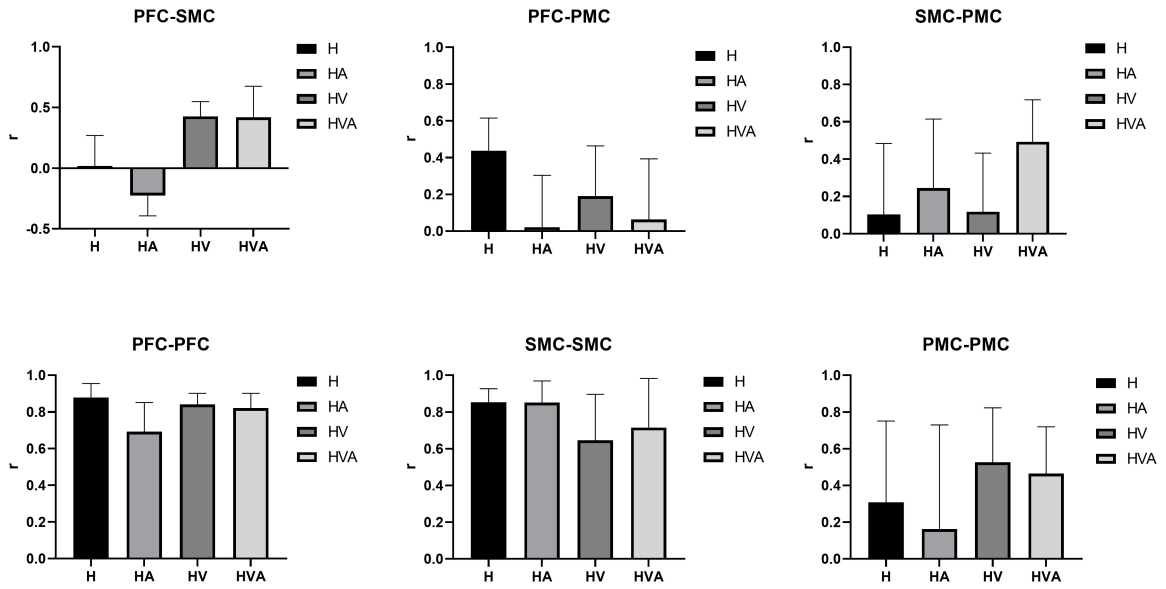

FIGURE 10
Statistical analysis of the correlation coefficients (r) under four experimental conditions between different regions of interest (ROIs). The ROIs include the bilateral dorsolateral prefrontal cortex (PFC, channels 8–12), somatosensory area (SMC, channels 14, 15, 17, 19–21, and 23), and premotor cortex (PMC, channels 13, 16, 18, 22, and 24). The abbreviations in the figure represent haptic (H), haptic + auditory (HA), haptic + visual (HV), and haptic + visual + auditory (HVA).

than that without auditory feedback, which may be related to the interaction effect between visual and auditory feedback (**Figure 8**).

As shown in **Figures 6**, **7**, the HV and HVA groups demonstrated higher degrees of activation in the SMC and PFC regions than the H and HA groups. Previous studies have shown that the PFC is associated with decision-making and motor strategy development. Specifically, the PFC assists in regulating the response and behavior generated by environmental stimuli (Wood and Grafman, 2003) and participates in the attentional demands of trajectory planning. Thus, activation of the PFC reflects its role in maintaining attention and regulating postural control (Woollacott and Shumway-Cook, 2002, Drew et al., 2004). In contrast, the SMC plays a vital role in the early stages of motor learning and is mainly involved in observing motor tasks and integrating multiple sensory inputs (Bhattacharjee et al., 2020). It is usually activated in response to somatosensory stimuli such as haptic stimuli, disturbances, and passive movements. Thus, activation of the SMC and PFC regions during active upper-limb training represents the increased attention of the participants. As can be seen from the results of this study, interaction patterns that incorporate visual feedback may help to engage the attention of users.

As shown in **Figure 7**, the cortical activation levels were similar under the HV and HA interaction modes in SMC and PFC regions, whereas activation under the HVA condition was significantly higher than in the other interaction modes. This indicates that the higher activation levels under HVA conditions may not result from individual visual or auditory feedback; instead, these may result from a combination of multiple feedback modalities. Similar results have been reported in previous studies. For example, Leff et al. (2011) showed that the motion control system of the arm can adapt to a kinematic environment using auditory feedback and that the effect of auditory feedback is similar to that of visual feedback. Furthermore, Radziun and Ehrsson (2018) hypothesized that neuron populations integrate auditory signals with visual, tactile, and proprioceptive signals from the upper limbs, suggesting that the four interactions among vision, touch, proprioception, and sound are more conducive to the perception of limb ownership. In addition, studies have shown that auditory stimuli are effective at perceiving speed, regularity, and periodicity of motion (Kapur et al., 2005). Therefore, in future designs, auditory feedback design objects can incorporate the carrier signal, loudness, and pitch height (Konttinen et al., 2010).

As shown in **Figures 9**, **10**, the correlation between the SMC and PMC was the strongest under the HVA mode. Notably, the PMC is responsible for motor initiation and motor control coding of skilled motor sequences (Sabes, 2000, Inoue and Sakaguchi, 2014). This suggests that HVA training modalities can provide sufficient feedback to stimulate the motor cortex to better facilitate motor initiation and control, which may be advantageous in the early stages of motor activity. In addition, some studies have shown that multimodal stimuli are generally perceived more accurately and faster than unimodal stimuli, reaching the threshold of neural activation earlier (Forster et al., 2002, Shams and Seitz, 2008). As task complexity increases, users prefer multimodal interactions, suggesting that users self-manage by shifting from unimodal interactions to multimodal interactions as their cognitive demands increase (Oviatt et al., 2004). Previous studies have shown that when visual information is input, the movement pattern is controlled according to the target location. In response, the movement policy responds quickly. In the absence of visual input, the response is slower but easier to recall later (Kovacs et al., 2010). Therefore, multimodal fusion should be employed during the early stages of motor learning. As the patient's motor function continues to improve, the stimulation can be gradually reduced to maintain a greater cognitive load and enhance memory.

In summary, we studied the cortical activation patterns under four different VR training modes based on end-effector upper-limb rehabilitation robots. The results show that upper-limb rehabilitation robot training can activate the lateral SMC, PMC, and PFC. In addition, the HVA training mode displayed higher levels of brain

activation and stronger connectivity among cortical regions. These results may contribute to the development of rehabilitation robots and provide a physiological basis for robot design and rehabilitation strategy formulation. Moreover, fNIRS can be a useful tool for studying the cortical effects of rehabilitation robots.

The limitations of this study must be considered. First, the form of auditory feedback used in this study was relatively simple and may not have strongly excited the nerves, thus affecting the experimental results. Second, some researchers have suggested that after training with multimodal stimuli, multimodal processing may be activated even if only a single modal stimulus is present (Shams and Seitz, 2008), which may have influenced the results of the experiments. In addition, the target users of this technology are older adults and people with upper extremity dysfunction; however, this hypothesis was tested only in young, healthy participants, and the number of participants was small. In the future, more participants should be included, including patients with neurological injuries, to investigate these initial findings in greater depth.

In the future, we will increase the modalities of robotic auditory stimulation to explore whether multiple auditory feedback tones lead to higher neural activity levels. In addition, elderly people and people with brain injuries will be included. Furthermore, the effects of other training modes, forces, and trajectories of the rehabilitation robot on cortical activation should be investigated to provide more comprehensive and systematic evidence.

5. Conclusion

In this study, we used fNIRS to investigate the significant activation of the parietal and prefrontal cortices during a VR training task. We have integrated visual and auditory feedback based on haptic feedback to form a multilevel VR training mode. With the integration of more sensory feedback, neuronal activity generally increased, which was reflected in the degree of cortical activation and connectivity of the ROIs. This indicates that multimode VR is more helpful in activating the cerebral cortex and promoting the connection of brain regions. The results may provide a specific theoretical basis for the human-computer interaction design of upper limb rehabilitation robots and provide an optimal interactive mode for rehabilitation robots.

Data availability statement

The raw data supporting the conclusions of this article will be made available by the authors, without undue reservation.

Ethics statement

The studies involving human participants were reviewed and approved by University of Shanghai for Science and Technology. The patients/participants provided their written informed consent to participate in this study.

Author contributions

JZ and PS designed the experiment. WH and QM collected the data. JZ and YH analyzed the data and prepared all figures. JZ drafted the manuscript. SL and HY provided critical revisions. All authors approved the manuscript to be published.

Funding

This study was supported by the National Natural Science Foundation of China (61903255).

Acknowledgments

We thank Duojin Wang for his assistance with the experimental equipment and Sailan Liang for her indispensable assistance in the recruitment of participants during the experiments. We also thank Zhuo Jian for his technical support on the robotic experimental platform.

Conflict of interest

The authors declare that the research was conducted in the absence of any commercial or financial relationships that could be construed as a potential conflict of interest.

Publisher's note

All claims expressed in this article are solely those of the authors and do not necessarily represent those of their affiliated organizations, or those of the publisher, the editors and the reviewers. Any product that may be evaluated in this article, or claim that may be made by its manufacturer, is not guaranteed or endorsed by the publisher.

References

Bhattacharjee, S., Kashyap, R., Abualait, T., Annabel Chen, S. H., Yoo, W. K., and Bashir, S. (2020). The role of primary motor cortex: more than movement execution. *J. Mot. Behav.* 53, 258–227. doi: 10.1080/00222895.2020.1738992

Blank, A. A., French, J. A., Pehlivan, A. U., and O'malley, M. K. (2014). Current Trends in robot-assisted upper-limb stroke rehabilitation: promoting patient engagement in therapy. *Curr. Phys. Med. Rehabil. Rep.* 2, 184–195. doi: 10.1007/s40141-014-0056-z

Cao, W., Chen, C., Hu, H., Fang, K., and Wu, X. (2020). Effect of Hip assistance modes on metabolic cost of walking with a soft exoskeleton. *Ieee Trans. Auto. Sci. Eng.* 18, 426–436. doi: 10.1109/TASE.2020.3027748

Carlen, M. (2017). What constitutes the prefrontal cortex? *Science* 358, 478. doi: 10.1126/science.aan8868

Collins, D., Neelin, P., Peters, T., and Evans, A. (1994). Automatic 3D intersubject registration of Mr volumetric data in standardized Talairach space. *J. Comput. Assist. Tomogr.* 18, 192–205. doi: 10.1097/00004728-199403000-00005

Cope, M., and Delpy, D. (1988). System for long-term measurement of cerebral blood and tissue oxygenation on newborn infants by near infra-red transillumination. *Med. Biol. Eng. Comput.* 26, 289–294. doi: 10.1007/BF02447083

Deutsch, J. E., Merians, A. S., Adamovich, S., Poizner, H., and Burdea, G. C. (2004). Development and application of virtual reality technology to improve hand use and gait of individuals post-stroke. *Restor. Neurol. Neurosci.* 22:371.

Drew, T., Prentice, S., and Schepens, B. (2004). Cortical and brainstem control of locomotion. *Prog. Brain Res.* 143, 251–261. doi: 10.1016/S0079-6123(03)43025-2

Eldridge, A. (2006). Issues in Auditory Display. *Artif. Life* 12, 259–274. doi: 10.1162/artl.2006.12.2.259

Forster, B., Cavina-Pratesi, C., Aglioti, S. M., and Berlucchi, G. (2002). Redundant target effect and intersensory facilitation from visual-tactile interactions in simple reaction time. *Exp. Brain Res.* 143, 480–487. doi: 10.1007/s00221-002-1017-9

Freides, D. (1974). Human information processing and sensory modality: cross-modal functions, information complexity, memory, and deficit. *Psychol. Bull.* 81, 284–310. doi: 10.1037/h0036331

Grafton, S. T., Fagg, A. H., and Arbib, M. A. (1998). Dorsal premotor cortex and conditional movement selection: A Pet functional mapping study. *J. Neurophysiol.* 79, 1092–1097. doi: 10.1152/jn.1998.79.2.1092

Grefkes, C., and Fink, G. R. (2014). Connectivity-based approaches in stroke and recovery of function. *Lancet Neurol.* 13, 206–216. doi: 10.1016/S1474-4422(13)70264-3

Han, C. H., Hwang, H. J., Lim, J. H., and Im, C. H. (2018). Assessment of user voluntary engagement during neurorehabilitation using functional near-infrared spectroscopy: a preliminary study. *J. Neuroeng. Rehabil.* 15:27. doi: 10.1186/s12984-018-0365-z

Hogan, N., Krebs, H. I., Rohrer, B., Palazzolo, J. J., Dipietro, L., Fasoli, S. E., et al. (2006). Motions or muscles? Some behavioral factors underlying robotic assistance of motor recovery. *J. Rehabil. Res. Dev.* 43, 605–618. doi: 10.1682/JRRD.2005.06.0103

Holper, L., Biallas, M., and Wolf, M. (2009). Task complexity relates to activation of cortical motor areas during uni- and bimanual performance: a functional Nirs study. *Neuroimage* 46, 1105–1113. doi: 10.1016/j.neuroimage.2009.03.027

Inoue, Y., and Sakaguchi, Y. (2014). Periodic change in phase relationship between target and hand motion during visuo-manual tracking task: Behavioral evidence for intermittent control. *Hum. Mov. Sci.* 33, 211–226. doi: 10.1016/j.humov.2013.10.002

Jacky, A., Sheehan, E., Tsai, N., Greg, J., and Martin, D. (2015). mproving fluid intelligence with training on working memory: a meta-analysis. *Psychon Bull Rev* 22, 366–377. doi: 10.3758/s13423-014-0699-x

Jasper, H. (1958). The ten-twenty electrode system of the international federation. *Electroencephalogr. Clin. Neurophysiol.* 10, 371–375.

Kaplan, M. S. (1988). Ms: Plasticity after brain lesions: Contemporary concepts. *J. Head Trauma Rehabil.* 4, 984. doi: 10.1097/00001199-198906000-00013

Kapur, A., Tzanetakis, G., Virjibabul, N., Wang, G., Cook, P. R., and Columbia, B. (2005). *A Framework for Sonification of Vicon Motion Capture Data. Digital Audio Effects (DAFX-05)*, Madrid. 20–22.

Konttinen, N., Mononen, K., Viitasalo, J., and Mets, T. (2010). The effects of augmented auditory feedback on psychomotor skill learning in precision shooting. *J. Sport Exerc. Psychol.* 26, 306–316. doi: 10.1123/jsep.26.2.306

Kovacs, A., Boyle, J., Grützmacher, N., and Shea, C. H. (2010). *Coding of on-line and preplanned movement sequences*. Netherlands: Springer. doi: 10.1016/j.actpsy.2009.10.007

Krebs, H. I. (2009). A working model of stroke recovery from rehabilitation robotics practitioners. *J. NeuroEng. Rehabil.* 6, 6–6. doi: 10.1186/1743-0003-6-6

Krebs, H. I., Palazzolo, J. J., Dipietro, L., Ferraro, M., Krol, J., Rannekleiv, K., et al. (2003). Rehabilitation robotics: performance-based progressive robot-assisted therapy. *Auton. Robots* 15, 7–20. doi: 10.1023/A:1024494031121

Leff, D. R., Orihuela-Espina, F., Elwell, C. E., Athanasiou, T., Delpy, D. T., Darzi, A. W., et al. (2011). Assessment of the cerebral cortex during motor task behaviours in adults: a systematic review of functional near infrared spectroscopy (fnirs) studies. *Neuroimage* 54, 2922–2936. doi: 10.1016/j.neuroimage.2010.10.058

Lieberman, J., and Breazeal, C. (2007). *Tikl: Development of a Wearable Vibrotactile Feedback Suit for Improved Human Motor Learning*. Piscataway: Ieee Press. doi: 10.1109/ROBOT.2007.364093

Luara, F. D. S., Christ, O., Mate, K., Schmidt, H., Krüger, J. R., and Dohle, C. (2016). Movement visualisation in virtual reality rehabilitation of the lower limb: a systematic review. *Biomed. Eng. Online* 15, 144. doi: 10.1186/s12938-016-0289-4

Maciejasz, P., Eschweiler, J. R., Gerlach-Hahn, K., Jansen-Troy, A., and Leonhardt, S. (2014). A survey on robotic devices for upper limb rehabilitation. *J. Neuroeng. Rehabil.* 11, 1–29. doi: 10.1186/1743-0003-11-3

Nesbitt, K. V. (2004). *Ms-Taxonomy: A Conceptual Framework for Designing Multi-sensory Displays. International Conference on Information Visualisation*. (London, UK). doi: 10.1109/IV.2004.1320213

Okamoto, M., Dan, H., Sakamoto, K., Takeo, K., Shimizu, K., Kohno, S., et al. (2004). Three-dimensional probabilistic anatomical cranio-cerebral correlation via the international 10-20 system oriented for transcranial functional brain mapping. *NeuroImage* 21, 99–111. doi: 10.1016/j.neuroimage.2003.08.026

Oldfield, R. C. (1969). Handedness In Musicians. *Br. J. Psychol.* 60, 91–99. doi: 10.1111/j.2044-8295.1969.tb01181.x

Oviatt, S., Coulston, R., and Lunsford, R. (2004). *When do we interact multimodally? Cognitive load and multimodal communication patterns*. Portland: Oregon Health & Science University. doi: 10.1145/1027933.1027957

Periánez, J. A., Maestú, F., Barceló, F., Fernández, A., Amo, C., and Alonso, T. O. (2004). Spatiotemporal brain dynamics during preparatory set shifting: Meg evidence. *Neuroimage* 21, 687–695. doi: 10.1016/j.neuroimage.2003.10.008

Peters, M. (1998). Description and validation of a flexible and broadly usable handedness questionnaire. *Laterality* 3, 77–96. doi: 10.1080/713754291

Radziun, D., and Ehrsson, H. H. (2018). Auditory cues influence the rubber-hand illusion. *J. Exp. Psychol.* 44, 1012–1021. doi: 10.1037/xhp0000508

Rehme, A. K., Eickhoff, S. B., Rottschy, C., Fink, G. R., and Grefkes, C. (2012). Activation likelihood estimation meta-analysis of motor-related neural activity after stroke. *Neuroimage* 59, 2771–2782. doi: 10.1016/j.neuroimage.2011.10.023

Rehme, A. K., Fink, G. R., Von Cramon, D. Y., and Grefkes, C. (2011). The role of the contralesional motor cortex for motor recovery in the early days after stroke assessed with longitudinal Fmri. *Cereb. Cortex* 21, 756–768. doi: 10.1093/cercor/bhq140

Sabes, P. N. (2000). The planning and control of reaching movements. *Curr. Opin. Neurobiol.* 10, 740–746. doi: 10.1016/S0959-4388(00)00149-5

Scholkmann, F., Kleiser, S., Metz, A. J., Zimmermann, R., and Wolf, M. (2014). A review on continuous wave functional near-infrared spectroscopy and imaging instrumentation and methodology. *Neuroimage* 85, 6–27. doi: 10.1016/j.neuroimage.2013.05.004

Secoli, R., Milot, M. H., Rosati, G., and Reinkensmeyer, D. J. (2011). Effect of visual distraction and auditory feedback on patient effort during robot-assisted movement training after stroke. *J. Neuroeng. Rehabil.* 8:21. doi: 10.1186/1743-0003-8-21

Shams, L., and Seitz, A. R. (2008). Benefits of multisensory learning. *Trends Cogn.* 12, 411–417. doi: 10.1016/j.tics.2008.07.006

Shamy, M. C. F. (2010). The treatment of psychogenic movement disorders with suggestion is ethically justified. *Mov. Disord.* 25, 260–264. doi: 10.1002/mds.22911

Sigrist, R., Rauter, G., Riener, R., and Wolf, P. (2013). Augmented visual, auditory, haptic, and multimodal feedback in motor learning: a review. *Psychon. Bull. Rev.* 20, 21–53. doi: 10.3758/s13423-012-0333-8

Stefan, K. (2000). Induction of plasticity in the human motor cortex by paired associative stimulation. *Brain* 123, 572–584. doi: 10.1093/brain/123.3.572

Veldsman, M., Cumming, T., and Brodtmann, A. (2015). Beyond bold: Optimizing functional imaging in stroke populations. *Hum. Brain Mapp.* 36, 1620–1636. doi: 10.1002/hbm.22711

Wang, D., Huang, Y., Liang, S., Meng, Q., and Yu, H. (2022). The identification of interacting brain networks during robot-assisted training with multimodal stimulation. *J. Neural Eng.* 20:016009. doi: 10.1088/1741-2552/acae05

Wang, F., Mao, M., Duan, L., Huang, Y., Li, Z., and Zhu, C. (2018). Intersession Instability in fnirs-Based Emotion Recognition. *IEEE Trans. Neural Syst. Rehabil. Eng.* 26, 1324–1333. doi: 10.1109/TNSRE.2018.2842464

Wood, J. N., and Grafman, J. (2003). Human prefrontal cortex: processing and representational perspectives. *Nat. Rev. Neurosci.* 4, 139–147. doi: 10.1038/nrn1033

Woollacott, M., and Shumway-Cook, A. (2002). Attention and the control of posture and gait: a review of an emerging area of research. *Gait Posture* 16, 1–14. doi: 10.1016/S0966-6362(01)00156-4

Yamada, T., Umeyama, S., and Matsuda, K. (2012). Separation of fnirs signals into functional and systemic components based on differences in hemodynamic modalities. *PLoS One* 7:e50271. doi: 10.1371/journal.pone.0050271

Ye, J. C., Tak, S., Jang, K. E., Jung, J., and Jang, J. (2009). Nirs-Spm: statistical parametric mapping for near-infrared spectroscopy. *Neuroimage* 44, 428–447. doi: 10.1016/j.neuroimage.2008.08.036

Yu, N., Estévez, N., Hepp-Reymond, M., Kollias, S., and Riener, R. (2011). fmri assessment of upper extremity related brain activation with an Mri-compatible manipulandum. *Int. J. Comput. Assist. Radiol. Surg.* 6, 447–455. doi: 10.1007/s11548-010-0525-5

Frontiers in
Human Neuroscience

Bridges neuroscience and psychology to understand the human brain

The second most-cited journal in the field of psychology, that bridges research in psychology and neuroscience to advance our understanding of the human brain in both healthy and diseased states.

Discover the latest Research Topics

See more →

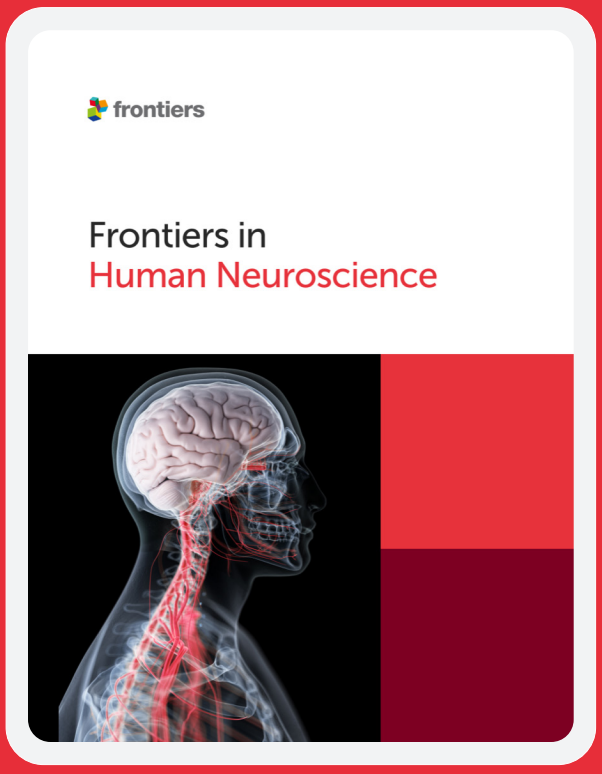

Frontiers

Avenue du Tribunal-Fédéral 34
1005 Lausanne, Switzerland
frontiersin.org

Contact us

+41 (0)21 510 17 00
frontiersin.org/about/contact